THE TETRASPANIN TSPAN18 REGULATES GPVI INDUCED PLATELET ACTIVATION AND Ca^{2+} MOBILISATION

By

REBECCA LOUISE GAVIN

A thesis submitted to the University of Birmingham for the degree of DOCTOR OF PHILOSOPHY

School of Biosciences
College of Life and Environmental Sciences
University of Birmingham
September 2014

ABSTRACT

Platelet activation and subsequent thrombus formation are important for preventing excessive blood loss at sites of vascular injury, a process termed haemostasis. However, excessive platelet activation at sites of atherosclerotic plaque rupture can lead to thrombus formation, which may occlude the vessel and cause heart attack or stroke. The platelet collagen receptor GPVI is essential for thrombus formation, but is largely dispensable for haemostasis.

Tetraspanins are transmembrane proteins which compartmentalise the membrane through formation of dynamic tetraspanin-enriched microdomains. Due to regulation of a wide range of partner proteins, tetraspanins have been implicated in many cellular processes, including platelet activation, though most platelet tetraspanins have not been characterised.

The aim of this thesis was to investigate the novel platelet tetraspanin Tspan18, using the Tspan18 knockout mouse. Tspan18 was shown to have a role in platelet activation and platelet Ca^{2+} signalling specifically downstream of GPVI. Tspan18 also appeared to have a role in haemostasis, as Tspan18 deficient mice displayed a severe bleeding phenotype. The bleeding was shown to be driven by non-haematopoietic cells and is therefore unlikely to be platelet-driven. Additionally, Tspan18-induced Ca^{2+} mobilisation was shown to be dependant on functioning Orai1 Ca^{2+} channels and a novel interaction between Tspan18 and the Orai family was identified. Together, these findings suggest a role for Tspan18 in platelet activation and regulation of Ca^{2+} mobilisation, potentially via interaction with Orai proteins.

ACKNOWLEDGEMENTS

Firstly, I would like to say thank you to all members of the Tomlinson lab, past and present, who have offered me support, friendship and advice over the past four years. Mike, you have been a fantastic mentor; your encouragement and unwavering optimism made even the toughest problems approachable. I would like to say thank you for your guidance and patience, and for always being genuinely enthusiastic about my project. Jing, your brilliance in the lab was truly amazing – I hope at least a little bit of it rubbed off on me at some point. Thank you for your kindness and for looking after all of us. Lizzie and Jas, Thank you for being there when I needed to talk through my data and complain about science. The past four years wouldn't have been half as funny without you, so thank you for making the office and the lab such a great place to work. Pete, thank you for your advice and help with the Tspan18 project, especially with the paper.

Prof Steve Watson and all the members of his group have given me countless help and advice throughout my PhD. Thank you to all of you for sharing your expertise and equipment and for always making me feel welcome in your lab.

Thank you to the many people from across Biosciences and the IBR who have offered help, equipment and guidance when I needed it. Thank you to Steve Publicover and Frank Michellangeli for taking the time to help and advise me on my project and for offering use of your lab equipment. Thank you to everyone who contributed to discussions in Friday lab meeting for your help and advice on my data. Also thank you to all members of the Rappoport lab who have been fantastic office mates and good friends. Thank you to Roy Bicknell and Victoria Heath for letting me dabble in endothelial biology and for help during the early stages of my PhD. I would also like to express my gratitude to the very hardworking staff at the BMSU who looked after my animals. I really appreciate all the work you have done behind the scenes which has enabled me to generate this data.

Massive thanks also go to Gareth Lewis for all of your brilliant advice, for continuing to be a wonderful friend and for being the first person to encourage me to do a PhD.

I would also like to thank my family for their support in everything I do. Mum and Dad, you taught me to be strong and determined and your encouragement has always empowered me to believe in myself. Thank you for your enduring confidence in me, for always offering your reassurance and understanding, and for always being ready with a large glass of wine!

Finally, and most importantly, thank you to my husband Alex. When I have felt like everything else is against me, I could always rely on you to be on my side. You are always willing to listen to my problems, even when you are stressed about your own. Thank you for believing in me and for supporting me unconditionally through everything.

TABLE OF CONTENTS

LIST OF FIGURES AND TABLES

CHAPTER 1

CHAPTER 2

CHAPTER 3

CHAPTER 4

CHAPTER 5

CHAPTER 6

APPENDICES

ABBREVIATIONS

ACD	Acid citrate dextrose
ADAM10	A disintegrin and metalloprotease domain-containing protein 10
ADP	Adenosine diphosphate
AMP	Adenosine monophosphate
ANOVA	Analysis of variance
AP-1	Activator protein 1
ATP	Adenosine triphosphate
BSA	Bovine serum albumin
CAD	CRAC activation domain
cAMP	Cyclic adenosine monophosphate
CCG	Cysteine-cysteine-glycine motif
CD19	Cluster of differentiation 19
cGMP	Cyclic guanylyl monophosphate
CLEC-2	C-type lectin like receptor 2
CRAC	Ca^{2+} release activated Ca^{2+} current
CRP	Collagen related peptide
Ct	Cycle threshold
DAG	Diaceyl-glycerol
DNA	Deoxyribonucleic acid
DTSSP	3, 3'-dithiobis [sulfosuccinimidylpropionate]
EGTA	Ethylene glycol tetraacetic acid
ELISA	Enzyme-linked immunosorbant assay
EMT	Epithelial mesenchymal transition
EP3	Prostaglandin E receptor 3
ER	Endoplasmic reticulum
EWI-2	Immunoglobulin super family member 8
FACS	Fluorescence activated cell sorting
FBS	Foetal bovine serum
FEVR	Familial exudative vitreoretinopathy
FITC	Fluorescein isothiocyanate
FVa	Factor Va
FVIIa	Factor VIIa
FXa	Factor Xa
FXIIa	Factor XIIa
GC	Guanylyl cyclase
GDP	Guanosine diphosphate
GFP	Green fluorescent protein
GPCR	G-protein coupled receptor
GPO	Glycine-proline-hydroxyproline
GPVI	Glycoprotein VI
GTP	Guanosine triphosphate
HCV	Hepatitis C virus
HMEC	Human microvascular endothelial cells
HUVEC	Human umbilical vein endothelial cells
ICAM-1	Intercellular adhesion molecule 1
Ig	Immunoglobulin
IP_3	Inositol triphosphate
ITAM	Immunoreceptor tyrosine based activation motif

LacZ	Lactose operon
LAT	Linker for activation of T-cells
LTA	Light transmission aggregometry
MAPK	Mitogen-activating protein kinase
mRNA	Messenger ribonucleic acid
NFAT	Nuclear factor of activated T-cells
NO	Nitric oxide
PAGE	Polyacrylamide gel electrophoresis
Panx-1	Pannexin-1
PAR	Protease activated receptor
PBS	Phosphate buffered saline
PCR	Polymerase chain reaction
PDE	Phosphodiesterase
PEI	Polyethylenimine
PGI_2	Prostaglandin I2
PIP_2	Phosphatidyl inositol 4, 5-bisphosphate
PKA	Protein kinase A
PKC	Protein kinase C
PKD2	Protein kinase D2
PKG1	Protein kinase G 1
PLCβ	Phospholipase C β
PLCγ	Phospholipase C γ
PMA	Phorbol 12-myristate 13-acetate
PSGL-1	P selectin glycoprotein ligand 1
RhoA	Ras homologue gene family member A
SAM	Sterile α motif
SCID	Severe combined immunodeficiency
SDS	Sodium dodecyl sulphate
SERCA	Sarco/endoplasmic reticulum Ca^{2+}-ATPase
SH2	Src homology 2
SH3	Src homology 3
siRNA	Short interfering ribonucleic acid
SNP	Single nucleotide polymorphism
SOAR	STIM1 Orai1 activating region
SOCE	Store operated Ca^{2+} entry
SPCA2	Secretory pathway Ca^{2+}-ATPase
SR	Sarcoplasmic reticulum
STIM	Stromal interaction molecule
STIM-C	STIM1 C-terminal
STIM-N	STIM1 N-terminal
TM	Transmembrane domain
TP	Thromboxane receptor
TRPC	Transient receptor potential cation channel
TxA_2	Thromboxane A2
UP	Uroplakin
VASP	Vasodilator-stimulated phosphoprotein
VCAM-1	Vascular cell adhesion protein 1
VEGF	Vascular endothelial growth factor
vWF	Von Willebrand factor
Xgal	5-bromo-4-chloro-3-indolyl-β-D-galactopyranoside

CHAPTER 1

GENERAL INTRODUCTION

1.1 PLATELETS

Platelets are small, anuclear blood cells which have roles in many biological processes, though the best characterised is their role in haemostasis and prevention of blood loss. Platelets are formed from mature megakaryocyte progenitors in the bone marrow, which extend cytoplasmic processes, called proplatelets, into the circulation where budding and fragmentation results in platelet formation (J. E. Italiano, 2013). Once in the bloodstream, platelets are maintained at the edges of the flow and are therefore in close proximity to the endothelial lined vessel wall. Abnormalities in platelet production can cause thrombocytopenia (low platelet count) which is associated with an increased risk of bleeding (J. E. Italiano, 2013).

1.1.1 Haemostasis

At sites of vascular injury, the body prevents excessive blood loss via a process called haemostasis. Damage to a blood vessel induces an immediate reaction from surrounding smooth muscle cells, endothelial cells and platelets. This is a highly regulated process, involving several key stages which act to reduce blood loss and to initiate the wound healing response.

Firstly, vasoconstriction occurs via contraction of smooth muscle cells, which form the muscular wall of the vessel, causing narrowing of the lumen to reduce blood flow (van Hinsbergh, 2012). One example of the multiple stimuli which can induce smooth muscle cell contraction is thromboxane A_2 (TxA_2), which is released by platelets at sites of vascular injury. This vasoconstrictor activates a G-protein coupled receptor, stimulating G_q protein responses,

leading to activation of myosin-light chain kinase and induction of muscle cell contraction (Wilson, Susnjar, Kiss, Sutherland, & Walsh, 2005).

Following vasoconstriction, primary haemostasis occurs, which involves activation of platelets. Platelets are maintained in the circulation in an inactive state, but at sites of vascular injury they become activated and aggregate together to form a platelet plug and therefore stem the loss of blood. Formation of this platelet plug, or thrombus, involves activation of multiple signalling receptors on the platelet surface, to induce platelet activation, shape change, adhesion and aggregation (Broos, Feys, De Meyer, Vanhoorelbeke, & Deckmyn, 2011). These signalling mechanisms are discussed in more detail in sections 1.1.2 and 1.1.4.

The final stage of haemostasis, secondary haemostasis, involves activation of the coagulation cascade and formation of a fibrin clot. Initiation of the coagulation cascade is marked by complex formation between plasma protease factor VIIa (FVIIa) and tissue factor, which promotes thrombin generation (Chou et al., 2004; B Nieswandt, Pleines, & Bender, 2011). Thrombin acts not only to promote platelet activation, but also induces fibrin formation from fibrinogen. Finally, cross-linking of fibrin produces a fibrin mesh which acts to reinforce the thrombus. A process called clot retraction also occurs, during which actin stress fibres within the platelets contract to reduce the size of the clot and to protect the clot from disruption by the blood flow (Stegner & Nieswandt, 2011).

Together, these immediate responses at sites of vascular damage can prevent excessive blood loss. The role that platelets play within this system

and the ability to activate quickly is vital for successful haemostasis. However, regulation of platelet activation is important to prevent thrombus formation and disruption to blood flow at sites away from vascular damage.

1.1.2 Thrombus formation

The mechanisms underlying thrombus formation are well characterised and the impact that platelet activation and thrombus formation has during haemostasis is depicted in figure 1.1. Within an undamaged vessel, the endothelium inhibits platelet activation in order to prevent unwanted thrombus formation. For example, endothelial secretion of both prostaglandin I_2 (PGI_2) and nitric oxide (NO) reduce platelet activation (figure 1.1, A). PGI_2 is produced in endothelial cells by PGI_2 synthase from the precursor prostaglandin H_2. PGI_2 reduces platelet activation through G-protein coupled receptor (GPCR) activation and subsequent G-protein mediated increases in cytosolic cyclic adenosine monophosphate (cAMP), which leads to reduced intracellular Ca^{2+} concentration (Mitchell, Ali, Bailey, Moreno, & Harrington, 2008; Schwarz, Walter, & Eigenthaler, 2001). NO, also synthesised by endothelial cells, inhibits adhesion and platelet aggregation through activation of guanylyl cyclase and thus increased cyclic guanylyl monophosphate (cGMP), which also reduces intracellular Ca^{2+} (Mitchell et al., 2008; S Moncada & Higgs, 2006). Additionally, endothelial cells express the ecto-nucleotidase CD39, which hydrolyses platelet-secreted adenosine diphosphate (ADP) into adenosine monophosphate (AMP), thus reducing ADP-induced platelet activation (Marcus et al., 1997; van Hinsbergh, 2012).

However, following injury to the vessel wall and exposure to the sub-endothelial matrix, platelets become activated. An initial interaction between exposed collagen and the platelet occurs via the glycoprotein von Willebrand factor (vWF), which allows for initial tethering of the platelet to collagen fibres within the high shear environment of the vessel (Stegner & Nieswandt, 2011) (figure 1.1, B). This tethering process then allows for an interaction to form between the platelet collagen receptor glycoprotein VI (GPVI) and collagen (Stegner & Nieswandt, 2011). Activation of GPVI by collagen binding initiates a phosphorylation signalling cascade resulting in platelet activation (Stegner & Nieswandt, 2011). Activated platelets undergo a period of shape change, during which rearrangement of the actin cytoskeleton mediates platelet adhesion, clot retraction and secretion of secondary mediators. Positive feedback mediators such as ADP and TxA_2, which are secreted from platelet dense granules, act to potentiate platelet activation and recruit more platelets from the blood flow to the site of injury (Stegner & Nieswandt, 2011) (figure 1.1, C). Finally, thrombus formation is stabilised via activation of platelet surface integrins such as αIIbβ3, which mediates platelet-platelet interactions, and α2β1, α5β1 and α6β1 which bind collagen, fibronectin and laminin respectively (Stegner & Nieswandt, 2011). In addition, the platelet plug is supported by a mesh of fibrin, which is formed via the cleavage of fibrinogen by thrombin, a process driven by the coagulation cascade and secondary haemostasis (figure 1.1, D). The precise mechanisms behind this complex process and the interplay which balances inhibitory and activatory signals in platelets are discussed in more detail in section 1.1.4.

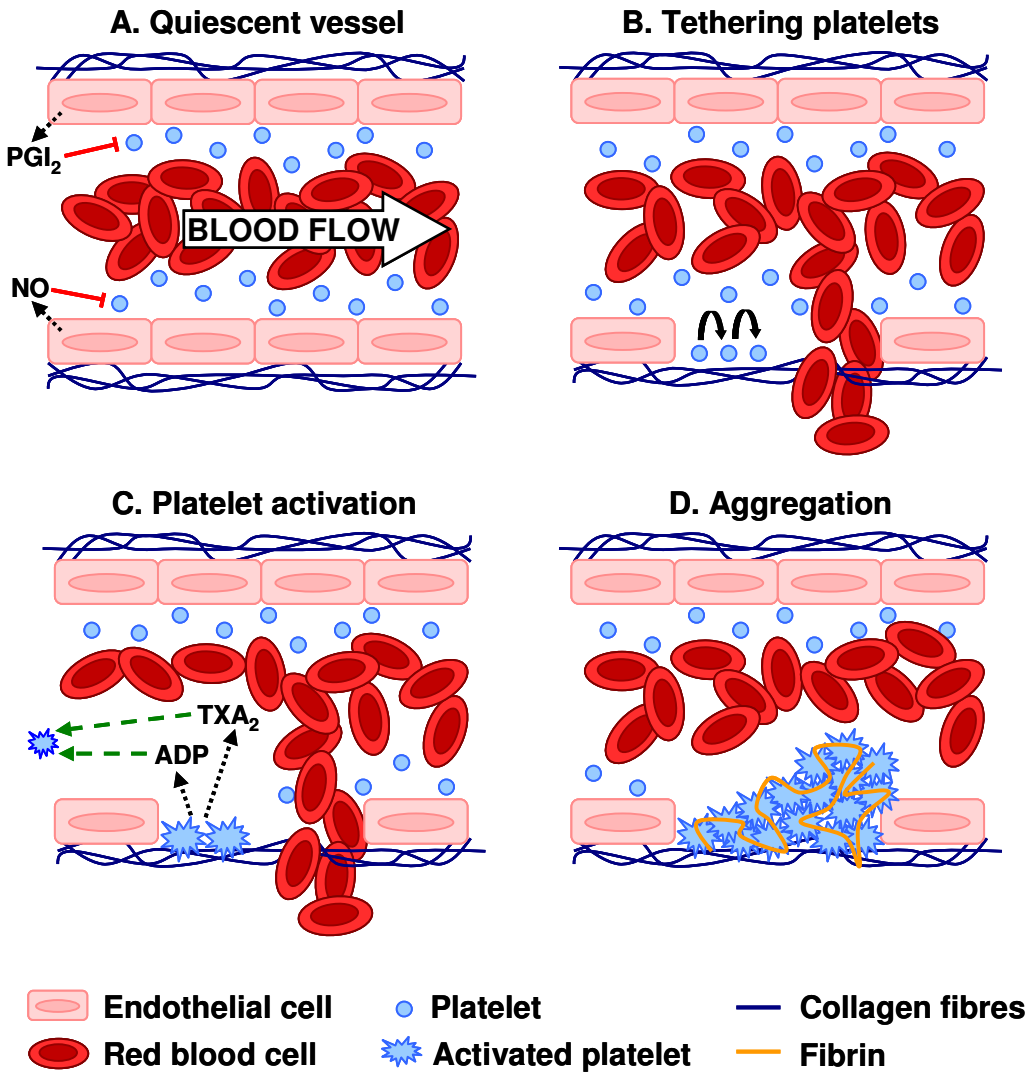

Figure 1.1 – Thrombus formation prevents excessive blood loss at sites of vascular injury. In a quiescent, uninjured vessel, the endothelium releases anti-thrombotic agents such as PGI_2 and NO to inhibit platelet activation (A). Following injury to the endothelium, components of the basal membrane such as collagen are exposed, and blood cells and plasma leak out of the damaged vessel. Platelets react to the exposed collagen and tether to collagen fibres via vWF. Black arrows represent deceleration of the platelets from the flow of blood due to this initial tethering stage (outline in more detail in section1.1.4) (B). The initial tethering process slows the platelet and allows an interaction between collagen and GPVI to form, which induces platelet activation, shape change and secretion of secondary mediators, such as ADP and TxA_2 (C). Integrin activation induces aggregation, and fibrin drives formation of the haemostatic plug (D).

1.1.3 Platelets in health and disease

Although platelet activation has an important role during haemostasis, recent research has implicated platelets in several other biological processes and

platelet activation and thrombus formation has also been implicated in several disease processes. For example, interaction between platelets and lymphatic endothelial cells has been shown to be important for normal development and function of the lymphatic system, especially in preventing backflow of blood into the lymphatic vessels at lymphovenous junctions. Podoplanin, expressed on the lymphatic endothelium, activates the platelet receptor C-type lectin like receptor 2 (CLEC-2), which leads to platelet aggregation and prevents leakage of blood components into the lymphatic system (Bertozzi et al., 2010; Finney et al., 2012; Hess et al., 2014; Suzuki-Inoue et al., 2010; Uhrin et al., 2010). Additionally, at lymphovenous junctions which display impaired valve function, thrombus formation within the lymphatic environment can be protective against blood-lymphatic mixing (Hess et al., 2014). CLEC-2 is also important in development and maintenance of lymph nodes and in mice with platelets deficient in CLEC-2, blood filled lymph nodes and fibrosis was observed due to reduced lymph node integrity (Bénézech & Nayar, 2014). Platelet CLEC-2 and GPVI mediated signalling has also been implicated in maintaining vascular integrity during inflammation, when lymphocytes transmigrate through the vessel wall (Boulaftali et al., 2013). This is particularly important in high endothelial venules, through which lymphocytes transmigrate to reach the lymph nodes. Podoplanin-induced CLEC-2 signalling and platelet activation is important to maintain integrity of these vessels (Herzog et al., 2013). Finally, platelets have also been shown to play an important role in facilitating the closure of the ductus arteriosus; a vessel between the aorta and the pulmonary artery which must be closed after birth

to prevent post natal mortality. Platelets support remodelling and contribute to the thrombotic sealing of this area (Echtler et al., 2010).

Platelets have also been implicated in poor cancer prognosis, as they can coat the surface of tumour cells in the blood stream and are able to facilitate adhesion to the vessel wall, tumour growth and metastasis (Lowe, Navarro-Nunez, & Watson, 2012). One mechanism which has been widely studied is the interaction between platelet CLEC-2 and tumour cell podoplanin. Podoplanin is highly expressed on cancer cells and several studies have linked podoplanin to increased metastasis and malignant tumour progression (Mishima et al., 2006; P. Yuan et al., 2006). Investigation into activation of platelet CLEC-2 by tumour cell podoplanin, implicated a role for CLEC-2 induced platelet aggregation in tumour growth and metastasis (Suzuki-Inoue et al., 2007, 2010). Interestingly, if podoplanin-induced platelet activation is suppressed, then a significant reduction in pulmonary metastasis is observed (Miyata et al., 2014), which highlights the potential for therapeutic targeting of platelets to combat cancer metastasis. Platelets also play additional roles in cancer progression, for example activation of protease activated receptor (PAR) pathways can lead to release of angiogenic factors such as vascular endothelial growth factor (VEGF), which promote vessel growth and therefore mediates tumour growth (J. E. I. Italiano et al., 2008; Lowe et al., 2012).

In addition to being necessary during haemostasis, thrombus formation is also heavily implicated in both heart attack and stroke, as arterial thrombus formation at sites of atherosclerotic plaque rupture can lead to occlusion of the vessel. Formation of atherosclerotic plaques occurs as a result of severe inflammation of the endothelium caused by deposits of cholesterol and

accumulation of macrophages (Palomo, Toro, & Alarcón, 2008; Sakakura et al., 2013). Progression of plaque formation eventually leads to narrowing of the vessel and potential disruption to blood flow. Rupture of an unstable plaque induces thrombus formation, as the surrounding platelets are exposed to damaged endothelium and components of the sub-endothelium matrix, all of which induce platelet activation and aggregation. The coagulation cascade has also been implicated in atherothrombosis, as coagulation factors such as FXI regulates thrombus formation at sites of acutely ruptured plaques (van Montfoort et al., 2014), FVIIa contributes to activation of initial thrombus formation, and factor XIIa (FXIIa) has been shown to stabilise the thrombus during pathological atherothrombosis (Kuijpers et al., 2014). Culmination of thrombosis and the coagulation cascade at sites of plaque rupture can produce blood clots which completely occlude the vessel, preventing blood flow within the artery and causing heart attack or stoke. New roles for platelets in the early stages of plaque formation are also being investigated. It appears that activated platelets can interact with and activate the endothelium at sites prior to plaque formation. Therefore platelets could potentially be promoting inflammation and thus initiating plaque formation (Rondina, Weyrich, & Zimmerman, 2013).

A better understanding of the mechanisms behind platelet activation could provide potential future targets for anti-thrombotic therapies for heart attack, which is currently one of the principle causes of mortality worldwide (Mendis, Puska, & Norrving, 2011).

1.1.4 Multiple signalling pathways balance inhibitory and activating stimuli in platelets

Inappropriate platelet activation at sites distant from vascular damage needs to be avoided in order to prevent unwanted thrombus formation, therefore inhibitory signals to maintain platelets in a 'resting' state are vitally important. However, it is also crucial that platelet activatory signals are robust enough to overcome inhibition of platelet activation when required. The fine balance of these positive and negative signals, which was briefly outlined in section 1.1.2, involves a multitude of signalling receptors and signal transduction pathways.

One important physiological platelet inhibitor is NO, which is secreted by endothelial cells to keep the platelets in a 'resting' state within a healthy vessel. Inhibition of platelet activation by endothelial-secreted NO occurs predominantly via the cGMP-PKG signalling pathway. NO diffuses across the platelet membrane and activates the NO-sensitive enzyme guanylyl cyclase (GC), thus increasing the production of cGMP (Smolenski, 2012). Increased levels of cGMP in the platelet lead to activation of protein kinase G 1 (PKG1), which then acts on a range of different substrates; inducing phosphorylation and ultimately inhibiting platelet activation. The importance of PKG1 within the inhibitory NO-cGMP pathway was demonstrated by the prothrombic phenotype observed in PKG1 knockout mice; mice lacking PKG1 showed an increase in platelet adhesion and platelet activation in the presence of NO (Massberg et al., 1999). One example of a PKG1 substrate is vasodilator-stimulated phosphoprotein (VASP), which has an important role in the regulation of actin cytoskeleton dynamics. Mice lacking VASP show

increased adhesion and defective inhibition via the NO-cGMP pathway, suggesting that phosphorylation of VASP by PKG1 has an important role in platelet inhibition (Massberg et al., 2004).

PGI_2 which is also released by the endothelium is another important inhibitor of platelet activation, though it acts through a different mechanism to NO. PGI_2 binds to a GPCR on the platelet surface and triggers a signalling pathway through activation of the associated G-proteins. Specifically, binding of PGI_2 leads to activation of the Gs G-protein through promotion of the GTP-bound active form of the protein (Smolenski, 2012). Active GTP-bound Gs then goes on to activate adenylate cyclase (AC) which stimulates synthesis of cAMP. In a similar mechanism as described for cGMP, cAMP utilises a kinase to continue the signalling cascade, specifically activating protein kinase A (PKA); upon cAMP binding to the regulatory subunits of PKA, the catalytic domains dissociate and go on to phosphorylate its substrates. Substrates of PKA include VASP and also the intracellular Ca^{2+} store channel protein IP_3 receptors (Smolenski, 2012). Both PKA and PKG1 act on many different substrates and phosphorylation of these substrates ultimately leads to modulation of the actin cytoskeleton to prevent platelet shape change and regulation of Ca^{2+} release from intracellular stores to prevent platelet activation (Smolenski, 2012). Despite the need for these inhibitory signals in platelets, mechanisms exist to reduce cAMP and cGMP levels in the platelet, as balancing these cyclic nucleotides is vital for balancing platelet inhibition and activation. Regulation of cAMP and cGMP occurs mainly through degredation via the phosphodiesterase (PDE) family of proteins. In platelets, PDE2 and PDE3 specifically degrade cAMP and PDE5 specifically degrades

cGMP (Smolenski, 2012). Activation of the PDE proteins occurs via a negative feedback loop, which helps to keep the cytosolic levels of cAMP and cGMP in check. However, to ultimately be able to induce platelet activation when required at sites of vascular damage, strong activatory signals need to be produced to overcome these inhibitory effects.

The process of platelet activation at sites of vascular damage involves multiple cell surface receptors. Investigation into their signalling has demonstrated that platelet surface receptors rely on two key downstream signalling pathways. Receptors such as GPVI/FcRγ and CLEC-2 rely on tyrosine phosphorylation signalling cascades downstream of immunoreceptor tyrosine based activation motif (ITAM) and hemITAM motif activation respectively. Other platelet receptors such as PAR, thromboxane receptors (TP) and P2Y receptors are GPCRs which rely on G-protein activated signalling pathways (Bernhard Nieswandt & Watson, 2003; Stegner & Nieswandt, 2011). Ultimately, these pathways converge to reduce cAMP and increase intracellular Ca^{2+} which amplifies platelet activation and stabilises platelet adhesion through integrin activation, as demonstrated by the diagram in figure 1.2.

Exposure of collagen fibres at sites of vascular damage acts as the initial signal to stimulate platelet activation. However, in arterial shear conditions, the platelets must undergo a process of tethering, to decelerate the platelet, before direct interaction with collagen and platelet activation can occur. This process is reliant on the adhesive glycoprotein GPIb-V-IX complex, which interacts with vWF multimers which become immobilised on exposed collagen fibres (M Moroi et al., 1997). Without this initial stage of platelet tethering,

platelet activation is impaired, as demonstrated by the bleeding disorder Bernard-Soulier syndrome, which is caused by the lack or dysfunction of the GPIb-V-IX complex (Berndt & Andrews, 2011). Interaction of GPIb-V-IX with vWF not only facilitates tethering of the platelet at the site of injury, but also induces weak activation of the integrin αIIbβ3, and can induce intracellular Ca^{2+} mobilisation (Stegner & Nieswandt, 2011).

Although the capture of platelets from the blood flow is reliant on the GPIb-vWF interaction, this is not sufficient to provide firm adhesion of the platelet to the exposed collagen fibre. In order to achieve this, strong activation signals are required. The platelet collagen receptor GPVI is able to produce the activatory signals required, following capture of the platelet. GPVI is a transmembrane Ig super family receptor, which interacts with collagen fibres via glycine-proline-hydroxyproline (GPO) repeats, which induces cross-linking of the receptor (Watson, Auger, McCarty, & Pearce, 2005). Following cross-linking, GPVI signals via the ITAM motif found in the intracellular tail of the associated FcRγ chain, which eventually leads to activation of phospholipase Cγ (PLCγ), causing increased cytosolic Ca^{2+} concentration via release from intracellular stores, and influx from the extracellular environment (Bernhard Nieswandt & Watson, 2003; Y. a Senis, Mazharian, & Mori, 2014). The complex signalling cascade of this important platelet collagen receptor is described in more detail in section 1.1.5 and is represented in figure 1.3. Interestingly, mice lacking GPVI/FcRγ do not display vastly prolonged bleeding times, which suggests that although this receptor has an important role in platelet activation, some level of redundancy with other receptors on the platelet surface might occur (B Nieswandt, Schulte, et al., 2001).

However, mice lacking GPVI/FcRγ are protected against arterial thrombosis in the transient middle cerebral artery occlusion model of stroke and display reduced damage to brain tissue due to a reduction in thromboinflammation (Kleinschnitz et al., 2007). This presents GPVI as an attractive target for treatment of ischemic coronary disease, as there is the potential to reduce artherothrombosis without increasing the risk of bleeding or brain injury after reperfusion (Kleinschnitz et al., 2007). Additionally, GPVI has been implicated in inflammation models other than those following pathological vascular events such as stroke. Both GPVI and CLEC-2 have a role in maintenance of vascular integrity during inflammation (Boulaftali et al., 2013) and GPVI has also been implicated in promotion of inflammation in rheumatoid arthritis (Boilard et al., 2010).

The role of GPVI is not limited to platelet activation through increasing cytosolic Ca^{2+} concentration. This receptor also has an important role in activation of platelet integrins through an 'inside-out' mechanism, which converts them from inactive to an active state (Y. a Senis et al., 2014). Integrins are adhesion receptors, which exist as heterodimeric transmembrane proteins made from α and β subunits. Integrins play a vital role in mediating cell adhesion and specifically in platelets, this is important during platelet activation and thrombus formation (B Nieswandt et al., 2011; Stegner & Nieswandt, 2011). In a resting platelet, integrins are held in an inactive state and have low affinity for their ligands; this is important to prevent platelet adhesion away from sites of vascular damage and prevent inappropriate platelet adhesion. Upon activation of platelet surface receptors, integrins shift to an active state with high binding affinity for their ligands. This

shift is triggered by inside-out signalling from platelet surface receptors such as GPVI, and others including GPCRs and ITAM mechanisms (B Nieswandt et al., 2011; Stegner & Nieswandt, 2011). In addition to the role in adhesion that these integrins play on the platelet surface, outside-in signalling mechanisms are triggered following binding of integrins to their ligands. A broad variety of cytosolic integrin-binding proteins play a role in promoting platelet spreading and clot retraction follwing integrin activation.

Three different β1 integrins have been identified in platelets; α2β1, α5β1 and α6β1. Activation of α2β1 facilitates firm adhesion of the platelet to exposed collagen fibres (Inoue, Suzuki-Inoue, Dean, Frampton, & Watson, 2003). Additionally, α5β1 and α6β1 help to further stabilise adhesion of the platelet through interactions with fibronectin and laminin respectively (Stegner & Nieswandt, 2011). However, the β1 integrins are suggested to play more of a supportive role and are considered not to be essential for firm platelet adhesion (B Nieswandt et al., 2011; Stegner & Nieswandt, 2011). This is demonstrated by the lack of severe disruption to thrombus formation following loss of α2β1, suggesting that loss of the β1 integrins can be compensated by other platelet surface protein which contribute to adhesion (B Nieswandt, Brakebusch, et al., 2001). In addition to the β1 integrins, the platelet surface is also populated with two β3 integrins; αIIbβ3 and αVβ3. The αVβ3 integrin is expressed at very low levels on the platelet surface and is poorly understood however αIIbβ3 is the most abundant integrin on the platelet surface and has been widely studied due to the vital role it plays in thrombus formation (B Nieswandt et al., 2011). Loss of the integrin αIIbβ3 on the platelet surface results in increased bleeding and lack of thrombus formation

in mice (Hodivala-dilke et al., 1999; Tronik-Le Roux et al., 2000), and mutations leading to lack or dysfunction of αIIbβ3 in humans causes the bleeding disorder Glanzmann's thrombasthenia (Sebastiano, Bromberg, Breen, & Hurford, 2010). This demonstrates that loss of this particular integrin cannot be compensated through alternative interactions and confirms the importance of the role it plays in platelet aggregation. This particular integrin is vital in forming platelet-platelet interactions through association with fibrinogen, which forms a bridge with αIIbβ3 integrins on opposing platelet surfaces, therefore allowing platelet aggregation and thrombus growth (Watson et al., 2005). It has also been suggested that vWF is another ligand for this integrin and that this interaction is important for platelet-platelet interactions to occur within high shear environments (Ruggeri, Dent, & Saldívar, 1999).

In addition to the initial activatory signals from GPVI, other platelet surface proteins are also important in potentiating platelet activation and driving thrombus formation, including G-protein coupled receptors such as the PAR receptors, TPα/TPβ receptors and the P2Y1/P2Y12 receptors. The PAR receptors are activated by the prothrombotic agent thrombin, which is produced locally at sites of vascular damage through the coagulation cascade. Gq-coupled responses from PAR activation lead to downstream phospholipase Cβ (PLCβ) activation and ultimately increased Ca^{2+} concentration through release from intracellular stores (De Candia, 2012). G12/13-coupled responses from PAR activation leads to downstream activation of Ras homologue gene family member A (RhoA), from its inactive guanosine diphosphate (GDP)-bound form into its active guanosine

triphosphate (GTP)-bound form (De Candia, 2012). Once active, this small GTPase can trigger phosphorylation events which lead to myosin light chain phosphorylation, which has been shown to drive platelet shape change. The process of shape change within the platelet is driven by dynamic changes to the cytoskeleton and allows for the normally discoid platelet to spread and adhere strongly to exposed collagen fibres. Changes to the cytoskeleton can also drive secretion of secondary mediators, such as ADP and TxA_2, through trafficking of platelet dense granules to the plasma membrane (Broos et al., 2011; Stegner & Nieswandt, 2011).

Platelet-secreted ADP activates P2Y1 and P2Y12 receptors on the platelet cell surface which activate downstream Gq and Gi signalling respectively. As described above, activation of Gq-proteins induces increased Ca^{2+} concentrations through activation of PLCβ. Activation of Gi-coupled signalling inhibits adenylyl cyclase, which normally converts adenosine triphosphate (ATP) into cAMP, thus Gi signalling reduces cAMP activity (Jin, Daniel, & Kunapuli, 1998). The action of cAMP inhibits many platelet activatory processes such as degranulation leading to secretion, rearrangement of the cytoskeleton and increasing intracellular Ca^{2+} (Schwarz et al., 2001; Stegner & Nieswandt, 2011). Therefore Gi-protein induced inhibition of andenylyl cyclase promotes secretion, shape change and platelet activation through reduction of cAMP.

Platelet secreted TxA_2 activates TPα/TPβ receptors, which also activate Gq-proteins. Therefore activation of TP receptors drives increasing Ca^{2+} concentration and inhibition of cAMP production, as outlined above (Stegner & Nieswandt, 2011).

P2X1 adenosine triphosphate (ATP)-gated cation channels also contribute to platelet activation, through direct flux of Ca^{2+} into the cell. Following binding of ATP, P2X1 allows flux of Ca^{2+} and other cations into the platelet. The Ca^{2+} signal provided by P2X1 receptors is important for platelet shape change, and promotion of dense granule secretion (Mahaut-Smith, Jones, & Evans, 2011). The activation of P2X1 has also been shown to amplify platelet activation via synergy with other platelet receptors and can increase signalling responses to low doses of platelet agonists such as thrombin and collagen (Mahaut-Smith et al., 2011).

These platelet receptors, which are shown in figure 1.2, demonstrate some of the signalling pathways involved in platelet activation. Further signalling receptors also contribute to platelet activation; CLEC-2 signals in a very similar mechanism to GPVI, with the intracellular tail utilising a hemITAM motif to initiate tyrosine phosphorylation signalling cascade (May et al., 2009; Y. a Senis et al., 2014). Receptors such as adrenergic receptors, prostaglandin E receptor 3 (EP3) and 5-hydroxytimamine 2A receptors signal through G-protein coupled mechanisms (Broos et al., 2011; Stegner & Nieswandt, 2011). Additional receptors which contribute to platelet activation as well as new levels of regulation of currently known platelet receptors are still being identified. For example, the selective anion channel pannexin-1 (Panx-1) has recently been shown to facilitate Ca^{2+} mobilisation and platelet aggregation, potentially through secondary activation of the P2X1 receptors on the platelet surface (Taylor, Wright, Vial, Evans, & Mahaut-Smith, 2014).

Culmination of signalling from all of these different receptors allows for maximal platelet activation, and also promotes regulation of this vital process.

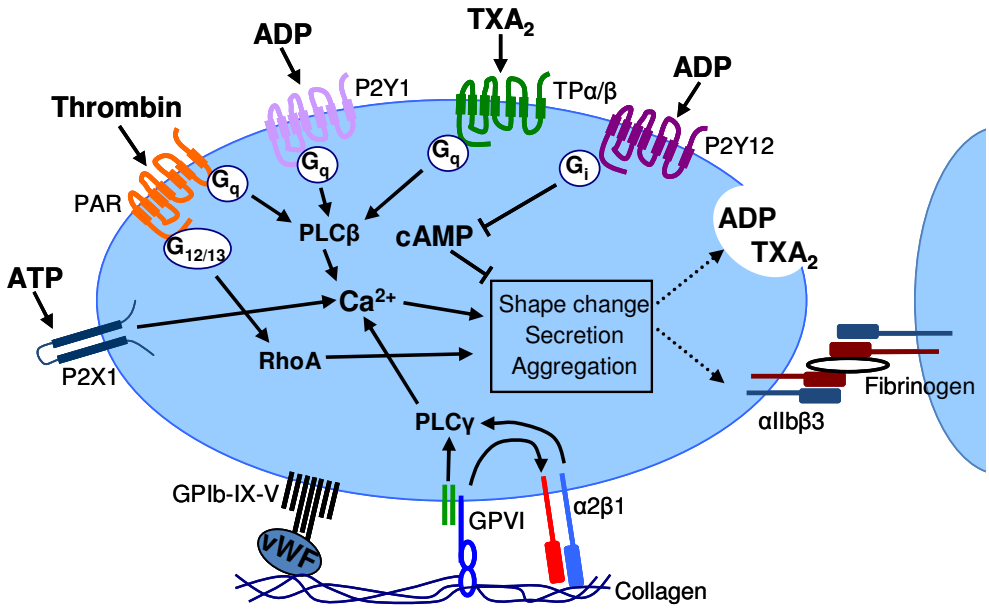

Figure 1.2 – Multiple surface receptors contribute to platelet activation and aggregation. The primary wave of platelet activation is mediated by adhesion to exposed extracellular matrix at sites of injury. Tethering of the GPIb-IX-V complex to collagen via vWF slows the platelet from the blood flow and allows interaction between GPVI and collagen to form. Once bound to collagen, GPVI signals via an ITAM motif within the FcRγ chain which initiates a phosphorylation cascade resulting in increased cytosolic Ca^{2+}, secretion of secondary mediators such as ADP and TxA_2, platelet activation and activation of integrin α2β1 to stabilise adhesion to collagen. ADP activates the P2Y1 and P2Y12 receptors, coupled to Gq and Gi proteins respectively. TxA_2 activates TPα and TPβ receptors, coupled to Gq proteins. Thrombin is generated at sites of vascular injury and as well as contributing to fibrin generation, activates the PAR receptors, coupled to Gq and G12/13 proteins. These secondary wave agonists amplify and sustain platelet activation through increasing cytosolic Ca^{2+}, decreasing cAMP activity and inducing shape change. Ca^{2+} influx via ATP-gated P2X1 channels amplifies platelet activation. Ultimately, this leads to activation of integrin αIIbβ3, which mediates platelet-platelet interaction, thus driving aggregation.

1.1.5 Downstream signalling from the platelet collagen receptor GPVI

The platelet collagen receptor GPVI has two extracellular immunoglobulin (Ig) domains and a proline-rich Src homology 3 (SH3)-binding domain within the short intracellular tail, to allow for interaction of kinase proteins (Masaaki Moroi & Jung, 2004). The functional receptor is associated with the FcRγ chain, which contains an ITAM motif within the intracellular tail, which is defined by two YxxL/I motifs separated by 6-12 residues (Horii, Kahn, & Herr,

2006; Masaaki Moroi & Jung, 2004). GPVI itself does not possess intrinsic kinase activity, therefore transfer of the signal to induce platelet activation is reliant on Src family kinases to complete a complex tyrosine phosphorylation cascade (Y. a Senis et al., 2014). This signalling cascade is outlined in figure 1.3 and is discussed in more detail below.

Following cross-linking of GPVI induced by binding collagen, activation of the downstream phosphorylation cascade begins with the Src family kinases Lyn or Fyn phosphorylating two tyrosine residues within the ITAM motif in the cytosolic tails of the associated FcRγ chain (Dütting, Bender, & Nieswandt, 2012; Stegner, Haining, & Nieswandt, 2014; Zahid et al., 2012). Phosphorylation of the ITAM recruits Syk, via 2 Src homology 2 (SH2) domains, which enables phosphorylation of Syk by Lyn. Syk can then go on to phosphorylate the linker for activation of T-cells (LAT) and enable formation and activation of the LAT signalosome; a scaffold of adaptor proteins which recruits PLCγ2 close to the plasma membrane (Dütting et al., 2012; Stegner et al., 2014; Zahid et al., 2012). These adapters include SLP-76 and also Gads, which aid in linking LAT to SLP-76 (Hughes et al., 2008). Completion of the LAT signalosome promotes activation of PLCγ2, which in turn produces diaceylglycerol (DAG) and inositol trisphosphate (IP_3) from hydrolysis of phosphatidyl inositol 4, 5 bisphosphate (PIP_2). IP_3 can then stimulate flux of Ca^{2+} from the intracellular Ca^{2+} store, into the cytosol, via IP_3 receptors. In turn, depletion of Ca^{2+} from the intracellular store induces influx of Ca^{2+} from the extracellular environment in a process called store operated Ca^{2+} entry (SOCE) (Smyth et al., 2010; Stegner et al., 2014), which is discussed in more detail in section 1.2. The overall increase in cytosolic Ca^{2+} induces platelet

activation, shape change and secretion via several key Ca^{2+} activated proteins. For example, the protein kinase C (PKC) isoform PKCα has been shown to be important in platelet secretion downstream of increases in Ca^{2+} concentration (Konopatskaya et al., 2009). PKCα regulates secretion via activation of protein kinase D 2 (PKD2) and mutation or loss of either PKCα or PKD2 in platelets leads to reduced secretion of dense granules, decreased aggregation and decreased thrombus formation (Konopatskaya et al., 2009, 2011). The GPVI signalling pathway is vitally important to initiate strong activatory signals to promote platelet aggregation through integrin activation, shape change and secretion of secondary mediators. This signalling cascade is reliant on Ca^{2+} signalling to produce platelet activation.

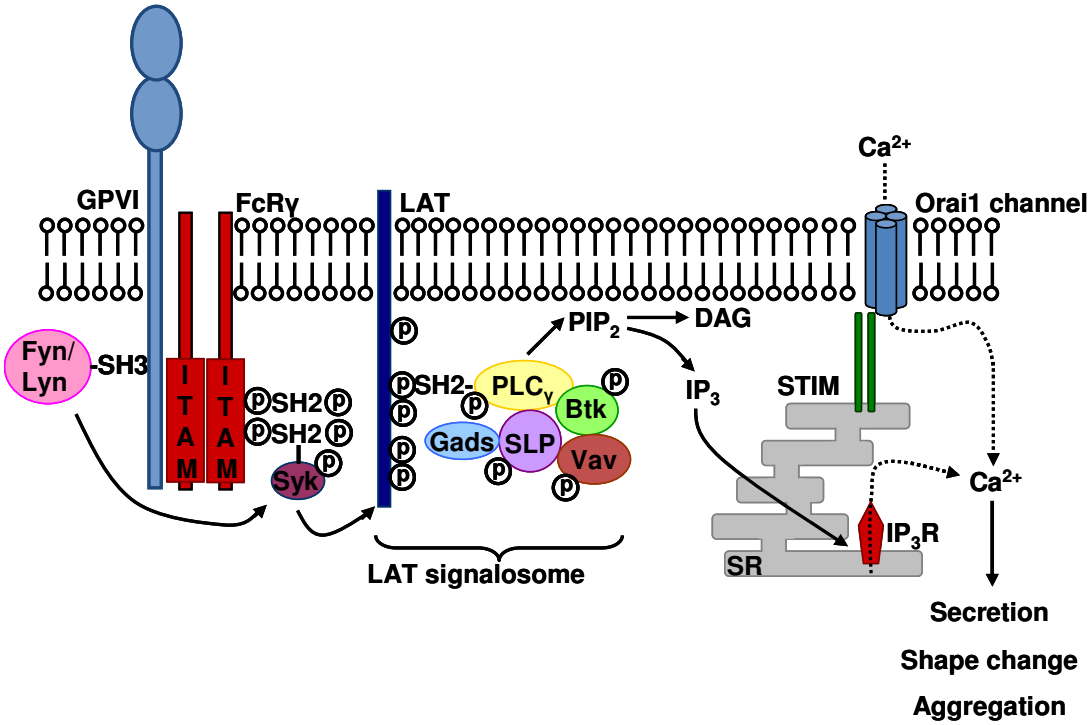

Figure 1.3 – The GPVI signalling pathway. Following GPVI activation by collagen, phosphorylation of the ITAM motif in the intracellular tails of the FcRγ chain via Fyn and Lyn occurs. This leads to recruitment of Syk and a downstream phosphorylation cascade which induces formation of the LAT signalosome and recruitment of PLCγ2 to the membrane. Active PLCγ2 induces production of IP_3, which stimulates flux of Ca^{2+} from the intracellular Ca^{2+} store into the cytosol via IP_3 receptors. Depletion of Ca^{2+} from the intracellular store induces flux from the extra cellular environment via Orai channels during store operated Ca^{2+} entry. Increased intracellular Ca^{2+} induces secretion of secondary mediators, alterations to the actin cytoskeleton to induce shape change, and aggregation.

1.2 STORE OPERATED Ca^{2+} ENTRY

The process of SOCE facilitates flux of Ca^{2+} into the cell following depletion of intracellular Ca^{2+} stores and as such is vitally important for sustaining high levels of intracellular Ca^{2+} during signalling events. The influx of Ca^{2+} from the extracellular environment also enables replenishment of the depleted intracellular Ca^{2+} stores, therefore enabling the cell to undergo future signalling events (Smyth et al., 2010). As Ca^{2+} acts as a signal transducer in many different signalling pathways across multiple cell types, regulation of the mechanism of Ca^{2+} entry is vital, to prevent unwanted signalling activation and to ensure enough Ca^{2+} is available to the cell when required.

1.2.1 Overview of Orai and STIM as key regulators of SOCE

Many different signalling pathways utilise Ca^{2+} as a secondary signalling mechanism to activate specific responses in the cell. Following stimulation of cell surface receptors, activation of PLC leads to hydrolysis of PIP_2, which releases IP_3 as a soluble messenger. IP_3 can then diffuse through the cytoplasm where it binds to the IP_3 receptor; a conformational change in the receptor occurs, which induces opening of the channel to allow flux of Ca^{2+} into the cytosol (Lewis, 2007; Smyth et al., 2010). In most cell types, IP_3 receptors are located on the membrane of the endoplasmic reticulum (ER), which acts as the intracellular Ca^{2+} store (Lewis, 2007; Smyth et al., 2010).

Following depletion of Ca^{2+} from the ER, subsequent influx of Ca^{2+} from the extracellular environment occurs via a pathway called the Ca^{2+} release activated Ca^{2+} (CRAC) current, which is reliant on two key proteins: the Ca^{2+}

sensory molecule stromal interaction molecule (STIM1 and 2) and the CRAC channel protein family (Orai1, 2 and 3) (Soboloff et al., 2006).

In a resting state, STIM proteins are found within the membrane of the ER where they bind Ca^{2+} via the EF hand motif, which holds the protein in a folded conformation (for more detail on STIM structure, refer to section 1.2.2). Dissociation of Ca^{2+} from STIM, driven by store depletion, induces a conformational change and oligomerization of STIM. STIM proteins then translocate to areas of the ER which are adjacent to the plasma membrane and form puncta, which are able to interact with Orai within the plasma membrane (Soboloff, Rothberg, Madesh, & Gill, 2012). Interaction of STIM with Orai proteins induces clustering and enables formation of functional pore-forming channels. The formation of functional Orai channels is believed to require either 4 or 6 subunits, though the exact structure is still debated (discussed in more detail in section 1.2.3). Following formation of the functional channel, Ca^{2+} is able to flux into the cell (Soboloff et al., 2006, 2012). Orai channels are highly selective for Ca^{2+} ions, utilising a selectivity filter mechanism which requires important residues both within the pore and outside of the pore on the extracellular side of the channel (Hou, Pedi, Diver, & Long, 2012).

Orai channels are not the only Ca^{2+} channels found on the cell surface, and channels of the transient receptor potential cation channel (TRPC) family have also been considered as potential CRAC channels (Smyth et al., 2010). TRPC channels can associate with STIM proteins and they are sometimes activated downstream of PLC stimulation and depletion of intracellular stores. However, channels formed by TRPC proteins are less selective for Ca^{2+} than

those formed by Orai1 (Smyth et al., 2010). The consequence of interaction between TRPC with STIM and Orai proteins and the level of coordination between them is not fully understood. However, it is widely accepted that when TRPC channels are activated downstream of store depletion, the non-selective channels which are formed are distinct from CRAC channels (Smyth et al., 2010). The widely accepted mechanism of SOCE is depicted in figure 1.4 and includes Orai proteins as the primary channel forming unit.

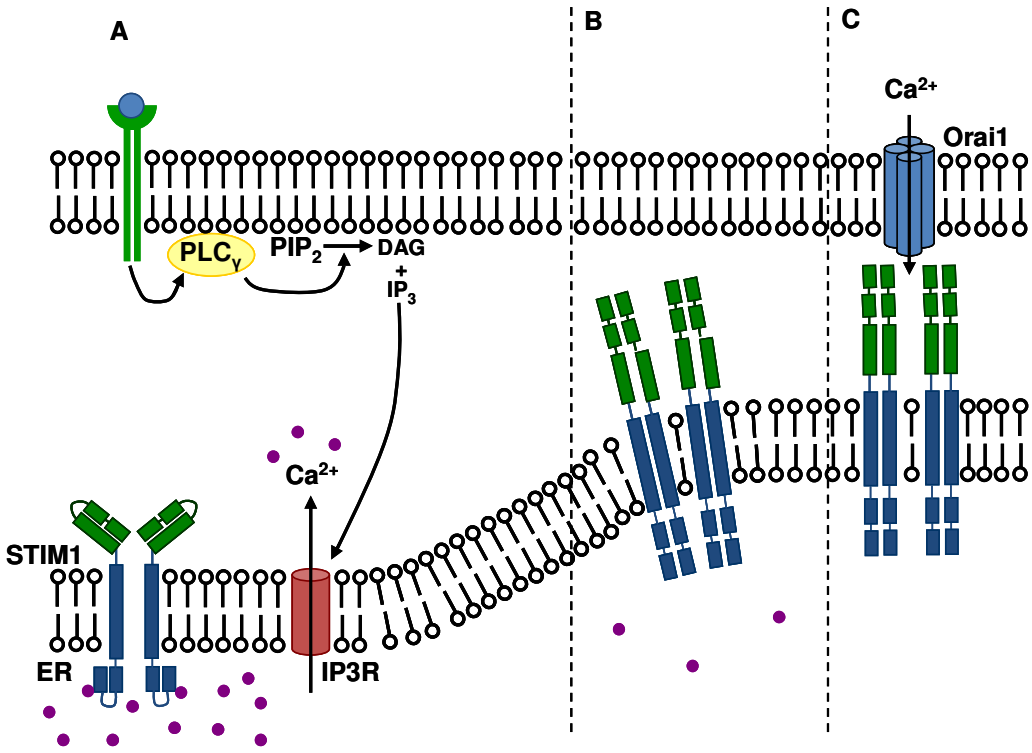

Figure 1.4 – The role of STIM and Orai in SOCE. When Ca^{2+} within the ER lumen binds STIM, the protein is held in an inactive conformation. Activation of IP_3 receptors downstream of cell surface receptor signalling enables flux of Ca^{2+} out of the ER and into the cytosol (A). Ca^{2+} becomes depleted and dissociates from STIM, inducing a conformational change, oligomerization and relocation to areas of the ER close to the plasma membrane (B). STIM form puncta close to the plasma membrane and interact with Orai proteins, to induce clustering and activation of the channels, to allow flux of extracellular Ca^{2+} into the cell (C).

1.2.2 Different isoforms of STIM and Orai

The STIM family consists of STIM1 and STIM2 and although these two isoforms are both widely expressed, STIM1 is localised within the ER membrane and the plasma membrane, whereas STIM2 is found only in the ER (Smyth et al., 2010). STIM1 and STIM2 share approximately 65% sequence homology and have similar domain structure (Stathopulos, Zheng, & Ikura, 2009). However, oligomerization and activation of STIM2 occurs more slowly than STIM1 (Stathopulos, Zheng, Li, Plevin, & Ikura, 2008) which is thought to be due to differences in the kinetics of the Ca^{2+} binding domain at the N-terminus of STIM (see section 1.2.3 for more detail on STIM structural domains) (Stathopulos et al., 2009). Additionally, differences in the C-terminal domain of STIM1 and STIM2, which are involved in binding Orai1, demonstrate the isolated mechanisms of these two isoforms. The phenylalanine residue at position 394 within the C-terminal domain of STIM1 has been shown to be important for interaction with and activation of Orai1, as mutation of this residue to a histidine leads to ineffective association and gating of Orai1 (X. Wang et al., 2014). The equivalent residue within the C-terminal of STIM2, leucine 394, generates partial interaction and activation of Orai1, but not to the full capacity observed for STIM1 (X. Wang et al., 2014). Interestingly, a role for STIM2 in replenishing intracellular stores following low levels of store depletion has been suggested (Thiel, Lis, & Penner, 2013). Whereas STIM1 was activated in response to strong signals (complete store depletion), STIM2 was activated in response to weaker stimuli, which suggests a potential mode of regulation of SOCE, depending on the level of store depletion (Thiel et al., 2013). Overall, it seems likely that STIM1 is the

main regulator of SOCE in the cell, whereas STIM2 has a role in regulating basal cytosolic and intracellular store Ca^{2+} levels. (Baba, Matsumoto, & Kurosaki, 2014; Smyth et al., 2010).

Within the Orai family of transmembrane proteins, there are 3 different isoforms; Orai1, Orai2 and Orai3. All three proteins have similar sequence, including conserved residues such as glutamate at position 106, which is important for ion selectivity. All three are also able to reconstitute functional channels which are stimulated by store depletion and which are highly selective for Ca^{2+} ions (Gwack et al., 2007). However, Orai1 is often the more highly expressed of the three and has been the most widely studied (Hoth & Niemeyer, 2013). It is not yet clear whether Orai proteins are able to heteromultimerise in order to form functional channels, though Orai1 has been immunoprecipitated with Orai2 and Orai3, suggesting an interaction, and in some cases, loss of Orai1 results in compensation by Orai2 and Orai3 (Gwack et al., 2007). However, the extent of cooperation between the different isoforms is most probably cell-specific, as Orai2 and Orai3 do not always reconstitute channel function in the absence of Orai1. It is therefore difficult to assess the exact roles of the different isoforms in general terms (Hoth & Niemeyer, 2013). Some studies have suggested that Orai3 displays structural differences to Orai1, particularly within the intracellular termini domains, though the functional effects of these differences and the physiological implications have not yet been elucidated (Shuttleworth, 2012).

1.2.3 The molecular mechanism of STIM1 activation

STIM1 is a single transmembrane protein, with the N-terminal (STIM1-N) located within the lumen of the ER acting as a Ca^{2+} sensor, and the C-terminal (STIM1-C) located in the cytosol, acting to interact with and stimulate Orai channel proteins (X. Yang, Jin, Cai, Li, & Shen, 2012). STIM1-N contains tandem EF-hand motifs which bind Ca^{2+} in the ER lumen alongside a sterile α motif (SAM) (Stathopulos et al., 2009, 2008). STIM1-C contains the STIM1 Orai1 activating region (SOAR), which has been recognised as essential for oligomerization and activation of Orai1. SOAR is comprised of two coiled-coil domains, which have been shown to form a STIM1-C homodimer which is held in a v-shaped folded conformation by an inhibitory helix within the CC1 domain, as shown in figure 1.5 (X. Yang et al., 2012).

Upon Ca^{2+} depletion in the ER lumen, dissociation of Ca^{2+} from the EF hand motif exposes hydrophobic regions within the EF-SAM domain, driving dimerisation of STIM1-N, which drives the conformational changes required to induce 'unfolding' of STIM1-C and allow interaction with Orai1, as shown in figure 1.5 (Stathopulos et al., 2009, 2008). It is believed that this occurs through dimerisation of the inhibitory helices, which releases the SOAR dimer into an unfolded conformation, which is able to span the distance between the ER membrane and the plasma membrane (Zhou et al., 2013). Oligomerization of STIM1 occurs and interaction with Orai1 induces channel formation and Ca^{2+} influx. Recently, a positively charged region at the tip of the SOAR domain was identified to be vitally important for interaction with and activation of Orai1 (X. Wang et al., 2014; X. Yang et al., 2012).

1.2.4 The molecular mechanism of Orai1 activation

The basic structure of Orai1 is relatively well defined, though the mechanisms and 3D structure required for clustering and in functional pore formation are highly debated. Orai1 has 4 transmembrane domains (TM1-4) with intracellular termini, 2 extracellular regions, and a glycosylation site within the second extracellular region at Asparagine 223 (Smyth et al., 2010; Srikanth & Gwack, 2012). The N and C terminals are regarded as important sites for associating proteins to interact with Orai1, including interaction of STIM1 (Srikanth & Gwack, 2012). The coiled-coil domain within the C terminus of STIM1 is particularly important for re-arrangement and co-localisation of Orai1 subunits with STIM1. It is widely accepted that TM1 of each Orai1 subunit lines the pore of the channel and mutation of arginine 91 within TM1 leads to non-functional channels and severe combined immunodeficiency (SCID) in humans due to the detrimental effects of reduced Ca^{2+} signalling on cells of the immune system (Feske et al., 2006). The mutation which occurs (arginine 91 to tryptophan 91) increases the hydrophobicity between the TM1 and N-terminal regions, thus causing loss of pore function, without disrupting interaction with STIM1 (Feske et al., 2006; Smyth et al., 2010). Several residues are important in ion selectivity of the channel including glutamate 106, which is found on the extracellular side of the protein and is conserved across the family, and which if mutated to aspartate induces a reduction in channel selectivity (Smyth et al., 2010). An additional 3 residues found within the extracellular region between TM1 and TM2 are also involved in forming the selectivity filter for the channel, though they are not conserved across the family (Smyth et al., 2010).

The dynamics of multimer formation and the state of resting Orai1 subunits within the membrane is widely debated. For example, some groups have demonstrated that functional Orai1 channels are formed from tetramers, as outlined in figure 1.5, and that these tetramers may be formed through dimerisation of resting Orai1 dimers (Penna et al., 2008). However, there is not a consensus of opinion on the resting state of Orai1 subunits, as some groups argue that the multimeric channel could be pre-formed as homotetramer in the membrane ready for activation (Madl et al., 2010).

Similarly, there is also debate over the exact composition of the functional Orai1 channels. Several different experimental techniques, including use of preassembled Orai1 multimers (Mignen, Thompson, & Shuttleworth, 2008), single-molecule photo-bleaching (Ji et al., 2008) and high resolution microscopy (Maruyama et al., 2009), have demonstrated that functional channels exist as tetramers, as depicted in figure 1.5. However more recently, another group using crystallography demonstrated that functional Orai1 channels exist as hexamers (Hou et al., 2012). In this study, a detailed 3D analysis of a functional channel formed from drosophila Orai1, which has 73% sequence identity to human within the TM domains, was completed. The six TM1 helices formed the lining of the pore and TM2 and TM3 helices were packed in closely around this inner ring. TM4 helices were excluded to an outer ring and the TM4 cytoplasmic extensions of neighbouring subunits were packed together in pairs via an antiparallel coiled-coil helix arrangement. This was held in place through interaction of hydrophobic residues, isoleucine 316 and leucine 319, within these regions, believed to provide stability to the whole structure (Hou et al., 2012). However, recent functional analysis of the

hexamer structure has raised questions to its true functional relevance (Thompson & Shuttleworth, 2013). These functional studies highlighted that the hexamer channels were not selective for Ca^{2+} ions, as they were permeable to both Na^{+} and Cs^{+} monovalent ions (Thompson & Shuttleworth, 2013), which is in sharp contrast to the highly Ca^{2+}-selective nature of Orai channels normally. The hexamer structure which had been proposed was confirmed using cross-linking and size exclusion chromatography (Hou et al., 2012), but further analysis is required to convince the field that this isn't simply a non-selective channel which fails to mimic the true fingerprint of a normal CRAC channel. In summary, although the transmembrane helices arrangement and interaction of STIM1 via the TM4 C-terminal extensions is widely accepted, the number of Orai subunits required and the resting state of the channel is widely disputed.

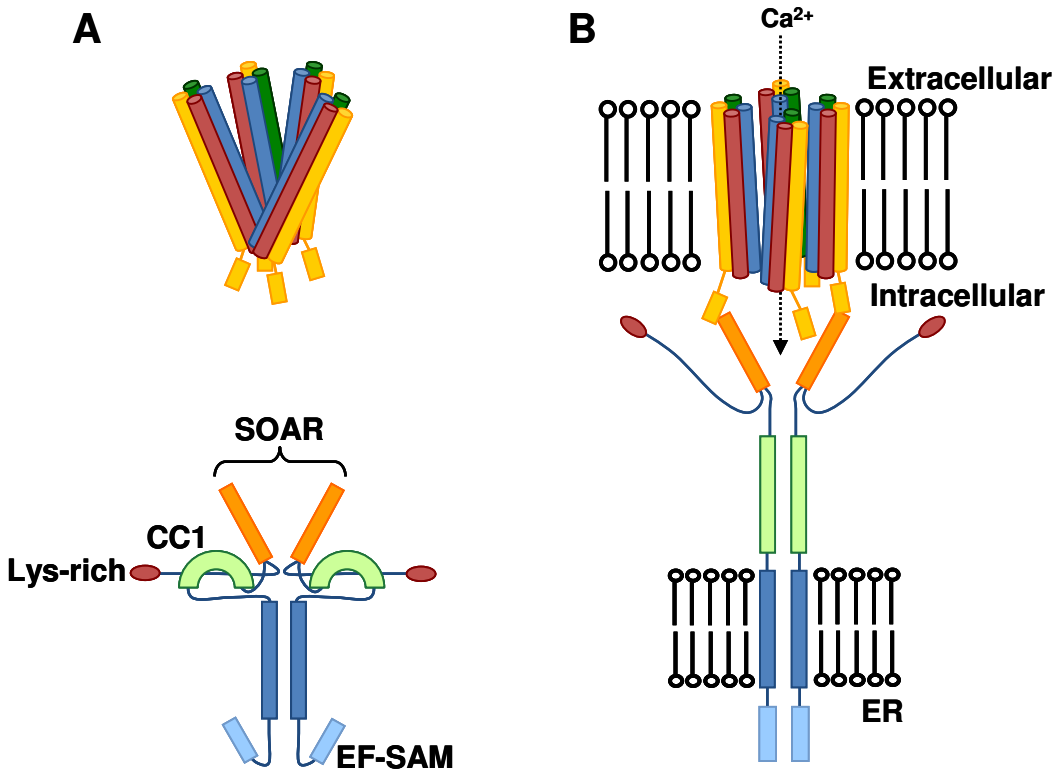

Figure 1.5 – The conformational changes required for STIM1 activation and Orai1 channel formation. As shown by the upper panel, Orai1 channels are formed through multimerisation of Orai1 units in either tetramer or hexamer complexes. The TM1 (blue) of each subunit lines the pore of the channel and TM4 (yellow) creates the outer ring of the structure. TM4 extensions (yellow) extend into the cytoplasm. As shown by the lower panel, STIM1 is held in an inactive, folded conformation when Ca^{2+} is bound to the EF-hand motif in the ER lumen, this conformation is stabilised by the inhibitory CC1 domain (A). When activated through dissociation of Ca^{2+} STIM1 dimerises via the EF-SAM domain and STIM1 extends towards the plasma membrane and oligomerises. The interaction between STIM1 SOAR and the TM4 extensions and TM1 membrane-proximal regions of Orai1 promotes Orai1 multimerisation and opening of the channel to allow flux of Ca^{2+} into the cell. Lysine rich regions in the C-terminal of STIM1 interact close to the plasma membrane (B).

1.2.5 SOCE is vital for GPVI signalling

As discussed throughout section 1.1, thrombus formation is heavily reliant on Ca^{2+} signalling, as increases in cytosolic Ca^{2+} in platelets leads to downstream secretion, shape change and aggregation. Typically, the concentration of Ca^{2+} found in a resting platelet, as with many non-excitable cells, is within the region of 100 nM, however this can increase by 10-100 fold

during platelet activation (Rink & Sage, 1990). This large increase in intracellular Ca^{2+} concentration provides the driving force behind many of the platelet activatory responses which lead to aggregation, and is made possible through the process of SOCE. Once SOCE channels at the membrane are activated, the influx of Ca^{2+} into the platelet is driven by the large concentration gradient of Ca^{2+} in the blood in comparison to intracellular levels. Typically, circulating free Ca^{2+} concentrations are within the range of 1.0 – 1.3 mM and total blood Ca^{2+} concentration, including bound Ca^{2+} which forms a complex with serum proteins such as albumin, is normally within the range of 2.2 – 2.6 mM. This large difference in extracellular and intracellular Ca^{2+} concentration allows for rapid influx of Ca^{2+} into the platelet via open SOCE channels, and therefore rapid signal transduction and platelet activation.

Influx of Ca^{2+} from the extracellular environment specifically via SOCE is vital in platelets, as demonstrated by the finding that both STIM1 and Orai1 are important for normal platelet activation and thrombus formation (Bergmeier et al., 2009; Braun et al., 2009; David Varga-Szabo, Braun, et al., 2008). Interestingly, it seems that SOCE is especially important in facilitating signalling downstream of GPVI, more so than downstream of other platelet activatory pathways.

In platelets, Ca^{2+} is stored within the dense tubular system, or sarcoplasmic reticulum (SR), as well as within lysosome-related organelles (D Varga-Szabo, Braun, & Nieswandt, 2009). Although the precise mechanism of store release in platelets is not clear, STIM1 has been identified on platelets (Grosse et al., 2007; David Varga-Szabo, Braun, et al., 2008) and both STIM1

and STIM2 have been shown to be localised to the acidic lysosome-related organelles (Zbidi et al., 2011). STIM1 has been recognised as the primary Ca^{2+} sensor, as platelets deficient in STIM2 did not display marked differences in Ca^{2+} mobilisation, platelet activation or thrombus formation (Gilio et al., 2010). In contrast, platelets deficient in STIM1 had reduced release of Ca^{2+} from the intracellular stores after stimulation with thapsigargin, which indicates a reduced Ca^{2+} store content, and also showed reduced influx of Ca^{2+} via SOCE (David Varga-Szabo, Braun, et al., 2008). Ca^{2+} entry in response to a range of platelet agonists was also reduced, though aggregation of the platelets was only impaired downstream of GPVI activation. The defects observed within GPVI-ITAM reliant processes, and normal activation of the platelets through G-protein coupled pathways, suggest that STIM1 and SOCE are vitally important downstream of GPVI, but might not be vital in activation of platelets through other signalling pathways (David Varga-Szabo, Braun, et al., 2008). During *in vivo* analysis, mice with STIM1 deficient platelets displayed reduced thrombus formation in two different models and were also protected from cerebral ischemia in a model of stroke (David Varga-Szabo, Braun, et al., 2008)

Orai1 is also expressed in human and mouse platelets, and Orai1 is more highly expressed than either Orai2 or Orai3 (Braun et al., 2009). To date there have been two different mouse models used to study the role of Orai1 in platelets; knock out mice lacking expression of Orai1 ($Orai1^{-/-}$) (Braun et al., 2009) and knock in mice expressing a loss of function mutant of Orai1 ($Orai1^{R93W}$) (Bergmeier et al., 2009). Similarly to STIM1 depletion, loss of Orai1 in $Orai1^{-/-}$ mice resulted in reduced SOCE, and reduced Ca^{2+}

mobilisation across a range of platelet agonists, though release of Ca^{2+} from the intracellular stores appeared normal (Braun et al., 2009). Despite defective Ca^{2+} mobilisation across a range of agonists, Orai1 deficient platelets displayed reduced aggregation only downstream of GPVI activation (Braun et al., 2009), again suggesting that SOCE is important for platelet activation downstream of ITAM-induced signalling but not G-protein coupled signalling. During *in vivo* analysis, mice with Orai1 deficient platelets were protected form arterial thrombus formation, similarly to mice with STIM1 deficient platelets (Braun et al., 2009). These findings demonstrating loss of Ca^{2+} mobilisation and aggregation defects suggests that Orai1 is the primary SOCE channel in platelets, as Orai2 and Orai3 were not able to compensate for the loss of Orai1. Additionally, the potential role for the Ca^{2+} channel TRPC1 in platelet SOCE has been dismissed, as mice deficient in TRPC1 show no defect in SOCE, platelet activation or in vivo thrombus formation (David Varga-Szabo, Authi, et al., 2008). Some similarities were observed in assessment of the Orai1^{R93W} mice, as Ca^{2+} mobilisation following stimulation by multiple agonists was reduced and SOCE following stimulation with thapsigargin was also reduced (Bergmeier et al., 2009). In results similar to those seen with Orai1$^{-/-}$ mice, Orai1^{R93W} mice had normal release of Ca^{2+} from the intracellular stores, but reduced flux of Ca^{2+} from the extracellular environment (Bergmeier et al., 2009; Braun et al., 2009). However, Orai1^{R93W} mice displayed normal aggregation responses across a range of platelet agonists, and normal aggregate formation on collagen under flow (Bergmeier et al., 2009). The authors suggested that the release of Ca^{2+} from the intracellular stores would have been sufficient to allow aggregation to occur

normally, which is in conflict of the findings with the Orai1$^{-/-}$ mice, which displayed defective aggregation downstream of GPVI activation (Bergmeier et al., 2009; Braun et al., 2009). Despite the differences between these two models, platelets responses from the Orai1^{R93W} mice such as integrin activation, P-selectin exposure and phosphatidyl serine exposure were all impaired, which suggests that impairment of Orai1 in platelets and resulting reductions in intracellular Ca^{2+} concentrations does have an impact on normal platelet function (Bergmeier et al., 2009). The differences observed across the two models may be a result of the variation in experimental design, or could be due to the different methods of mouse model generation. Importantly, both studies agree that Orai1 is a major component of SOCE in platelets and that without Orai1, platelet Ca^{2+} signalling is greatly reduced.

The GPVI-specific defects observed in both STIM1 and Orai1 deficient platelets suggest that SOCE is important downstream of ITAM-induced signalling, but not G-protein induced signalling. Platelet aggregation was normal downstream of agonists such as thrombin and ADP, which activate G-protein coupled pathways, despite Ca^{2+} signalling being reduced in response to these agonists. This could suggest that these pathways rely not only on Ca^{2+} signals during platelet activation, but that another activatory signal could be sufficient for aggregation downstream of G-protein signalling in platelets. Alternatively, non-GPVI pathways may not require such a large increase in Ca^{2+} concentration in order to activate downstream platelet activation and therefore may rely on non-SOCE mechanisms, such as TRPC. TRPC1 and TRPC6 have been shown to have no role in SOCE in platelets, but instead it has been suggested they could be activated downstream of other pathways

such as DAG (Ramanathan et al., 2012). Other TRPC channels are known to be activated downstream of G-protein mechanisms (Lang, Münzer, Gawaz, & Borst, 2013). Therefore activation of STIM1 and Orai1 deficient platelets by non-GPVI agonists may be possible through utilisation of other Ca^{2+} entry mechanisms. This is an area which needs further clarification, as TRPC channels have been shown to form complexes with Orai and STIM proteins, therefore these processes are likely to be linked (Jardin, Gómez, Salido, & Rosado, 2009; Jardin, Lopez, Salido, & Rosado, 2008; Lang et al., 2013).

1.3 TETRASPANINS

Tetraspanins are a large family of small transmembrane proteins that are highly conserved throughout evolution and of which there are 33 members in human, displayed in figure 1.6. These proteins are expressed throughout the body and have been implicated in multiple biological processes through regulation of specific partner proteins. In addition to forming interactions with partner proteins, tetraspanins interact with each other to form tetraspanin enriched microdomains, which act as platforms for optimal signalling, adhesion and proteolysis (Stéphanie Charrin, Jouannet, Boucheix, & Rubinstein, 2014; Hemler, 2014).

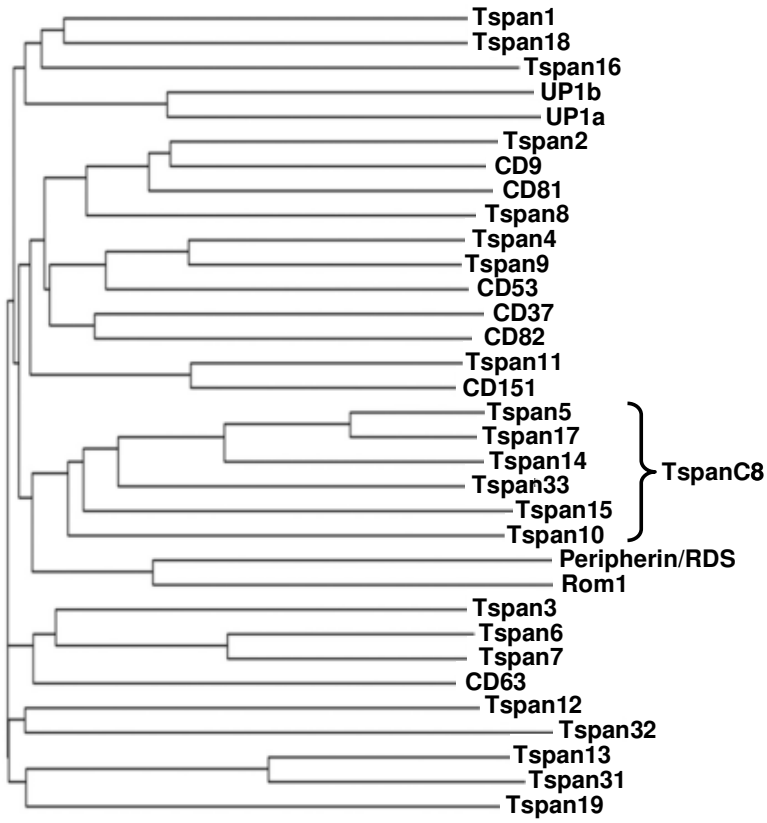

Figure 1.6 – The tetraspanin family of identified proteins. The sequence alignment tool, Cluster Omega, was used to compare the amino acid sequence alignment of the 33 human tetraspanins. The data is displayed in the form of a dendogram to show how closely the different members of the family are related. Adapted from Haining et al, 2011.

1.3.1 Tetraspanin structure

As their name suggests, tetraspanin proteins are characterised by four transmembrane domains, short intracellular tails and two extracellular loops of unequal size, as demonstrated by the diagram in figure 1.7. The most highly conserved area within the tetraspanin family is the cysteine-cysteine-glycine (CCG) motif within the large extracellular loop which, along with the 2-6 other cysteine residues within this region, form disulphide bonds which maintain the structure of the large extracellular loop (Kitadokoro et al., 2001). Tetraspanins also undergo post-translational modifications including palmitoylation at cysteine residues within the intracellular loop and cytoplasmic tails at membrane proximal regions, N-linked glycosylation within the large extracellular loop (up to 3 predicted sites), and ubiquitination of the cytoplasmic tails (Stéphanie Charrin et al., 2009).

Determining the exact 3D structure of tetraspanins has proven to be a difficult task and no full atomic resolution structure of a whole tetraspanin exists, though a few key studies have attempted to elucidate the structure of these proteins. The cryo-electron microscopy structure of the tetraspanin uroplakins (UP) UPIa and UPIb complex has been revealed, which showed that these proteins form a compact, rod-like structure which protrudes approximately 3.5-5 nm above the plasma membrane (Min, Wang, Sun, & Kong, 2006). The rod-like structure was believed to be driven by the tightly bound bundle formed by the transmembrane helices. Additionally, the extracellular region of the protein formed a ‘mushroom-like’ structure (Min et al., 2006). Using crystallography, the structure of the large extracellular region of CD81 has also been resolved (Kitadokoro et al., 2001), and following this, computational

modelling methods were used to predict the rest of the structure (Michel Seigneuret, 2006). Additionally, structural studies of the importance of the large extracellular region of CD81 in ligand interactions has provided further information on the functional basis of tetraspanin structure (Rajesh et al., 2012). These studies have outlined a tightly packed transmembrane region made of left-handed coiled coil helices. The small extracellular loop emerges from transmembrane 1, into transmembrane 2 and is comprised of a β-strand which contains a hydrophobic region (figure 1.7). The large extracellular loop connects transmembrane regions 3 and 4 and contains 5 α-helices, which form a 'mushroom-like' structure (figure 1.7). The large extracellular loop is divided into 2 regions; helices A, B and E make up the membrane proximal region, which associates closely with the hydrophobic region of the small extracellular loop via a hydrophobic groove, which holds the two extracellular regions closely together. The two smaller helices, C and D, make up the variable region of the large extracellular loop, alongside the conserved CCG motif. The disulphide bonds formed between the CCG motif and the 2 additional cysteine residues in this region holds the variable domain in the correct conformation, which is held on the opposite side of the protein to the small extracellular loop (figure 1.7). Although CD81 and UPIa/UPIb share only 12-13% sequence identity, these studies suggest a very similar structure, which suggests these defining features could be ubiquitous across the tetraspanin family.

Despite these characteristics which are shared across the tetraspanin family, the variable region within the large extracellular loop of tetraspanin proteins is known to differ greatly. The variable region of the large extracellular loop,

containing helices C and D, has been shown through sequence alignment and subsequent structure prediction to be highly variable in both size and the number of cysteine residues present (M Seigneuret, Delaguillaumie, Lagaudrière-Gesbert, & Conjeaud, 2001). This suggests that the variable region will differ in 3D structure across the tetraspanin family. This is potentially due to a role for this region in regulating tetraspanin-partner protein interactions (María Yáñez-Mó, Barreiro, Gordon-Alonso, Sala-Valdés, & Sánchez-Madrid, 2009); the different structures potentially offer specificity to each separate tetraspanin. This is discussed in more detail in section 1.3.2.

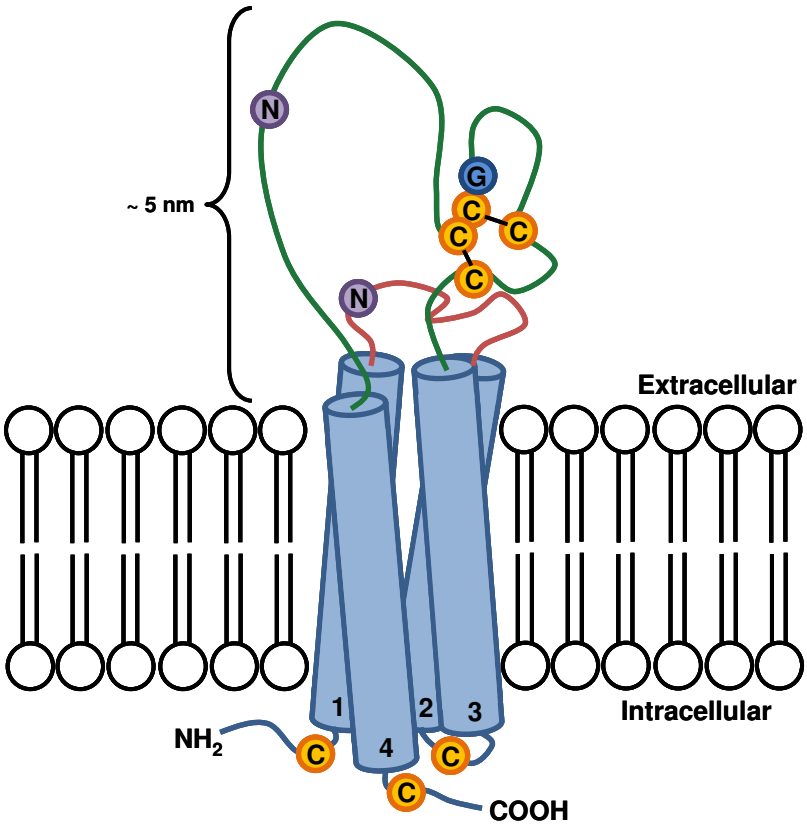

Figure 1.7 – The conserved structure of tetraspanin proteins. Proteins from across the tetraspanin family are characterised by several conserved structural features. They have four transmembrane regions, labelled 1-4, which are tightly packed to form a rod-like structure. They also have intracellular tails, marked in blue, which contain cysteine residues, marked in yellow, which are often sites for palmitoylation close to the plasma membrane. They also have a small extracellular loop which links TM1 and TM2, marked in red, and a large extracellular loop, marked in green, which contains the variable region believed to be important in partner protein binding. The extracellular loops often contain sites for N-linked glycosylation, as marked in purple. Additionally, all tetraspanins contain a conserved CCG motif within the large extracellular loop which, along with other conserved residues, forms between 2 and four disulphide bonds, which help to stabilise the structure.

1.3.2 Tetraspanin interactions

Investigation into tetraspanin function revealed a role for these proteins in organisation of membrane proteins into tetraspanin enriched microdomains, thus promoting compartmentalisation of the membrane (Stéphanie Charrin, Manié, Billard, et al., 2003; Hemler, 2005; Rubinstein, 2011). Formation of

these domains is a complex process, but is believed to occur via two distinct levels of interaction.

The primary tetraspanin interaction occurs between the tetraspanin and its specific partner protein. This is a relatively strong interaction which can withstand stringent detergent conditions, such as Triton X-100 (Yauch, Berditchevski, Harler, Reichner, & Hemler, 1998) and digitonin (Serru et al., 1999). Studies utilising chimeric proteins have helped to highlight which tetraspanin domains are important in tetraspanin-partner protein interaction, specifically highlighting the role of the variable region within the extracellular domain (see section 1.3.1 for more information on tetraspanin structure). For example, the high affinity interaction of the tetraspanin CD81 with the E2 envelope protein of hepatitis C virus (HCV) requires the variable region (Drummer, Wilson, & Poumbourios, 2002; Higginbottom et al., 2000), and the variable region within the large extracellular loop of the tetraspanin CD9 is important for normal adhesive function of intercellular adhesion molecule 1 (ICAM-1) and vascular cell adhesion molecule 1 (VCAM-1) on endothelial cells during leukocyte extravasation (Barreiro, Ovalle, Higginbottom, & Monk, 2005). Additionally, transmembrane regions have been implicated as important for some tetraspanin-partner protein interactions. The interaction between the tetraspanin uroplakins and their partners relies on transmembrane region 3 (Min et al., 2006) and the interaction between the tetraspanin CD81 and immunoglobulin super family member 8 (EWI-2) is reliant on transmembrane regions 3 and 4 (Montpellier et al., 2011).

The secondary level of interaction involves clustering of primary tetraspanin-partner protein complexes together via tetraspanin-tetraspanin interaction.

These small complexes are thought to be supported by interactions with lipids within the plasma membrane. Palmitoylation of the intracellular regions of tetraspanins enables interaction with the lipid bilayer and reinforces tetraspanin-tetraspanin interactions (Stéphanie Charrin et al., 2002; Stéphanie Charrin, Manié, Thiele, et al., 2003). The hypothesis that tetraspanins associate with lipids in the membrane is supported by the ability to precipitate tetraspanins with cholesterol in biochemical assays (Serru et al., 1999) and by the disruption of tetraspanin-tetraspanin interactions in palmitoylation mutants. Subsequent formation of large tetraspanin enriched microdomains from these small clusters is thought to be a highly dynamic process, which potentially occurs as a result of stimuli to induce formation of specialist structures within the membrane (Stéphanie Charrin et al., 2009). These tetraspanin enriched microdomains have been shown to be highly dynamic in terms of tetraspanin movement into and out of the microdomain (Barreiro et al., 2008; Espenel et al., 2008). Additionally, these microdomains are separate from lipid rafts in the membrane (Hemler, 2003).

Together, this builds an image of tetraspanins as membrane organisers, which can interact directly with partner proteins and other tetraspanins. These dynamic interactions can drive formation of tetraspanin enriched microdomains, and thus regulate partner protein function.

1.3.3 Tetraspanin function

Tetraspanins have been identified across a range of different cell types and have been implicated in a wide variety of cellular processes. Further

investigation into these proteins has revealed use of specific mechanisms in order to regulate partner protein function and thus have an impact on trafficking, signalling, adhesion and proteolysis within the cell.

In some cases, tetraspanins have an important role in maturation and trafficking of partner proteins to the cell surface. For example, the tetraspanin CD81 is required for cell surface expression of its partner, the B-lymphocyte antigen cluster of differentiation 19 (CD19). in CD81 knockout mice, expression of CD19 on the surface of B cells was 50% reduced (Shoham et al., 2003) and in human patients lacking CD81 there was complete loss of cell surface CD19 (Zelm et al., 2010). In both cases, this was due to impaired trafficking of CD19 from the ER to the golgi. CD19 is an important co-receptor in B-cell receptor signalling and in enhancing B cell activation, therefore lack of CD81, which disrupts surface expression of CD19, leads to reduced B cell antibody responses in both mouse and human (Shoham et al., 2003; Zelm et al., 2010).

Tetraspanins can also regulate particular signalling processes through regulation of their partner proteins. One example of this is the tetraspanin Tspan12, which has been shown to interact with and regulate the Wnt receptor Frizzled 4 (Junge et al., 2009). Following activation, Frizzled 4 recruits co-receptors such as Lrp5 and downstream signalling activates the TCF/LEF family of transcription factors. This process is particularly important in development of the retinal vasculature and mutations in Frizzled 4 or Lrp5 cause familial exudative vitreoretinopathy (FEVR), in which under development of the retinal vasculature causes blindness (Ye, Wang, & Nathans, 2010). Tspan12 does not directly activate or promote signalling of

Frizzled 4, but instead is thought to be responsible for promoting clustering of the receptor required for downstream signalling (Junge et al., 2009). The importance of this interaction was highlighted when mutations in human Tspan12 were also found to cause FEVR and blindness (Nikopoulos et al., 2010; Poulter et al., 2012).

Another important function of some tetraspanins is to regulate adhesion, which is an important process for many cellular events. An example of this is the role that the tetraspanins CD9 and CD151 play during leukocyte adhesion to endothelial cells and therefore subsequent extravasation from the blood flow at sites of inflammation. The endothelial adhesion molecules ICAM-1 and VCAM-1 are important for interaction with leukocyte integrins to reinforce firm adhesion of the leukocyte and to allow extravasation (Nourshargh, Hordijk, & Sixt, 2010). It has been shown that ICAM-1 and VCAM-1 are co-localised with CD9 and CD151 (Barreiro et al., 2005), and that the tetraspanins act to promote formation of nano-platforms on the endothelial cell surface which are enriched in ICAM-1 and VCAM-1 and therefore allow more efficient leukocyte adhesion (Barreiro et al., 2008). Knockdown of either tetraspanin resulted in decrease surface expression of the adhesion molecules, reduce leukocyte adhesion and reduced leukocyte transmigration (Barreiro et al., 2005). Additionally, the tetraspanin CD63 also has a role in facilitating leukocyte extravasation through regulation of P-selectin (Doyle et al., 2011). Both CD63 and P-selectin are localised to intracellular organelles such as lysosomes and Weibel-Palade bodies and upon activation of the endothelium, is rapidly trafficked to the cell surface, when it interacts with P-selectin glycoprotein ligand 1 (PSGL-1) on leukocytes and thus promotes

leukocyte recruitment (M Yáñez-Mó et al., 1998). In the absence of CD63, P-selectin expression at the cell surface was reduced, which caused a reduction in leukocyte recruitment and delayed extravasation, mimicking the phenotypes observed in P-selectin knockout mice (Doyle et al., 2011). Together, these studies demonstrate the important roles for tetraspanins in regulation of leukocyte recruitment and extravasation during the inflammatory response. In addition to this, there have been multiple studies on the role of the tetraspanin CD151 in interaction with and regulation of the integrins α3β1, α6β1, and α6β4 (Sterk & Geuijen, 2002). CD151 directly interacts with these laminin binding integrins via association with the α subunit of the integrin (Hemler, 2014). Several modes of action have been documented for the mechanism by which CD151 regulates these partner proteins. For example, CD151 limits the diffusion of the α6 subunit in the membrane, thus making the integrins more available for functions such as adhesion (X. H. Yang et al., 2012). CD151 has also been shown to regulate the distribution and recycling of α3 and α6 subunits, which is important during cell migration (Winterwood, Varzavand, Meland, Ashman, & Stipp, 2006; X. H. Yang et al., 2008). The role that CD151 plays in regulation of these integrins has resulted in implication of CD151 in pathological angiogenesis and tumour cell growth, invasion and metastasis (Bailey et al., 2011; H.-X. Wang, Li, Sharma, Knoblich, & Hemler, 2011).

Finally, tetraspanin proteins have also been implicated in regulation of proteolysis through interaction with partner proteins such as the ectodomain sheddase a disintegrin and metalloprotease domain-containing protein 10 (ADAM10). ADAM10 has a wide range of cleavage targets including Notch,

which has roles in development, amyloid precursor protein, which is the pathogenic peptide which causes Alzheimer's disease and the endothelial junction molecule VE-cadherin amongst many others. A subfamily of six tetraspanins, termed the TspanC8s (highlighted in figure 1.6) were all shown to interact with ADAM10 (Dornier et al., 2012; Haining et al., 2012). In addition to these tetraspanins regulating the maturation and cell surface expression of ADAM10, they were also shown to promote its proteolytic activity (Prox et al., 2012). The authors predict that different tetraspanins within this subfamily may regulate targeting of ADAM10 to specific substrates in the cell and thus regulate proteolytic cleavage events in the cell (Haining et al., 2012).

Tetraspanins are implicated in a wide variety of processes, though it can often be difficult to elucidate the exact mechanism for each specific tetraspanin as functional redundancy can occur across the family. However, as demonstrated by the examples above, several specific interactions with partner proteins have been identified and the exact mechanism of tetraspanin regulation elucidated. Knowledge of the precise mechanisms of tetraspanin function and the partner proteins they co-ordinate allows for a better understanding of the 'fine-tuning' involved in regulation of many different cellular events.

1.3.4 Platelet tetraspanins

Tetraspanins have been identified in platelets, though most of the platelet tetraspanins are understudied and their role in platelet activation poorly

understood. Study of megakaryocyte mRNA has suggested that there could be as many as 18 tetraspanins in platelets (Macaulay et al., 2007; Protty et al., 2009), though only 10 have been identified using proteomics (Lewandrowski et al., 2009) and only five (CD9, CD63, CD151, Tspan9 and Tspan32) confirmed using specific antibodies (Haining, Yang, & Tomlinson, 2011; Protty et al., 2009).

Initial investigation into the role of the tetraspanins CD151 and Tspan32 on platelets identified defective thrombus formation in knockout mice for either tetraspanin (Goschnick et al., 2006; Lau et al., 2004; Orlowski et al., 2009). The CD151 knockouts displayed increased bleeding in vivo, and reduced platelet spreading and clot retraction during in vitro assays (Lau et al., 2004). Additionally, during in vivo models of thrombus formation through $FeCl_3$ induced, or laser induced injury, thrombi formed by the CD151 deficient mice were small and unstable (Orlowski et al., 2009). Assessment of the Tspan32 deficient mice produced very similar results; impaired spreading and clot retraction in vitro and reduced thrombus formation in vivo (Goschnick et al., 2006). In both cases, it was proposed that the phenotypes observed were due to defective signalling from the integrin αIIbβ3, though the exact mechanism by which these tetraspanins might control integrin function is not known. It is possible that CD151 and Tspan32 could promote the active conformation of the integrin and thus increase activity, or that they might be involved in recruitment of other signalling proteins to promote downstream signalling.

Conversely, characterisation of mice lacking either CD9 or CD63 yielded no major platelet phenotypes, though a mild increase in thrombus size in the

CD9 knockout mice suggested a potential negative regulatory role for this tetraspanin (Mangin, Kleitz, Boucheix, Gachet, & Lanza, 2009; Schröder et al., 2009). Such a subtle phenotype seemed surprising considering CD9 is the second most highly expressed protein on the cell surface (Protty et al., 2009), though similar observations have been made for this tetraspanin across other cell types in which it is expressed. An exception to this was observed on oocytes, where CD9 appears to play a vital role in fertilisation. CD9 deficiency leads to female infertility due to defective sperm-egg fusion, an event which is critical for fertilisation (Kaji et al., 2000; Le Naour, Rubinstein, Jasmin, Prenant, & Boucheix, 2000; Miyado et al., 2014).

Although the specific role of most other platelet tetraspanins is yet to be investigated, several platelet surface proteins have been identified as tetraspanin associated. The integrin α6β1, the scavenger receptor CD36, the choline transporter CD92 and the ectodomain sheddase ADAM10 have all been identified as tetraspanin associated proteins on various cell types and, through a proteomics approach, have been observed as components of tetraspanin microdomains specifically on platelets (Haining et al., 2011). Additionally, the platelet collagen receptor GPVI has been identified as being tetraspanin associated, though there is no evidence for tetraspanin interactions with other important platelet surface proteins such as GPIb, αIIbβ3, α2β1 or α5β1 in co-immunoprecipitation experiments (Protty et al., 2009). These tetraspanin associated proteins, depicted in figure 1.8, provide hints to currently uncharacterised roles for tetraspanins on platelets. For example, the ecto-domain sheddase ADAM10, which is known to interact with the TspanC8 subfamily of tetraspanins (discussed in section 1.3.3), is

important as a negative regulator of platelet activation, through cleavage of receptors such as GPVI and thus cessation of signalling. The mechanism behind regulation of this process may be better understood if the exact role of tetraspanins in ADAM10 activation on platelets was known.

The fine tuning of partner protein function by tetraspanins is important in many cell types, and it appears it is also important in platelet function. The emerging roles of tetraspanins on platelets provide greater insight into the mechanisms behind platelet activation. If the specific tetraspanin-partner protein interactions on platelets can be elucidated and the mechanisms of platelet activation better understood, then future development of more specific anti-platelet therapies is possible.

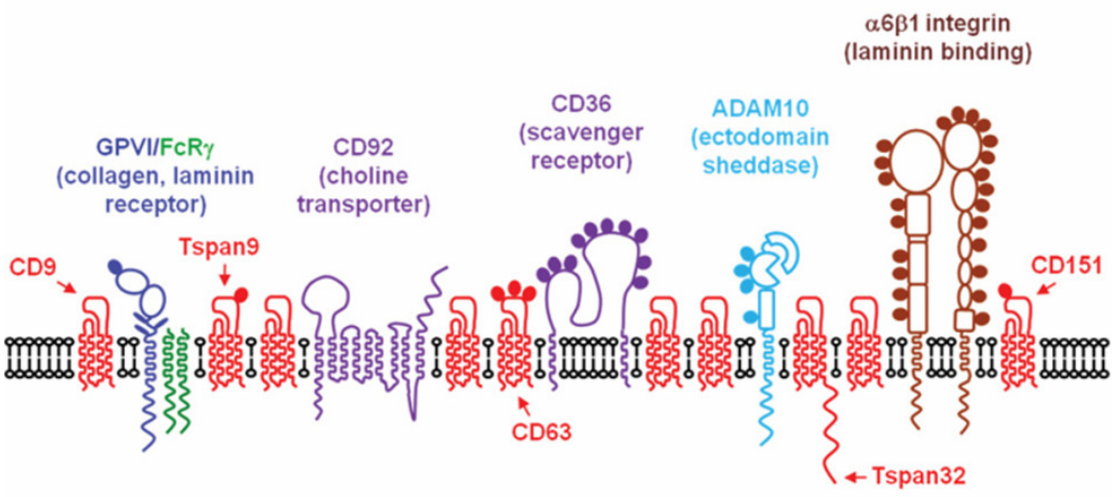

Figure 1.8 – Tetraspanin associated proteins in platelets. Tetraspanin proteins are represented in red; the five which have been identified on platelets using antibodies are labelled. The proteins shown in the microdomain have been identified as tetraspanin associated in other cell types as well as in a proteomics screen in platelets. Adapted from Haining et al, 2011.

1.3.5 Tspan18

The tetraspanin Tspan18 was initially identified as a novel tetraspanin in an mRNA screen of embryonic chick spinal cord and was initially termed 'neurospanin' (Perron & Bixby, 1999). Northern blot analysis was used to monitor fold changes in expression, and up-regulation of Tspan18 was observed during development of the brain, especially during the period of axon growth, suggesting a potential role for Tspan18 in early development of the nervous system (Perron & Bixby, 1999). Further to this initial study, Tspan18 has been implicated in the migration of chick neural crest cells; a process which is important during embryogenesis. Tspan18 was shown to regulate cadherin-6B levels; down regulation of Tspan18 via a FoxD3-dependant mechanism was required to allow down regulation of cadherin-6B expression and therefore crest cell migration (Fairchild & Gammill, 2013). Migration of neural crest cells is dependant on the process of epithelial-to-mesenchymal transition (EMT), which allows tightly packed epithelial cells to depolarise and become mesenchymal cells capable of migration. The novel role of Tspan18 in this process has implications not only in the mechanism of EMT, but also potentially in other migrating mechanisms such as cancer metastasis (Fairchild & Gammill, 2013).

In addition to the role for Tspan18 in the developing nervous system, this tetraspanin has been identified as a susceptibility locus for mutations causing schizophrenia within the Han Chinese ethnic group (J. Yuan et al., 2013; Yue et al., 2011). In a study using a genome-wide association approach, three single-nucleotide polymorphisms (SNPs) within the Tspan18 gene were identified to be linked with increased susceptibility for schizophrenia, though

the functional role for Tspan18 during pathogenesis of this disorder is not known (Yue et al., 2011). A more recent study confirmed this link with one of the SNPs identified, in an independent population (J. Yuan et al., 2013).

Aside from expression in the nervous system, Tspan18 has also been identified in cells of the vasculature, such as endothelial cells, platelets and CD4-positive T cells (Bailey et al., 2011; Colombo, 2010; Lewandrowski et al., 2009; Macaulay et al., 2007; Protty et al., 2009). The strong endothelial expression profile of Tspan18 was revealed during real time polymerase chain reaction (PCR) studies on human cells and mouse tissues. Tspan18 messenger ribonucleic acid (mRNA) was most highly expressed in human umbilical vein endothelial cells (HUVEC) and human microvascular endothelial cells (HMEC) in comparison to smooth muscle cells, fibroblasts, and in the cell lines PBL, DAMI, DG75, K562, HBP-AII, HEL, MDA-MB-231, RAJI, U937, HEK293T, or Jurkat cells (Colombo, 2010). In mouse tissue, Tspan18 mRNA was found to be highest in lung tissue in comparison to brain, heart, kidney, liver, muscle, spleen and thymus, which is consistent with a preferential expression in endothelial cells (Colombo, 2010). Additionally, analysis of transcriptomic data from serial analysis of gene expression experiments indicated that Tspan18 is most highly expressed in endothelial cell libraries (Bailey et al., 2011). Together, these data strongly suggest that Tspan18 is expressed in endothelial cells. Proteomics screens have also identified Tspan18 in human platelets (Lewandrowski et al., 2009), human and mouse megakaryocytes and CD4-positive T cells (Macaulay et al., 2007; Protty et al., 2009). Also, Tspan18 mRNA has been identified in human and mouse platelets (Haining et al., 2012; Rowley et al., 2011). Together, these

real time PCR and proteomics studies suggest that Tspan18 is expressed in both endothelial cells and platelets, though there are currently no publications which investigate the role of this tetraspanin within the vasculature.

Interestingly, when assessed alongside a panel of other tetraspanins, only expression of Tspan18 was able to induce activity of a Ca^{2+} responsive nuclear factor activated T-cells (NFAT) luciferase reporter; expression of the tetraspanins CD9, CD63, CD151, Tspan32 and Tspan9 had no significant effect on the reporter (Colombo, 2010). This work also demonstrated that Tspan18 induced NFAT activation independently of non-receptor tyrosine kinases of Src, Syk and Btk families, PLCγ, and IP_3 receptors; over-expression of Tspan18 still promoted NFAT activation in specific DT40 knockout cell lines for these proteins (Colombo, 2010). Additional functional studies demonstrated that the action of Tspan18 mimicked the action of the ionophore ionomycin, further implying a role for Tspan18 in regulation of Ca^{2+} mobilisation (Colombo, 2010).

Although no partner protein has yet been identified for Tspan18, these findings suggest that Tspan18 could be interacting with and regulating a Ca^{2+} channel, or other protein involved in Ca^{2+} entry. It is therefore possible that Tspan18 may have a role in regulation of Ca^{2+} signalling in cell types such as platelets, and thus a role in platelet signalling and activation.

A useful tool for investigating the role of Tspan18 further is the Tspan18 knockout mouse. The Tspan18 knockout mouse was obtained from the Mutant Mouse Regional Resource Centre and was originally generated by Genentech Inc. and Lexicon Pharmaceuticals Inc. They aimed to create an

extensive collection of knockouts, providing a resource to screen for new drug targets. In total, a mouse knockout library of 472 secreted and transmembrane proteins was produced, including Tspan18 (Tang et al., 2010). The Tspan18 gene has a total of 10 exons and the start codon is found in exon 4 (NCBI accession NM_183180.1). To knockout Tspan18, homologous recombination was used to target exons 4 and 5 in embryonic stem cells derived from strain 129/SvEvBrd (see figure 1.9 for targeting strategy). The resulting chimeras were crossed with C57BL/6J albino mice to generate mice which were heterozygous for Tspan18. These progeny were intercrossed to generate wildtype, heterozygous and homozygous mutant progeny. Disruption of Tspan18 was confirmed by Southern hybridisation analysis (Tang et al., 2010).

No notable phenotype was observed during a broad phenotypic screen completed by Genentech Inc. which included analysis of development, metabolism, and the immune and cardiovascular systems (Tang et al., 2010). No in-depth platelet function tests were completed. A minor increase in anxiety response in female knockout mice was observed in an open field test when compared to wildtype gender matched littermates (Tang et al., 2010).

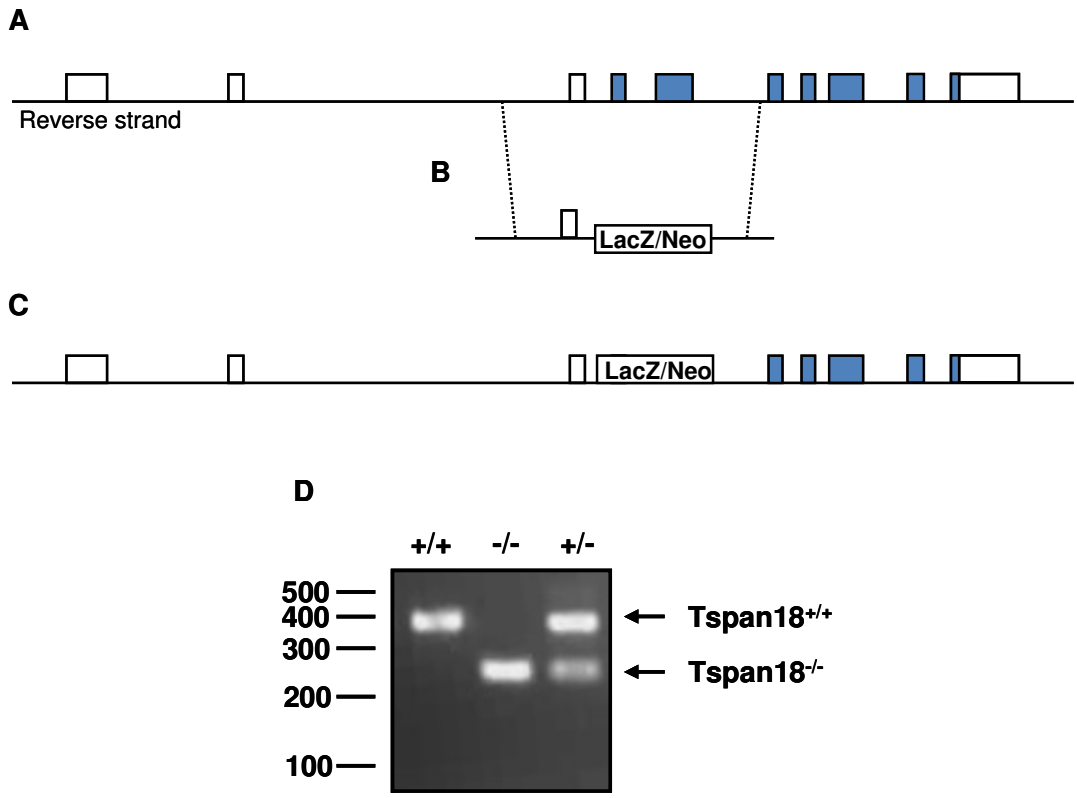

Figure 1.9 – Targeting strategy involved in generating the Tspan18 knockout mouse by homologous recombination. Blue filled boxes represent coding exons and empty boxes represent untranslated regions. The diagrams shown represent the wildtype Tspan18 gene structure (A), the target vector, pKOS-50 (B) and the resulting gene structure after homologous recombination (C) (Tang et al. 2010). Wildtype, mutant and heterozygous progeny were identified by PCR of tissue taken from ear clips, using primers outlined in chapter 2, section 2.8.2 (D).

1.4 PROJECT OBJECTIVES

The main aim of the work completed in this thesis was to characterise the function of the tetraspanin Tspan18 in platelets by using the Tspan18 knockout mouse and cell line models. The Tspan18 knockout mouse was available from the Mutant Mouse Regional Resource Centre, after being generated by Lexicon Pharmaceuticals and Genentech (Tang et al., 2010).

CHAPTER 2

MATERIALS AND METHODS

2.1 MICE, REAGENTS AND CELL CULTURE

2.1.1 Mice

Procedures using mice completed at the University of Birmingham, UK, were undertaken with the correct approval and licensing from the United Kingdom Home Office, under the project licence number 30/2721 and the personal licence number IE639FEE9. Tspan18 deficient mice were generated during collaboration between Genentech Inc. and Lexicon Pharmaceuticals Inc. (Tang et al., 2010). The mice were purchased from the Mutant Mouse Regional Resource Centre. The Tspan18 mouse colony was sustained by breeding heterozygous pairs which produced Tspan18 wildtype, heterozygous and mutant progeny. Therefore, wildtype littermates were used as controls alongside Tspan18 deficient mice in experiments. C57Bl/6 wild type mice were purchased as required from Harlan Laboratories, UK, or Charles River, UK.

2.1.2 Plasmids

The NFAT/activator protein 1 (AP-1) luciferase transcriptional reporter construct has been described previously (Shapiro, Mollenauer, Greene, & Weiss, 1996; Michael G Tomlinson et al., 2004). The pEF6 mock vector and pEF6-LacZ expression constructs were purchased from Invitrogen. All N-terminal FLAG-tagged tetraspanin expression constructs were made by cloning the tetraspanins into the pEF6-FLAG vector (Haining et al., 2012;

Protty et al., 2009). The Myc-tagged pCDNA3.1 Orai1, Orai2 and Orai3 expression constructs and the dominant negative FLAG-tagged MO70 Orai1 E106Q expression construct were purchased from Addgene (Gwack et al., 2007).

2.1.3 Antibodies

Listed in table 2.1 below are details of antibodies used across all experiments within this thesis, including the host species and the source.

Antibody	Host species	Source
Mouse α2 FITC	Rat	Emfret Analytics
Mouse αIIb FITC	Rat	Emfret Analytics
Mouse α6 FITC	Rat	Emfret Analytics
Mouse ADAM10 FITC	Rat	R&D Systems
Mouse CD9 FITC	Rat	Emfret Analytics
Mouse GPIb FITC	Rat	Emfret Analytics
Mouse GPVI FITC	Rat	Emfret Analytics
Mouse CLEC-2 FITC	Rat	Prof. Steve Watson
Rat IgG_{2a} FITC	Rat	AbD Serotec
Human/mouse tubulin (DM1A)	Mouse	Sigma
Phosphotyrosine (4G10)	Mouse	Millipore
Mouse IgG1 (MOPC)	Mouse	Sigma
Human CD9	Mouse	Prof Leonie Ashman
Human GPIb	Mouse	Prof Leonie Ashman
Human ADAM10	Mouse	R&D Systems
Rabbit IgG	Rabbit	Upstate Cell Signalling
Human/mouse Orai1-NT (4041)	Rabbit	ProSci
Human/mouse Orai1-CT (4281)	Rabbit	ProSci
FLAG	Rabbit	Sigma
FLAG (clone M2)	Mouse	Sigma
MYC (9BII)	Mouse	Cell Signalling Technology

Table 2.1 – Details of all antibodies used in western blotting, flow cytometry and immunoprecipitation experiments.

2.1.4 Cell culture

All cells were kept in a humidified incubator at 37°C, 5% CO_2. The DT40 chicken B cell line was obtained from laboratory stocks and was maintained in RPMI media with added supplements: 10% heat inactivated foetal bovine serum (FBS), 1% chicken serum, 4 mM glutamine, 100 units/ml penicillin, 100 µg/ml streptomycin and 50 µM β2-mercaptoethanol (Michael G Tomlinson et al., 2004). The HEK293T human embryonic kidney cell line was obtained from laboratory stocks and was maintained in DMEM media with added supplements: 10% heat inactivated FBS, 4 mM glutamine, 100 units/ml penicillin and 100 µg/ml streptomycin (Haining et al., 2012). HUVEC were isolated by infusing the veins of umbilical cords with collagenase to dislodge the cells, or were obtained from Phil Stone (University of Birmingham, UK). HUVEC were grown on cell culture plates pre-treated with 0.1% (w/v) gelatine diluted in phosphate buffered saline (PBS) and were used up to passage six. They were maintained in M199 media with added supplements: 10% heat inactivated FBS, 4 mM glutamine, 0.3% bovine brain extract (Maciag, Cerundolo, Ilsley, Kelley, & Forand, 1979) (provided by Dr. Victoria Heath, University of Birmingham), 90 µg/ml heparin (Sigma), 100 units/ml penicillin and 100 µg/ml streptomycin (Kaur et al., 2011). Human dermal fibroblasts were obtained from Dr. Victoria Heath and were maintained in DMEM media with added supplements: 10% heat inactivated FBS, 4 mM glutamine, 100 units/ml penicillin and 100 µg/ml streptomycin (Kaur et al., 2011).

2.2 TRANSFECTION

2.2.1 Transfection by electroporation

DT40 B cells were transiently transfected by electroporation for use in the NFAT/AP-1 luciferase reporter assay, as previously described (Michael G Tomlinson et al., 2004). Briefly, cells were suspended at $1.5x10^7$ cells/400 µl in serum free media and were incubated with 20 µg NFAT/AP-1 luciferase transcriptional reporter (Shapiro et al., 1996; Michael G Tomlinson et al., 2004), 2 µg pEF6-LacZ (Invitrogen) and 10 µg of either pEF6 mock vector (Invitrogen), or pEF6 FLAG-tagged tetraspanin (Haining et al., 2012; Protty et al., 2009) for 10 mins before electroporation at 350 V and 500 µF using a Gene-Pulser and capitance extender (Bio-Rad). Cells were incubated for 10 mins and then suspended in 8 ml complete serum-containing media.

2.2.2 Transfection by polyethylenimine (PEI)

HEK293T cells were transiently transfected using PEI (Sigma), for use in biochemical assays, as described (Ehrhardt et al., 2006; Haining et al., 2012). Briefly, cells were set up in complete media 24 hours before transfection. Opti-mem serum-free media (Gibco) was incubated with deoxyribonucleic acid (DNA) and PEI (1 mg/ml stock) for 10 mins to allow DNA/PEI complexes to form. The mix was added to the cells, which were used for experiments 48 hours after transfection. Cell counts, and volume of reagents used are listed in table 2.2.

Plate	Cells	Media	Opti-mem	DNA	PEI
6-well	3×10^5	2 ml	100 µl	1 µg	4 µl
6 cm	1×10^6	3 ml	300 µl	3 µg	12 µl
10 cm	3×10^6	10 ml	1 ml	9 µg	36 ml
15 cm	6×10^6	20 ml	2 ml	18 µg	72 ml

Table 2.2 – Reagents and quantities required for PEI transfection of HEK293T cells.

2.3 PLATELET PREPARATION

2.3.1 Mouse platelet preparation

Both washed platelets and platelet rich plasma were prepared as previously described (Hughes et al., 2008). Briefly, mice at 10-12 weeks old were terminally anaesthetised using isoflurane and blood was drawn from the exteriorised descending aorta directly into 150 µl acid citrate dextrose (ACD; 120 mM sodium citrate, 110 mM glucose, 80 mM citric acid) when preparing washed platelets, or citrate concentrated solution (4%, Sigma) when preparing platelet rich plasma. Withdrawn blood was then diluted in 200 µl of modified Tyrode's buffer (134 mM NaCl, 0.34 mM Na_2HPO_4, 2.9 mM KCl, 12 mM $NaHCO_3$, 20mM HEPES, 5 mM glucose, 1 mM $MgCl_2$, pH 7.3). Platelet rich plasma was extracted from the whole blood by centrifugation; 2 x 6 min at 200 g to allow separation of platelet rich plasma from red blood cells. Washed platelets were prepared with an additional centrifugation step to pellet the platelets and separate them from the plasma; 6 min at 1000 g in the presence of 1 µg/ml PGI_2 (Sigma). PGI_2 was used to inhibit platelet activation and aggregation through increased cAMP and decreased intracellular Ca^{2+} concentration (Best, Martin, Russel, & Preston, 1977; Salvador Moncada, 1982). Platelets were then suspended in modified Tyrode's buffer, counted and concentration adjusted as required.

2.3.2 Human platelet preparation

Preparation of human platelets was approved by the University of Birmingham Ethics Committee and donors provided informed consent before donating blood, which was taken by a trained phlebotomist (Laura Cronin, Elizabeth Haining, or Farhat Khanim). Records of donors and volume of blood taken were completed in line with the ethical approval requirements. Washed human platelets were prepared as outlined previously (Pearce et al., 2004). Briefly, 50 ml of blood from healthy donors was drawn directly into 5 ml concentrated sodium citrate to act as an anticoagulant. 5 ml of pre-warmed ACD was added to the blood as further anti-coagulant and blood was centrifuged at 200 g for 20 min. The supernatant (platelet rich plasma) was extracted and centrifuged at 1000 g for 10 min in the presence of PGI_2 (1 µg/ml). The platelet pellet was suspended in modified Tyrode's buffer, counted and the volume adjusted as required.

2.4 PLATELET FUNCTION ASSAYS

2.4.1 Assessment of mouse blood cell counts

Blood was drawn from the exteriorised descending aorta of terminally anaesthetised mice, as described in section 2.3.1. A 60 µl sample of whole blood was analysed using Pentra 60 whole blood counting equipment (ABX Diagnostics). All cell count readings were normalised for the added volume of the ACD and Tyrode's buffer.

2.4.2 Assessment of cell surface expression of platelet receptors

Blood was drawn from the exteriorised descending aorta of terminally anaesthetised mice, as described in section 2.3.1. 5 µl of whole blood was stained for 30 min at room temperature with fluorescein isothiocyanate (FITC)-conjugated anti-mouse antibodies (Emfret), at a dilution of 1:10 in Tyrode's buffer, as directed by the manufacturer's guidelines. Samples were analysed on a fluorescence activated cell sorting (FACS) Caliber (BD Biosciences) and platelets were gated by size on forward and side scatter and fluorescence was measured as geometric mean fluorescence intensity, which was normalised against an IgG control antibody using Cellquest Pro software.

2.4.3 Light transmission aggregometry

Washed mouse platelets were prepared as described in section 2.3.1 and suspended at $2x10^8$ platelets/ml ready for aggregation, as previously described (Hughes et al., 2008; Y. A. Senis et al., 2009). Briefly, aggregation was measured in glass cuvettes, using a volume of 300 µl at 37°C with stirring. Initial resting platelet readings were taken for 1 min, followed by stimulation by injection of 3 µl agonist (100 x concentrations). Aggregation was measured by light transmission using aggregometer model 460VS (Chronolog, Lab Medics) and measurements recorded using a chart reader (Chronolog, Lab Medics).

2.4.4 Measurement of platelet secretion

Secretion of secondary mediators from platelet dense granules during aggregation was assessed via binding of platelet secreted ATP to an added firefly luciferin/luciferase premix (chromolume, Chrono-Log Corporation). Firefly luciferase is an enzyme which catalyses the chemical reaction which leads to the generation of light from luciferin. The reaction, which is described by the equation below, requires ATP to produce lucifryl adenylate from luciferin. In turn, oxyluciferin is formed in an excited state; as it returns to the ground level, a photon of light is emitted. Therefore, the amount of ATP secreted from the platelets can be measured through the amount of light detected. ATP concentration was calculated using an ATP standard to calibrate the measurements (Hughes et al., 2008; Y. A. Senis et al., 2009).

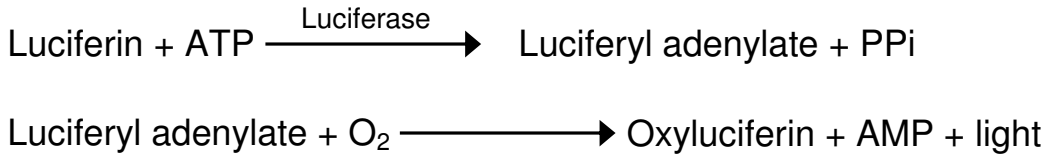

2.4.5 Platelet spreading

Analysis of platelet spreading was undertaken as previously described (Hughes et al., 2008; Y. A. Senis et al., 2009). Briefly, glass cover slips were coated with collagen related peptide (CRP) (10 µg/ml) or Fibrinogen (100 µg/ml) overnight. Cover-slips were blocked with 5mg/ml of denatured and filtered fatty acid free bovine serum albumin (Sigma) for 1 hour. Washed mouse platelets were prepared as described in section 2.3.1, suspended at $2x10^7$ platelets/ml and incubated on the cover-slips for 45 min at 37℃ in the presence of 10 µM indomethacin (Sigma) and 2 U/ml apyrase (Sigma) to inhibit platelet aggregation. Platelets spread on fibrinogen coated cover-slips were also activated with 1 unit/ml thrombin. Non-adherent platelets were washed away with phosphate buffered saline (PBS) and cover slips were fixed with 4% paraformaldehyde in PBS for 10 min. Platelets were imaged using a 60X Plan APO 1.4NA oil immersion objective with a TE2000 (Nikon) microscope with Digital Sight DS-Qi1MC camera (Nikon) using NIS elements AR software (Nikon). The area of single, in focus platelets was measured using thresholding in ImageJ Software for 150 platelets per condition.

2.4.6 Aggregate formation under flow

Blood was drawn from the exteriorised descending aorta of terminally anaesthetised mice into 300 µl modified Tyrode's buffer with heparin and PPACK (134 mM NaCl, 0.34 mM Na_2HPO4, 2.9 mM KCl, 12 mM $NaHCO_3$, 20mM HEPES, 5 mM glucose, 1 mM $MgCl_2$, pH 7.3, 15 u/ml heparin, 40 µM PPACK) to prevent thrombin generation (Hughes et al., 2010). Flow cells in a 24-well plate format (Fluxion) were coated with 30 µg/ml collagen for one hour and blocked with 5 mg/ml of denatured and filtered fatty acid free bovine serum albumin (Sigma) at 4°C overnight. Blood was incubated with DiOC6 membrane dye (0.2 µM) (Molecular Probes) at 37°C for 10 minutes and then perfused through the flow cell at shear rates of 300, 1000 or 3000 s^{-1} at 37°C using the Bioflux 200 microfluidic flow system (LabTech). Images were continuously taken by fluorescence microscopy with a TE2000 (Nikon) microscope with Digital Sight DS-Qi1MC camera (Nikon) using NIS elements AR software (Nikon), using a 40x plan APO 1.4 NO oil immersion DIC objective.

2.4.7 Platelet Ca^{2+} signalling measurements

Washed mouse platelets prepared as outlined in section 2.3.1, were suspended at $1x10^8$ platelets/ml in modified Tyrode's buffer and incubated with Fura2-AM (Invitrogen) (10 µM) and pluronic F-127 (Molecular Probes) (0.2 µg/ml) for 30 min at 37 ^oC (Inoue et al., 2003). Platelets were then washed in the presence of PGI_2 (1 µg/ml) by centrifugation at 1000 g for 6 min to removed excess dye. Platelets were suspended at $1x10^8$ platelets/ml in

modified Tyrode's buffer and 600 µl used for Ca^{2+} measurements, taken in a LS50B luminescence spectrometer (Perkin Elmer) in which excitation was alternated between 340 nm and 380 nm and measurements taken at 509 nm. Quantitative evaluation of Ca^{2+} concentration was calculated from the raw ratio values following calibration and use of the equation outlined below. Calibration of each value was achieved by obtaining the maximum and minimum ratio values. The maximum value was measured after lysing the platelets with 0.1% Triton X-100 in the presence of 1.5 mM Ca^{2+}. The minimum value was measured after addition of 20mM ethylene glycol tetraacetic acid (EGTA) to chelate the Ca^{2+} in the media. The Grynkiewicz equation was used to convert the raw data 340/380 nm ratio values into Ca^{2+} concentration values (Grynkiewicz, Poenie, & Tsienb, 1985). The equation is defined below, where Kd = the dissociation constant of fura-2 (224 nM), R = measured fluorescence ratio value, Rmax = maximum ratio value, Rmin = minimum ratio value, S_{f2}/S_{b2} = the ratio of fluorescence intensity at 380 nm in the absence of Ca^{2+} and at Ca^{2+}-saturation.

$$[Ca^{2+}] = Kd \times \frac{(R - R_{min})}{(R_{max} - R)} \times \frac{(S_{f2})}{(S_{b2})}$$

2.4.8 Platelet phosphotyrosine blotting

Measurement of phosphorylation downstream of platelet surface receptor activation was completed as previously described (Hughes et al., 2008; Y. A. Senis et al., 2009). Briefly, washed mouse platelets were prepared as

described in section 2.3.1 and suspended at $5x10^8$ platelets/ml. Lotrafiban (10 µm), indomethacin (10 µm), and apyrase (2 units/ml) were included in the suspension buffer to inhibit platelet aggregation. Platelets were held at 37°C in a water bath without stirring, activated with CRP for 90 or 300 seconds and samples of 50 µl taken for resting and stimulated platelets. Samples were lysed in an equal volume of 2x reducing sample buffer (0.1 M Tris pH 6.8, 4% sodium dodecyl sulphate (SDS), 20% glycerol, 5% 2 β-mercaptoethanol in dH_20 containing bromophenol blue), separated by SDS- polyacrylamide gel electrophoresis (PAGE) using 4-12% gradient gels (Invitrogen) and visualised by western blotting as described in section 2.7.1, using an anti-phosphotyrosine 4G10 antibody.

2.5 IN VIVO ASSAYS

2.5.1 Tail bleeding

The tail bleeding assay was used to assess haemostasis and was completed as described previously (Senis et al., 2009). Litter-matched mice at 8-10 weeks old were administered 0.05 mg/kg of the analgesic buprenorphine by subcutaneous injection prior to maintenance under continued isoflurane anaesthesia. 3 mm of the tail tip was removed using a razor blade and the tail left to hang freely without disruption. Resulting blood drops were collected into pre-weighed 1.5 ml microfuge tubes. The assay continued for 20 min, or until a maximum blood loss of 15% as estimated by weight (blood loss allowed = (mouse weight*0.15*70)/30, where a single drop of blood is estimated to be 30µl and total blood volume is assumed to be 70 µl/g. For example, for a mouse weighing 20g: 20*0.15*70/30 = 7 drops allowed) was reached, or until bleeding ceased (judged as no blood fall for 5 min). To end the procedure, the tail tip was cauterised.

2.5.2 Thrombus formation following chemical injury

This experiment was completed in Wurzburg, Germany, as previously described (Braun et al., 2009). Briefly, platelets of mice were fluorescently labelled with Dylight-488 conjugated anti-GPIX Ig derivative. Injury was induced to mesenteric arterioles by topical application of $FeCl_3$ (20%) for 10 s.

Adhesion and aggregation of platelets was measured by fluorescence microscopy until complete occlusion of the vessel or a final time of 40 min.

2.5.3 Thrombus formation following mechanical injury

This experiment was completed in Wurzburg, Germany, as previously described (Braun et al., 2009). Briefly, an ultrasonic flow probe was placed around the abdominal aorta of anaesthetised mice and thrombosis was induced by a single firm compression with forceps. Blood flow was monitored until complete occlusion occurred; otherwise experiments were stopped manually after 30 minutes.

2.5.4 Generating chimeric mice

To generate chimeric mice with Tspan18 wildtype haematopoietic cells and knockout non-haematopoietic cells, and vice versa, an irradiation approach was used, as previously described (Hughes et al., 2010). Briefly, the drinking water of 6-week old C57BL/6 wild type or Tspan18 deficient mice was treated with the antibiotic Baytrill for 1 week to reduce the risk of infection during the experiment. The mice were then lethally irradiated with two separate doses at 500 Gy, 3 hours apart. One hour after the second dose of irradiation, the mice were injected via the tail vein with embryonic liver cells suspended in PBS, which had been harvested at embryonic day E16.5 and stored as a single cell suspension in freezing solution (90% FBS, 10% DMSO) at -80 ^{o}C. Mice were left to recover over a period of 6 weeks to allow reconstitution of

the haematopoietic system from the injected cells. Genotyping of haematopoietic and non-haematopoietic cells was used to confirm success of the experiment, as outlined in sections 2.8.1 and 2.8.2. Embryonic liver was selected for injecting in to the irradiated mice, as full and long term reconstitution of the multiple lineages within the haematopoietic system, including erythrocytes, T-cells, mast cells and macrophages, has been observed following transplant of foetal liver (Ema & Nakauchi, 2015; Forrester, Bernstein, Rossant, & Nagy, 1991). The embryonic stem cells which are derived from foetal liver have been shown to have the ability to reconstitute the haematopoietic system, and are relatively easy to harvest in significant quantities in comparison to other sources of stem cells such as bone marrow. As such, many studies within the field of platelet function testing have utilised this method of haematopoietic reconstitution (Hess et al., 2014; Hughes et al., 2010; Suzuki-Inoue et al., 2010).

2.6 NFAT/AP-1 LUCIFERASE REPORTER ASSAY

2.6.1 Measurement of luciferase signalling

NFAT activity was monitored using a reporter assay, as described previously (Michael G Tomlinson et al., 2004). DT40 cells were transfected as described in section 2.2.1 and after 16 hours, cells were counted, suspended at $2x10^6$ cells/ml and 50 µl aliquoted into triplicate wells in a 96-well plate. An equal volume (50 µl) of media containing agonist was added to each well; cells were either left unstimulated, were stimulated with 50 ng/ml Phorbol 12-myristate 13-acetate (PMA) (Merck Millipore) and 1 µM ionomycin (Merck Millipore), or were inhibited with 2 mM cyclosporin A (Merck Millipore) for 6 hours. After incubation, cells were lysed in 11 µl harvest buffer (10% Triton X-100, 1 mM DTT, 200 mM potassium phosphate buffer; 450 mM K_2HPO_4, 46 mM KH_2PO_4) for 5 min. 100 µl from each well was transferred to an opaque 96-well plate and 100 µl assay buffer added (10 mM ATP, 20 mM $MgCl_2$ in 0.2 M potassium phosphate buffer); luciferase activity was measured in a plate-reading Mithras LB940 luminometer (Berthold Technologies) after injection of 50 µl luciferin (1 mM) (Cambridge Bioscience).

Luciferase activity data were normalised for transfection efficiency to β-galactosidase activity using a kit (Applied Biosystems) as described previously (Michael G Tomlinson et al., 2004). Briefly; cell pellets of $1x10^6$ cells were lysed in 80 µl lysis buffer for 5 mins. Lysed cells were incubated with galacton reaction buffer in the dark for 1 hour and activity was measured

in a plate-reading Mithras LB940 luminometer (Berthold Technologies) after injection of light emission accelerator.

Data was not normally distributed due to normalisation of the values to β-galactosidase activity; therefore data were transformed into logarithmic values for analysis. As a result, positive and negative error bars were calculated separately, to avoid presenting misleading quantities due to the logarithmic data. For graphical representation, data were converted back into linear values.

2.6.2 Analysis of protein expression following measurement of signalling

For analysis of protein expression, whole cell lysate samples were separated by SDS-PAGE and analysed by western blot. To prepare the samples, frozen DT40 whole cell pellets were lysed in 20µl lysis buffer (1% Triton X-100, 10mM Tris pH 7.5, 150mM NaCl, 1mM EDTA, 0.02% sodium azide) containing 1% protease inhibitor cocktail (Sigma) per 1 x 10^6 cells for 30 minutes on ice. The supernatant was mixed with 2x non-reducing SDS-PAGE sample buffer (0.1 M Tris pH 6.8, 4% SDS, 20% glycerol in dH_20 containing bromophenol blue), boiled for 5 min and 40µl of each sample was loaded into a 12% gel and separated by SDS-PAGE electrophoresis. The gels were transferred onto an Immobilon FL PVDF membrane (Millipore), as described in section 2.7.1.

2.7 BIOCHEMICAL ASSAYS

2.7.1 Western blotting

For visualisation of protein expression, gels from SDS-PAGE electrophoresis were transferred onto either methanol activated Immobilon FL low fluorescence membranes (Millipore) for development using the Odyssey infra-red scanner, or methanol activated Immobilon FL PVDF membranes for development on film. Membranes were blocked in 5% milk or 3% bovine serum albumen (BSA) (First Link, UK) in TBST (20 mM Tris, 137 mM NaCl, 0.1% Tween, pH 7.6) for at least 1 hour, incubated with primary antibody (1 µg/ml) diluted in 3% BSA in TBST overnight, washed in TBST, and incubated with secondary antibody diluted in 3% BSA in TBST for 2 hours. Immobilon FL membranes were blotted with secondary antibodies conjugated to infra-red dye (IR dye) 800 CW or 680 (LI-COR Biosciences) and were scanned using the Odyssey infra-red scanner (LI-COR Biosciences). PVDF membranes were blotted with HRP-conjugated secondary antibodies (Pierce), developed using Pierce ECL western blot substrate (Thermo Scientific) and exposure to film.

2.7.2 Immunoprecipitation in HEK293T cells

Immunoprecipitation in HEK293T cells was completed as previously described (Haining et al., 2012). Briefly, transfected HEK293T cells in 6-well plates were lysed in either 1% cold Triton X-100 (1% Triton X-100, 10 mM Tris

pH 7.5, 150 mM NaCl, 1 mM EDTA, 0.02% sodium azide) or 1% digitonin (1% digitonin, dissolved in 100% methanol, diluted 1:10 in lysis buffer; 10 mM Tris pH 7.4, 150 mM NaCl, 0.02% NaN_3) for 30 min on ice. Insoluble material was removed by centrifugation at 20,000 g 10 min, and the supernatant incubated with rotation for 1.5 hours at 4°C with protein G sepharose 4B beads (Invitrogen), which had been coupled to an anti-FLAG M2 antibody; 20 µl beads and 1 µg antibody per sample, incubated with rotation at 4°C overnight. After incubation, the beads were washed 4 times with 1 ml lysis buffer, and mixed with 50 µl non-reducing SDS-PAGE sample buffer. Samples were boiled for 5 min, 20 µl was loaded onto 12% gels and separated by SDS-PAGE gel electrophoresis. Gels were transferred onto an Immoblin FL membrane as outlined in section 2.7.1.

2.7.3 Immunoprecipitation in human platelets

Immunoprecipitation using human platelets was completed as previously described (Haining et al., 2012). Briefly, platelets were prepared as described in section 2.3.2 at a density of 1 x 10^9 platelets/ml. 500 µl platelets were lysed in 500 µl 2x Brij97 lysis buffer (2% Brij97, 20 mM Tris pH 7.5, 150 mM NaCl, 2 mM $CaCl_2$, 2 mM $MgCl_2$, 0.02% sodium azide) containing 20 µl protein sepharose G beads for pre-clearing, with rotation at 4°C for 1 hour. Following lysis, the immunoprecipitation protocol and gel loading was completed as described in section 2.7.2.

2.7.4 Biotinylation

Sulfo-NHS-LC-biotin reacts with amine groups and therefore labels lysine residues and the primary amine at the N-terminus of proteins. The reagent is largely membrane impermeable, thus predominantly labels cell surface proteins. Biotin was used to label HEK293T cells, as described previously (Haining et al., 2012; Y. A. Senis et al., 2009). Briefly, transfected HEK293 T cells in a 6-well plate were first washed 3 times with PBS, then 1 ml of sulfo-NHS-LC-biotin (Pierce) (1 mg/ml) was added and incubated on a rocker for 30 min at room temperature. The biotinylation reaction was quenched using glycine (100 mM), the cells were harvested and either lysed and treated as outlined in the immunoprecipitation protocol outlined in section 2.7.2, or were used as whole cell lysates, without immunoprecipitation.

2.7.5 Cell surface cross-linking

3, 3'-dithiobis[sulfosuccinimidylpropionate] (DTSSP) (Pierce) was used as a membrane impermeable chemical cross-linker, as previously described (Haining et al., 2012). It consists of amine-reactive groups at either end, linked by a spacer of 1.2 nm in length. Therefore, if two cell surface proteins are closely associated, with either their N-termini or lysine residues in close proximity, these proteins will be covalently cross-linked together by DTSSP. The spacer can subsequently be cleaved with reducing agents. Transfected HEK293T cells were washed with PBS and treated with 2 mM DTSSP on a rocker at 4℃ for 30 min. 0.1 M glycine solution was added to each well to

quench the cross-linking reaction. Samples were lysed and immunoprecipitation completed as outlined in section 2.7.2.

2.7.6 Enzyme linked immunosorbent assay (ELISA)

Blood was drawn from the exteriorised descending aorta of terminally anaesthetised mice, as described in section 2.3.1, using only sodium citrate as an anticoagulant. Plasma was separated from the whole blood by centrifugation at 1000 g for 10 min. Following extraction, plasma samples were stored at -80^{o}C until use. Measurement of plasma concentration of vWF and FVIII was achieved using kits containing pre-coated micro-titre plates, following the manufacturer's guidelines (Bioassay Technology Laboratory and My Biosource, respectively). At completion of the assay, the plates were read at 450 nm using a microtitre plate reader (Anthos Zenyth 340rt). Concentration was calculated by extrapolation from a five-point standard curve generated with provided standard solutions of known concentration.

2.8 PCR

2.8.1 Genotyping mouse tissue

For identification of littermates and to provide tissue for genotyping, tissue was clipped from the ears of 1-2 week old mice and stored at -20^{o}C until use. Tissue samples were incubated at 55^{o}C overnight with 500 µl lysis buffer (100 mM Tris-HCl, 5 mM EDTA, 0.2% SDS, 200 mM NaCl) with 5 µl proteinase K (Sigma). After incubation, samples were centrifuged at 10,000 g for 2 min to pellet the insoluble material, and the supernatant was added to an equal volume of isopropanol to precipitate the DNA. Samples were centrifuged at 20,000 g for 20 min, the supernatant aspirated and the pellet suspended in 50 µl DNAse free water. DNA samples were incubated at 50 ^{o}C for 30 min and stored long term at 4 ^{o}C. Each 20 µl PCR reaction contained 10 µl RedTaq master mix (Sigma), 7.4 µl water, 1.6 µl primers (Lexicon, primer sequences outlined in table 2.3), and 1 µl DNA. The following PCR program was used: 5 min at 95^{o}C, followed by 35 cycles of 1 min at 95^{o}C, 1 min at 58^{o}C, 1 min at 72^{o}C, and a final 5 min at 72^{o}C. PCR products were run on 2% agarose gels and visualised using SYBR safe DNA gel stain (Life Technologies).

2.8.2 Genotyping from mouse blood

For assessment of chimeric mice, genotyping analysis of haematopoietic cells was necessary to confirm successful reconstitution of the haematopoietic cells from the transplanted cells. Blood samples were taken from the mice 6 weeks

post irradiation and were incubated with 1 ml ACK red cell lysis buffer (150 mM NH_4Cl, 10 mM $KHCO_3$, 0.1 mM Na_2EDTA, pH 7.2) for 5 min at room temperature before being centrifuged to pellet the intact white blood cells; the supernatant was discarded and the cell pellet saved. This process was repeated three times to remove all traces of red blood cells from the sample. The lysis, DNA extraction and PCR protocol outlined in section 2.8.1 was then used.

Wildtype specific (absent in targeted allele)	
5' primer name	DNA498-24
3' primer name	DNA498-13
Predicted band size	376 bp
5' primer sequence	5' – AGGATGGGATAACTGTCTGG
3' – primer sequence	5' – GCAGCGCATCGCCTTCTATC
Mutation specific (absent in wildtype allele)	
5' primer name	Neo3A
3' primer name	DNA498-13
Predicted band size	227 bp
5' primer sequence	5' – GCAGCGCATCGCCTTCTATC
3' – primer sequence	5' – GCAGCGCATCGCCTTCTATC

Table 2.3 – An outline of primer sequences of the primers used in PCR for genotyping of mouse tissue.

2.8.3 Real time quantitative PCR

Following siRNA knock down in HUVEC, 48 hours after transfection the cells were harvested and split to be used for experiments or for analysis by RT-PCR. RNA was extracted from HUVEC using a Total RNA Purification Kit (Norgen Biotek), according to the manufacturer's guidelines, and the resulting yield of RNA was measured using a spectrophotometer (Nanodrop). To generate the template required for the real-time PCR reaction, cDNA was generated from the extracted RNA using a High Capacity cDNA Reverse

Transcriptase kit (Invitrogen), which required the following PCR program to generate the cDNA: 25°C for 10 min, 37°C for 120 min, 85°C for 5 min. The cDNA product was stored at -20°C short-term before use in the RT-PCR reaction, which utilised FAM-TAMRA TaqMan hydrolysis probes (Applied Biosciences) and GAPDH as the internal house keeping control gene. RT-PCR samples were analysed using an ABI Prism 700 Sequence Detection system (Applied Biosciences) and the following PCR program: 50°C for 2 min, 95°C 10 min, followed by 44 cycles of 95°C for 15 sec, 60°C for 1 min. MIQE guidelines were followed (Bustin et al., 2009); water controls were included to check for contamination and the efficiency of each experiment, which was required to be within 10% of the house keeping gene to be considered valid, was calculated from standard curves, generated from 2-fold serial dilutions of the cDNA in the PCR reaction mix.

To calculate relative mRNA expression in each sample, the cycle threshold values (Ct) for Tspan18 were compared to the Ct of the housekeeping gene, GAPDH. Ct marks the point of intersection between the amplification curve and the threshold line and was set at the exponential phase of amplification. To calculate the expression ratio of the gene of interest and to control for differences in efficiency of amplification across experiments, the Pfaffl method was used, for which the equation is outlined below (Pfaffl, 2001).

$$\text{Ratio} = \frac{(E_{\text{target}})^{\Delta Ct_{\text{target}}}}{(E_{\text{ref}})^{\Delta Ct_{\text{ref}}}}$$

Where E_{target} is the real time PCR efficiency of the target gene (in this case, Tspan18) and E_{ref} is the real time PCR efficiency of the housekeeping gene (in this case, GAPDH). The ΔCt_{target} is the Ct of control – knockdown sample for the target gene (Tspan18) and the ΔCt_{ref} is the Ct of control – knockdown sample for the housekeeping gene (GAPDH) (Pfaffl, 2001).

2.9 ENDOTHELIAL FUNCTION ASSAYS

2.9.1 siRNA Transfection of HUVEC

HUVEC were transiently transfected using RNAiMAX (Invitrogen) and short interfering RNA (siRNAs) (Ambion) to knock-down proteins of interest during endothelial functional assays, as previously described (Kaur et al., 2011). In brief, cells were set up in complete media 24 hours before transfection. A duplex mix, containing siRNA duplex (20 µM stock) and Opti-mem serum-free media, and a lipofectamine mix, of lipofectamine (RNAiMAX) and Opti-mem, were incubated for 10 mins. The two mixes were combined and incubated for a further 10 mins. The cells were washed twice with PBS and the duplex/lipofectamine mix with additional Opti-mem media added to the plate. The cells were incubated at 37^{o}C for 4 hours before the media was changed to complete HUVEC media without antibiotics. Cells were used in endothelial functional assays 48 hours after transfection. Cell counts, amount of DNA and volume of reagents used are listed in the table below (Kaur et al., 2011).

Plate size	Cells plated	siRNA mix		Lipofectamine mix		Final volume
		siRNA	Opti-mem	RNAiMAX	Optimem	
6-well	1.75 x 10^5	2.5 µl	167.5 µl	6-well	3 µl	1 ml
6 cm	3.6 x 10^5	3.6 µl	241.4 µl	6 cm	4.3 µl	2 ml
10 cm	1 x 10^6	10 µl	670 µl	10 cm	12 µl	4 ml

Table 2.4 – Reagents and quantities required for siRNA knock down in HUVEC

2.9.2 Scratch wound assay

HUVEC were seeded at 3.5 x 10^5 cells per well of a gelatine-coated 6-well plate 24 hours before transfection, using siRNA, as described above. 48 hours after transfection, HUVEC monolayers were wounded with a plastic pipette tip and cell migration was monitored using a 20X objective with a TE2000 (Nikon) microscope with Digital Sight DS-Qi1MC camera (Nikon) using NIS elements AR software (Nikon). Images were taken every 15 minutes for 12 hours and migration of the cells to close the wound was assessed using ImageJ software (Kaur et al., 2011). Samples were taken to analyse knockdown efficiency by real time PCR, as described above.

2.9.3 Co-culture tube formation assay of angiogenesis

Fibroblasts were grown to confluence in a 12-well plate. HUVEC which had been transfected with siRNA, as described above, 24 hours previously were plated on top of the fibroblast culture at 3 x 10^4 cells/ml, using 1 ml per well. For six days the cells were left to grow, being given fresh media every other day. Following this incubation period, the tubes formed by the HUVEC were stained; cells were washed with PBS and fixed using 1 ml chilled ethanol (70%) for 30 min. Fixed cells were then incubated with anti-human CD31 antibody (1.29 µg/ml) in 400 µl buffer (1% BSA in PBS) at 37 ^oC for 40 min. Cells were washed with PBS, and incubated with anti-mouse IgG alkaline phosphatase (Sigma) (1:500) in 400 µl buffer (1% BSA in PBS) at 37 ^oC for 40 min. Cells were washed with PBS then dH_2O before addition of 500 µl SigmaFast BCIP/NBT substrate (Sigma) dissolved in dH_2O and were

incubated at room temperature for 25 min. The reaction was stopped by washing with excess dH_2O. The plates were then imaged using a light microscope and tubule formation was assessed using AngioSys software (Kaur et al., 2011).

CHAPTER 3

TSPAN18 REGULATES GPVI INDUCED PLATELET ACTIVATION AND PLATELET Ca^{2+} SIGNALLING

3.1 INTRODUCTION

3.1.1 Tspan18 is a platelet tetraspanin

The expression of tetraspanins in platelets has been studied using several techniques including proteomics, mRNA analysis, and use of antibodies to confirm and quantitate protein expression (Haining et al., 2011). One specific proteomics screen demonstrated that Tspan18 is one of the tetraspanins expressed on human platelets (Lewandrowski et al., 2009). Additionally, Tspan18 has been identified at the mRNA level in human and mouse megakaryocytes (Macaulay et al., 2007; Protty et al., 2009) and human and mouse platelets (Haining et al., 2012; Rowley et al., 2011). Aside from platelets, Tspan18 has also been identified in endothelial cells (Colombo, 2010) and $CD4^+$ T-cells (Protty et al., 2009), at the mRNA level, however a lack of antibodies has limited further investigation into its expression profile.

Selected platelet tetraspanins have been investigated using knockout mouse models and some have been implicated in regulation of platelet activation. For example, mice lacking either CD151 or Tspan32 displayed impaired platelet function. This was proposed to be caused by defective signalling from the major platelet integrin αIIbβ3 (Goschnick et al., 2006; Lau et al., 2004; Orlowski et al., 2009; Wright et al., 2004). However, investigation into the CD9 and CD63 knockout mice yielded no major platelet phenotype except a mild increase in thrombus size in the CD9 knockouts (Mangin et al., 2009; Schröder et al., 2009). The role of Tspan18 in platelet function has not yet been investigated.

When characterising platelet function, genetically modified mouse models are often used, as the effectiveness of *in vitro* assays is limited by the inability to culture or transfect these cells (B Nieswandt, Aktas, Moers, & Sachs, 2005). Therefore, to assess the role of Tspan18 in platelets, the Tspan18 knockout mouse was used. The Tspan18 knockout mouse was obtained from the Mutant Mouse Regional Resource Centre and was originally generated by Genentech Inc. and Lexicon Pharmaceuticals Inc, as outlined in section 1.3.5 (Tang et al., 2010).

3.2 AIMS

The aim of this chapter was to assess the role of Tspan18 in platelet function and haemostasis by using Tspan18 deficient mice. Both *in vivo* models and well defined *in vitro* assays were used to ascertain whether Tspan18 has a role in platelet activation or haemostasis.

3.3 RESULTS

3.3.1 Normal blood cell numbers and expression of platelet surface receptors in Tspan18 deficient mice

To evaluate blood cell counts in the Tspan18 deficient mice, blood was taken from anaesthetised mice and analysed using the Pentra 60 from ABX Diagnostics. No significant difference was observed between Tspan18 deficient and wildtype mice for platelet count, platelet volume, white blood cell count, or red blood cell count (figure 3.2, A-D). Examination of the different white blood cell populations also distinguished no difference between Tspan18 deficient and wildtype mice (figure 3.2, E).

To assess expression of the cell surface receptors which are important in platelet activation, flow cytometry was used. Blood was taken from anaesthetised mice, stained with FITC-tagged antibodies for specific platelet surface proteins and mean fluorescence intensity values were corrected with an Ig control stain. Tspan18 deficient platelets displayed normal expression of GPIb, the integrins α6 and αIIb, the metalloproteinase ADAM10, the tetraspanin CD9, and the signalling receptors, GPVI and CLEC-2 (figure 3.3).

Taken together, these data suggest that Tspan18 does not have a role in blood cell production or regulation of surface expression of the platelet surface proteins tested.

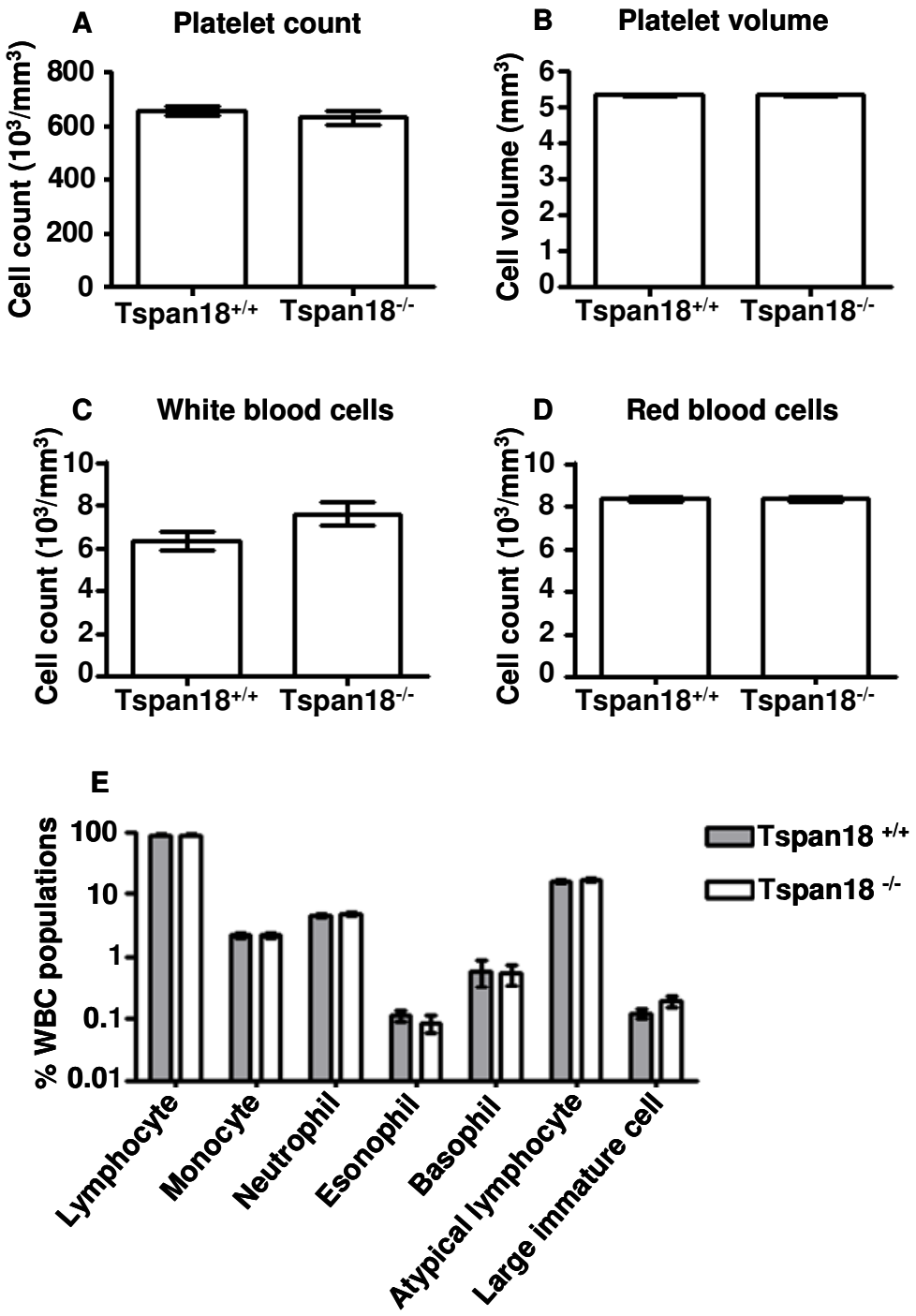

Figure 3.1 - Whole blood cell counts in Tspan18 deficient mice are normal. Blood was collected from anaesthetised mice and analysed by whole blood counting on a Pentra 60 from ABX diagnostics. Platelet count (A), platelet volume (B), white blood cell count (C), and red blood cell count (D) were assessed. Data were analysed by T-test. Error bars represent the standard error of the mean from 30 pairs of mice. White blood cell populations were also measured (E), and these data were normalised by arcsin transformation and analysed by two-way analysis of variance (ANOVA) with Bonferroni post-test. Error bars represent the standard error of the mean from 30 pairs of mice.

A

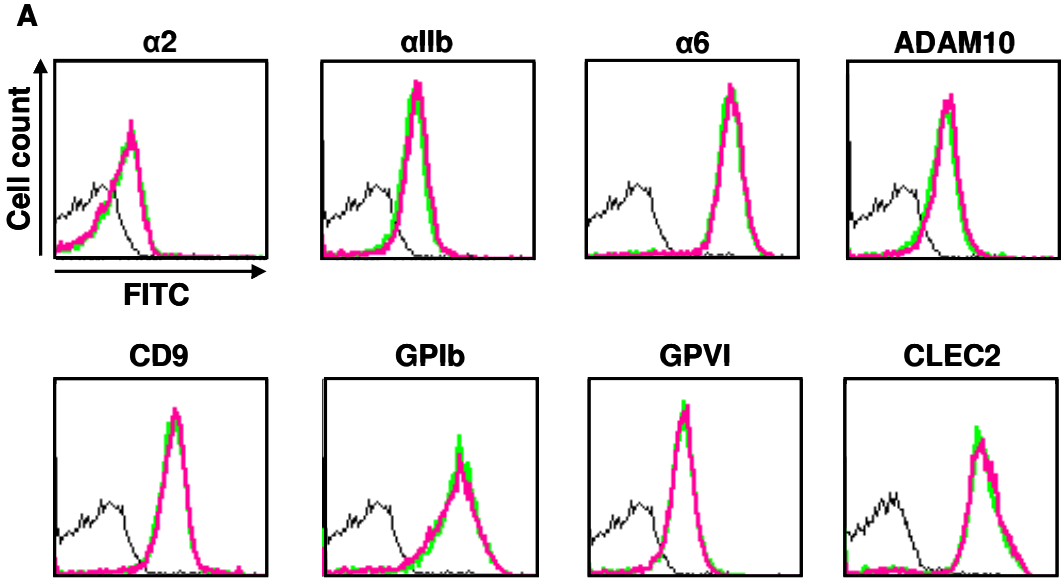

B

	Tspan18 $^{+/+}$	Tspan18 $^{-/-}$
α2	30.63 +/- 2.25	31.20 +/- 2.10
αIIb	323.85 +/- 33.39	311.94 +/- 37.39
α6	37.33 +/- 9.01	35.69 +/- 2.17
ADAM10	11.86 +/- 0.97	11.37 +/- 0.68
CD9	117.62 +/-27.54	125.69 +/- 26.68
GPIb	191.30 +/- 27.70	188.91 +/- 34.27
GPVI	41.60 +/- 3.72	37.89 +/- 4.81
CLEC2	153.09 +/-40.97	155.64 +/- 46.68

Figure 3.2 – Platelets from Tspan18 deficient mice express normal levels of the major platelet surface receptors. Blood was collected from anaesthetised mice, stained with FITC-tagged antibodies for specific platelet surface proteins, and analysed by flow cytometry. Representative overlay traces are shown; green = wildtype platelets, pink = Tspan18 deficient platelets, and black = control Ig staining for wildtype platelets (control Ig staining for Tspan18 deficient platelets yielded the same results, data not shown) (A). The mean fluorescence intensity values from 5 pairs of mice were collated and the mean +/- standard deviation values are displayed (B). All data were analysed by T-test.

3.3.2 Tspan18 deficient platelets display disrupted aggregation downstream of GPVI

To assess platelet activation and aggregation in Tspan18 deficient platelets, light transmission aggregometry (LTA) was used. LTA, or Born aggregometry, is considered to be the gold standard in platelet function testing and relies on the principle that more light can transmit through a suspension of aggregated platelets, than a suspension of resting platelets (Born, 1962). The percentage aggregation of platelets can therefore be assessed in terms of percentage light transmission. Use of agonists which activate specific platelet surface receptors enabled assessment of specific signalling pathways important in platelet activation. Analysis of both washed platelets and platelet rich plasma was completed. Washed platelets provided a clean system in which to assess platelet function, without additional effects of plasma factors, as the platelets were washed out of the plasma and into buffer. Platelet rich plasma allowed analysis of platelet activation by the agonist ADP, which activates P2Y receptors which become desensitised upon washing, and also provided more physiological conditions.

Initially, platelets were washed out of whole blood into modified Tyrode's buffer and stimulated with CRP (provided by Dr. R. Farndale), which is a synthetic peptide of GPO repeats cross-linked at N- and C- terminal cysteine or lysine residues. This peptide specifically activates platelets via the platelet collagen receptor GPVI (Farndale, 2006). In response to an intermediate dose of CRP, Tspan18 deficient platelets displayed defective aggregation. In response to a high dose of CRP, Tspan18 deficient platelets were able to aggregate, but a delayed response in aggregation was observed (figure 3.4).

The reduction in aggregation was significant when compared to wildtype platelets at both intermediate and high doses of CRP, though the phenotype was not as severe at high doses of agonist (figure 3.4). Washed platelet aggregation was also assessed downstream of signalling pathways other than GPVI, using agonists which activate other platelet surface proteins. Thrombin (Sigma) is a potent platelet agonist, which stimulates platelet activation through cleavage of the PAR family of GPCRs (Brass, 2003; De Candia, 2012). CLEC-2 Ab (provided by Prof. S. Watson) activates the C-type lectin receptor CLEC-2 on platelets via a Src and Syk tyrosine kinase family dependant mechanism (Eble et al., 2006; May et al., 2009). Collagen (HORM) (Nycomed Austria) can activate platelets indirectly, via vWF and the GPIb-V-IX complex, or directly via the integrin α2β1 and the platelet surface receptor GPVI (Farndale, 2006; Bernhard Nieswandt & Watson, 2003).

When stimulated by thrombin, CLEC-2 antibody or collagen, washed Tspan18 deficient platelets displayed normal aggregation; no difference was observed in comparison to wildtype platelets (figure 3.5). Analysis of Tspan18 deficient platelet response to doses of collagen lower than 1 µg/ml were attempted, but the lack of response from wildtype platelets at such low doses prevented further investigation (data not shown).

Following platelet activation, secretion of secondary mediators is an important step in driving thrombus formation, as it provides positive feedback to activate and recruit more platelets to the growing thrombus. Secretion of ATP from dense granules was measured via addition of a luciferin/luciferase mix to the platelet solution and measurement of luminescence output. Consistent with the aggregation data, secreted ATP was significantly reduced in Tspan18

deficient platelets in comparison to wildtype controls when activated with the GPVI-specific agonist, CRP, at either intermediate or high doses (figure 3.6, A). However, when Tspan18 deficient platelets were stimulated with thrombin, CLEC-2 antibody or collagen, secretion was normal across multiple doses of agonist (figure 3.6, B-D).

When aggregation was assessed in platelet rich plasma, the Tspan18 deficient platelets again demonstrated defective aggregation downstream of CRP, at several different doses of agonist (figure 3.7). Aggregation in platelet rich plasma was also assessed downstream of other platelet agonists. PAR4 peptide (AYPGKF) (provided by Dr. R. Farndale) was used as a thrombin substitute. ADP (Sigma) induces platelet activation via two GPCRs; P2Y1 and P2Y12 activate phospholipase C and suppress cAMP formation respectively, thus leading to platelet activation (Jin et al., 1998; Zhang et al., 2001). In response these other agonists, Tspan18 deficient platelets aggregated completely normally (figure 3.8, A-B). Interestingly, a minor defect in aggregation was observed in Tspan18 deficient platelets to a low dose of collagen, the physiological ligand of GPVI (figure 3.8 C). This suggests that Tspan18 deficient platelets are more susceptible to defects in platelet rich plasma, than when they have been washed out of the plasma, as no defects were observed following collagen stimulation in washed platelets.

Together, these data outline a defect during platelet aggregation and secretion, specifically downstream of the platelet collagen receptor, GPVI, which could be partially rescued through high doses of agonist. This is evidence of a mild but specific fault in platelet activation within the GPVI

signalling pathway and suggests a role for Tspan18 in GPVI-induced platelet activation.

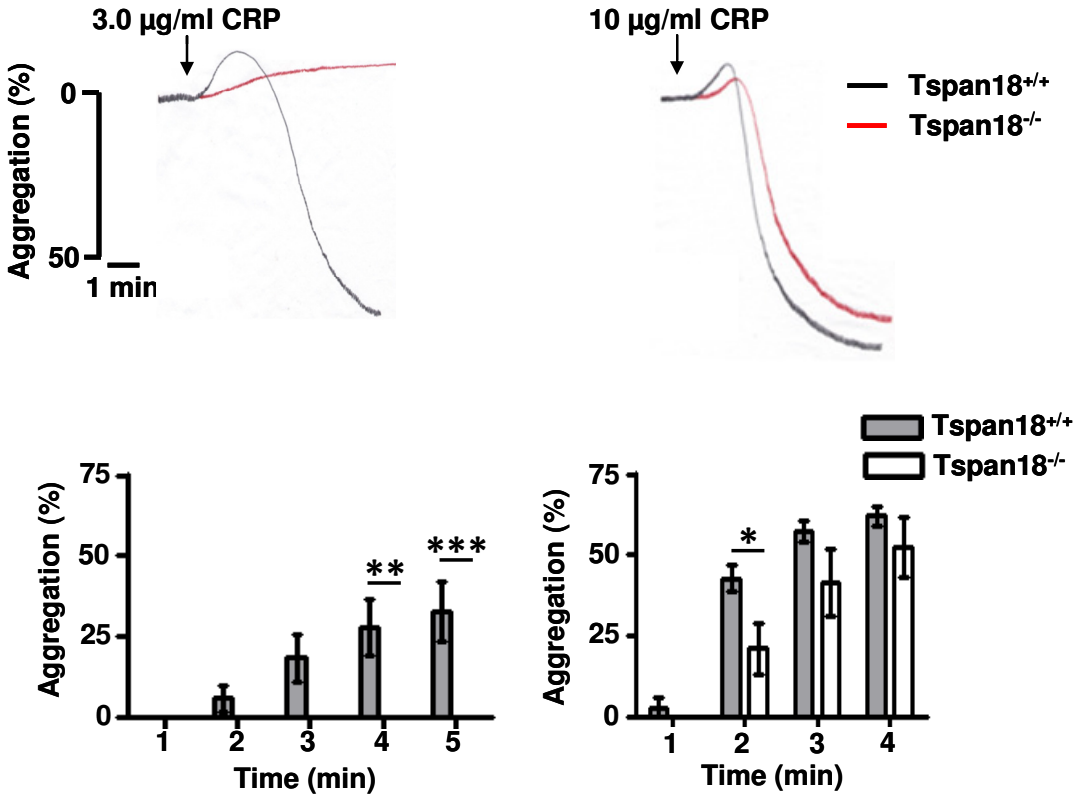

Figure 3.3 – Washed Tspan18 deficient platelets display reduced aggregation downstream of GPVI. Blood was collected from anaesthetised mice; platelets were isolated from the whole blood and washed in modified Tyrode's buffer. Washed platelets were activated with two different doses of CRP and aggregation was measured via light transmission with stirring, a representative trace is shown in the upper panels. Collated data of % aggregation at minute intervals were assessed and is shown in the lower panels. All data were normalised by arcsin transformation and analysed by two-way ANOVA with Bonferroni post-test (* denotes $P < 0.05$, ** denotes $P < 0.01$ and *** denotes $P < 0.001$). Error bars represent the standard error of the mean from 5-9 pairs of mice.

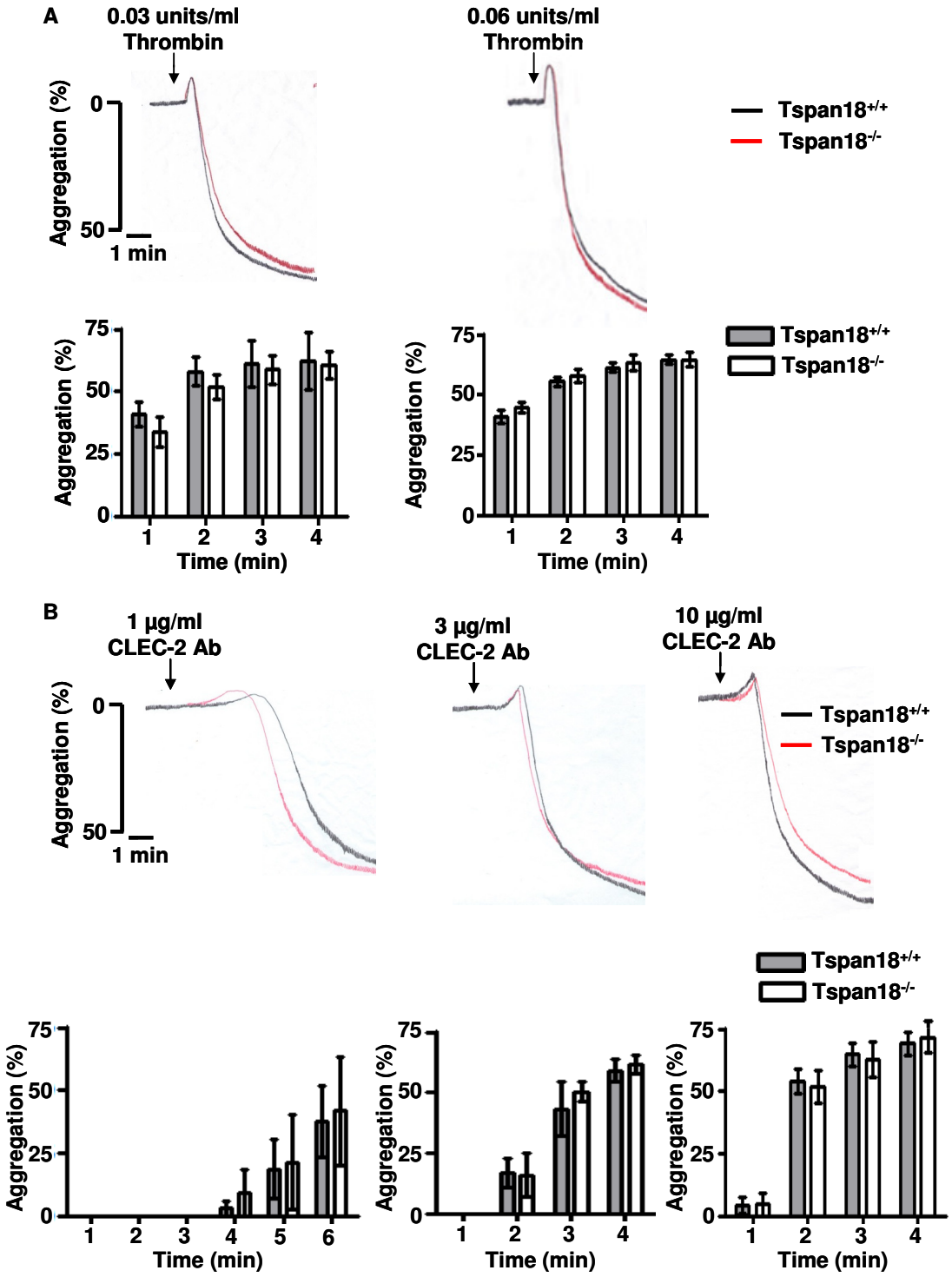
A
0.03 units/ml
Thrombin
0.06 units/ml
Thrombin
Aggregation (%)
0
50
1 min
Tspan18+/+
Tspan18-/-
75
50
25
0
1
2
3
4
Time (min)
B
1 µg/ml
CLEC-2 Ab
3 µg/ml
CLEC-2 Ab
10 µg/ml
CLEC-2 Ab
5
6

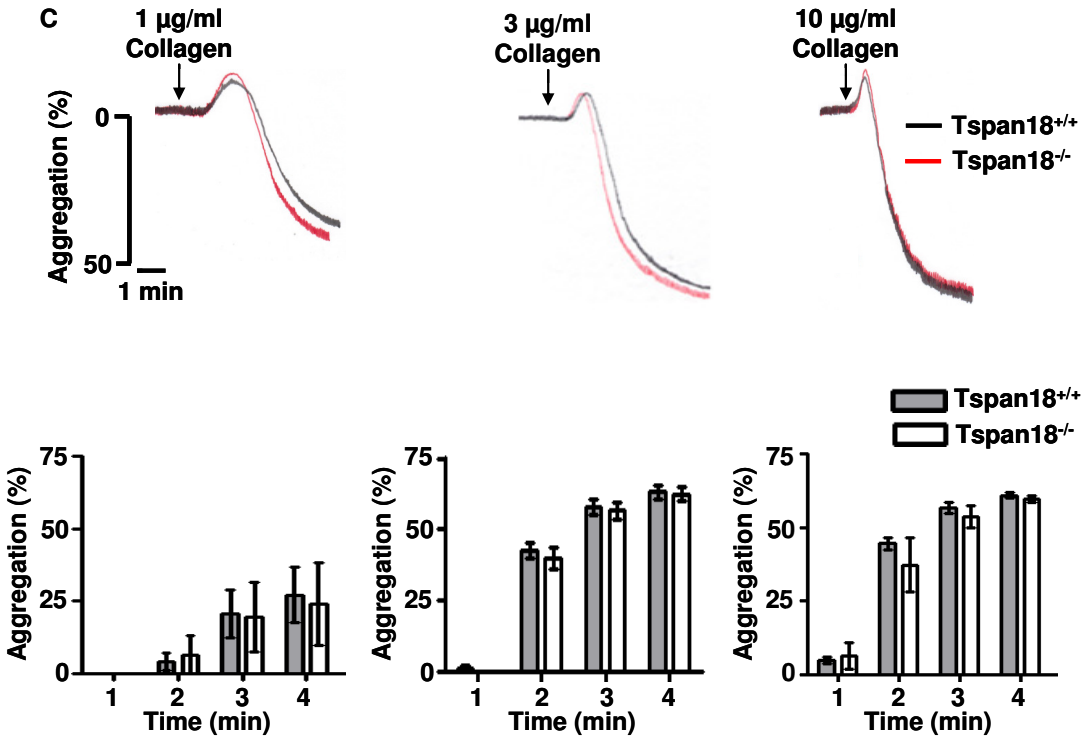

Figure 3.4 – Washed Tspan18 deficient platelets display normal aggregation to thrombin, CLEC-2 mAb and collagen. Blood was collected from anaesthetised mice; platelets were isolated from whole blood and washed in modified Tyrode's buffer. Washed platelets were activated with thrombin (A), CLEC-2 antibody (B), or collagen (C). Aggregation was measured via light transmission with stirring, representative traces are shown in the upper panels. Collated data of % aggregation at minute intervals were assessed and is shown in the lower panels. All data were normalised by arcsin transformation and analysed by two-way ANOVA with Bonferroni post-test. Error bars represent the standard error of the mean from 3-7 pairs of mice. Note that no wildtype platelet response was observed at doses of collagen lower than 1 µg/ml (data not shown).

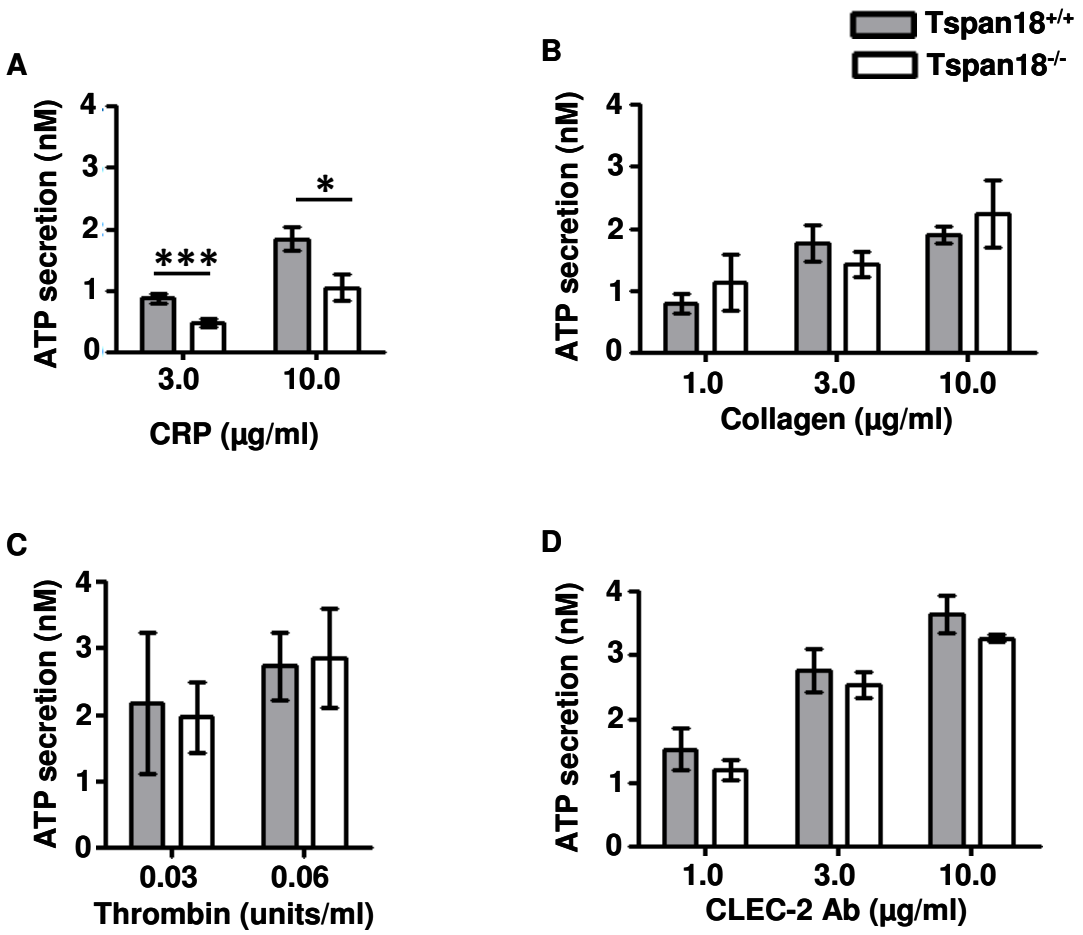

Figure 3.5 – Washed Tspan18 deficient platelets display reduced secretion downstream of GPVI. Blood was collected from anaesthetised mice; platelets were isolated from whole blood and washed in modified Tyrode's buffer. Following activation with CRP (A), collagen (B), thrombin (C) or CLEC-2 antibody (D), secretion of ATP from platelet dense granules was measured using an added firefly luciferin/luciferase mix (chromolume, Chrono-Log Corporation). All data were analysed by T-test (*** denotes $P < 0.001$, * denotes $P < 0.05$). Error bars represent the standard error of the mean from 3-9 pairs of mice.

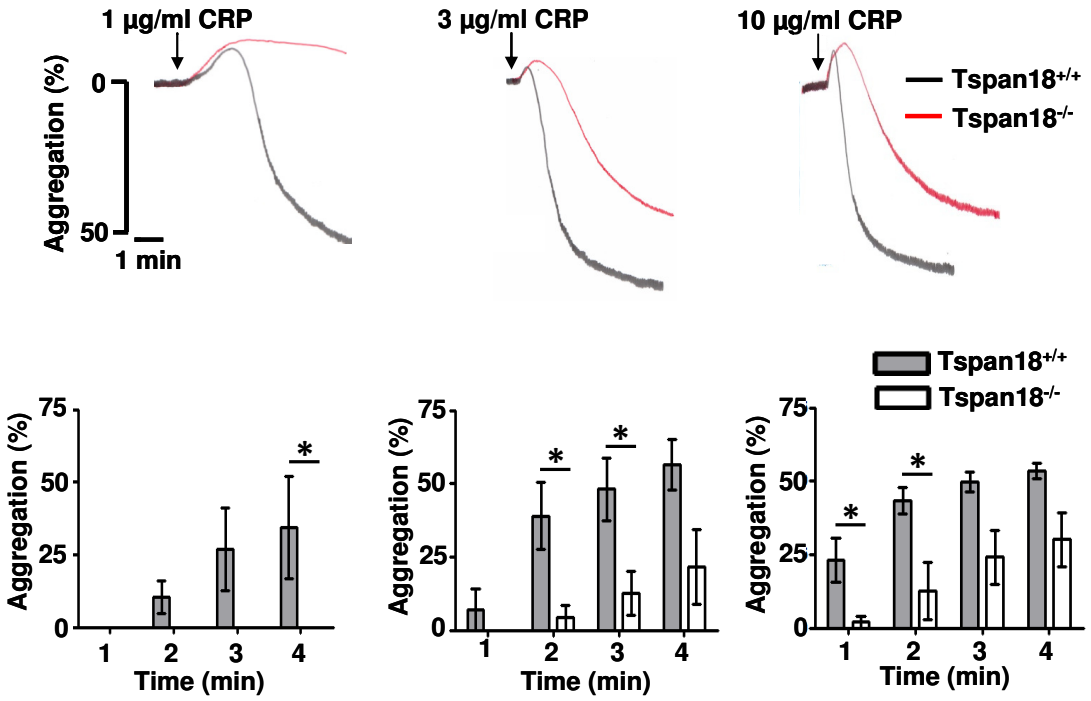

Figure 3.6 – Tspan18 deficient platelets in platelet rich plasma display defective aggregation downstream of GPVI activation. Blood was collected from anaesthetised mice; platelets were isolated from whole blood and collected as platelet rich plasma. Platelets were activated with CRP. Aggregation was measured via light transmission with stirring, representative traces are shown in the upper panels. Collated data of % aggregation at minute intervals were assessed and is shown in the lower panels. All data were normalised by arcsin transformation and analysed by two-way ANOVA with Bonferroni post-test (* denotes P< 0.05). Error bars represent the standard error of the mean from 3-4 pairs of mice.

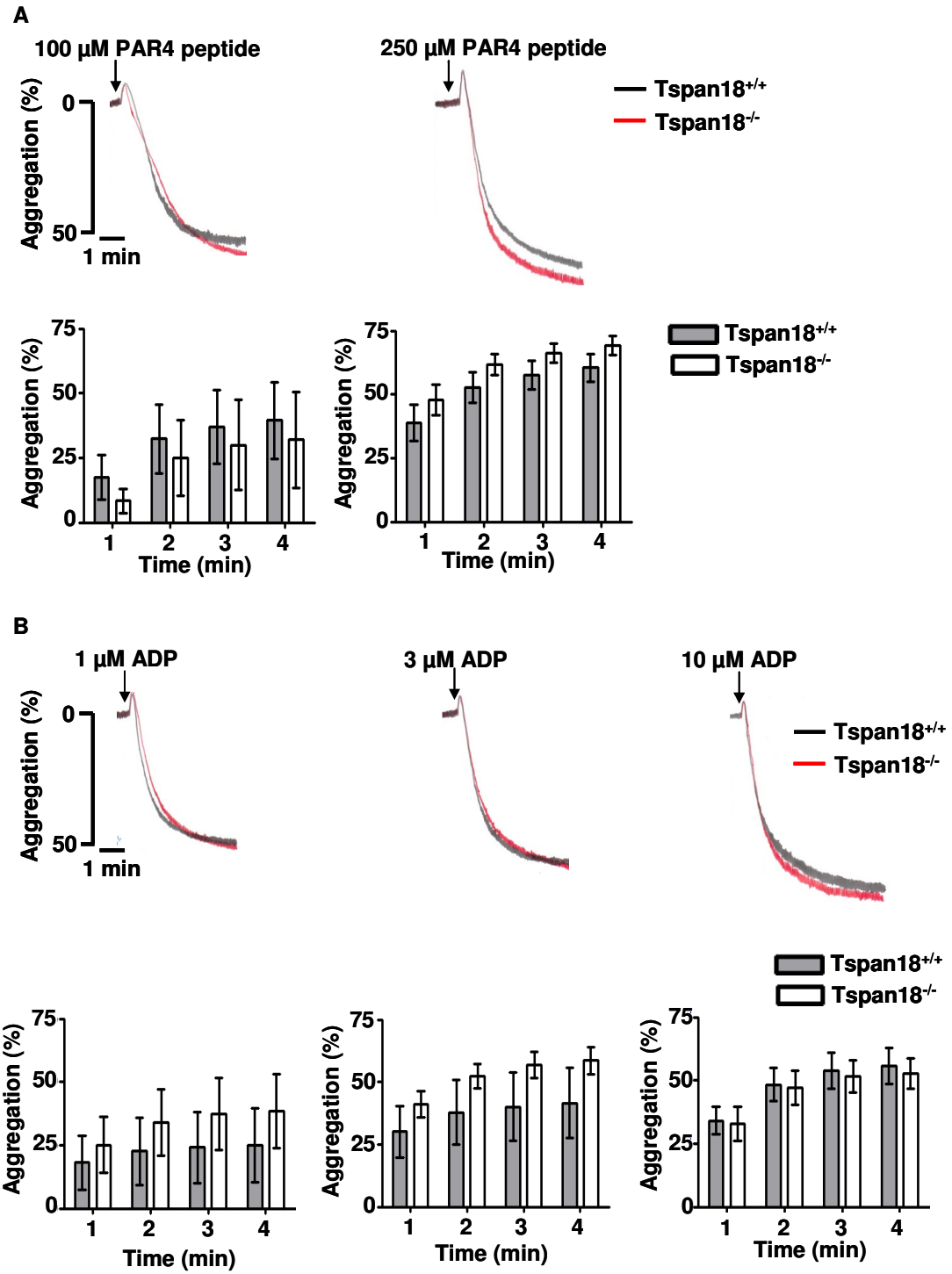
A
100 µM PAR4 peptide
250 µM PAR4 peptide
Tspan18+/+
Tspan18-/-
Aggregation (%)
0
50
1 min
75
25
1
2
3
4
Time (min)
B
1 µM ADP
3 µM ADP
10 µM ADP

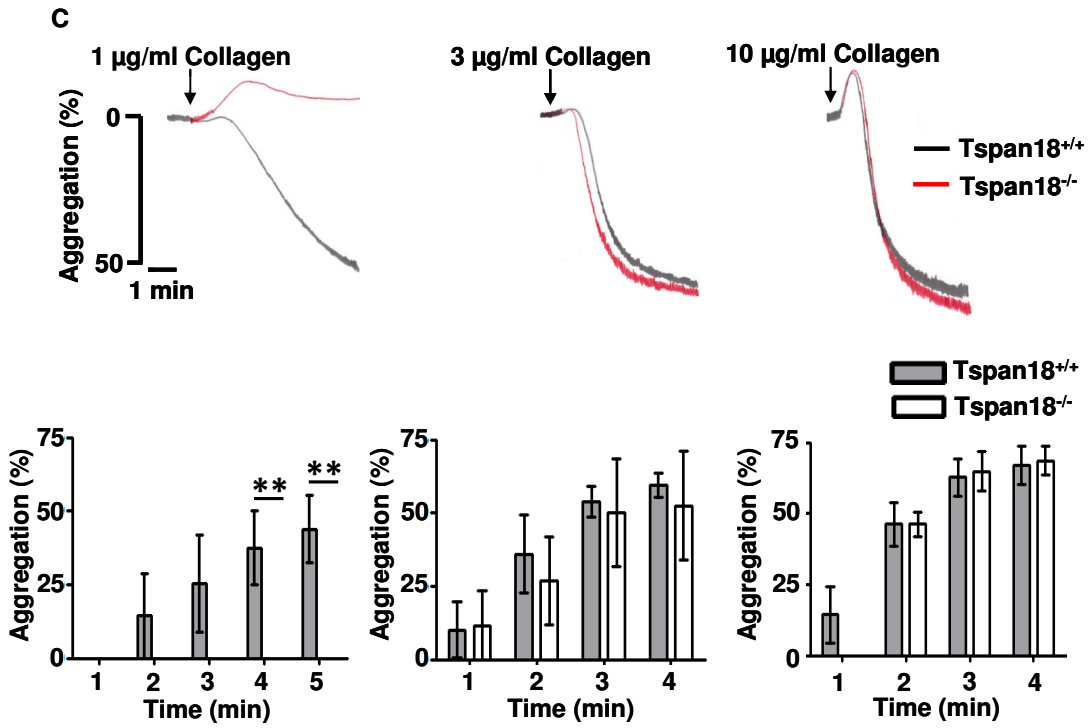

Figure 3.7 – Tspan18 deficient platelets in platelet rich plasma display normal aggregation to PAR4 peptide and ADP, but mildly defective aggregation to collagen. Blood was collected from anaesthetised mice; platelets were isolated from whole blood and collected as platelet rich plasma. Platelets were activated with PAR4 peptide (A), ADP (B), or collagen (C). Aggregation was measured via light transmission with stirring, representative traces are shown in the upper panels. Collated data of % aggregation at minute intervals were assessed and is shown in the lower panels. All data were normalised by arcsin transformation and analysed by two-way ANOVA with Bonferroni post-test (** denotes $P < 0.01$). Error bars represent the standard error of the mean from 4-5 pairs of mice.

3.3.3 Tspan18 deficient platelets display disrupted spreading downstream of GPVI

To further investigate the role of Tspan18 in platelet function, a platelet spreading assay was used, in which the ability of platelets to spread on immobilised agonist was assessed. As previously, blood was taken from anaesthetised mice and the platelets washed out from the whole blood into modified Tyrode's buffer. Platelets were then spread on glass cover slips pre-treated with immobilised agonist before being fixed, imaged and analysed for surface area using ImageJ software.

When Tspan18 deficient platelets were exposed to cover slips coated in CRP, a significant reduction in the area spread was observed when compared to wildtype control platelets (figure 3.9, A). However, when Tspan18 deficient platelets were exposed to cover slips coated with fibrinogen, no difference in the area spread was observed (figure 3.9, B).

Taken together with the data from the aggregation experiments, this outlines a clear disruption to platelet function specifically downstream of CRP stimulation, suggesting defective signalling within the GPVI signalling pathway.

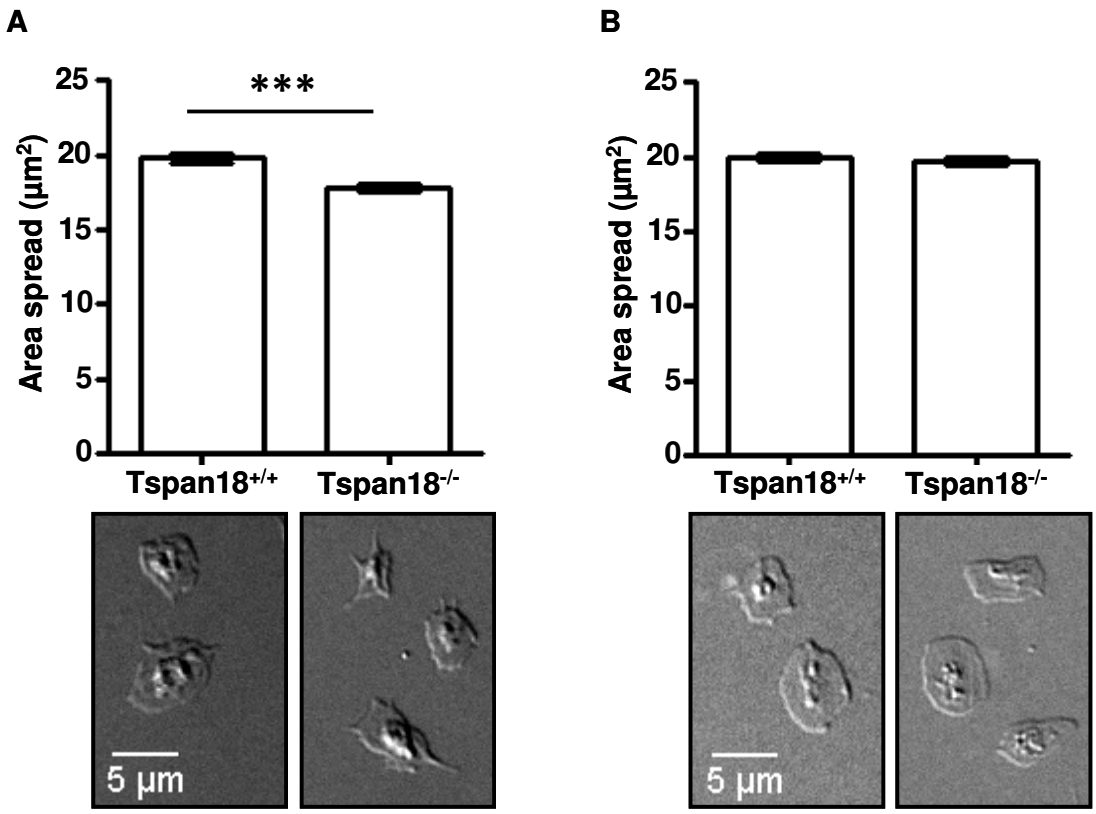

Figure 3.8 – Washed Tspan18 deficient platelets display reduced spreading downstream of GPVI. Blood was collected from anaesthetised mice; platelets were isolated from whole blood and washed in modified Tyrode's buffer. Washed platelets were exposed to cover slips coated with CRP (A) or fibrinogen (B) and the area of the adhered platelets was measured. Representative images are shown. All data were analysed by T-test (*** denotes $P < 0.001$). Error bars represent the standard error of the mean from 4 pairs of mice (150 platelets were analysed per mouse).

3.3.4 Protein tyrosine phosphorylation induced by GPVI is normal in Tspan18 deficient platelets

Following the observations from the platelet function tests that outlined a potential role for Tspan18 in regulation of platelet activation via GPVI, it was important to assess whether Tspan18 had a role in regulation of signalling from the GPVI receptor itself. Once activated, GPVI signals via an ITAM motif within the associated FcRγ chain, which leads to a complex phosphorylation cascade (Bernhard Nieswandt & Watson, 2003; Watson et al., 2005). Therefore, functionality of GPVI can be assessed by measuring downstream phosphorylation. Blood was taken from anaesthetised mice; platelets were isolated from the blood, washed in modified Tyrode's buffer and stimulated with CRP. Samples were taken into reducing sample buffer, separated by SDS-PAGE and western blotted with an anti-4G10 antibody to show phosphorylated tyrosine residues. To quantitate phosphorylation, band intensity was measured using the Odyssey infra red imaging system (LICOR).

No observable difference was noted in the pattern of tyrosine phosphorylation following GPVI stimulation between Tspan18 deficient and wildtype platelets. This was true for basal levels of phosphorylation and at two time points post-stimulation (figure 3.10, A). No difference was observed after measurement of band intensity of the band observed at approximately 72 kDa, which corresponds to phosphorylated Syk, at any of the time points across three different doses of agonist (figure 3.10, B). Similarly, no significant difference was observed after measurement of the band at 135 kDa, which corresponds to phosphorylated PLCγ (figure 3.10, C). However, close inspection of the intensity of the pp135 band after stimulation with 3 μg/ml CRP may suggest

an increase in phosphorylation in Tspan18 deficient platelets in comparison to wildtype. This may warrant further investigation, though does not appear to suggest a major phenotype.

These data demonstrate normal signalling from GPVI, which implies that Tspan18 may be having an effect further downstream in this signalling pathway.

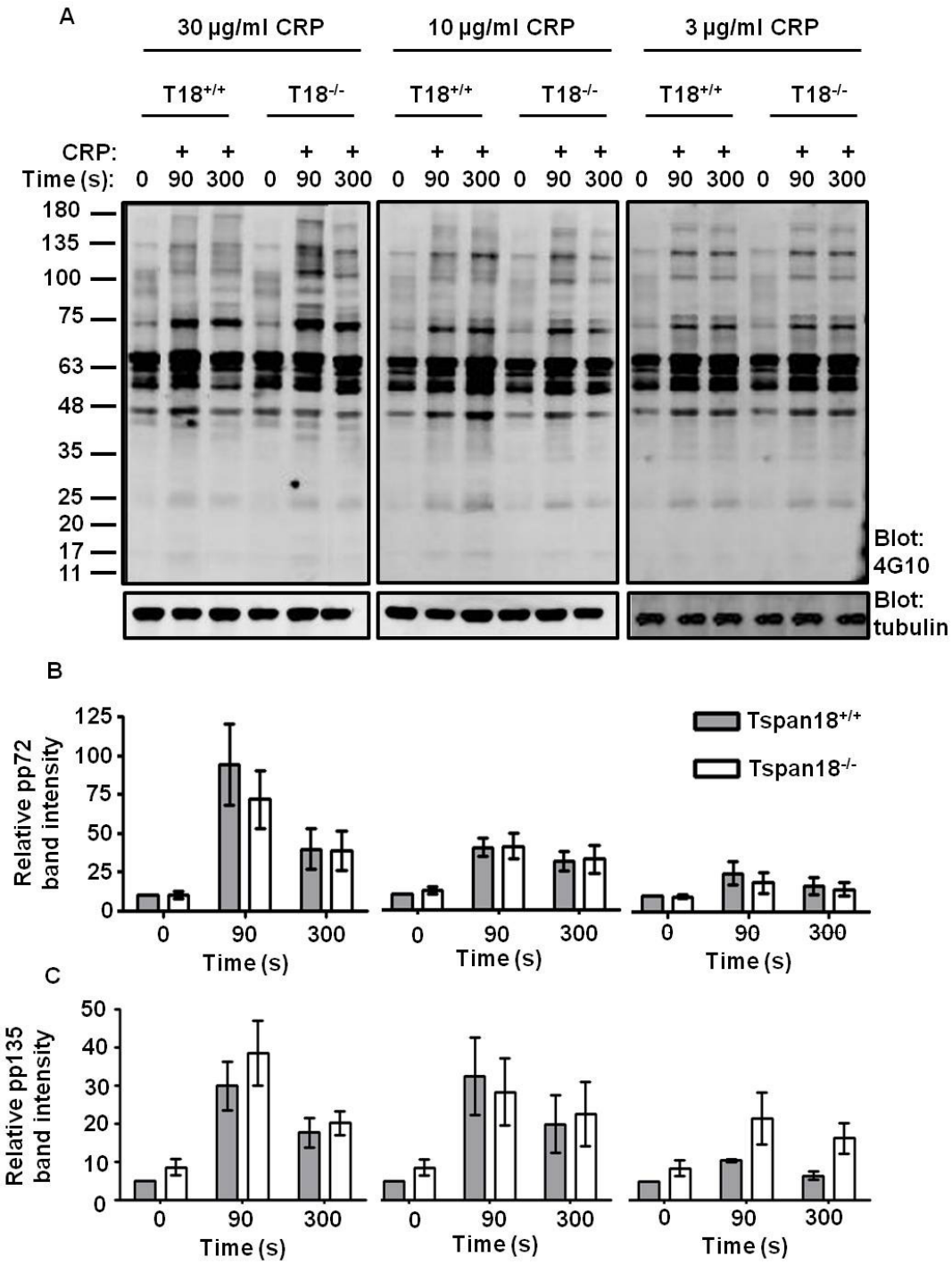

Figure 3.9 – Protein tyrosine phosphorylation induced by GPVI is normal in Tspan18 deficient platelets. Blood was collected from anaesthetised mice; platelets were isolated from whole blood and washed in modified Tyrode's buffer. Platelets were activated with three different doses of CRP. Samples were taken at several time-points, separated by SDS-PAGE and blotted with an anti-phosphotyrosine antibody, 4G10. A representative blot from 5 separate experiments is shown (A). The band at pp72, corresponding to phosphorylated Syk (B) and pp 135 corresponding to phosphorylated PLCγ (C), were quantitated using the Odyssey infra-red (LICOR) imaging system. All data were normalised by logarithmic transformation and analysed by two-way ANOVA with Bonferroni post-test. Error bars represent the standard error of the mean from 5 separate experiments.

3.3.5 Tspan18 deficient platelets have reduced SOCE and reduced global Ca^{2+} signalling

It has been shown previously that platelet activation, and specifically the GPVI signalling pathway, is reliant on SOCE (Braun et al., 2009; David Varga-Szabo, Braun, et al., 2008). Additionally, previous studies, using cell line over expression models had suggested a role for Tspan18 in Ca^{2+} signalling (Colombo, 2010). Therefore, it is possible that the defects observed in platelet activation in Tspan18 deficient platelets were caused by defective Ca^{2+} signalling. To investigate the potential role for platelet Tspan18 in SOCE, Ca^{2+} signalling was measured in Tspan18 deficient platelets. Blood was taken from anaesthetised mice and platelets were isolated and washed in modified Tyrode's buffer. Platelets were then loaded with the Ca^{2+} sensitive fluorescent dye, Fura2-AM and Ca^{2+} measurements were taken using a luminescence spectrophotometer.

Initial investigation into the role of Tspan18 in Ca^{2+} signalling in platelets focussed on platelet response following agonist stimulation. Platelets were suspended in Tyrode's buffer containing 1.5 mM Ca^{2+} and were stimulated with different platelet agonists. Ca^{2+} measurements were taken to measure Ca^{2+} influx following platelet stimulation. After stimulation with CRP or collagen, a significant reduction in the rate of Ca^{2+} mobilisation was observed in Tspan18 deficient platelets (figure 3.11, A). Additionally, the maximal Ca^{2+} concentration observed was significantly reduced in Tspan18 deficient platelets in comparison to wildtype platelets (figure 3.11, B). However, both the rate of Ca^{2+} influx and the maximal Ca^{2+} concentration achieved in

Tspan18 deficient platelets was normal after stimulation with thrombin (figure 3.11).

This suggests that Ca^{2+} mobilisation and influx of Ca^{2+} from the extracellular environment appears to be reduced in Tspan18 deficient platelets downstream of GPVI activation.

To more specifically investigate the potential role of Tspan18 in SOCE, the platelets were treated with thapsigargin (Sigma) which acts to induce emptying of the intracellular Ca^{2+} stores via inhibition of sarco/endoplasmic reticulum Ca^{2+}-ATPase (SERCA) Ca^{2+} ion pumps in the endoplasmic and sarcoplasmic reticulum, thus preventing Ca^{2+} flux back into the stores (Lytton, Westlin, & Hanley, 1991).

Initially, the platelets were suspended in Ca^{2+}-free media and were stimulated the thapsigargin to measure release of Ca^{2+} from intracellular stores. Following stimulation with thapsigargin, 1.5 mM Ca^{2+} was added back to the extracellular buffer to allow SOCE to occur. Throughout the experiment, the cytosolic Ca^{2+} concentration was measured to monitor release of Ca^{2+} from the intracellular stores and influx from the extracellular environment . The rate of entry of Ca^{2+} from the extracellular environment was reduced to 0.0026 s^{-1} in Tspan18 deficient platelets, in comparison to 0.0038 s^{-1} in the wildtype control platelets (figure 3.12, A). However, the final, maximal change in Ca^{2+} concentration was not significantly different between Tspan18 deficient and wildtype platelets (figure 3.12, B).

The reduction in Ca^{2+} entry from the extracellular environment was preceded by a reduction in the release of Ca^{2+} from the intracellular stores. This was

observed following thapsigargin treatment in the presence of Ca^{2+} free media, prior to Ca^{2+} being added back to the extracellular buffer. The rate of release of Ca^{2+} from the stores was reduced to 0.010 s^{-1} in Tspan18 deficient platelets when compared to a rate of 0.022 s^{-1} in wildtype control platelets (figure 3.13, A). Although a reduction in the rate of Ca^{2+} release from the stores was observed, there was no significant difference in maximal concentration of Ca^{2+} achieved in Tspan18 deficient platelets (figure 3.13, B). This suggests that Tspan18 deficient platelets have mildly defective release of Ca^{2+} from intracellular stores, resulting in slower accumulation of Ca^{2+} in the cytosol following thapsigargin stimulation.

Together, these data suggest defective release of Ca^{2+} from the intracellular store and defective SOCE in Tspan18 deficient platelets. However, this Ca^{2+} signalling defect appears to only limit platelet activation and Ca^{2+} signalling downstream of GPVI. It is therefore not surprising that no major difference in maximal Ca^{2+} concentration was observed after such a strong stimulus as thapsigargin.

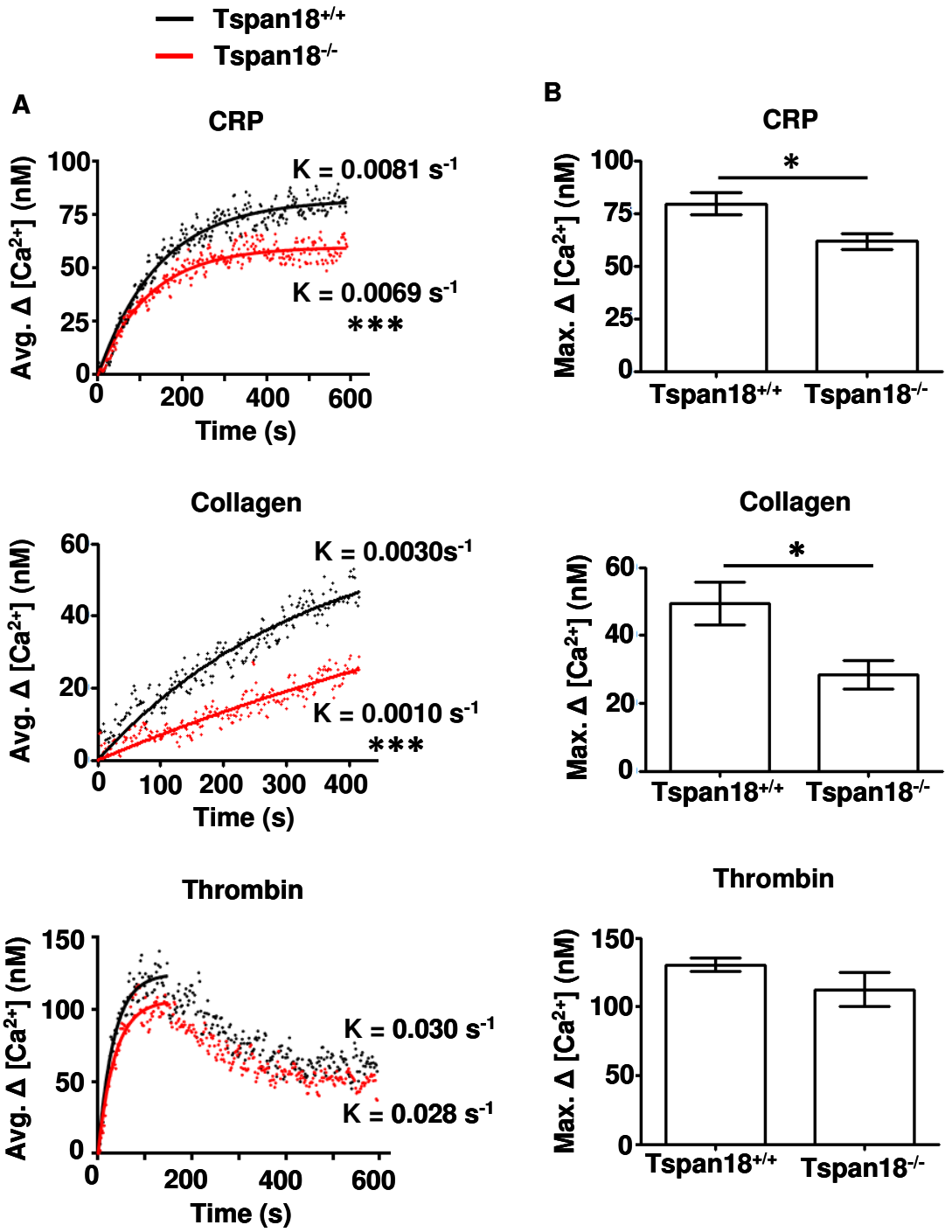

Figure 3.10 – Global Ca^{2+} signalling is reduced in Tspan18 deficient platelets downstream of GPVI. Blood was collected from anaesthetised mice; platelets were isolated from whole blood and washed in modified Tyrode's buffer. The platelets were loaded with the Ca^{2+} sensitive dye Fura-2 AM and Ca^{2+} measurements taken using a luminescence spectrophotometer. Platelets were stimulated with CRP, collagen or thrombin as indicated, in the presence of 1.5 mM extracellular Ca^{2+}. Average data from 4 separate experiments were fitted to a non-linear regression using an exponential one-phase association equation (A). Rate constants (K) were compared using an F-test (*** denotes $P < 0.01$). The maximal change in $[Ca^{2+}]$ was also calculated (B). Data were analysed by T-Test (* denotes $P < 0.05$). Error bars represent the standard error of the mean from 4 separate experiments.

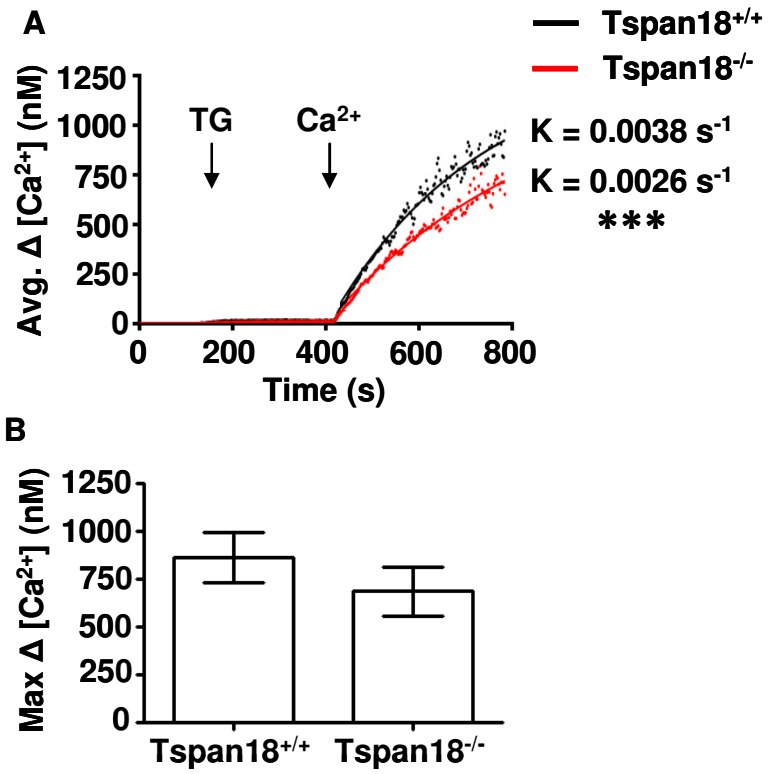

Figure 3.11 – Store operated Ca^{2+} entry is reduced in Tspan18 deficient platelets. Blood was collected from anaesthetised mice; platelets were isolated from whole blood and washed in modified Tyrode's buffer. The platelets were loaded with the Ca^{2+} sensitive dye Fura-2 AM and Ca^{2+} measurements taken using a luminescence spectrophotometer. Platelets were stimulated with thapsigargin (TG) to induce emptying of the intracellular Ca^{2+} stores and Ca^{2+} was then added back to the extracellular media at 1.5 mM to allow SOCE to occur. Average data from 5 separate experiments were fitted to a non-linear regression using an exponential one-phase association equation (A). Rate constants (K) were compared using an F-test (*** denotes $P < 0.001$). The maximal change in $[Ca^{2+}]$ was calculated (B). Data were analysed by T-Test. Error bars represent the standard error of the mean from 5 separate experiments.

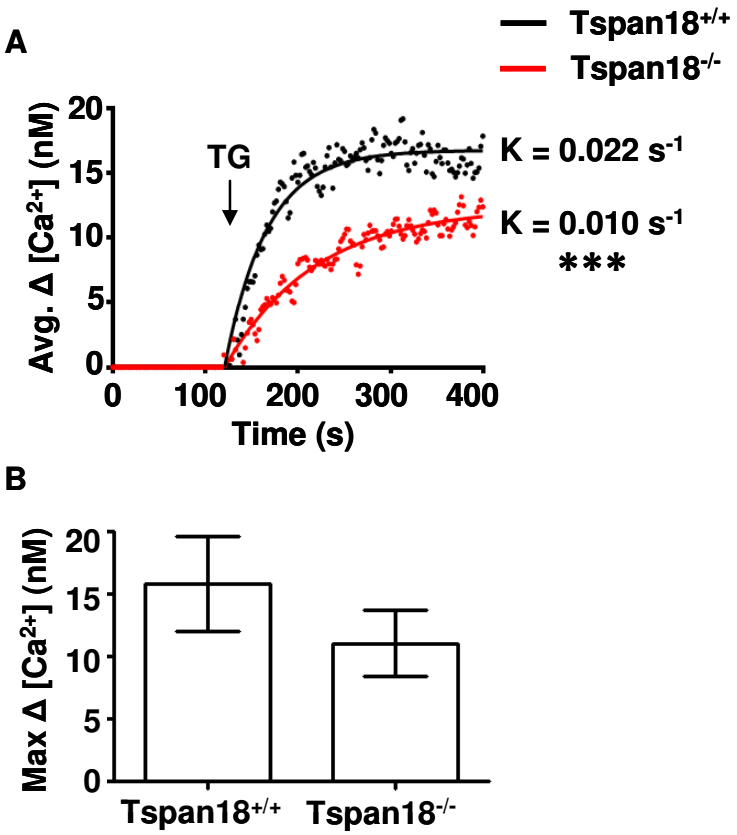

Figure 3.12 - Release of Ca^{2+} from intracellular stores is reduced in Tspan18 deficient platelets within Ca^{2+} free media. Blood was collected from anaesthetised mice; platelets were isolated from whole blood and washed in modified Tyrode's buffer. The platelets were loaded with the Ca^{2+} sensitive dye Fura-2 AM and Ca^{2+} measurements taken using a luminescence spectrophotometer. Platelets were treated with thapsigargin (TG) to induce emptying of the intracellular Ca^{2+} stores. Average data from 5 separate experiments were fitted to a non-linear regression using an exponential one-phase association equation (A). Rate constants were compared using an F-test (*** denotes $P < 0.001$). The maximal change in $[Ca^{2+}]$ was also calculated (B). Data were analysed by T-Test. Error bars represent the standard error of the mean from 5 separate experiments.

3.3.6 Aggregate formation under flow is normal for Tspan18 deficient platelets

While *in vitro* platelet function tests which utilise washed platelets or platelet rich plasma are well characterised and provide a detailed view of specific signalling pathways involved in platelet activation, other assays can be employed to provide a more physiological view of platelet function. One assay which better mimics *in vivo* conditions of platelet aggregation is the flow adhesion assay, which was completed using the Bioflux system from Fluxion. Platelets were fluorescently stained in whole blood, which was perfused through collagen-coated capillaries and aggregate formation was monitored using fluorescence microscopy. The blood was perfused through the capillaries at rates of 300 s^{-1} (to represent venous shear) or 1000 s^{-1} (to represent arterial shear).

No difference was observed in the dynamics of aggregate formation between blood from Tspan18 deficient mice and wildtype mice for either the high or low shear rates tested (figure 3.14, A and figure 3.15, A). Additionally, there was no difference in the final area of the flow cell covered by platelet aggregates when quantified using ImageJ software (figure 3.14, B and figure 3.15, B).

The lack of phenotype observed in this *in vitro* flow adhesion assay is consistent with the largely normal aggregation to collagen which was observed (figure 3.5).

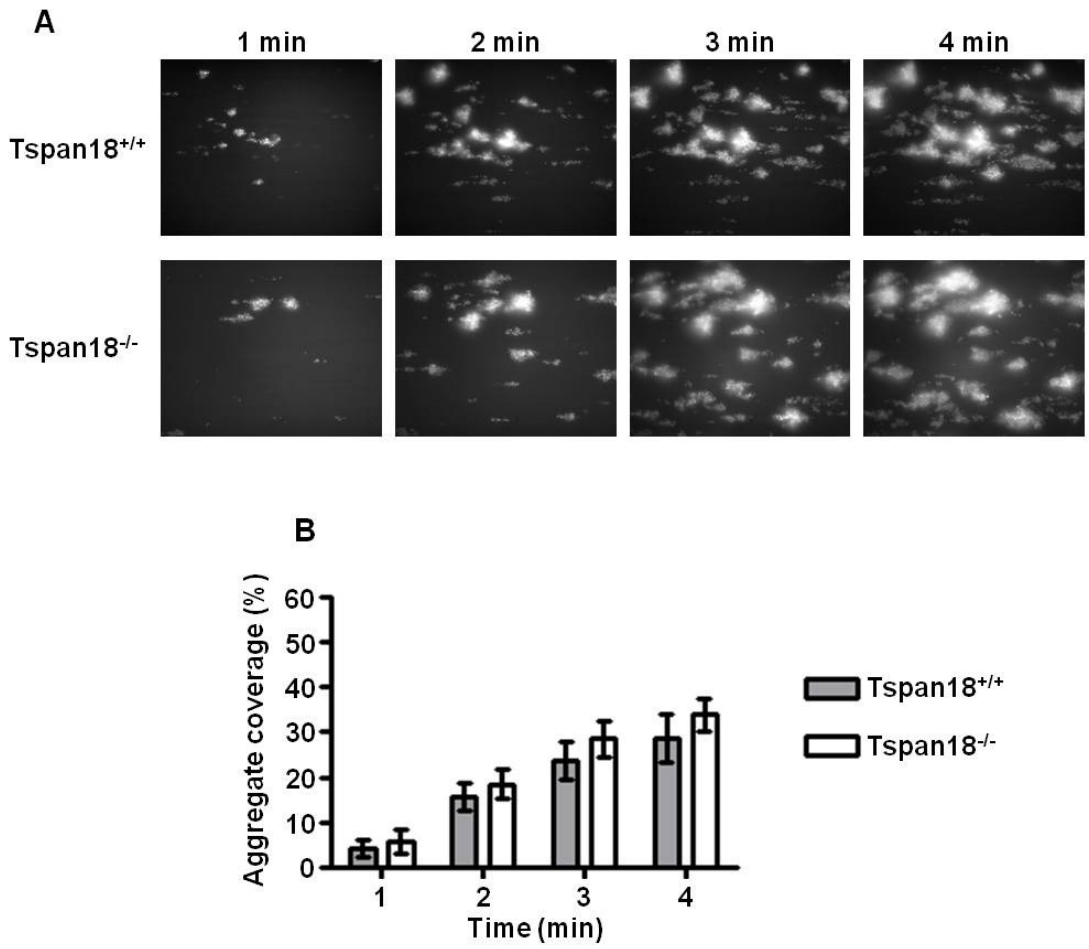

Figure 3.13 – Aggregate formation under arterial shear conditions in the Tspan18 knockout platelets is normal. Whole blood from wildtype and Tspan18 deficient mice was perfused over a collagen-coated flow cell (30 µg/ml) using the Fluxion Bioflux system at a shear rate of 1000s-1. Representative fluorescence images at minute-interval time points show normal aggregate formation by the Tspan18 deficient platelets (A). Coverage of the flow cell by aggregates was measured at minute intervals, using thresholding in ImageJ (B). Data were normalised by arcsin transformation and analysed by two-way ANOVA with Bonferroni post-test. Error bars represent standard error of the mean from 3 pairs of mice.

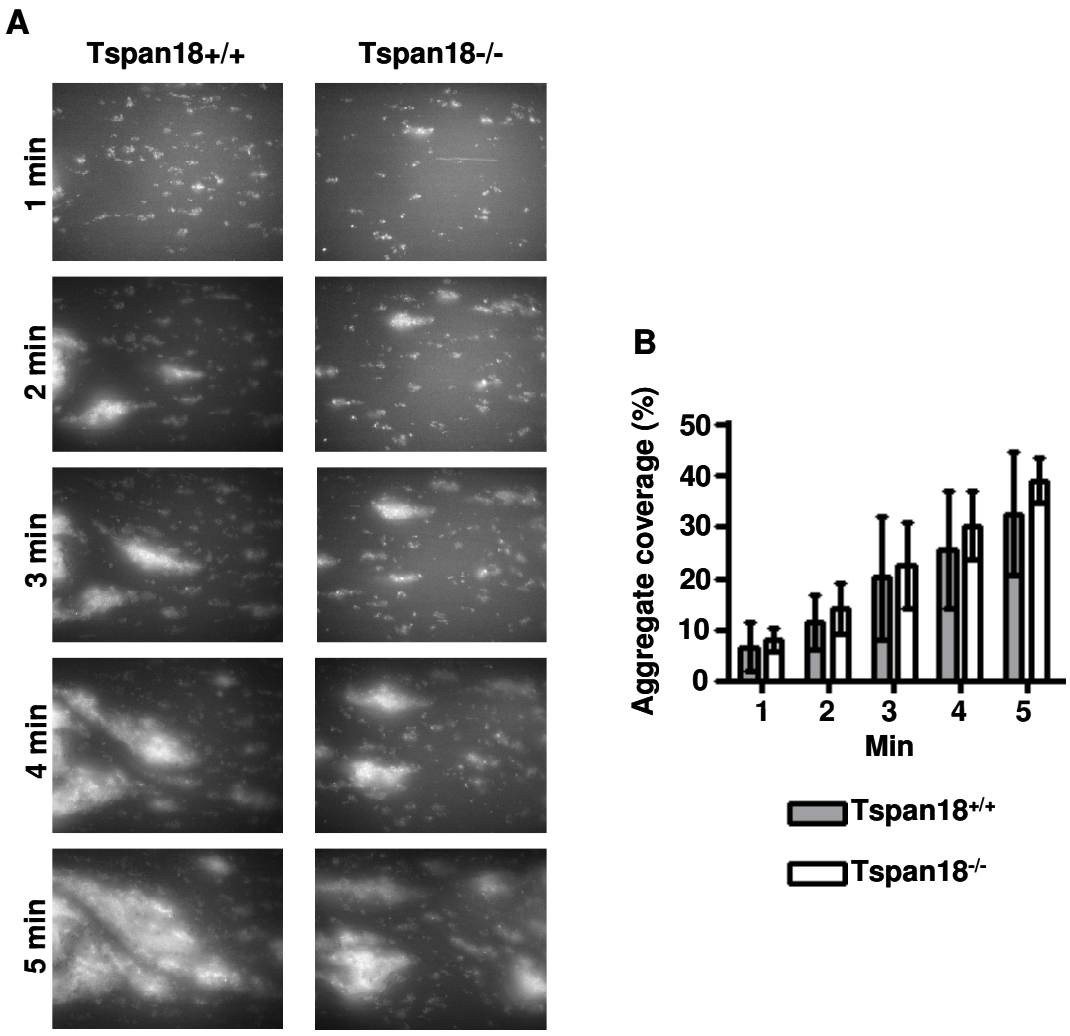

Figure 3.14 – Aggregate formation under venous shear conditions in the Tspan18 knockout platelets is normal. Whole blood from wildtype and Tspan18 deficient mice was perfused over a collagen-coated flow cell (30 µg/ml) using the Fluxion Bioflux system at a shear rate of 300s-1. Representative fluorescence images at minute-interval time points show normal aggregate formation by the Tspan18 deficient platelets (A). Coverage of the flow cell by aggregates was measured at minute intervals, using thresholding in ImageJ (B). Data were normalised by arcsin transformation and analysed by two-way ANOVA with Bonferroni post test. Error bars represent standard error of the mean from 3 pairs of mice.

3.3.7 Thrombus formation *in vivo* is normal in Tspan18 deficient mice

To provide further physiological assessment of the role of Tspan18 *in vivo*, two different models of thrombus formation were used to provide assessment of thrombus formation and the dynamics of thrombus growth. These were carried out by Ina Theilmann in the lab of Bernard Nieswandt, Wurzburg, Germany.

The first model used was mechanical injury of the abdominal aorta, during which the exposed vessel was injured using forceps and blood flow was monitored with a Doppler flow-meter. Previous studies have demonstrated that thrombus formation in this model is mainly triggered by collagen (Braun et al., 2009; Grüner et al., 2005). No significant difference in vessel occlusion was observed in Tspan18 deficient mice in comparison to wildtype control mice (figure 3.16).

The second model used was the $FeCl_3$ injury model, in which exteriorised mesentery arterioles were exposed to chemical injury by topical application of $FeCl_3$. The platelets were labelled with a fluorescent stain and thrombus formation monitored via fluorescence microscopy. This model of thrombus formation has previously been shown to be a highly thrombin dependant process, as loss of GPVI is only partially protective against thrombus formation (Braun et al., 2009; Renné et al., 2005). There was no difference observed in the onset of thrombus formation, as the first thrombi appeared in Tspan18 deficient mice at a similar time as in wildtype mice (figure 3.17, A). Additionally, there was no difference in the time to complete occlusion of the vessel (figure 3.17, B).

These *in vivo* models provided an insight into the physiological affects of Tspan18 deficiency on thrombus formation, showing that Tspan18 does not play a role in thrombus formation in these particular *in vivo* models.

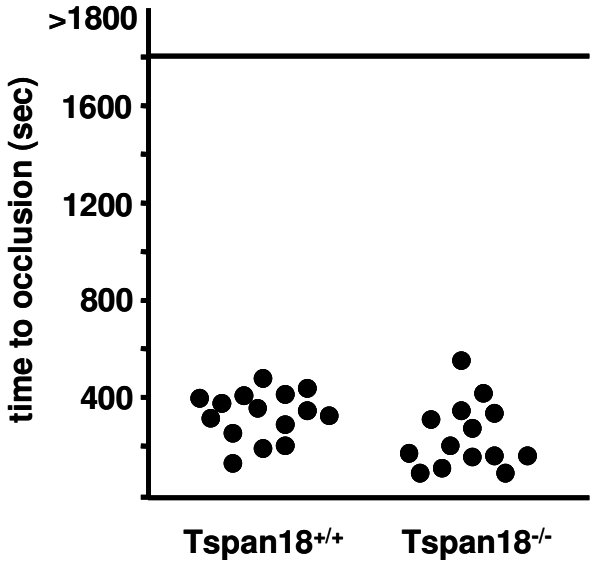

Figure 3.15 – Thrombus formation *in vivo* is normal in Tspan18 deficient mice following mechanical injury. Mice were anaesthetised, the abdominal aorta was exposed and the vessel was mechanically injured through a single firm compression with forceps. Blood flow was monitored with a Doppler flow meter and time until complete occlusion of the vessel measured. Each symbol represents one individual. Data were analysed by T-test. Data collated by Ina Theilmann from the Nieswandt laboratory, Wurzburg, Germany, as part of a collaboration.

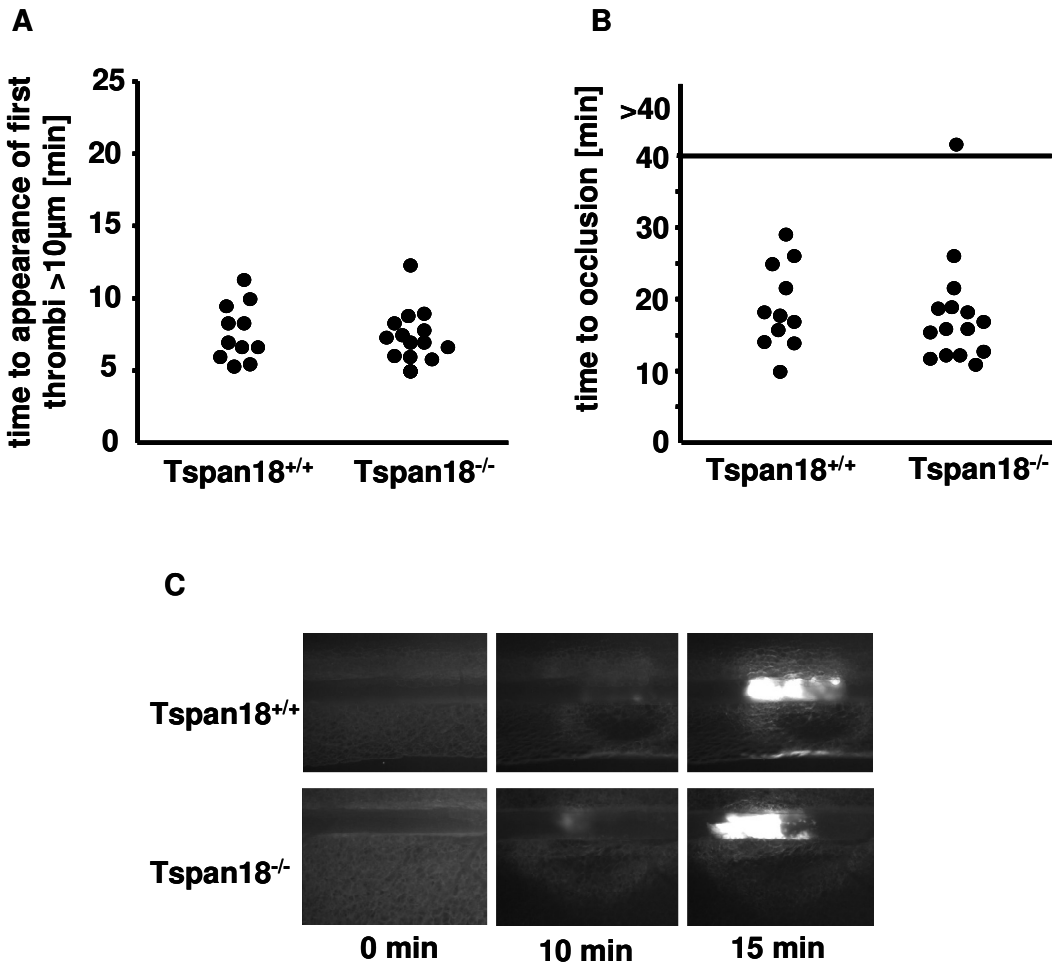

Figure 3.16 – Thrombus formation *in vivo* is normal in Tspan18 deficient mice following chemical injury. Mice were anaesthetised and the mesentery was exteriorised through an abdominal incision. Platelets were fluorescently labelled (Dylight 488 conjugated anti-GPIX Ig derivative). Small mesenteric arterioles were exposed to $FeCl_3$ induced chemical injury via topical application. The time for appearance of the first thrombi (A) and the time until complete occlusion of the vessel (B) were measured using fluorescence intravital microscopy. Representative fluorescence images before and after injury are shown (C). Each symbol represents one individual. Data were analysed by T-test. Data collated by Ina Theilmann from the Nieswandt laboratory, Wurzburg, Germany, as part of a collaboration.

3.3.8 Haemostasis is disrupted in Tspan18 deficient mice

To provide a broad analysis of haemostasis in the Tspan18 deficient mice, a tail bleeding assay was used. Given the observation of normal thrombus formation in Tspan18 deficient mice and the relatively mild platelet phenotype observed, a major disruption to haemostasis was not predicted. Mice were anaesthetised, 3 mm was amputated from the tip of the tail and blood loss was monitored over a maximum period of 20 minutes. Due to restrictions on the Home Office licence permitting this work, the mice were limited to a maximum loss of 15% of total blood, calculated by bodyweight.

The Tspan18 deficient mice bled significantly more than wildtype littermates (figure 3.18). Additionally, several of the Tspan18 deficient mice bled severely enough to cause premature termination of the assay by cauterisation of the wound, to prevent blood loss excessive to that permitted by the licence. The phenotype observed could therefore have been more severe if the assay had been permitted to continue. The Tspan18 deficient mice appear to show a heterogeneous population, in which some individuals bleed but other individuals did not bleed, whereas the wildtype mice demonstrate a homogenous population in which the variance is small, and none of the mice bleed. The variable phenotype observed is discussed in more detail in section 3.4 (discussion of this chapter) and in chapter 5.

These data demonstrate a clear disruption to haemostasis in Tspan18 deficient mice, despite only a mild platelet functional defect and normal thrombus formation *in vivo*.

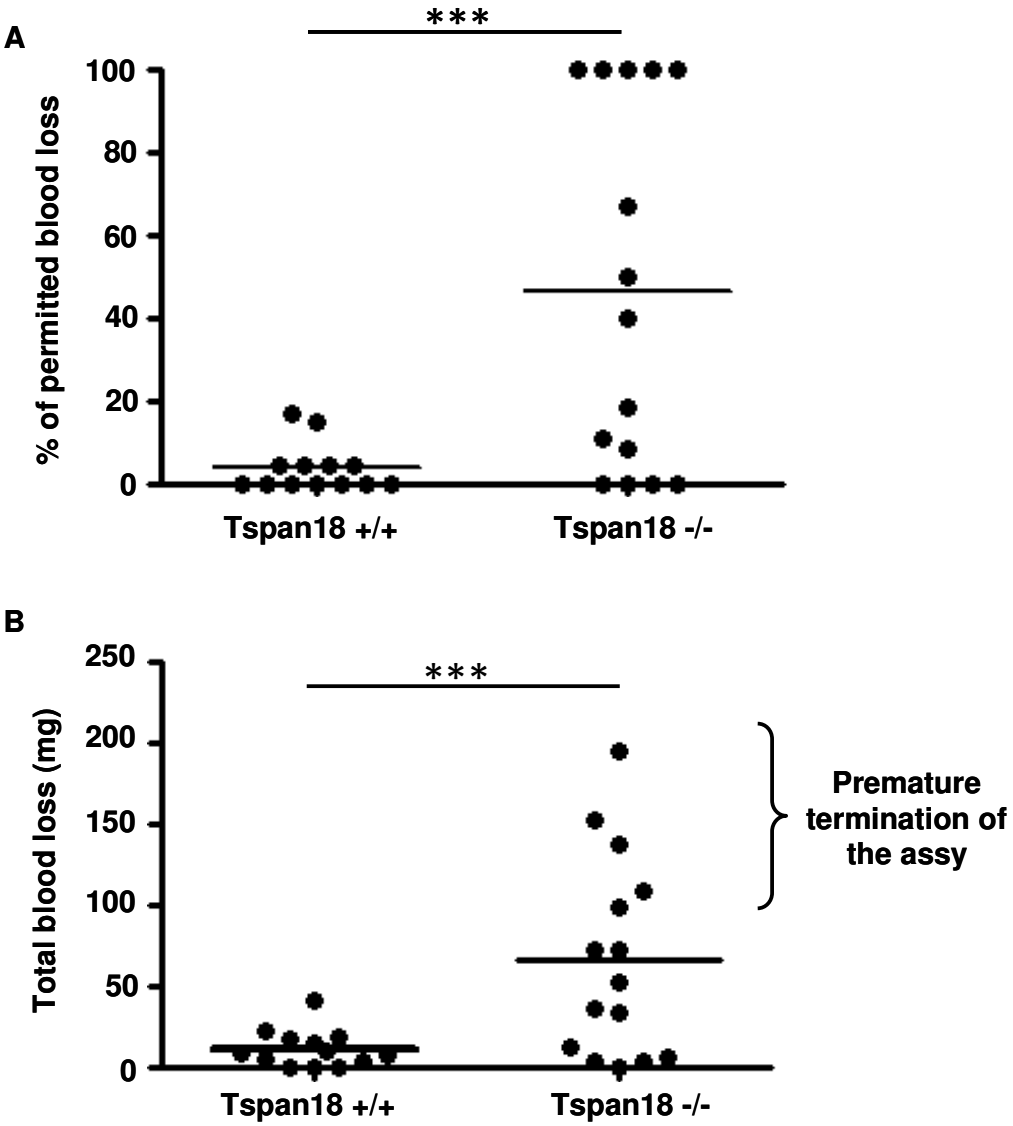

Figure 3.17 – Impaired haemostasis in the tail bleeding assay in Tspan18 deficient mice. The tail tip of anaesthetised mice was amputated and amount of blood lost was measured. Each symbol represents an individual. Data were analysed by Fisher's exact test; individuals were ranked as 'bleeding' or 'not bleeding' where 'bleeding' was defined as one or more drop of blood, equivalent to 30 µl lost (*** denotes $P < 0.001$). Data displayed is either the % of total permitted blood loss (A); each mouse was permitted to lose a maximum of 15% of total blood determined by body weight, due to restrictions on the Home Office animal licence, or as total volume of blood lost with a bracket to indicate termination of the assay for individuals which lost 100% of permitted blood (B).

3.4 DISCUSSION

The main aim of the work in this chapter was to characterise the role of Tspan18 in platelets by using the Tspan18 knockout mouse. When platelet function was assessed, defective aggregation, secretion and spreading was observed, specifically downstream of the platelet collagen receptor GPVI, though induction of tyrosine phosphorylation from GPVI itself was normal. Additionally, Ca^{2+} signalling following CRP stimulation and SOCE were reduced in Tspan18 deficient platelets. Together, these data suggested a role for Tspan18 in platelet activation, potentially via regulation of Ca^{2+} signalling, specifically downstream of GPVI. In addition to the specific, yet mild, defect in platelet activation, the Tspan18 deficient mice displayed a severe disruption to haemostasis, as they bled significantly more than wildtype controls. Additionally, thrombus formation was shown to be normal in two different *in vivo* models.

Although the precise role of Tspan18 on platelets is not known, the data presented in this chapter suggest a specific function for this tetraspanin in regulation of the GPVI signalling pathway. As the GPVI signalling pathway is reliant on Ca^{2+} signalling, and specifically SOCE (Braun et al., 2009; David Varga-Szabo, Braun, et al., 2008), it is possible that Tspan18 could regulate Ca^{2+} signalling, or more specifically, SOCE in platelets. This hypothesis is supported by previous studies on Tspan18 which reported a potential role for Tspan18 in Ca^{2+} signalling in a cell line over-expression system (Colombo, 2010).

Interestingly, some of the functional defects observed in Tspan18 deficient platelets replicated similar observations made in platelets deficient for the SOCE channel Orai1. The mice used to study Orai1 in platelets were generated as chimeras; lethally irradiated wildtype mice, which received a transplant of Orai1$^{-/-}$ or control cells to reconstitute the haematopoietic system, as the whole body knockouts displayed early lethality and growth retardation, making study of platelets difficult (Braun et al., 2009). Similar to the results described in this chapter, Orai1 deficient platelets displayed defective aggregation specifically downstream of GPVI, and also a reduction in SOCE and Ca^{2+} signalling following activation by platelet agonists (Braun et al., 2009). These similarities suggest that Tspan18 and Orai1 could share a common signalling pathway, and that Tspan18 could have a role in interaction with and regulation of Orai1 or another member of the SOCE pathway.

However, the phenotypes observed in Orai1 deficient platelets were more severe than those observed for Tspan18 deficient platelets; a reduction in Ca^{2+} signalling was observed downstream of all platelet agonists, not just CRP, and there was a disruption to thrombus formation *in vivo*, as assessed by the mechanical injury method (Braun et al., 2009). The cause for this difference in severity of phenotypes may be due to the level of regulation that Tspan18 might provide within the SOCE pathway. It could be possible that Tspan18 is important in fine-tuning the process of SOCE, rather than entirely regulating its function. In which case, removal of Tspan18 could disrupt the efficiency of Ca^{2+} entry, but might not inhibit it completely, leading to less severe phenotypes. This could also explain the subtle phenotype observed in reduced SOCE following stimulation by thapsigargin in Tspan18 deficient

platelets. In comparison to Orai1 deficient platelets, the alteration in SOCE is markedly reduced (Bergmeier et al., 2009; Braun et al., 2009). Again, if Tspan18 has a role in fine-tuning the mechanism of extracellular Ca^{2+} entry via Orai1, then it's removal may well disrupt Ca^{2+} entry without blocking it completely. Removal of Orai1 removes the ability of Ca^{2+} to enter the cell from the extracellular environment, whereas removal of Tspan18 may just disrupt this process resulting in a lower rate of Ca^{2+} flux rather than complete inhibition of this process. Differences observed across different studies are not an uncommon occurrence; previous studies on the role of Orai1 in platelets have not always produced similar results. A model utilising a loss of function mutant for Orai1 ($Orai1^{R93W}$) demonstrated a reduction in Ca^{2+} mobilisation in $Orai1^{R93W}$ platelets, but did not report the same platelet functional defects observed in $Orai1^{-/-}$ deficient platelets (Bergmeier et al., 2009). This demonstrates how variations in experimental design and differences across different mouse models can lead to differences in severity and appearance of specific phenotypes.

The potential role of Tspan18 in platelet Ca^{2+} signalling needs further investigation, as although the Ca^{2+} signalling experiments undertaken in this chapter highlighted a disruption to Ca^{2+} mobilisation in the absence of Tspan18, the exact role of this tetraspanin could not be determined. In the presence of physiological levels of extracellular Ca^{2+} (1.5 mM), Tspan18 deficient platelets had a reduced SOCE capacity when stimulated with the GPVI agonists CRP and collagen. When Ca^{2+} measurements were taken following stimulation with platelet agonists in Ca^{2+}-free media, the signal could not be detected above the background noise, therefore no conclusions could

be drawn on the release of Ca^{2+} from intracellular stores following agonist stimulation (data not shown). However, in experiments utilising thapsigargin in Ca^{2+}-free media and then in the presence of 1.5 mM Ca^{2+}, a reduction in both intracellular store release and influx of Ca^{2+} from the extracellular environment was observed. This may suggest that Tspan18 has a role at several different levels of Ca^{2+} signalling in platelets, and future experiments to provide a more in depth analysis of the Ca^{2+} signalling in Tspan18 deficient platelets would be useful.

Additionally, following the observations made during measurement of Ca^{2+} signalling in the platelets, it may be useful to repeat the aggregation experiments and the measurement of protein phosphotyrosine induction experiment in the presence of physiological levels of Ca^{2+}. These experiments were completed in Tyrode's buffer without added Ca^{2+}, and as such more severe phenotypes could potentially be masked. If Tspan18 has a role in SOCE, as suggested by the changes in Ca^{2+} signalling following thapsigargin stimulation, then completing aggregation analysis in the presence of extracellular Ca^{2+} might demonstrate a more severe difference in the aggregation capability of Tspan18 deficient and wildtype platelets due to the lack of Ca^{2+} influx from the extracellular environment. This might also explain the slight difference in phosphotyrosine signalling observed for band pp135. The importance of taking extracellular Ca^{2+} into consideration in future experiments is further supported by the results observed during the aggregation experiments conducted in PRP. Defective aggregation was observed at higher does of CRP and at low doses of collagen in PRP, whereas defective aggregation in washed platelets was less severe. PRP

contains more extracellular Ca^{2+}, as the platelets have not been washed out of the plasma. It is therefore possible that the additional extracellular Ca^{2+} in PRP demonstrates a more marked phenotype within the Tspan18 deficient platelets, suggesting a SOCE defect.

Perhaps the most surprising result within this chapter was that despite normal thrombus formation and only a mild platelet functional phenotype in Tspan18 deficient mice, these animals had a severe disruption to haemostasis. It is unlikely that the increase in bleeding was caused by platelet functional defects, as the platelet phenotypes were so mild in the Tspan18 deficient mice, and mice lacking GPVI display only moderate bleeding (B Nieswandt, Schulte, et al., 2001). Additionally, the tail bleeding data clearly represents the Tspan18 deficient mice as a heterogeneous population, in which some individuals bleed and some do not, as the variance in the population was large. This is despite the fact that the disruption to platelet activation was consistently observed across all individuals, showing a clearly homogenous response. This suggests that another cell or tissue might be the driving force behind disrupted haemostasis. Other cells such as the endothelium, which is responsible for release of clotting factors such as vWF (Kanaji, Fahs, Shi, Haberichter, & Montgomery, 2012) and FVIII (Everett, Cleuren, Khoriaty, & Ginsburg, 2014), and vascular smooth muscle cells, which regulate vasoconstriction (Wilson et al., 2005), play vital roles in haemostasis. This suggests that Tspan18 could be important in one or more of these cell types in regulation of haemostasis, in addition to its role in the GPVI signalling pathway.

Key questions still need to be addressed in order to better understand the role of Tspan18 within the vasculature. Firstly, the potential role for Tspan18 in Ca^{2+} signalling and SOCE needs further investigation in order to better understand the role of Tspan18 in the GPVI signalling pathway. Secondly, the role of this tetraspanin in non-haematopoietic cells needs to be evaluated in order to assess the potential affect that Tspan18 could be having on haemostasis. The work in the following chapters aimed to investigate both of these areas further.

CHAPTER 4

TSPAN18 ACTIVATES Ca^{2+} SIGNALLING AND INTERACTS WITH THE STORE OPERATED Ca^{2+} ENTRY CHANNEL ORAI1

4.1 INTRODUCTION

4.1.1 Store operated Ca^{2+} entry

Following receptor activation at the cell surface, the primary phase of Ca^{2+} mobilisation occurs via release of Ca^{2+} from intracellular stores, often the ER, via IP_3 receptors (Berridge & Irvine, 1984; Smyth et al., 2010). Reduced Ca^{2+} concentration within the ER induces influx of Ca^{2+} from the extracellular environment during the secondary phase of Ca^{2+} mobilisation, known as SOCE. SOCE is important in maintaining sustained levels of Ca^{2+} in the cell and for replenishing depleted intracellular Ca^{2+} stores (Smyth et al., 2010). SOCE relies on STIM1 which acts as a Ca^{2+} sensor in the ER, and the Orai family of proteins (Orai1, 2 and 3), which are vital as the pore-forming subunits of channels at the plasma membrane (Smyth et al., 2010). Upon depletion of Ca^{2+} in the ER, a conformational change and oligomerization of STIM1 occurs, followed by rearrangement of STIM1 in the ER to punctate structures close to the plasma membrane (Liou, Fivaz, Inoue, & Meyer, 2007). An interaction between STIM1 and Orai at the plasma membrane induces multimerisation of Orai allowing formation of functional channels and flux of Ca^{2+} from the extracellular environment into the cell (Hou et al., 2012). As the basic outline of Ca^{2+} signalling and SOCE in figure 4.1 demonstrates, increases in intracellular Ca^{2+} concentration can then activate downstream targets such as calcineurin, leading to NFAT activation and transcription.

4.1.2 The NFAT/AP-1 luciferase reporter assay

The NFAT/AP-1 luciferase reporter assay is a useful tool for providing highly sensitive measurements of Ca^{2+} signalling. This transcriptional reporter utilises promoters for both NFAT and AP-1, and is therefore maximally activated by combined Ca^{2+} and mitogen-activated protein kinase (MAPK) signalling pathways (M G Tomlinson et al., 2007). The NFAT promoter of this reporter is activated by increased intracellular Ca^{2+}, which induces activation of the protein phosphatase calcineurin via the Ca^{2+} binding protein calmodulin. When activated, calcineurin dephosphorylates cytosolic NFAT within the serine rich region in the C-terminal tail, exposing a nuclear transduction signal. NFAT then translocates to the nucleus, where it interacts with other transcription factors and regulates gene transcription (Crabtree & Olson, 2002). The AP-1 promoter is activated downstream of the MAPK signalling cascade. Formation of AP-1 occurs via heterodimerisation of the transcription factors c-Jun and c-Fos, after upstream phosphorylation by the JNK and ERK pathways respectively (Karin, 1995). In cells transfected with the NFAT/AP-1 luciferase reporter, culmination of the MAPK and Ca^{2+} signalling pathways leads to AP-1 and NFAT activation; transcription of luciferase occurs and the magnitude of signalling assessed through addition of luciferin and measurement of luminescence (figure 4.1). The use of PMA to activate the MAPK pathway via PKC and RasGRP (Landau, 1982; Tognon et al., 1998) and ionomycin to raise free intracellular Ca^{2+} levels (Liu & Hermann TE, 1978) can activate the reporter (figure 4.1). The use of cyclosporin A, an immunosuppressant drug used after transplantation, to inhibit calcineurin and prevent phosphorylation and nuclear translocation of

NFAT (Handschumacher, Harding, Rice, Drugge, & Speicher, 1984; Mattila et al., 1990) inhibits the reporter (figure 4.1).

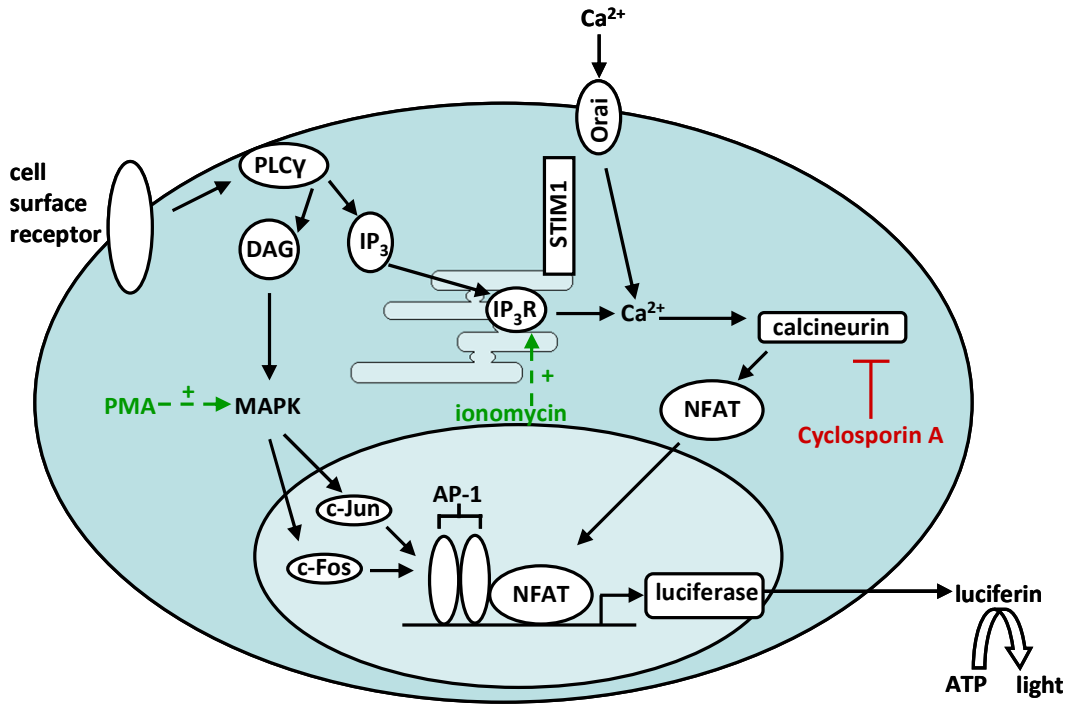

Figure 4.1 – Model of NFAT/AP-1 reporter activation. Measurement of Ca^{2+} and MAPK signalling pathways within cells is possible using the NFAT/AP-1 luciferase reporter assay. Use of PMA and ionomycin can induce activation of MAPK and Ca^{2+} pathways respectively, leading to luciferase transcription. The calcineurin inhibitor, cyclosporin A, inhibits downstream NFAT activation and therefore also luciferase transcription.

4.1.3 Tspan18 in NFAT activation and Ca^{2+} signalling

In previous studies using the NFAT/AP-1 luciferase reporter assay, Tspan18 was shown to be unique across a panel of six different tetraspanins, including CD9, CD63, CD151, Tspan32 and Tspan9, in its ability to activate NFAT signalling in DT40 B-cell and Jurkat T-cell lines (Colombo, 2010). It was confirmed that Tspan18 activated the luciferase reporter via the NFAT promoter, rather than the AP-1 promoter, which suggested a role for Tspan18

in upstream Ca^{2+} signalling (Colombo, 2010). This work also demonstrated that Tspan18 induced NFAT activation independently of non-receptor tyrosine kinases of Src, Syk and BtK families, PLCγ, and IP_3 receptors; over-expression of Tspan18 still promoted NFAT activation in specific DT40 knockout cell lines for these proteins (Colombo, 2010). The activation of NFAT by Tspan18 was also observed, using fluorescence microscopy, in HeLa cells containing green fluorescent protein (GFP)-tagged NFAT; translocation of activated NFAT-GFP to the nucleus was increased in cells transfected with Tspan18 in comparison to mock transfected cells (Tomlinson, unpublished data). Together, these data suggested a role for Tspan18 in regulation of Ca^{2+} signalling downstream of Ca^{2+} release from intracellular stores.

The work in the previous chapter outlined a role for Tspan18 within the GPVI signalling pathway and therefore in platelet activation, and although the precise mechanism was not elucidated, the data again suggested a role for this tetraspanin within the Ca^{2+} signalling pathway. Although previous studies have implicated Tspan18 in regulation of Ca^{2+} signalling, the precise mechanism of action and the potential partner protein(s) of this tetraspanin are still not known.

4.2 AIMS

There were three key aims driving the work in this chapter. Firstly, to identify whether a specific domain within the extracellular region of Tspan18 is important for activation of a Ca^{2+}-responsive NFAT reporter. Secondly, to determine whether Orai1 is important for Tspan18 induced activation of the NFAT reporter, and finally to determine whether Tspan18 interacts with the SOCE proteins STIM1 or Orai. The NFAT/AP-1 luciferase reporter assay was used to identify the domains of Tspan18 which are important in NFAT activation and to determine whether Tspan18 requires Orai1 in this process. An immunoprecipitation approach was used to identify potential Tspan18 interacting proteins within the SOCE signalling pathway.

4.3 RESULTS

4.3.1 Importance of the Tspan18 variable region in Tspan18 induced activation of a Ca^{2+} sensitive reporter in DT40 B cells

Findings from previous studies (Colombo, 2010), demonstrated that Tspan18 was specific across a panel of tetraspanins in its ability to activate an NFAT/AP-1 transcriptional reporter. This work also suggested that Tspan18 activated the reporter through regulation of Ca^{2+} mobilisation. To investigate this further, and to confirm these findings, the NFAT/AP-1 reporter was used.

Tspan18 was expressed alongside the Ca^{2+} responsive NFAT/AP-1 luciferase reporter in DT40 B cells. Cells were left unstimulated, inhibited with the calcineurin inhibitor cyclosporin A, or were treated with PMA and ionomycin as a positive control; PMA activates the MAPK signalling pathway and thus the AP-1 promoter and ionomycin activates Ca^{2+} signalling which leads to downstream NFAT activation, culminating in maximal activation of the reporter. In agreement with the preceding data, expression of Tspan18 induced a substantial increase in NFAT activation in unstimulated cells (figure 4.2, A). This increase was significant in comparison to both a mock transfection, which contained only an empty vector (pEF6) as a negative control, and to expression of another tetraspanin, CD9. When cells were treated with cyclosporin A, NFAT activation was inhibited, even when Tspan18 was expressed, demonstrating that Tspan18 is dependant on calcineurin (figure 4.2, A). Maximal activation of the reporter was observed in all transfections after treatment with PMA and ionomycin (figure 4.2, B). To

confirm protein expression of the FLAG-tagged tetraspanin constructs, samples were separated by SDS-PAGE electrophoresis and western blotted with an anti-FLAG antibody (figure 4.2, C).

In agreement with previous findings, these data demonstrate the ability of Tspan18 to activate NFAT and also highlights the dependence of this process on calcineurin, suggesting a role for Tspan18 in Ca^{2+} signalling.

Previous studies attempted to investigate which domains of Tspan18 were important in activating NFAT by using a chimeric construct. In the chimera, the transmembrane and intracellular regions of human Tspan18 were replaced with those of CD9. This chimera was able to activate NFAT (Colombo, 2010), demonstrating the importance of the extracellular region of Tspan18 in NFAT activation.

In order to locate more specifically which domain of Tspan18 is important for NFAT activation, a new chimera was made, in which only the variable region within the large extracellular loop of Tspan18 was present and the rest of the protein was CD9 (figure 4.3, A). The chimera, Tspan18 or CD9 were expressed alongside the NFAT/AP-1 luciferase reporter in DT40 B-cells and cells were left unstimulated, or treated with PMA and ionomycin as previously described. Expression of the chimera induced an increase in NFAT activation similar to that observed when Tspan18 was expressed, and which was significant in comparison to both mock transfected control and CD9 (figure 4.3, B). Maximal activation of the reporter was observed in all conditions after treatment with PMA and ionomycin (figure 4.3, C). As previously, similar protein expression of the FLAG-tagged tetraspanin constructs was confirmed

by SDS-PAGE electrophoresis and western blotting (figure 4.3, D). An opposite chimeric construct was also made, in which the variable region of CD9 was swapped into the structure of Tspan18. However, this construct could not be successfully expressed in the DT40 B cells (data not shown); therefore the ability of this construct to activate the NFAT luciferase reporter could not be assessed.

These data demonstrate the importance of the variable region of Tspan18 in activation of Ca^{2+} signalling, and suggest that only this region is required to induce NFAT activation, in the context of an intact tetraspanin.

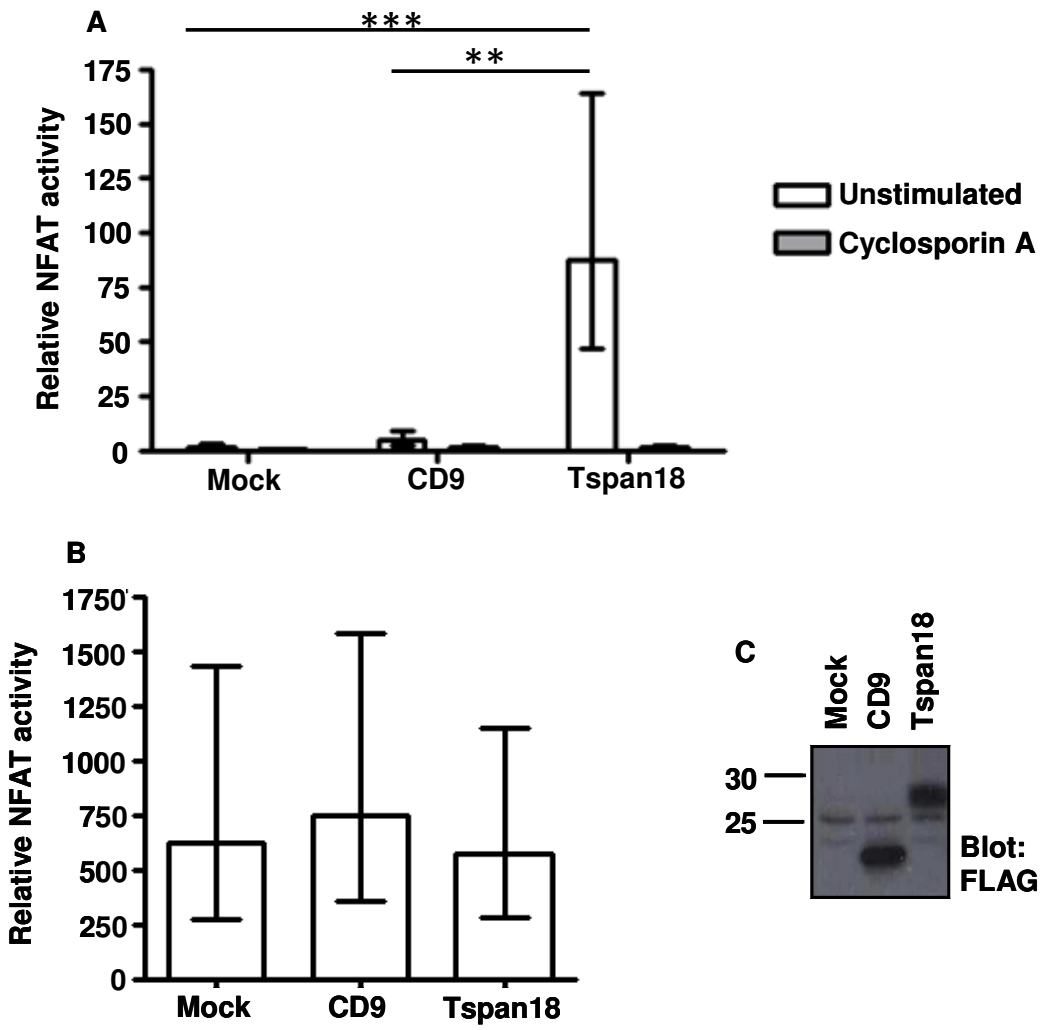

Figure 4.2 – Tspan18 activates a Ca^{2+} responsive NFAT luciferase reporter in DT40 B cells. DT40 B cells were transfected via electroporation with an NFAT-luciferase reporter, β-galactosidase expression construct, and either empty vector control, FLAG-tagged CD9, or FLAG-tagged Tspan18. Cells were left unstimulated or treated with the calcineurin inhibitor cyclosporin A (A), or were stimulated with PMA and ionomycin (B). Luciferase activity was measured in a luminescence plate reader after addition of luciferin. All data were corrected for β-galactosidase values, normalised by logarithmic transformation, and analysed by one-way ANOVA and Tukey's multiple comparison test (** denotes $P < 0.01$, *** denotes $P < 0.001$). Error bars represent the standard error of the mean from 3 separate experiments and were calculated asymmetrically due to logarithmic manipulation of the data; all values were converted back to linear values for presentation. Whole cell lysates from all experiments were separated by SDS-PAGE and western blotted with an anti-FLAG antibody; a representative blot is shown (C).

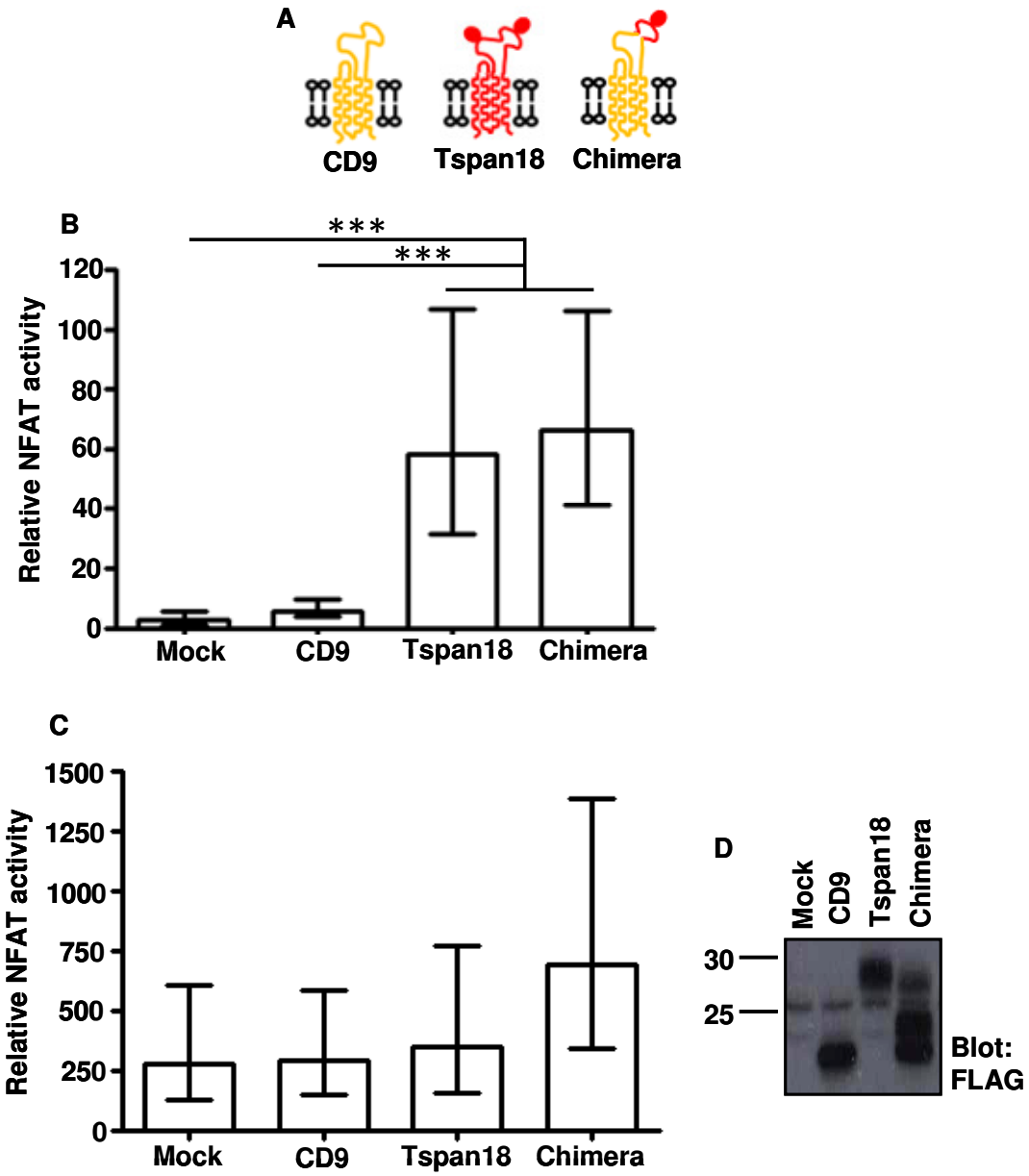

Figure 4.3 - The variable region of Tspan18 is sufficient to activate NFAT, in the context of an intact tetraspanin. A chimeric construct was made from CD9 and Tspan18, which included the variable region from the large extracellular loop of Tspan18 (A). DT40 B cells were transfected via electroporation with NFAT-luciferase reporter, β-galactosidase expression construct, and either empty vector control, FLAG-tagged CD9, FLAG-tagged Tspan18, or FLAG-tagged chimera. Cells were left unstimulated (B), or were stimulated with PMA and ionomycin (C). Luciferase activity was measured in a luminescence plate reader after addition of luciferin. All data were corrected for β-galactosidase values, normalised by logarithmic transformation, and analysed by one-way ANOVA and Tukey's multiple comparison test (*** denotes $P < 0.001$). Error bars represent the standard error of the mean from 6 separate experiments and were calculated asymmetrically due to logarithmic manipulation of the data; all values were converted back to linear values for presentation. Whole cell lysates from all experiments were separated by SDS-PAGE and western blotted with an anti-FLAG antibody; a representative blot is shown (D). This work was completed in collaboration with an undergraduate student, Adam Peall.

4.3.2 Dominant negative Orai1 inhibits Tspan18 induced NFAT activation

Data from previous studies had outlined a role for Tspan18 in Ca^{2+} signalling downstream of release of Ca^{2+} from intracellular stores, but upstream of calcineurin activation (Colombo, 2010). The resulting hypothesis therefore, was that Tspan18 might have a role in regulation of SOCE. To investigate the potential role of Tspan18 in SOCE, a dominant negative form of the SOCE channel Orai1, which has a mutation in the mouth of the channel causing loss of specificity for Ca^{2+}, was used (Gwack et al., 2007). In order to form functional pore-forming channels, Orai1 proteins cluster into multimer units (Hou et al., 2012; Mignen et al., 2008). Therefore expression of dominant negative Orai1 disrupts functional channel formation and reduces SOCE.

DT40 B-cells were transfected with the NFAT/AP-1 luciferase reporter and either Tspan18, dominant negative Orai1, Tspan18 and dominant negative Orai1, or dominant negative Orai1 and active calcineurin as a positive control. As previously, cells were left unstimulated, or were treated with PMA and ionomycin. Expression of Tspan18 alone induced a significant increase in NFAT activation above mock transfected control, as shown previously. However, when dominant negative Orai1 was co-expressed, a complete inhibition of Tspan18 induced NFAT activation was observed (figure 4.4, A). Dominant negative Orai1 also inhibited PMA and ionomycin signalling (figure 4.4, B); the predicted reduction of Ca^{2+} influx into the cell, caused by the mutated channel, would lead to reduced downstream calcineurin activation and therefore failure to activate the NFAT promoter of the reporter. When active calcineurin was expressed, an increase in NFAT activation was observed in both unstimulated (figure 4.4, A), and PMA/ionomycin treated

cells (figure 4.4, B), even though dominant negative Orai1 was present. The active calcineurin provided a positive control by bypassing the need for functioning Orai1 channels and increased Ca^{2+} concentration, therefore directly inducing NFAT activation. As previously, protein expression of FLAG-tagged Tspan18 and Myc-tagged dominant negative Orai1 was confirmed by SDS-PAGE electrophoresis and western blotting (figure 4.4, C).

This finding demonstrates the dependence of Tspan18 on functioning Orai1 channels in order to induce Ca^{2+} signalling and NFAT activation. This lends further evidence to the hypothesis that Tspan18 may regulate SOCE.

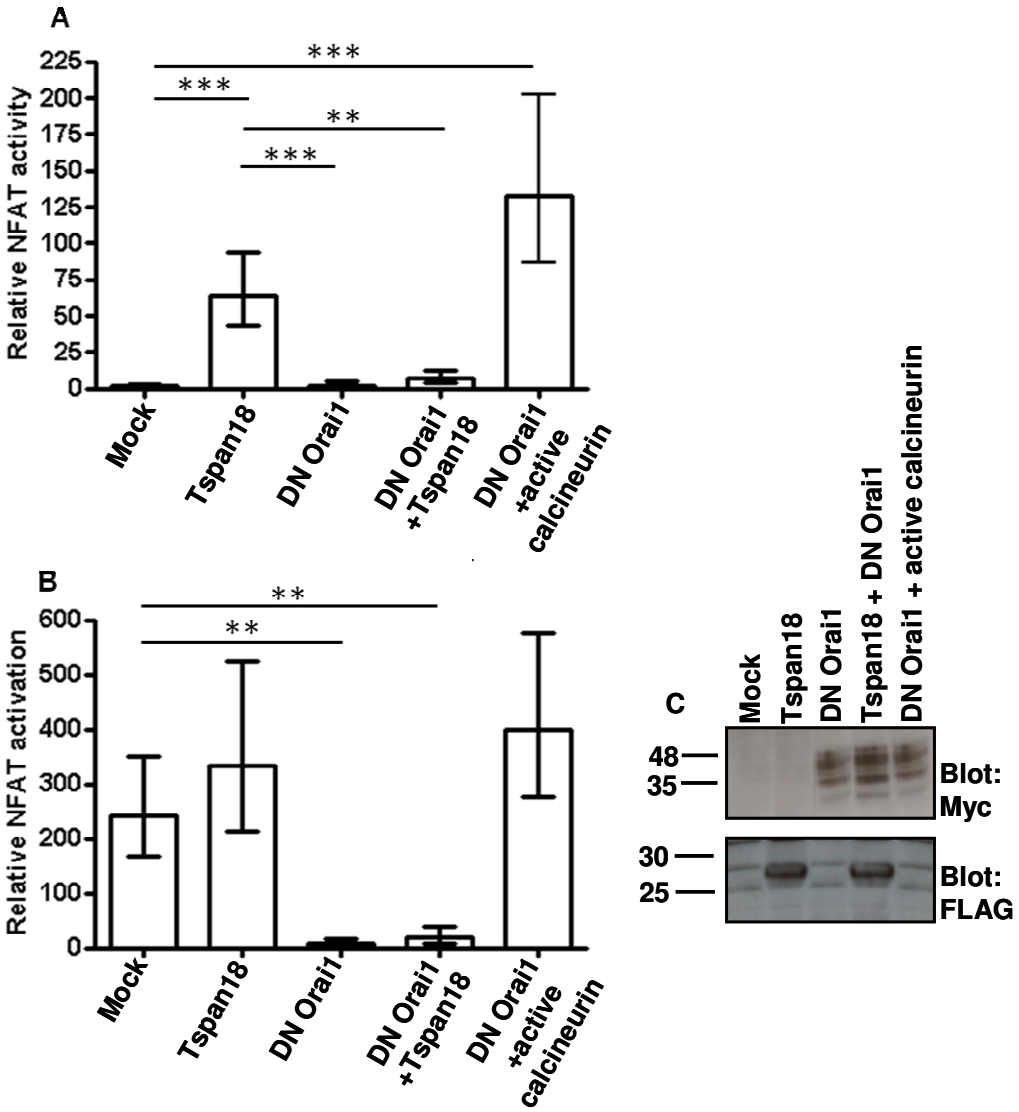

Figure 4.4 - Dominant-negative Orai1 inhibits Tspan18-induced NFAT activation. DT40 B cells were transfected via electroporation with NFAT-luciferase reporter, β-galactosidase expression construct, and either empty vector control, FLAG-tagged Tspan18, or Myc-tagged dominant negative (DN) Orai1. As a positive control, active calcineurin was used. Cells were left unstimulated (A) or stimulated with PMA and ionomycin (B). Luciferase activity was measured in a luminescence plate reader after addition of luciferin. All data were corrected for β-galactosidase values, normalised by logarithmic transformation, and analysed by ANOVA and Tukey's multiple comparison test (** denotes $P < 0.01$, *** denotes $P < 0.001$). Error bars represent the standard error of the mean from 6 separate experiments and were calculated asymmetrically due to logarithmic manipulation of the data; all values were converted back to linear values for presentation. Whole cell lysates from all experiments were separated by SDS-PAGE and western blotted with an anti-FLAG antibody and an anti-Myc antibody; a representative blot is shown (C). This work was completed in collaboration with a Masters student, Tammy Lloyd.

4.3.3 Tspan18 interacts with the Orai family of Ca^{2+} channels

To identify Tspan18-interacting proteins, focussing on potential partners from within the SOCE pathway, an immunoprecipitation approach was used. HEK293T cells were transfected with Myc-tagged Orai1, Orai2, Orai3, or STIM1 and either an empty vector negative control (pEF6), or FLAG-tagged Tspan18. Two different Orai1 constructs were used; Orai1 (a) and Orai1 (b). The cells were lysed in 1% digitonin lysis buffer, which is well established for identification of tetraspanin partner proteins (Haining et al., 2012). Following immunoprecipitation for the FLAG tag of Tspan18, samples were separated by SDS-PAGE and western blotted for the Myc tag of the proteins of interest. Band intensity was quantitated using the Odyssey infra-red imaging system (LI-COR). An interaction was detected between Tspan18 and Orai1, Orai2 and Orai3 when blotting immunoprecipitation samples with an anti-Myc antibody (figure 4.5, A). The relative band intensities demonstrated a significant increase above mock transfected control when Tspan18 was co-expressed with either of the Orai1 constructs, Orai2, or Orai3 (figure 4.5, panel B). The relative band intensity relating to the interaction between Tspan18 and Orai1 was much higher than that observed with Orai2 or Orai3 (figure 4.5, panel B). However, Orai2 and Orai3 were not expressed as highly as Orai1 in this system, as shown by the whole cell lysate anti-Myc western blot (figure 4.5, A). No interaction was observed between Tspan18 and the SOCE sensory molecule STIM1. Whole cell lysate samples blotted for the Myc tag confirmed expression of Orai1, Orai2, Orai3, and STIM1 and a FLAG blot confirmed expression of Tspan18 (figure 4.5, A).

The data presented here reveals an interaction between Tspan18 and the Orai channel family of SOCE proteins, which reinforces the hypothesis that Tspan18 may have a role in regulation of the SOCE pathway.

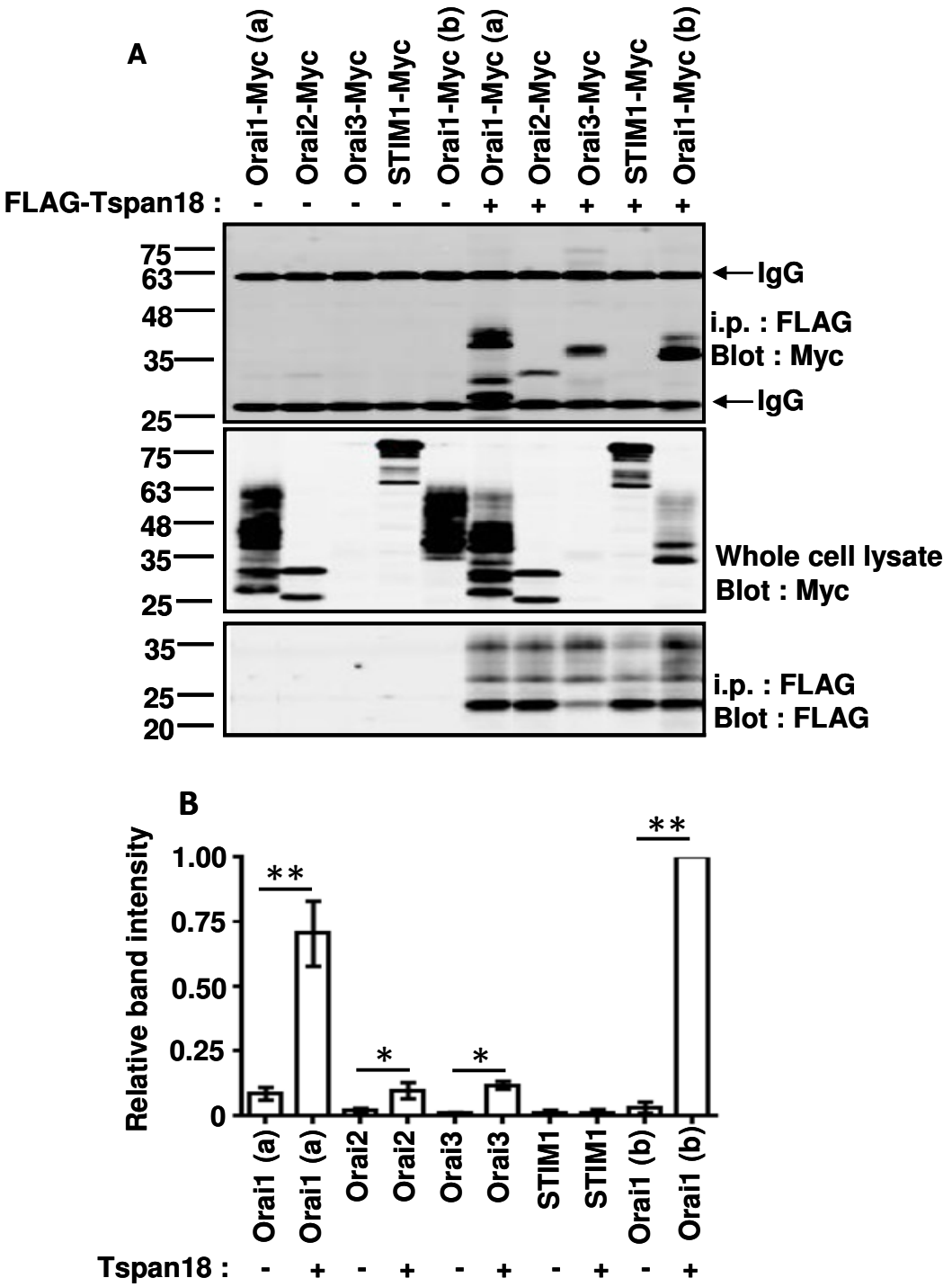

Figure 4.5 – Tspan18 interacts with the Orai family of Ca^{2+} channels. HEK293T cells were transfected using PEI with Myc-tagged Orai1, Orai2, Orai3 or STIM1 and either an empty vector control or FLAG-tagged Tspan18. Cells were lysed in 1% digitonin and immunoprecipitated with an anti-FLAG antibody. Samples were separated by SDS-PAGE and both immunoprecipitated and whole cell lysate samples blotted with anti-FLAG and anti-Myc antibodies, representative blots are shown (A). The blots were visualised using the Odyssey infra-red imaging system (LI-COR) and band intensity quantitatively measured (B). All data were normalised by logarithmic transformation and analysed by T-test (* denotes $P < 0.05$, ** denotes $P < 0.01$). Error bars represent standard error of the mean from 3 separate experiments.

4.3.4 Tspan18 forms a robust interaction with Orai1

Further study into the interaction between Tspan18 and Orai proteins was limited to Orai1. Orai1, rather than Orai2 or Orai3 has been previously shown to maintain the role of SOCE channel in platelets (Braun et al., 2009). As such, it was considered the most relevant potential partner protein in this project, and the most suitable to take forward into further studies.

To assess whether Tspan18 was unique in forming an interaction with the SOCE channel Orai1, an immunoprecipitation experiment in HEK293T cells was employed across a panel of different tetraspanins. The tetraspanins tested were CD9, CD63, CD151, Tspan32, Tspan9, Tspan18 and the Tspan18-CD9 chimera. After the HEK293T cells were transfected with Myc-tagged Orai1 and a FLAG-tagged tetraspanin, samples were lysed and blotted and band intensity quantitated, as described previously. The previously identified interaction between Tspan18 and Orai1 was observed and an interaction was also detected between the chimera and Orai1 when immunoprecipitation samples were blotted with an anti-Myc antibody (figure 4.6, A). When either Tspan18 or the chimera was expressed, the band intensity was significantly increased above mock transfected control containing empty vector (pEF6) (figure 4.6, B). However, the relative band intensity for the interaction between the chimera and Orai1 was reduced from the interaction between Tspan18 and Orai1, by approximately 75%. Additionally, a weak band was observed when Tspan32 was co-expressed alongside Orai1; relative band intensity was low, but still demonstrated a significant increase above control, suggesting that Orai1 may also be interacting with Tspan32. However, CD9, CD63, CD151 and Tspan9 did not

interact with Orai1 in this experiment. To act as a positive control, the well characterised tetraspanin-partner protein interaction between CD9 and CD9P-1 was used (S Charrin et al., 2001; Serru et al., 1999). CD9P-1 was successfully co-immunoprecipitated with CD9 (figure 4.6 A) and this was significant in comparison to mock transfected control (figure 4.6 B).

To assess how robust these interactions were, the experiment was repeated under more stringent lysis conditions. As previously, the panel of tetraspanins were expressed in HEK293T cells alongside Orai1. Samples were then lysed in 1% triton X-100 lysis buffer with 0.1% SDS, which disrupts tetraspanin microdomains and most weak interactions, including some tetraspanin-partner protein interactions (Stéphanie Charrin et al., 2009; Haining et al., 2012). Following immunoprecipitation and western blotting, band intensity was quantitated as described previously. Only the interaction between Orai1 and Tspan18 was maintained under stringent lysis conditions as the interactions with Tspan32 and the chimera were disrupted (figure 4.7, A) and this was significant when quantitated (figure 4.7, B). The interaction between CD9 and CD9P-1 was also lost in these stringent lysis conditions.

To further characterise the nature of the interaction between Tspan18 and Orai1 a cross-linking experiment was used. This allowed for comparison of this interaction with the well characterised interaction between Tspan14 and ADAM10 (Dornier et al., 2012; Haining et al., 2012), which was used as a positive control. It also allowed for further analysis of the interaction between the chimera and Orai1. Prior to lysis in 1% triton X-100 with 0.1% SDS and immunoprecipitation, the cells were treated with either the cell surface cross-linker DTSSP, or PBS control. DTSSP is a membrane impermeable chemical

cross-linker, linked by a spacer of 1.2 nm in length; if two cell surface proteins are closely associated, these proteins will be covalently cross-linked together by DTSSP, which can subsequently be cleaved with reducing agents. Samples were western blotted and band intensity measured as previously described. Following pre-treatment with DTSSP, the maximal level of interaction between Tspan18 and Orai1 was observed, whereas with pre-treatment with only PBS, there was a 50% decrease in band intensity which represented the interaction between Tspan18 and Orai1 (figure 4.8, A). Despite the reduction in band strength, the relative band intensity was still significantly increased from the control (figure 4.8, panel B). The interaction with the chimera and Orai1 was almost entirely lost in the stringent lysis conditions without the presence of the chemical cross-linker. Similarly, the interaction between ADAM10 and Tspan14 was almost entirely lost under stringent lysis without cross-linking.

Taken together, these data show that both Tspan18 and the chimera interact with the SOCE channel Orai1 and that this interaction is relatively specific across a panel of different tetraspanins. Additionally, the data demonstrates that the interaction between Tspan18 and Orai1 is very robust, being able to withstand stringent lysis conditions beyond that of the well characterised interactions between CD9 and CD9P-1 and Tspan14 and ADAM10. The cross-linking experiment also highlights the cell surface localisation of this interaction, as DTSSP, which is membrane impermeable, enhances the interaction. Finally, the data also demonstrates that the chimera has a reduced affinity for Orai1, as stabilisation of the interaction via cross-linking is required under stringent lysis conditions.

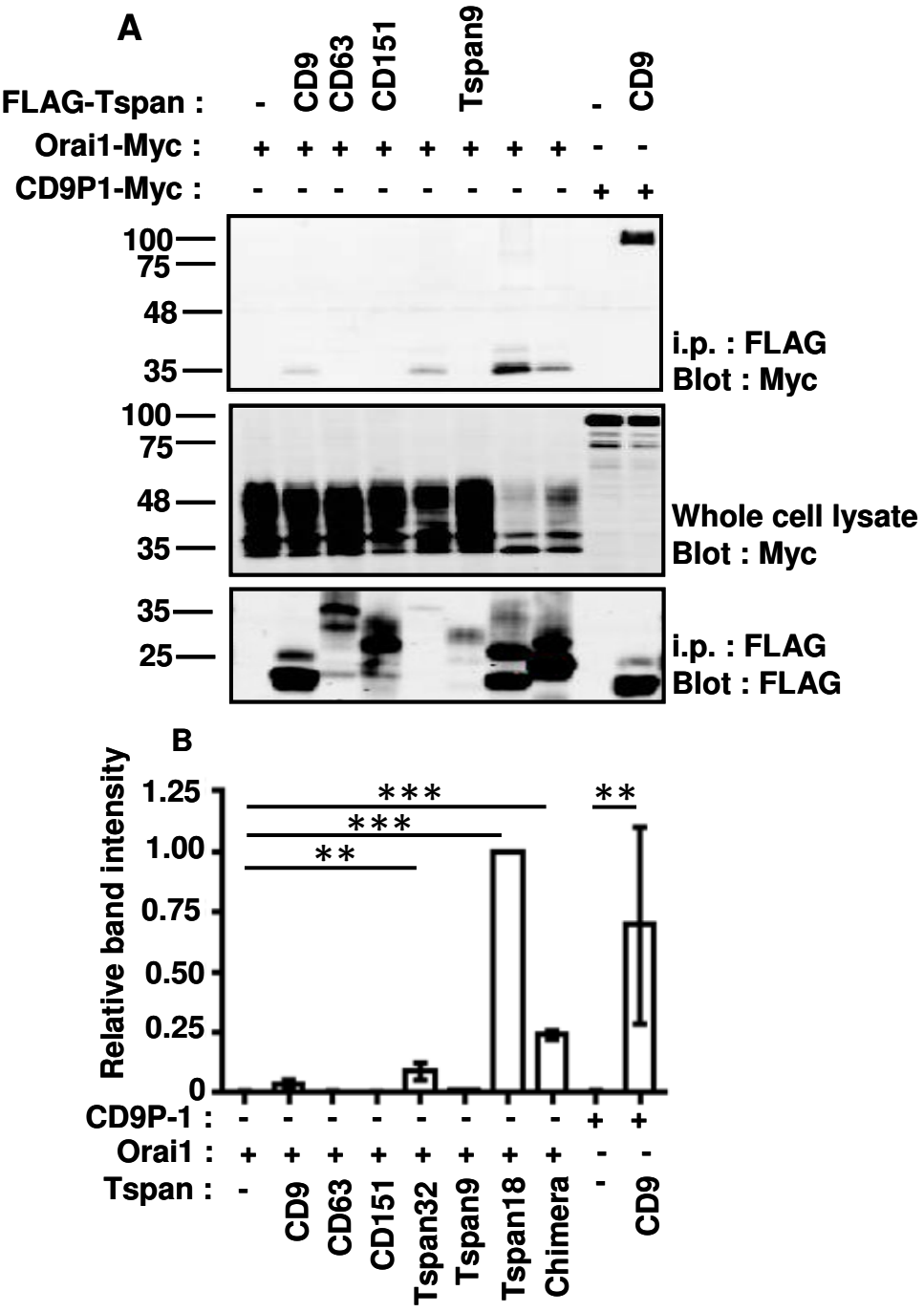

Figure 4.6 – Tspan18 interacts with Orai1. HEK293T cells were transfected using PEI with Myc-tagged Orai1 or CD9P-1 and either an empty vector control, or a FLAG-tagged tetraspanin. Cells were lysed in 1% digitonin and immunoprecipitated with an anti-FLAG antibody. Samples were separated by SDS-PAGE and both immunoprecipitated and whole call lysate samples blotted with anti-FLAG and anti-Myc antibodies, a representative blot is shown (A). The blots were visualised using the Odyssey infra-red imaging system (LI-COR) and band intensity quantitatively measured (B). All data were normalised by logarithmic transformation, and data for Orai1 immunoprecipitation were analysed by one-way ANOVA and Dunnet's post test and data for CD9P-1 immunoprecipitation were analysed by T-test (** denotes $P < 0.01$, ***denotes $P < 0.001$). Error bars represent standard error of the mean from 3 separate experiments.

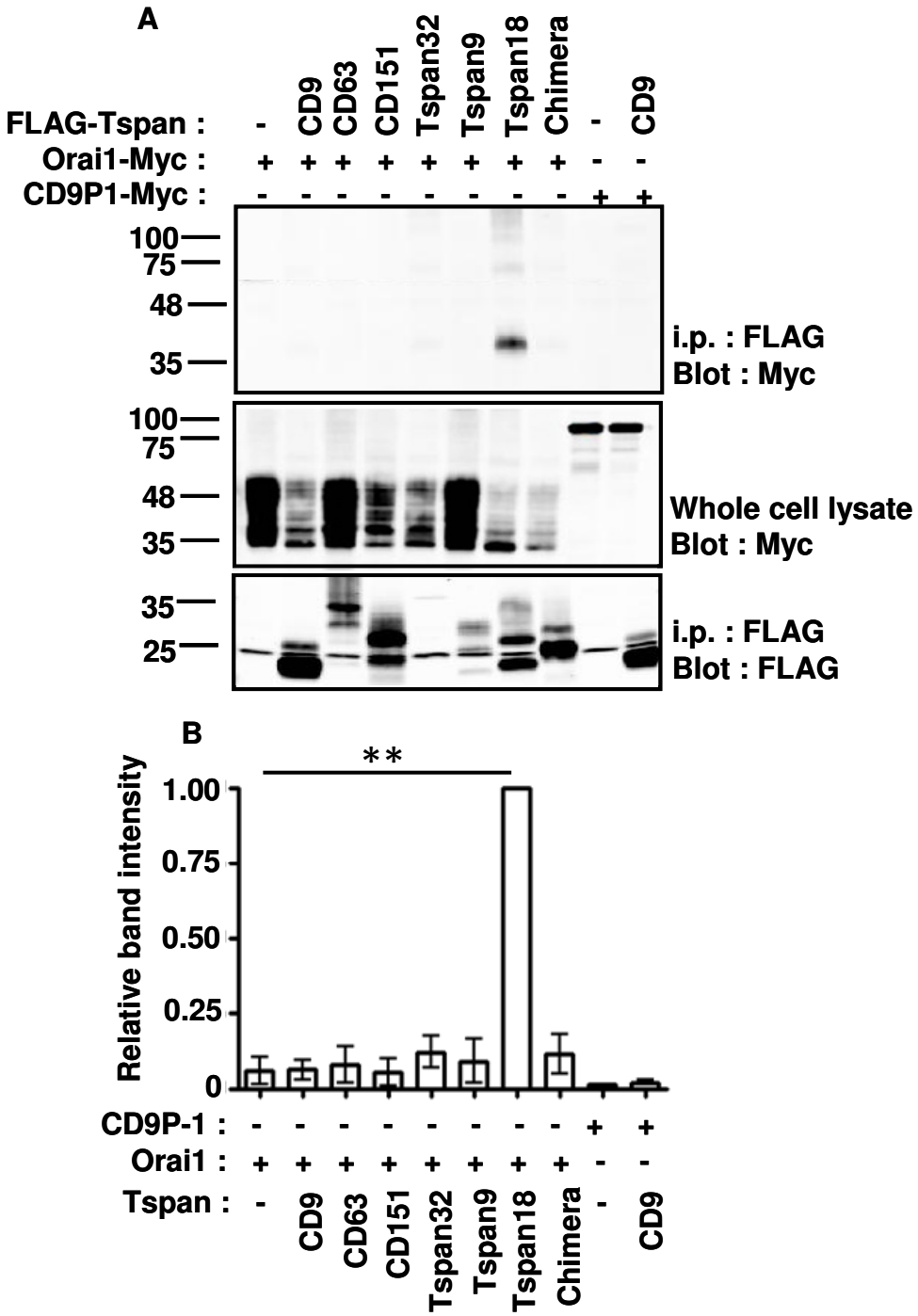

Figure 4.7 – Tspan18 interacts with Orai1 under stringent lysis conditions. HEK293T cells were transfected using PEI with Myc-tagged Orai1 or CD9P-1 and either an empty vector control, or a FLAG-tagged tetraspanin. Cells were lysed in 1% triton with 0.1% SDS and immunoprecipitated with an anti-FLAG antibody. Samples were separated by SDS-PAGE and both immunoprecipitated and whole call lysate samples blotted with anti-FLAG and anti-Myc antibodies, a representative blot is shown (A). The blots were visualised using the Odyssey infra-red imaging system (LI-COR) and band intensity quantitatively measured (B). All data were normalised by logarithmic transformation, data for Orai1 immunoprecipitation were analysed by one-way ANOVA and Dunnet's post test and data for CD9P-1 immunoprecipitation were analysed by T-test (** denotes $P < 0.01$). Error bars represent standard error of the mean from 3 separate experiments.

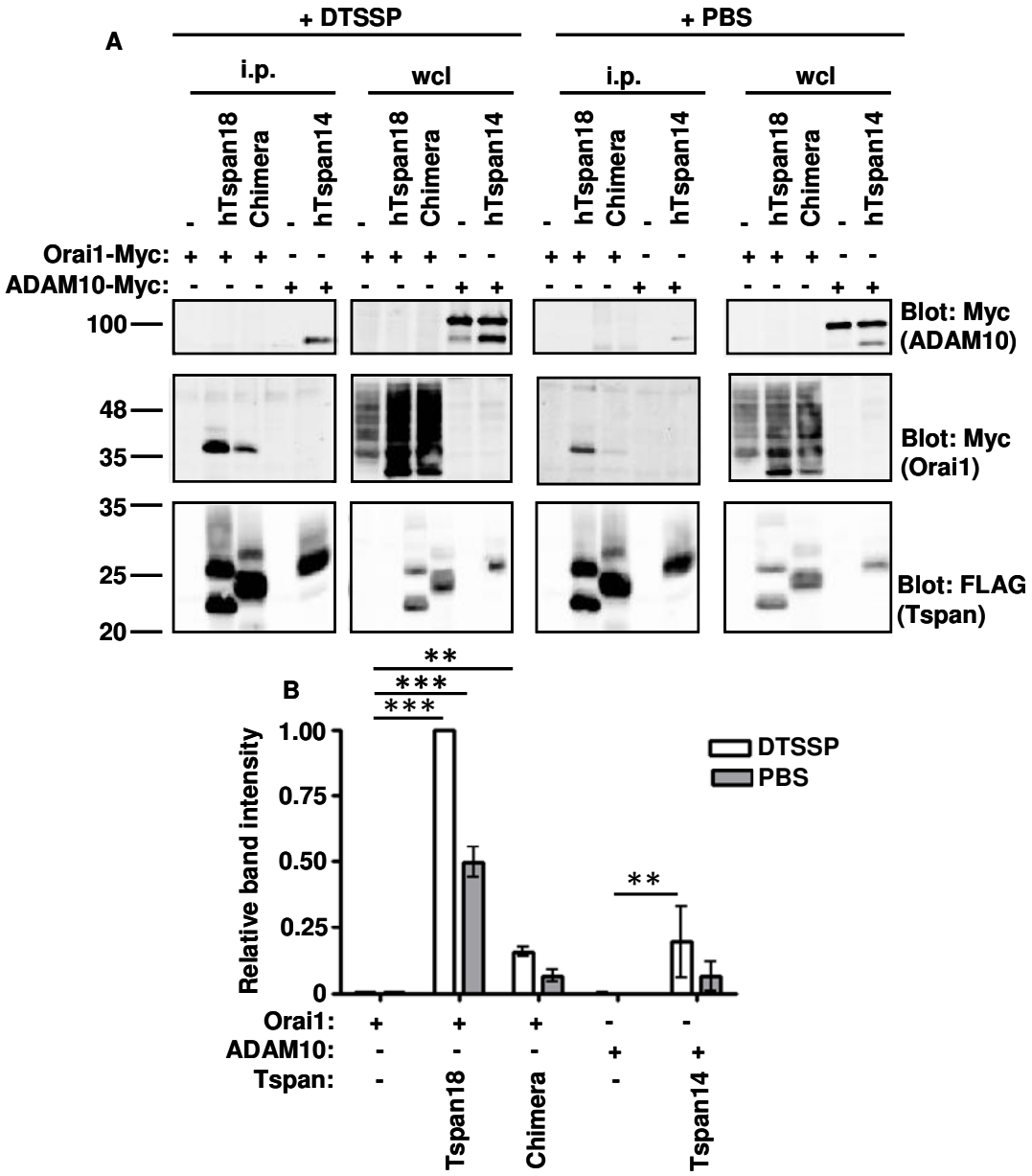

Figure 4.8 – A comparison of the Tspan18-Orai1 interaction under weak and stringent lysis conditions. HEK293T cells were transfected using PEI with Myc-tagged Orai1 or ADAM10 and either an empty vector control or a FLAG-tagged tetraspanin. Cells were incubated with either the chemical cross-linker DTSSP or PBS, then lysed in 1% Triton X-100 lysis buffer containing 0.1% SDS and immunoprecipitated with an anti-FLAG antibody. Samples were separated by SDS-PAGE and both immunoprecipitated and whole call lysate samples blotted with anti-FLAG and anti-Myc antibodies, a representative western blot is shown (A). The blots were visualised using the Odyssey infra-red imaging system (LI-COR) and band intensity quantitatively measured (B). All data were normalised by logarithmic transformation and analysed by one-way ANOVA and Tukey's multiple comparison test (** denotes $P < 0.01$, *** denotes $P < 0.001$). Error bars represent standard error of the mean from 4 separate experiments.

4.3.5 Tspan18 preferentially interacts with de-glycosylated Orai1

Orai1 has an N-linked glycosylation site at N223 in the extracellular loop between the third and fourth transmembrane domains (Prakriya et al., 2006). The glycosylated form of Orai1 was identified due to the appearance of a band at a higher molecular weight than predicted from the amino acid sequence when western blotting for Orai1; deglycosylated Orai1 is observed at approximately 35 kDa and the glycosylated form at 45 kDa (Gwack et al., 2007; Prakriya et al., 2006). The interaction observed between Tspan18 and Orai1 in the immunoprecipitation experiments conducted in this chapter occurred only with a form of Orai1 at approximately 35 kDa (see figures 4.5 – 4.8).

To test whether Tspan18 preferentially interacts with de-glycosylated Orai1, Tspan18 or empty vector control (pEF6) were expressed in HEK293T cells alongside Orai1. Samples were then lysed in 1% digitonin, treated with PNGase F (Sigma); an endoglycosidase, which cleaves N-linked glycoproteins at the link between asparagine and N-acetylglucosamines (Maley, Trimble, Tarentino, & Plummer, 1989) or PBS control, immunoprecipitated and western blotted as described previously. Following treatment with PNGase and immunoprecipitation for the Myc tag of Orai1 to enrich for this protein, only one band of approximately 35 kDa was observed (figure 4.9), representing de-glycosylated Orai1. However, without treatment with PNGase, two bands were observed at approximately 35 and 45 kDa (figure 4.9), representing glycosylated and de-glycosylated Orai1 respectively. When samples were immunoprecipitated for the FLAG tag of Tspan18 rather than the Myc tag of Orai1, only the lower molecular weight band at

approximately 35 kDa, representing de-glycosylated Orai1 was observed, with or without pre-treatment with PNGase (figure 4.9).

This clearly shows the two forms of Orai1; glycosylated and de-glycosylated and also demonstrates that Tspan18 only interacts with de-glycosylated Orai1.

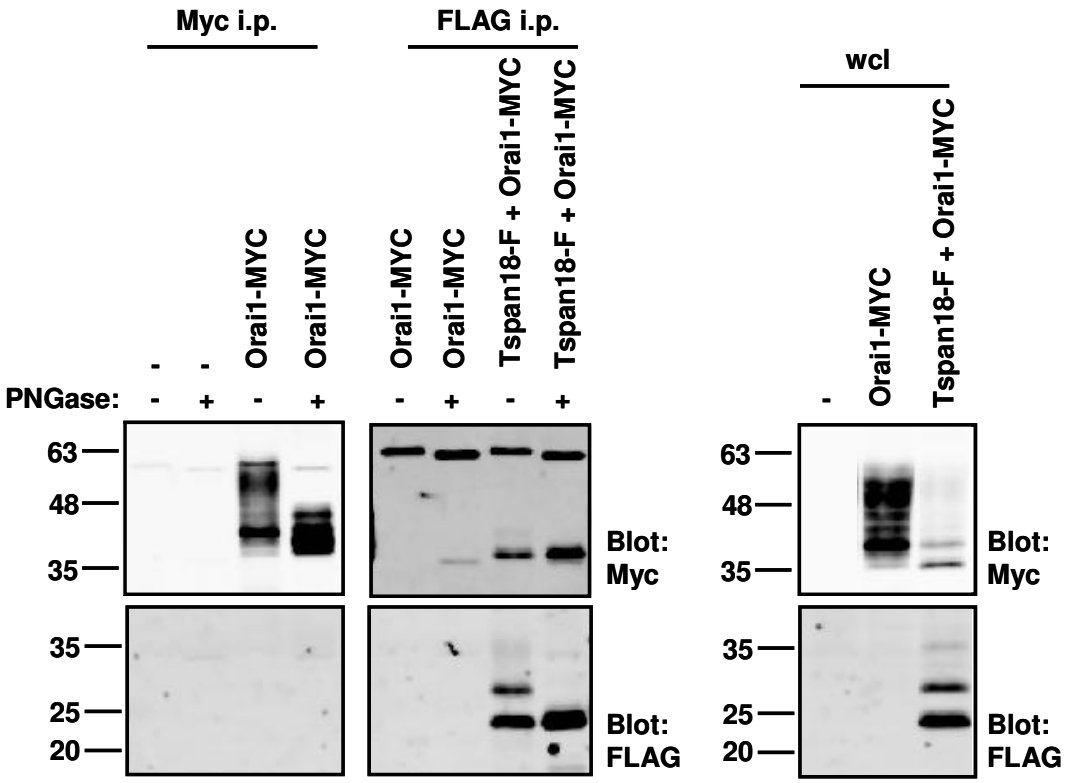

Figure 4.9 – Tspan18 interacts with the de-glycosylated form of Orai1. HEK293T cells were transfected using PEI with Myc-tagged Orai1 and either an empty vector control or FLAG-tagged Tspan18. Cells were lysed in 1% digitonin and immunoprecipitated with an anti-FLAG antibody. Samples were split and half treated with PNGase to cleave all N-linked glycosylations. Samples were separated by SDS-PAGE and both immunoprecipitated and whole cell lysate samples blotted with anti-FLAG and anti-Myc antibodies. A representative western blot is shown from two separate experiments.

4.4 DISCUSSION

The research completed in this chapter was focussed around three key aims; to investigate which region of Tspan18 was important for activation of the Ca^{2+}-responsive NFAT reporter, which has been previously investigated (Colombo, 2010), to assess the role of Orai1 in Tspan18-induced NFAT reporter activation, and to identify whether Tspan18 interacted with Orai or STIM proteins. The data presented in this chapter demonstrated that the variable region within the large extracellular loop of Tspan18 is sufficient to activate the NFAT reporter. Also, that Tspan18 is dependant on functioning Orai1 to induce Ca^{2+} signalling. Additionally, an interaction between Tspan18 and the Orai family of Ca^{2+} entry channels was observed; this interaction appeared to occur preferentially with only the de-glycosylated form of Orai1 and does appear to occur at the cell surface, within the HEK293T cell over-expression system. Together, these data strongly suggest a role for Tspan18 in regulation of SOCE via interaction with the Ca^{2+} channel Orai1.

The observation that the Tspan18-CD9 chimera was able to activate the NFAT reporter, confirmed that the variable region alone is sufficient to replicate the function of Tspan18 in the context of an intact tetraspanin. This could suggest that an interaction forms between Tspan18 and its partner protein via this variable region and that this interaction could be responsible for downstream Ca^{2+} signalling and NFAT activation. This would not be a novel idea within the tetraspanin field, as the variable region within the large extracellular loop across the tetraspanin family has often been suggested as

the most likely region for protein-protein interactions (Stipp, Kolesnikova, & Hemler, 2003). Several examples have been shown where the variable region of a tetraspanin is vital for normal function of the partner protein; association of CD151 with specific integrins occurs via a region within the large extracellular loop (Kazarov, Yang, Stipp, Sehgal, & Hemler, 2002), the high affinity interaction of CD81 with the E2 envelope protein of HCV requires the variable region (Higginbottom et al., 2000), and the variable region within the large extracellular loop of CD9 is important for normal adhesive function of ICAM-1 and VCAM-1 on endothelial cells during leukocyte extravasation (Barreiro et al., 2005).

Despite the functional ability of the chimera to activate the NFAT reporter, the interaction between Orai1 and the chimera was not maintained under stringent lysis, suggesting that this interaction was not as robust as that between Tspan18 and Orai1. This implies that domains other than the variable region of Tspan18 may be important in either maintaining a strong interaction with Orai1, or regulating the localisation of the tetraspanin to allow maximal interaction with Orai1. Domains other than the variable region within the large extracellular loop of tetraspanins have been shown to be important in interaction with partner proteins. For example, the transmembrane region 3 of the tetraspanin uroplakins is important for partner protein interaction (Min et al., 2006) and the EWI-2 interaction with the tetraspanin CD81 is reliant on transmembrane regions 3 and 4 (Montpellier et al., 2011). Therefore, domains from CD9 within the chimera could be partially disrupting the interaction.

The interaction between Tspan18 and Orai1 appeared to occur at the cell surface, as demonstrated by the cross-linking experiment. The cell surface cross-linker used, DTSSP, is membrane impermeable, therefore the increase in band intensity representing the Tspan18-Orai1 interaction under cross-linked conditions must represent cell surface interaction only. Tspan18 has previously been observed at the cell surface in stably transfected Jurkat T cells, using a surface biotinylation approach (Tomlinson, unpublished data). Together this suggests that Tspan18 may be interacting with and regulating Orai1 at the cell surface, though further investigation is required to characterise the nature of the interaction and the effect it has on Orai1 function.

The observation that Tspan18 interacts with the SOCE channel Orai1 supports the hypothesis that Tspan18 is involved in regulation of Ca^{2+} signalling; however the precise mechanism is still not known. Typically, tetraspanins regulate the function of their partner proteins in one of several key mechanisms. The TspanC8 sub family of tetraspanins, which all interact with the metalloproteinase ADAM10, regulate the biosynthesis and maturation of this protein (Dornier et al., 2012; Haining et al., 2012; Prox et al., 2012). It has also been speculated that these tetraspanins could be taking ADAM10 to specific locations in the cell. The tetraspanins CD9 and CD151 interact with and regulate the endothelial adhesion molecules ICAM-1 and VCAM-1 by clustering these proteins to form adhesive platforms for optimal leukocyte capture and extravasation at points of inflammation (Barreiro et al., 2008, 2005). Also, analysis of the lateral mobility of tetraspanins within the plasma membrane has shown highly dynamic interactions within tetraspanin enriched

microdomains, which could therefore impact on the lateral mobility of partner proteins (Espenel et al., 2008). The mechanism by which Tspan18 may regulate Orai1 could involve any of these processes. It is possible that the interaction observed between the chimera and Orai1 is due to a clustering mechanism. For example, the formation of complexes between Tspan18 and Orai1 as well as interactions formed between the chimera and Tspan18 could allow association of the chimera with Orai1 through incorporation into the tetraspanin microdomain. Therefore, the less direct interaction between the chimera and Orai1 may result in a less robust interaction which cannot withstand stringent lysis conditions.

It is interesting that Tspan18 only interacts with de-glycosylated Orai1, and this observation could provide clues to the mechanism by which Tspan18 regulates this Ca^{2+} channel. One hypothesis is that the interaction between these proteins occurs early in the biosynthesis of Orai1, prior to addition of post-translational modifications. However, the interaction between Tspan18 and Orai1 might not be limited to a role in early-stage biosynthesis. It has been shown that the de-glycosylated form of Orai1 is fully functional in its localisation and in its ability to allow flux of Ca^{2+} into the cell (Gwack et al., 2007). It could be possible that interaction with Tspan18 protects Orai1 from glycosylation and that de-glycosylated Orai1 has a specific and separate function in the cell. As the role of glycosylation on Orai1 and the affects that glycosylation has on its function have not yet been elucidated, it is difficult to predict why Tspan18 preferentially interacts with only the de-glycosylated form of this Ca^{2+} channel.

Further work is required to fully elucidate the mechanism by which Tspan18 may be regulating its partner protein, Orai1.

CHAPTER 5

THE HAEMOSTASIS DEFECT IN TSPAN18 KNOCKOUT MICE IS DUE TO TSPAN18 DEFICIENCY IN NON- HAEMATOPOIETIC CELLS

5. 1 INTRODUCTION

5.1.1 Tspan18 is an endothelial tetraspanin

Investigating the expression profile of Tspan18 is difficult due to the lack of antibodies; however Tspan18 expression can be monitored at the mRNA level. One study, which utilised publicly available large scale transcriptomic data from serial analysis of gene expression experiments, revealed that Tspan18 is more highly expressed in endothelial versus non-endothelial libraries (Bailey et al., 2011). Other studies using quantitative real time PCR identified Tspan18 at higher levels in human endothelial cells such as HUVEC and HMEC than other cell types such as smooth muscle cells, fibroblasts, hepatocytes, and cell lines of haematopoietic and non-haematopoietic origin (Colombo, 2010). Additionally, real time PCR on a range of mouse tissues including brain, heart, kidney, liver, lung, muscle, spleen and thymus, found Tspan18 mRNA levels to be highest in lung, suggesting an endothelial expression profile (Colombo, 2010). However, the role of Tspan18 on endothelial and other non-haematopoietic cells has not been studied.

5.1.2 The role of non-haematopoietic cells in haemostasis

The process of haemostasis is regulated not only by platelet activation and thrombus formation, but also by contributions of non-haematopoietic cells, including endothelial cells and smooth muscle cells. Vasoconstriction occurs at sites of injury to narrow the vessel and reduce blood flow, thus reducing

blood loss (van Hinsbergh, 2012). This process requires the contraction of vascular smooth muscle cells, which is regulated by vasoconstrictive agents and through activation of the nervous system (van Hinsbergh, 2012). Just one example of the multiple stimuli which acts as a vasoconstrictor is TxA_2. TxA_2 is released by platelets and induces contraction of vascular smooth muscle via activation of a G protein coupled pathway leading to increased intracellular Ca^{2+} concentrations, activation of myosin light chain kinase and muscle cell contraction (Wilson et al., 2005). The nervous system can also induce vasoconstriction, through production and release of norepinephrine from stimulated neurons of the sympathetic nervous system (Thomas, 2011). Norepinephrine can then go on to stimulate smooth muscle cell contraction, through increasing intracellular Ca^{2+} concentration, thus driving vasoconstriction (Thomas, 2011).

The endothelium can provide both negative signals to regulate haemostasis in normal vessels, and positive signals to promote thrombus formation at sites of vascular injury. The endothelium can inhibit platelet activation through release of inhibitory molecules such as PGI_2 and NO, and through expression of cell surface receptors, such CD39, which hydrolyses platelet-released ADP to prevent platelet activation (Becker, Heindl, Kupatt, & Zahler, 2000; Marcus et al., 1997; van Hinsbergh, 2012). When necessary, the endothelium can stimulate platelet activation and the clotting cascade via release of clotting factors such as vWF and FVIII. vWF mediates the adhesion of platelets to the exposed sub-endothelial matrix at sites of vascular injury. A small amount of vWF is produced in megakaryocytes and is stored in α-granules in platelets, to be released upon platelet activation (Blann, 2006). However, the majority

of vWF is stored in, and released from Weibel-Palade bodies within endothelial cells (Blann, 2006). Endothelial vWF alone has been shown to be sufficient to support haemostasis (Kanaji et al., 2012), and interestingly, exocytosis of the contents of Weibel-Palade bodies, following vessel injury, is regulated by increased intracellular Ca^{2+} signalling (Rondaij, Bierings, Kragt, van Mourik, & Voorberg, 2006). The clotting factor, FVIII is closely associated with vWF via a direct interaction which acts to stabilise FVIII in the blood stream (Everett et al., 2014). Upon activation initiated by a response to injury, FVIII dissociates from vWF and promotes the clotting cascade via interaction with other clotting factors.

5.1.3 Use of chimeric mice to investigate the role of Tspan18 in haemostasis

As described in the first results chapter, Tspan18 deficient mice displayed a severe disruption to haemostasis, as they bleed significantly more than wildtype mice in a tail bleeding assay. This is despite normal thrombus formation *in vivo* and only a mild platelet functional defect. Additionally, the bleeding observed appears more severe than that documented for either GPVI deficient mice (B Nieswandt, Schulte, et al., 2001), or mice with Orai1 deficient platelets (Braun et al., 2009), which suggests that the platelet defects alone can not explain the haemostasis phenotype observed. To investigate the role of non-haematopoietic cells in haemostasis, it is possible to use chimeric mice with different haematopoietic and non-haematopoietic compartments. To generate chimeric mice, whole embryonic livers were

harvested from the embryos of pregnant Tspan18 wildtype or Tspan18 deficient mice. A single cell suspension was generated from the whole liver and transplanted into lethally irradiated C57BL/6 wildtype or Tspan18 deficient mice to reconstitute the haematopoietic system. Therefore, mice with Tspan18 deficient platelets and wildtype endothelium (and other non-haematopoietic cells) as well as mice with Tspan18 deficient endothelium (and other non-haematopoietic cells) and wildtype platelets were generated.

5.2 AIMS

The aim of this chapter was to investigate the mechanism behind the bleeding phenotype observed in the Tspan18 deficient mice. By generating chimeric animals with wildtype haematopoietic cells and Tspan18 knockout non-haematopoietic cells, and vice versa, the role of haematopoietic and non-haematopoietic Tspan18 in haemostasis could be assessed.

5.3 RESULTS

5.3.1 Non-haematopoietic cells appear to drive the disruption to haemostasis in Tspan18 deficient mice

To investigate the role of Tspan18 in haemostasis and to elucidate the effects of platelet Tspan18 as opposed to non-haematopoietic Tspan18, chimeric mice were generated from both C57BL/6 wildtype mice and Tspan18 deficient mice, using lethal irradiation and injection of embryonic liver cells to reconstitute the haematopoietic system, as outlined in section 5.1.3. The tail bleeding assay was then repeated.

When assessed using the tail bleeding assay described in chapter 3, the C57BL/6 recipient mice did not bleed, whether they had Tspan18 wildtype or Tspan18 deficient platelets and other haematopoietic cells (figure 5.1). When Tspan18 deficient chimeras with either knockout or wildtype haematopoietic cells were tested, a significant increase in bleeding was observed. The bleeding mimicked the pattern observed for the Tspan18 whole body knockout mice, in which a heterogeneous population was observed, as some of the mice bled and some did not (figure 5.1). The chimeric mice were bled alongside 8 litter matched pairs of whole body Tspan18 wildtype or knockout animals as controls and, as previously, the Tspan18 deficient mice displayed an increase in bleeding and a highly heterogeneous population was observed whereas the wildtype mice did not bleed (figure 5.1).

These data demonstrate that mice with Tspan18 wildtype non-haematopoietic cells do not have a disruption to haemostasis, whereas mice with Tspan18

knockout non-haematopoietic cells display a disruption to haemostasis, regardless of the genotype of the haematopoietic cells. This suggests that the platelets in the Tspan18 deficient mice do not drive the bleeding phenotype, therefore suggesting a non-haematopoietic driving force behind the bleeding observed.

Genotyping analysis of post-transplant blood samples was carried out to assess success of the reconstitution of the haematopoietic system from the transplanted cells. Genomic DNA was isolated from white blood cells and used for PCR using primers specifically for wildtype Tspan18 (visualised at 376 bp) and gene targeted Tspan18 (visualised at 227 bp). In recipients of wildtype embryonic liver cells, only a band at 376 bp was visualised, representing wildtype Tspan18. In recipients of knockout embryonic liver cells, only a band at 227 bp was visualised, representing disrupted Tspan18 (figure 5.2). This demonstrated successful reconstitution of the haematopoietic system from the transplanted cells, and that generation of the chimeric animals had been achieved. Bands at both 376 bp and 227 bp were observed for tail tip tissue harvested from the mice post-transplant (figure 5.2). The appearance of both bands suggests both Tspan18 wildtype and deficient cells were present, which would be expected, as some blood contamination could have occurred during harvesting of this tissue which would mean that both haematopoietic and non-haematopoietic cells may have been present.

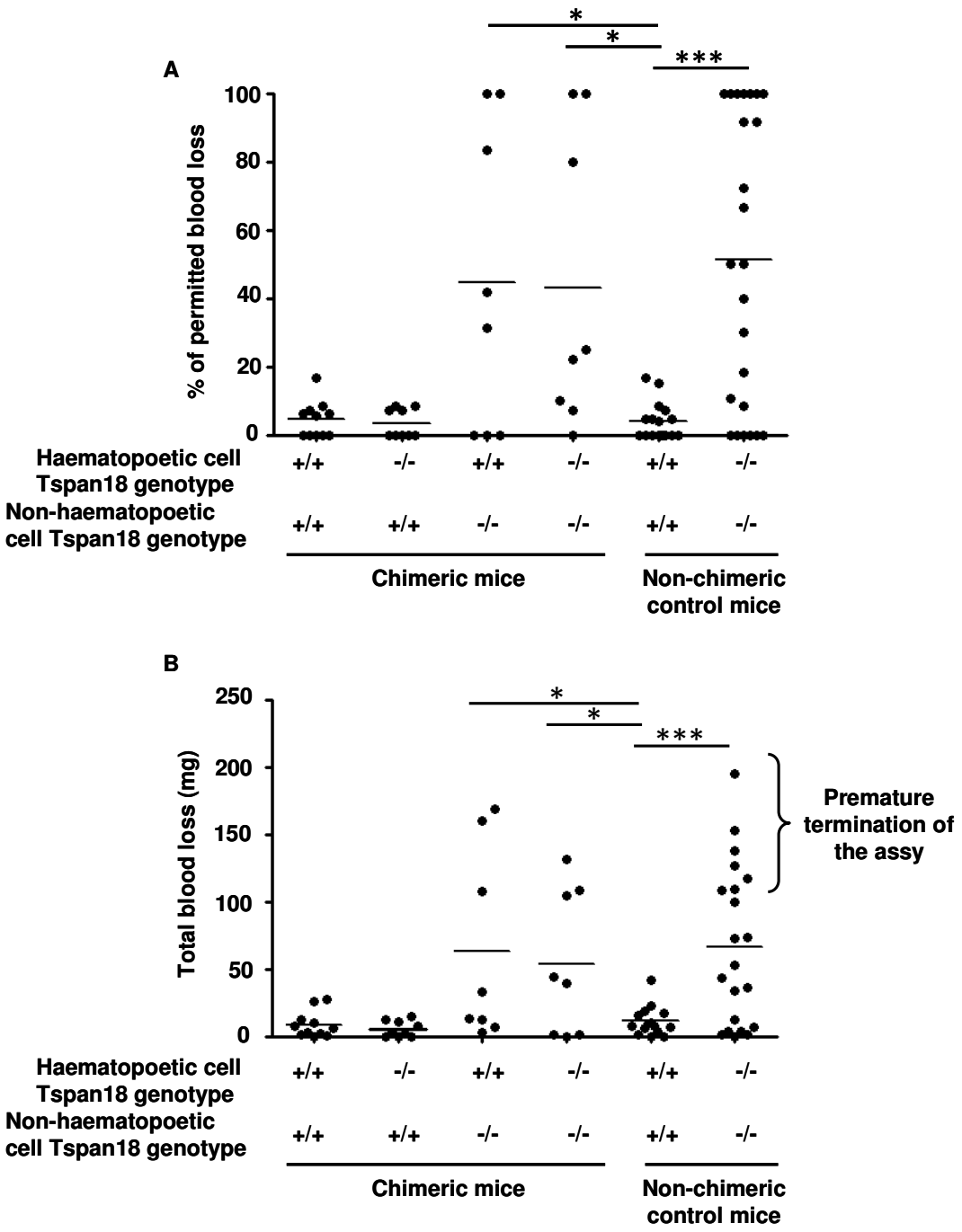

Figure 5.1 – Normal haemostasis in the tail bleeding assay in C57BL/6 chimeric mice, but impaired haemostasis in Tspan18-/- chimeric mice. The tail tip of anaesthetised mice was amputated and amount of blood lost was measured. Each symbol represents an individual. Data were analysed by Fisher's exact test; individuals were ranked as 'bleeding' or 'not bleeding' where 'bleeding' was defined as one or more drop of blood, equivalent to 30 µl lost (* denotes $P < 0.05$, *** denotes $P < 0.001$). Data displayed is either the % of total permitted blood loss (A); each mouse was permitted to lose a maximum of 15% of total blood determined by body weight, due to restrictions on the Home Office animal licence, or as total volume of blood lost with a bracket to indicate termination of the assay for individuals which lost 100% of permitted blood (B). Non-chimeric mouse data is a reproduction of all collated data for Tspan18 wildtype and knockout individuals, including 8 pairs which were bled in parallel to the chimeric mice.

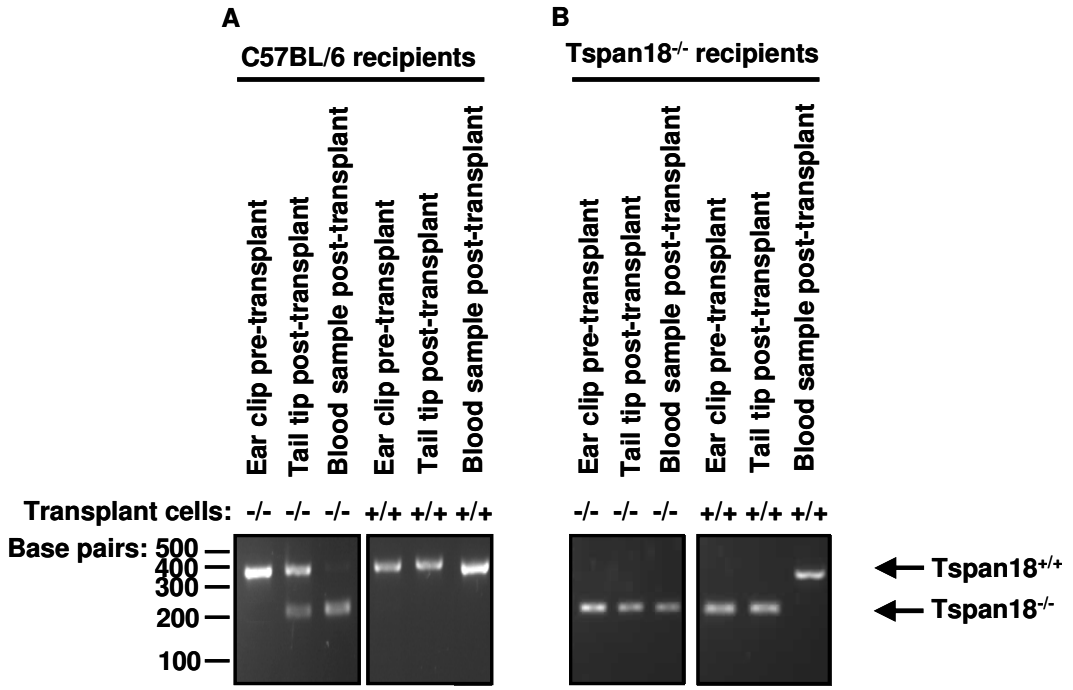

Figure 5.2 – Validation of Tspan18 chimeric mice by genotyping. 6-week old wildtype C57BL/6 (A) or Tspan18-/- (B) recipient mice were lethally irradiated prior to injection with embryonic liver cells from either Tspan18 deficient or wildtype mice. The mice recovered over 6 weeks to enable reconstitution of the haematopoietic system from the transplanted cells. Tissue samples were taken before transplantation and blood and tissue samples were taken after reconstitution of the haematopoietic system. Genomic DNA was isolated from the samples and the PCR products run on a gel to visualise Tspan18 wildtype and gene targeted bands (wildtype Tspan18 PCR product is visualised at 376 bp and disrupted Tspan18 PCR product visualised at 227 bp). A representative gel is shown.

5.3.2 Plasma levels of endothelial-derived clotting factors vWF and FVIII are normal in Tspan18 deficient mice

One known impact that the endothelium has on haemostasis is biosynthesis and release of specific clotting factors which, as described earlier, can act to promote platelet activation and the clotting cascade. As demonstrated by the data presented earlier in this chapter, non-haematopoietic cells appear to be driving the bleeding observed in Tspan18 deficient mice. Tspan18 is expressed in endothelial cells; therefore it is possible that an endothelial-derived defect is driving the bleeding.

To investigate the cause of the potentially endothelial-driven bleeding in the Tspan18 deficient mice, plasma concentrations of specific clotting factors were measured by ELISA. Blood was taken from anaesthetised mice and the plasma was separated by centrifugation. Mouse plasma concentration of vWF was measured using pre-coated micro-titre ELISA plates from BT-Laboratory and mouse plasma concentration of FVIII was measured using pre-coated micro-titre ELISA plates from My Biosource. The plasma concentration of both vWF and FVIII was found to be normal in plasma from Tspan18 deficient mice when compared to plasma from wildtype mice (figure 5.3 A and B).

Therefore endothelial Tspan18 does not appear to have a role in regulation of the basal levels of plasma vWF or FVIII. This suggests that either another mechanism, involving endothelial, or other non-haematopoietic cells, could be causing the bleeding in the Tspan18 deficient mice, or that Tspan18 might have a more complex role in regulating the function of these clotting factors;

the latter could be regulation of their release upon injury by Tspan18, which, in the case of vWF, has been previously shown to be a Ca^{2+} dependant mechanism (Rondaij et al., 2006).

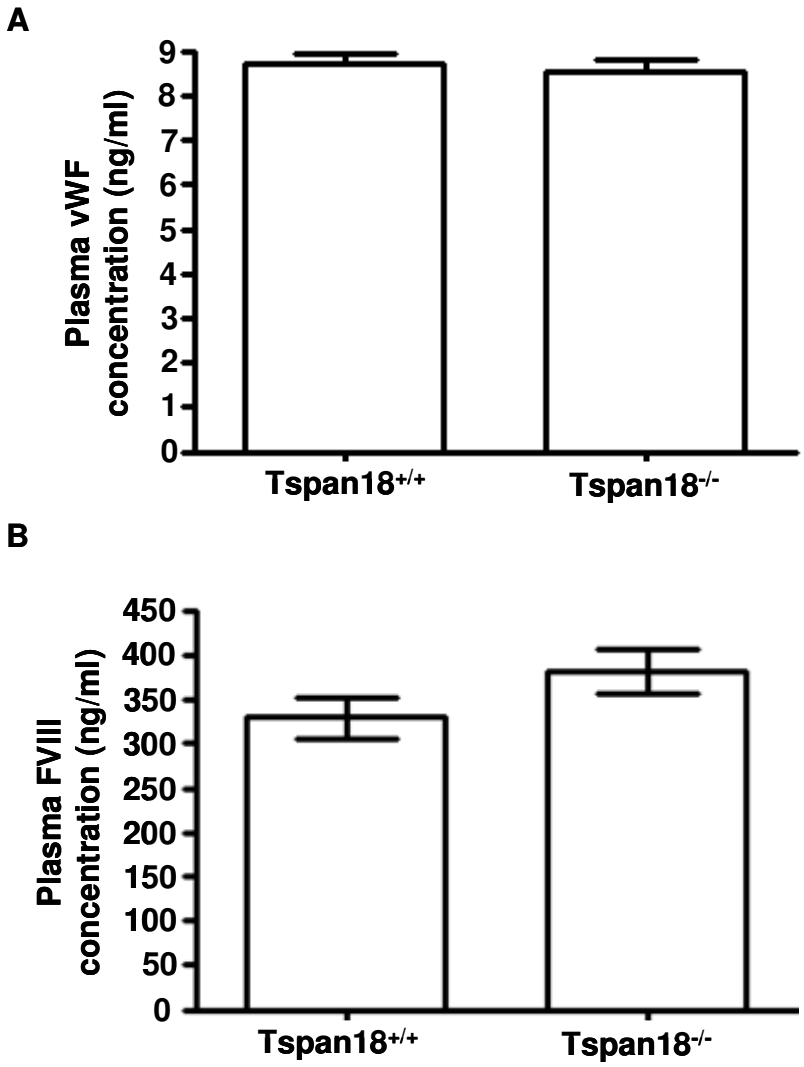

Figure 5.3 – Tspan18 deficient mice have normal levels of plasma vWF and FVIII. Blood was taken from anaesthetised mice and the plasma was isolated from whole blood by centrifugation. Concentration of vWF and FVIII was assessed by ELISA, using pre-coated micro-titre plates from BT-Laboratory for vWF (A) or My Biosource for FVIII (B). Error bars represent the standard error of the mean from 4 pairs of mice. All data were analysed by T-test.

5.3.3 Knockdown of Tspan18 in HUVEC appears to disrupt endothelial cell function

As a preliminary investigation into the potential role of Tspan18 on endothelial cells, *in vitro* assays using HUVEC were employed. Expression of Tspan18 was disrupted using two different siRNA duplexes in comparison to a control siRNA duplex. Optimisation of knockdown is outlined in appendix 2.

The first method of assessing endothelial cell function was the scratch wound assay; a confluent monolayer of HUVEC was wounded using a pipette tip and the migration of the cells to close the wound was monitored using time-lapse microscopy. In HUVEC which had been treated with the Tspan18 siRNA.1 duplex, a significant reduction in wound closure was observed at 6 and 12 hours post-wounding, in comparison to cells treated with the control siRNA (figure 5.4 A-C). Tspan18 knock down for both duplexes was assessed by real-time PCR, in comparison to the control siRNA (figure 5.4, D).

The second endothelial function assay was a co-culture tube-formation assay, in which HUVEC were cultured alongside fibroblasts and the formation of tube-like structures was assessed (figure 5.5, A). The number of junctions formed appeared to be reduced in HUVEC treated with either Tspan18 siRNA duplex (figure 5.5, C), though the length of the tubules and the number of tubules formed appeared mainly undisrupted (figure 5.5, A and D). Tspan18 knock down for both duplexes was assessed by real-time PCR, in comparison to the control siRNA (figure 5.5, E).

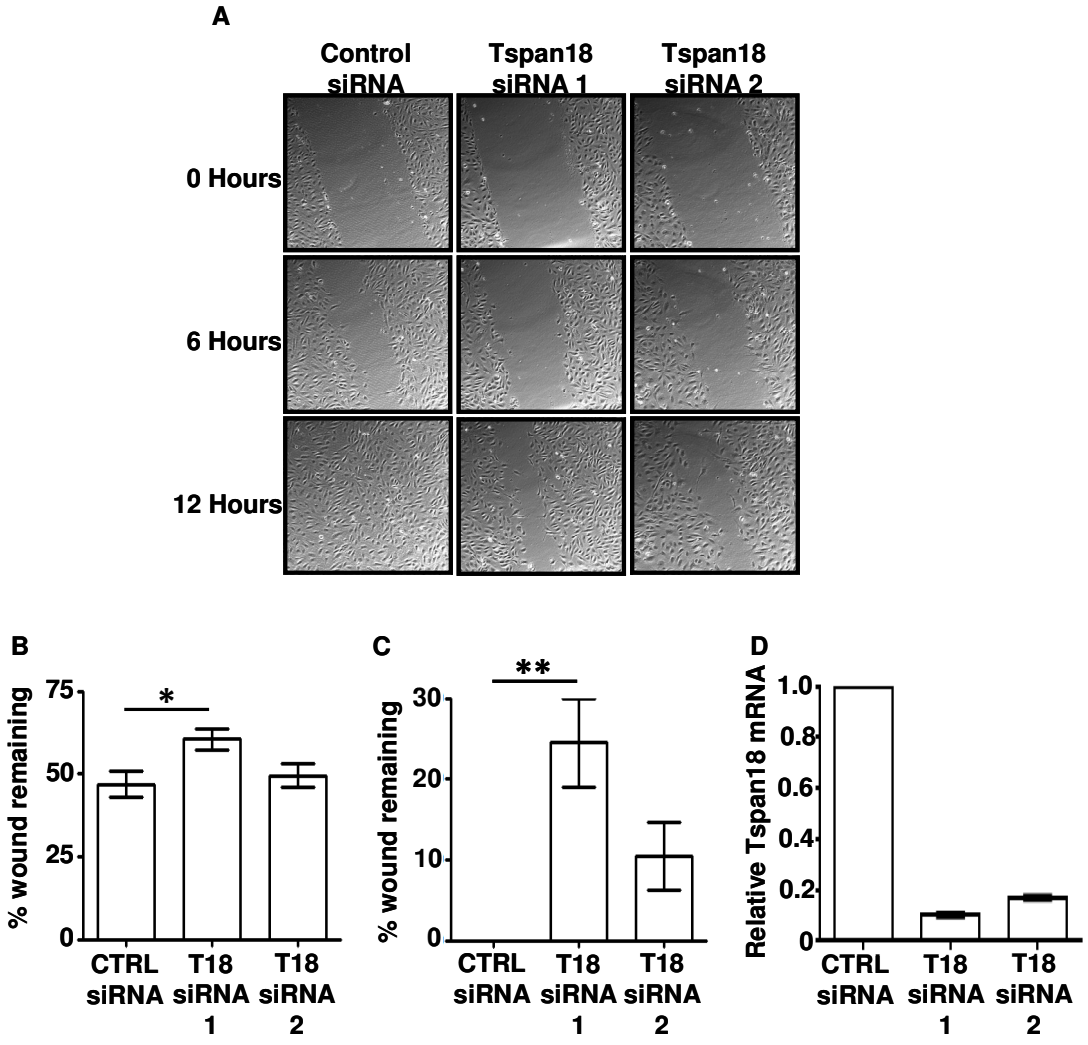

Figure 5.4 – Tspan18 knockdown disrupts endothelial function in a scratch wound assay. Tspan18 expression was disrupted in HUVEC using siRNA. The HUVEC were grown to be confluent before scratching a wound through the monolayer of cells with a pipette tip. Time-lapse microscopy was used to monitor the migration of the cells to close the wound; representative images are shown (A). Images were analysed using ImageJ software at 6 (B) and 12 (C) hours post-wounding, to quantitatively measure wound closure. All data were normalised by arcsin transformation and analysed by one-way ANOVA with Dunnet's multiple comparison (* denotes $P < 0.05$, ** denotes $P < 0.01$). Relative Tspan18 mRNA levels were assessed by real time PCR (D). Error bars represent the standard error of the mean from 3 separate experiments.

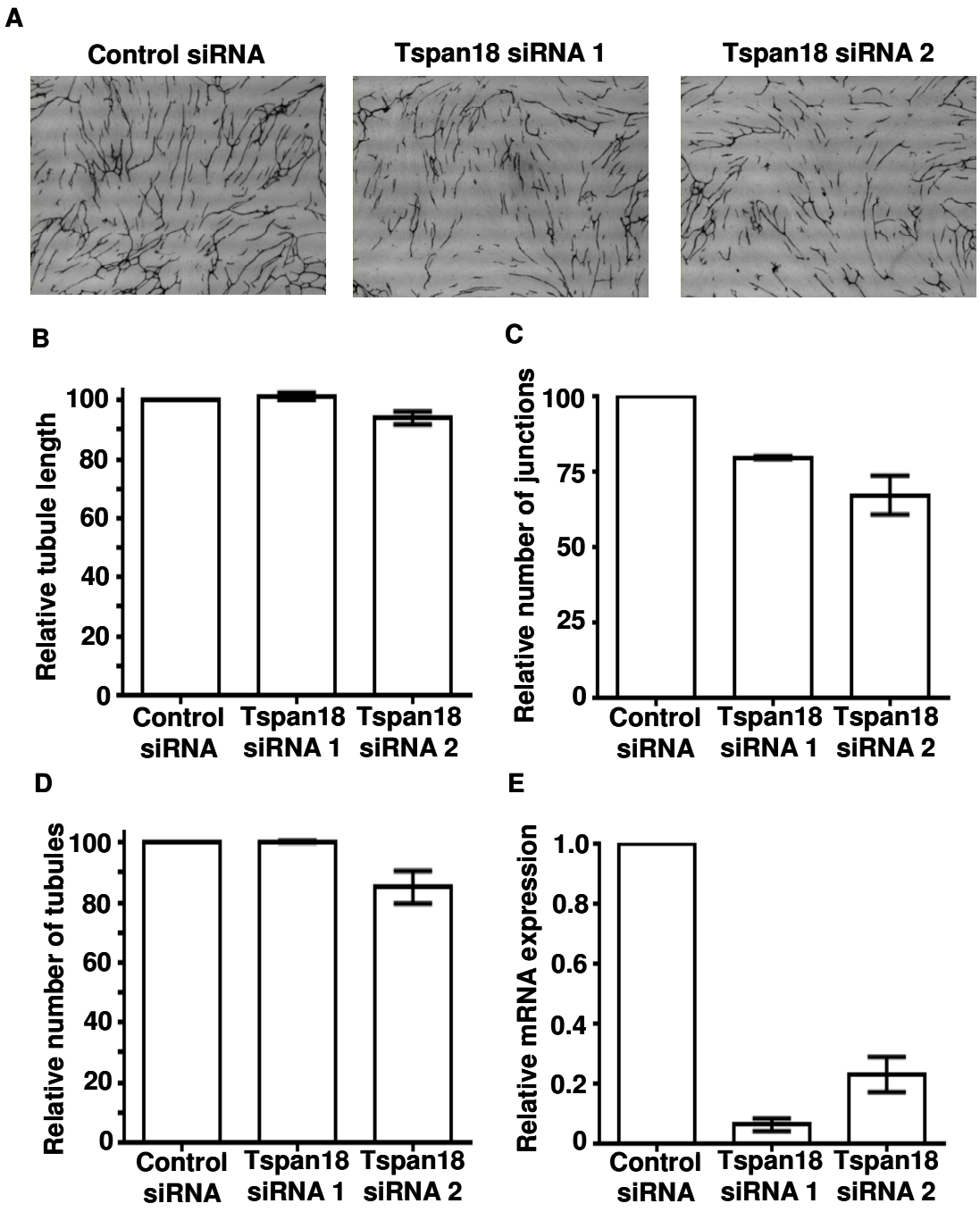

Figure 5.5 – Tspan18 knockdown disrupts endothelial function in a tube formation assay. Tspan18 expression was disrupted in HUVEC using siRNA and the HUVEC were seeded onto fibroblasts in a co-culture environment and cultured for 6 days to allow tube-like structures to form. The HUVEC were then fixed and stained for CD31, using an alkaline phosphatase conjugated secondary antibody for visualisation under a light microscope. Representative images are shown (A). The images were analysed by thresholding; the length of tubules (B), number of junctions (C) and number of tubules (D) were measured. Relative mRNA levels were assessed by real time PCR (E). Error bars represent the standard error of the mean from 2 separate experiments.

5.4 DISCUSSION

The main aim of the work in this chapter was to investigate the role of Tspan18 in haemostasis and to investigate whether non-haematopoietic derived dysfunction was the cause of disrupted haemostasis in the Tspan18 deficient mice. Chimeric mice derived from C57BL/6 wildtype animals displayed no bleeding phenotype, whether they had wildtype or Tspan18 deficient haematopoietic cells. However, chimeric mice derived from Tspan18 deficient animals displayed an increase in bleeding, whether they had wildtype or Tspan18 deficient haematopoietic cells, suggesting that the disrupted haemostasis in Tspan18 deficient mice is driven by defects in non-haematopoietic cells. Interestingly, Tspan18 is known to be expressed in endothelial cells; a cell type which plays multiple roles in haemostasis. It is therefore possible that endothelial Tspan18 has a role in regulation of haemostasis. However, the bleeding was not caused by disruption to basal plasma concentration of endothelial released vWF or FVIII. Preliminary investigation into the role of Tspan18 on endothelial cells appeared to highlight a role for Tspan18 in endothelial cell migration and tube formation, though further experiments are required to confirm these results.

The generation of chimeric mice, using embryonic foetal liver cells to reconstitute the haematopoietic system enabled the roles of Tspan18 in haematopoietic and non-haematopoietic cells within the process of haemostasis to be investigated. Use of foetal liver to reconstitute the haematopoietic system in mice is a widely used method, as embryonic stem

cells from the liver are able to provide long term reconstitution across the range of haematopoietic cell lineages (Ema & Nakauchi, 2015; Forrester et al., 1991). Use of PCR to genotype the chimeric mice demonstrated that the reconstitution method was successful and that only a minimal, if any, population of original haematopoietic cells remained after irradiation. Use of this method to drawn conclusions on the role of Tspan18 in haemostasis relies on the assumption that the platelets derived from the embryonic liver stem cell lineages have the same biology and function as those which were derived from the original adult mouse stem cells, prior to irradiation. In order to better understand this, platelet function tests such as those completed in chapter 3, could be completed on the reconstituted platelets from the chimeric mice, to assess whether they function in the same way as normal adult platelets.

Interestingly, the severity of bleeding observed in either Tspan18 deficient mice or the chimeric mice derived from Tspan18 deficient mice appears to vary widely across the population. This is in contrast to the largely consistent results observed for Tspan18 wildtype mice, which do not bleed. The unequal variance between these populations represents the heterogeneity within the Tspan18 knockout mice. Why there would be such a high levels of variance within this population is not known, but it suggests that certain individuals are more susceptible to bleeding than others. Similar results have been observed for the tail bleeding assay previously, as mice deficient in the tyrosine phosphatase CD148 demonstrated a bimodal distribution of bleeding (Y. A. Senis et al., 2009). Additionally, a similar distribution was also observed for GPVI deficient mice which had been generated on a mixed 129 x1 / SvJ x

C57Bl/6J background (Cheli et al., 2008). Through use of a genome wide single-nucleotide polymorphism screen, a modifier locus was identified, which was shown to affect the extent of disruption to haemostasis following GPVI deficiency (Cheli et al., 2008). Interestingly, the Tspan18 knockout mice were also generated on a mixed background (Tang et al., 2010). Therefore, the bimodal distribution of bleeding observed in the Tspan18 knockout mice could be the result of contribution of a modifier locus. Alternatively, the bimodal population could be the result of another factor, for example affects of the environment. If the bleeding phenotype is weak, but is exacerbated by stress, for example, then the increase in bleeding could be observed only in some individuals, when stress becomes a secondary factor.

As Orai1 has been identified as a novel partner protein for Tspan18 (see chapter 4), it is possible that Tspan18 is regulating Orai1 and Ca^{2+} signalling in endothelial cells. A disruption to endothelial Ca^{2+} signalling due to Tspan18 deficiency could impact on endothelial function and may drive the bleeding phenotype observed. However, it is also possible that Tspan18 could be interacting with a different partner protein and altering endothelial cell function in a different way. It would be interesting to assess the Orai1 endothelial cell specific knockout mouse for disruptions to haemostasis and to see whether these mice might phenocopy the results observed for Tspan18 knockout mice.

Although the basal plasma concentration of vWF and FVIII appear to be normal in Tspan18 deficient mice, it is still possible that Tspan18 has a role in regulation of one or both of these clotting factors. Deficiency or defective function of vWF is the cause of the bleeding disorder von Willebrand disease (vWD) and it might be possible that although the basal concentrations of vWF

are normal in Tspan18 deficient mice, there might be another defect which has not yet been investigated. For example, the release of this clotting factor following injury could be impaired, therefore studying basal plasma concentration alone cannot provide definitive evidence that these factors are functioning normally in the blood. It has been previously shown that release of vWF from Weibel-Palade bodies following injury, occurs via a Ca^{2+} regulated process (Rondaij et al., 2006). It is therefore feasible that although basal plasma levels of vWF are normal in the Tspan18 deficient mice, release of vWF from the endothelium following injury may well be disrupted, due to disrupted Ca^{2+} signalling, and could be causing the bleeding phenotype observed. An investigation into the injury-induced release of these clotting factors in Tspan18 deficient mice is required before a role for Tspan18 in regulation of vWF or FVIII function can be dismissed completely.

The role for Tspan18 in endothelial cells may not involve regulation of vWF or FVIII, but may include regulation of another aspect of endothelial function in haemostasis. For example, the endothelium can act to reduce thrombus and clot formation via inhibition of platelet adhesion and activation (van Hinsbergh, 2012). Release of PGI_2 by endothelial cells promotes anti-thrombotic effects by inhibiting platelet activation (Becker et al., 2000; Salvador Moncada, 1982; van Hinsbergh, 2012). Endothelial cells can also release NO, which aids in the platelet-inhibitory actions of PGI_2 (van Hinsbergh, 2012). In order to assess whether the levels of NO or PGI_2 are disrupted and are causing defective haemostasis, plasma concentrations could be measured. For example, to investigate plasma NO levels, a spectrophotometric approach could be used, in which plasma NO can be reduced to NO_2 for detection by

Griess reagent, which induces a colour change in response to high NO_2 and is therefore used for colorimetric detection of nitrite in samples (Giustarini, Rossi, Milzani, & Dalle-Donne, 2008).

Both the scratch wound assay and the tube formation assay were used to assess the effect on endothelial cell function following knockdown of Tspan18. In both cases, knockdown of Tspan18 appeared to disrupt endothelial cell function, as a reduction in wound closure and a reduction in tube formation was observed following disruption of Tspan18. This suggests that Tspan18 has a role in regulating normal endothelial cell function, but further work is required to confirm these results and to investigate whether endothelial Tspan18 has a role in haemostasis, or whether it is involved in another endothelial cell process.

It is possible that the mechanism by which Tspan18 regulates haemostasis could be separate from the endothelium, and may involve regulation of other cell types, such as vascular smooth muscle. The fine balance of positive and negative regulation of haemostasis is clearly disrupted in Tspan18 deficient mice; however to fully understand the mechanism by which Tspan18 may be regulating haemostasis, further investigation is required. Ideally, generation of an antibody for Tspan18 is required to be able to confirm the expression profile of this tetraspanin and therefore better hypothesise in which cell types it may be having an effect. An antibody against this tetraspanin would also enable investigation of endogenous protein and allow assessment of the Tspan18-Orai1 interaction at the endogenous level, rather than within an over-expression system. It would be interesting to investigate whether Tspan18 interacts with partner proteins other than Orai1, and whether the

disruption to haemostasis observed is due to defective Ca^{2+} signalling and SOCE, or whether there is another mechanism. Ca^{2+} signalling experiments in endothelial cells and other Tspan18 expressing cells would be useful to investigate this question.

CHAPTER 6

GENERAL DISCUSSION

6.1 Summary of key findings

The main aim of this thesis was to characterise the role of the tetraspanin Tspan18 in platelet function. Generation of the Tspan18 knockout mouse in a large scale mouse knockout project (Tang et al., 2010) provided the means to characterise the role of Tspan18 in platelets, and use of cell line models enabled investigation into the mechanism of Tspan18 action and identification of potential binding partners. Characterisation of Tspan18 deficient platelets highlighted a very specific role for Tspan18 in regulation of platelet activation downstream of collagen receptor GPVI signalling, as Tspan18 deficient platelets displayed defective aggregation, secretion and spreading downstream of the GPVI-specific agonist CRP. Additionally, Tspan18 deficient platelets had a reduced ability to mobilise Ca^{2+} following stimulation with CRP or collagen and following emptying of intracellular Ca^{2+} stores, the latter suggesting a SOCE defect. The Tspan18 deficient mice did not display any defect in thrombus formation in the two in vivo models tested, but a large increase in bleeding was observed in Tspan18 deficient mice compared to wildtype controls. This bleeding defect was concluded to most probably be caused by defective non-haematopoietic function, leading to a disruption to coagulation, rather than as a direct result of the mild platelet defects. During in vitro analyses, the variable region within the large extracellular loop of Tspan18 was shown to be important for Tspan18 to induce an increase in activation of a Ca^{2+} responsive reporter. Additionally, through use of a dominant negative form of the SOCE channel Orai1, the ability of Tspan18 to induce increased intracellular Ca^{2+} was shown to be dependant on functioning Orai1 channels. Finally, through an immunoprecipitation approach, a novel

partner protein was identified for Tspan18, as a robust interaction formed between Tspan18 and Orai1, for which the variable region was important. Taken together, these data highlight a novel tetraspanin-partner protein interaction that may outline a role for Tspan18 in regulation of Ca^{2+} entry by regulation of Orai1. In terms of platelet activation, Tspan18 appears to be particularly important in Ca^{2+} signalling downstream of GPVI activation. The ability of Tspan18 to activate Ca^{2+} is unique across a panel of different tetraspanins (Colombo, 2010) and the interaction between Tspan18 and Orai1 was specific. It is unlikely that other tetraspanins would be able to compensate for the role of Tspan18, as there are no close relatives to Tspan18 with similar sequence and there is no evidence for the closest relative, Tspan1, expression on platelets. The findings in this thesis therefore potentially represent a highly specific and unique mechanism.

6.2 The interaction between Tspan18 and Orai1

The interaction that was observed between Tspan18 and Orai1 is a novel tetraspanin-partner protein interaction which has not been observed previously. Although the interaction appeared to be highly robust, as it was able to withstand stringent lysis conditions, the interaction consistently only occurred with the low molecular weight form of Orai1, corresponding to de-glycosylated Orai1 (Gwack et al., 2007; Prakriya et al., 2006). The reason behind the specificity of Tspan18 interacting with only de-glycosylated Orai1 is unknown, though it is not the first time that Orai1 interacting proteins have been shown to preferentially interact with the de-glycosylated form. During

immunoprecipitation experiments using over-expressed Orai1 and STIM1 in HEK293T cells, STIM1 was shown to interact with the lower molecular weight form of Orai1 (Vig et al., 2006). Additionally, in experiments using soluble STIM1 fragment peptides to identify the regions of STIM1 which are important for activation of Orai1, it was shown that a region within the C-terminal of STIM1, named the CRAC activation domain (CAD), was sufficient to interact with Orai1 and induce channel opening (Park et al., 2009). When the CAD peptide was over-expressed in HEK293T cells alongside Orai1 and immunoprecipitation employed, the interaction was observed between CAD and the low molecular weight form of Orai1 (Park et al., 2009). Interestingly, it is not only the interaction between Orai1 and STIM1 which has demonstrated a preference for the lower molecular weight of the Ca^{2+} channel. In a study which outlined a role for secretory pathway Ca^{2+}-ATPase (SPCA2) in store-independent activation of Orai1, immunoprecipitation experiments for both endogenous and over-expressed protein demonstrated that the interaction which formed was between SPCA2 and the low molecular weight form of Orai1 (Feng et al., 2010). As of yet, there has been no explanation for the specific interaction between only the low molecular weight form of Orai1 and it's binding partners. However, the occurrence of this interaction across multiple binding partners and within experiments studying both over-expressed and endogenous protein, suggests that the interaction of Tspan18 with only de-glycosylated Orai1 is unlikely to be a co-immunoprecipitation artefact.

Further evidence for the interaction of Tspan18 with Orai1 was outlined through use of a cross-linking assay in chapter 4. The use of a membrane

impermeable surface cross-linker increased the signal observed for the interaction between Tspan18 and Orai1 and stabilised the interaction between the Tspan18/CD9 chimeric construct and Orai1. This suggests that the interaction between Tspan18 and Orai1 is preserved at the cell surface.

It is interesting that Tspan18 also appeared to interact with the other members of the Orai family; Orai2 and Orai3. However, the extent of these interactions were not investigated as far as the interaction with Tspan18 and Orai1, therefore it is not possible to discern the importance or relevance of these interactions. It is possible that Tspan18 only interacts with Orai2 and Orai3 indirectly, mediated by a common interaction with Orai1. It would be possible to test to robustness of these interactions using more stringent lysis conditions.

6.3 The mechanism of Tspan18 action

Despite the functional studies completed in both cell line models and the Tspan18 deficient platelets which suggested a role for Tspan18 in Ca^{2+} mobilisation, the mechanism of action of this tetraspanin is still unknown. As Tspan18 has been shown to interact with Orai1, it is reasonable to hypothesise that the interaction between Tspan18 and this Ca^{2+} channel could be regulating its function and thus effecting Ca^{2+} flux into the cell, as outlined in figure 6.1 A. However, exactly how Tspan18 is regulating Orai1 is more difficult to predict, as there are several viable mechanisms which may occur.

Firstly, as outlined in figure 6.1 B, Tspan18 could be regulating the biosynthesis, trafficking and therefore expression of Orai1. Tetraspanins have previously been observed regulating the expression and biosynthesis of their partner proteins. For example, the tetraspanin CD81 is required for trafficking of its partner, CD19, from the ER to the golgi and thus regulates the cell surface expression of CD19 (Shoham et al., 2003; Zelm et al., 2010). Additionally, the TspanC8 subfamily of tetraspanins have all been shown to interact with ADAM10, regulating its maturation, cell surface expression and proteolytic activity (Dornier et al., 2012; Haining et al., 2012; Prox et al., 2012). As other tetraspanins have been shown to interact with their partner proteins early during their biosynthesis, it is possible that Tspan18 interacts with Orai1 early in biosynthesis, within the ER or the golgi, and thus has a role in regulating its expression at the cell surface. SOCE is known to be highly sensitive to expression levels of both STIM and Orai proteins. Over-expression studies have shown that an imbalance of these proteins can disrupt SOCE, as over-expression of Orai without STIM, or visa versa, disrupts SOCE and reduces Ca^{2+} influx into the cell (Mercer et al., 2006; Soboloff et al., 2006). This clearly demonstrates the need for balance of both STIM and Orai expression for SOCE to occur optimally. Tspan18 could have a role in maintaining the correct levels of Orai1 in the cell for optimal SOCE. In order to begin to assess the potential role of Tspan18 in regulation of Orai1 expression, Orai1 antibodies were characterised for use in western blotting and immunoprecipitation experiments, as outlined in appendix 3. Two commercially available Orai1 antibodies were shown to western blot over-expressed human Orai1 protein in transfected HEK293T cells, but the level of

endogenous Orai1 in mouse platelets was either too low to detect, or the antibodies might not detect mouse Orai1 as well as human Orai1 (appendix figure 3a). Initial characterisation of the antibodies for immunoprecipitation was completed in human platelets (appendix figure 3b). To test the hypothesis that Tspan18 regulates the expression levels of Orai1, these antibodies could now be used for immunoprecipitation of Orai1 from wildtype and Tspan18 deficient platelets, followed by western blotting to detect endogenous expression levels in the presence and absence of Tspan18. Additional techniques, such as flow cytometry could also be utilised to assess the cell surface expression of Orai1 in Tspan18 knockout vs wildtype platelets, to assess the correct surface localisation of the protein as well as overall expression. However, this would rely on the use of good antibodies to the extracellular region of Orai1, which are not currently available.

Another feasible hypothesis, depicted in figure 6.1 C, is that Tspan18 may be regulating and facilitating the clustering of Orai1. One key example of tetraspanin proteins which facilitate clustering of their partner protein is the role that CD9 and CD151 play in regulation of ICAM-1 and VCAM-1, which are vital during leukocyte extravasation during inflammation. These tetraspanins promote formation of nano-platforms of these endothelial adhesion molecules, by clustering ICAM-1 and VCAM-1 to allow more efficient adhesion and transmigration of leukocytes (Barreiro et al., 2008, 2005; Nourshargh et al., 2010). Tspan18 could potentially be facilitating formation of functional Orai1 channels through clustering of Orai1 monomers in the membrane. As discussed in detail in chapter 1, the formation of Orai1 channels is not well characterised. Some groups have suggested that Orai1

channels are formed of 4 separate subunits (Ji et al., 2008; Maruyama et al., 2009; Mignen et al., 2008) and some have proposed 6 subunits are required (Hou et al., 2012). Some studies have outlined the presence of preformed channels in the membrane, which only require activation to allow Ca^{2+} influx into the cell (Madl et al., 2010), whereas other groups suggest that resting Orai1 is found as a dimer and that dimerisation of these dimers must occur for channel activation (Penna et al., 2008). It is possible that Tspan18 could be associated with Orai1 monomers and have a role in the regulation of clustering these monomers into higher order complexes to promote formation of Orai1 channels. Alternatively, Tspan18 could be involved in channel activation rather than channel formation, by providing a platform for preformed Orai1 channels to cluster, therefore inducing formation of Orai1-rich puncta to allow maximal Ca^{2+} influx. When activated, STIM1 proteins form puncta in areas of the ER which are adjacent to the plasma membrane (Smyth et al., 2010). This creates a platform for optimal interaction with Orai1 channels to induce Ca^{2+} influx. It is possible therefore that Tspan18 enables formation of similar Orai1 puncta in the plasma membrane to further enhance and drive channel activation and Ca^{2+} mobilisation. To test these hypotheses, fluorescence microscopy could be employed in cells transfected with tagged Orai1 to monitor puncta formation. This method has been used widely to study Orai1 clustering events and to elucidate the role of several different regulatory proteins in SOCE (Giurisato et al., 2014). Use of cells deficient in Tspan18 through siRNA knockdown would enable measurement of Orai1 puncta formation in the absence of Tspan18.

Alternatively, Tspan18 could be regulating Orai1 through an entirely distinct mechanism. The dynamic interactions formed within tetraspanin enriched microdomains within the membrane not only regulate compartmentalisation of the membrane, but can also affect the lateral mobility of specific membrane proteins (Espenel et al., 2008). If interaction with Tspan18 alters the lateral mobility of Orai1, this might alter potential interaction events between Orai1 monomers and thus affect the efficiency of functional channel formation. The ability to measure the minute details of membrane dynamics has been developed through use of single particle tracking analysis (Sako, Minoghchi, & Yanagida, 2000; Schütz, Kada, Pastushenko, & Schindler, 2000). This method utilises fluorescence microscopy to monitor the dynamics of single molecules within the membrane and enables measurement of diffusion coefficients, modes of motion and special and temporal behaviour of those molecules (Sako et al., 2000; Schütz et al., 2000). This technique has been utilised to demonstrate the highly dynamic nature of tetraspanin microdomains through monitoring the membrane dynamics of the abundantly expressed tetraspanin CD9 (Espenel et al., 2008). This technique could be utilised to monitor Orai1 lateral mobility and behaviour within the membrane in the presence or absence of Tspan18, to investigate whether Tspan18 has a role in regulation of the membrane dynamics of this Ca^{2+} channel.

Finally, it is possible that Tspan18 plays a role in incorporation of Orai1 into tetraspanin enriched microdomains which also contain GPVI. The platelet collagen receptor GPVI has been shown to be tetraspanin associated, so it is reasonable to assume it may be enriched in some tetraspanin microdomains (Protty et al., 2009). The importance of SOCE and especially the proteins

Orai1 and STIM1 have been highlighted in platelet activation downstream of GPVI signalling, though platelet activation via G-protein coupled processes does not appear to be so dependant on SOCE (Braun et al., 2009; David Varga-Szabo, Braun, et al., 2008). Therefore, there might be a currently uncharacterised mechanism which would explain the requirement for Orai1 specifically in GPVI induced platelet activation. If Tspan18 is responsible for bringing Orai1 into the microdomain with GPVI, this may allow for a platform for optimal signalling to occur, where downstream phosphorylation cascades function efficiently and in close proximity, allowing for maximal Ca^{2+} influx and platelet activation. However, platelet responses such as integrin activation and P-selectin exposure have also been previously shown to be Orai1-dependant processes, but not specific to GPVI pathways (Bergmeier et al., 2009). This suggests that Orai1 might be important across multiple platelet pathways, not just the GPVI pathway, though how exactly Tspan18 fits into this mechanism is as yet unknown.

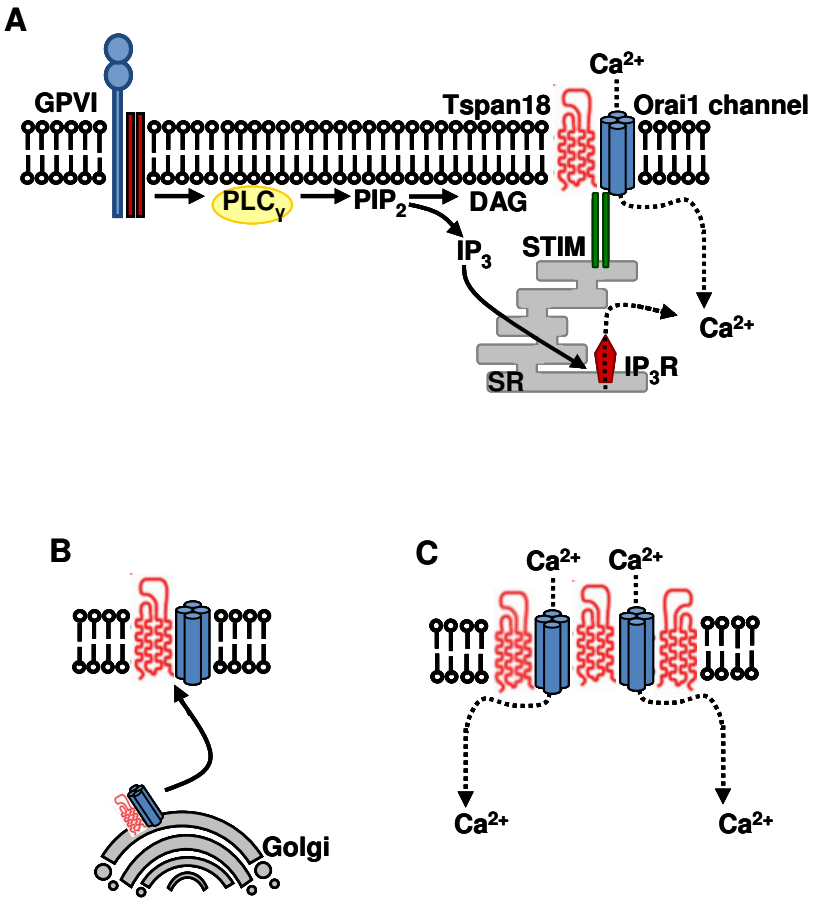

Figure 6.1 – Potential mechanisms of Tspan18 regulation of Orai1. Tspan18 interacts with the CRAC channel Orai1, though the mechanism by which Tspan18 regulates Orai1 is unknown. The interaction between Tspan18 and Orai1 suggests that Tspan18 may have a role in regulation of channel formation or channel activation and therefore effect intracellular Ca^{2+} concentrations (A). Tspan18 could be acting to regulate the biosynthesis and trafficking of Orai1 and therefore might be important for the correct cell surface expression of Orai1 (B). The Tspan18-Orai1 interaction may facilitate clustering of Orai1 within the plasma membrane and therefore enhance and assist in the formation of functional Orai1 channels to allow flux of Ca^{2+} into the cell (C).

6.4 The role of Tspan18 on non-haematopoietic cells

Although the main aim of this thesis was to characterise the role of Tspan18 in platelets, some of the results observed implicated Tspan18 in other, non-haematopoietic cell types. The work using chimeric mice, outlined in detail in chapter 5, demonstrated that the bleeding phenotype observed in the Tspan18 deficient mice was due to defects in non-haematopoietic cells rather

than the platelets. However, it still not known which cell types might be implicated in this disruption to haemostasis and the mechanism has not been elucidated.

It is possible that the bleeding defects observed in the Tspan18 deficient mice are caused by defective endothelial or smooth muscle cell function. Endothelial cells play multiple roles in haemostasis, not least through release of pro- and anti-thrombotic agents and coagulation factors, and smooth muscle cells are important during the process of vasoconstriction to reduce blood flow and limit blood loss (Thomas, 2011; van Hinsbergh, 2012). Tspan18 has been previously identified in endothelial cells through both SAGE analysis and by real time PCR of mouse tissues and human cells (Bailey et al., 2011; Colombo, 2010). Therefore it is possible to hypothesise that endothelial Tspan18 could have role in regulation of haemostasis. During preliminary investigation into the potential roles of Tspan18 in endothelial cells (outlined in chapter 5), knockdown of Tspan18 in HUVEC caused defective migration in a wound closure assay and defective tube formation in a co-culture assay. These data suggest that Tspan18 does have a role in maintaining normal endothelial cell function, but exactly what that role is and what effects this might have on endothelial function *in vivo* is still to be investigated.

One known impact that endothelial cells have on haemostasis is the release of the clotting factors vWF and FVIII from Weibel-Palade bodies in response to vascular injury (Blann, 2006). The response of endothelial cells to injury to release these clotting factors is believed to be a Ca^{2+} dependant process (Rondaij et al., 2006). Therefore it is possible that injury-induced release of

vWF and FVIII from Weibel-Palade bodies in endothelial cells is regulated by Tspan18 and might be defective in the Tspan18 deficient mice, causing the increase in bleeding. It is not necessarily the case that basal levels of these clotting factors would be affected, which could explain why normal basal plasma levels of vWF and FVIII were observed in the Tspan18 deficient mice.

An interesting recent investigation also highlighted the importance of the endothelium in driving the coagulation cascade by providing a surface for the prothrombinase complex to form (Ivanciu, Krishnaswamy, & Camire, 2014). The multiple steps within the coagulation cascade ultimately lead to formation of thrombin, which cleaves fibrinogen to form fibrin, which acts to stabilise the forming clot against disruption by the blood flow (Stegner & Nieswandt, 2011). Two important factors involved in this process are factor Xa (FXa) and factor Va (FVa), which drive thrombin formation. A recent study demonstrated that formation of prothrombinase from these factors is supported by the damaged endothelium rather than being entirely driven by the activated platelet cell surface as previously assumed (Heemskerk, Mattheij, & Cosemans, 2013; Ivanciu et al., 2014). This description of coagulation on the endothelial cell surface, distinct from the platelet thrombus, provides another mechanism by which endothelial cells regulate haemostasis. This process involves exposure of phosphatidylserine by the activated endothelium to provide the surface for prothrombinase activation (Ivanciu et al., 2014). Exposure of phosphatidylserine is a Ca^{2+} dependant process, which could therefore potentially be regulated by endothelial Tspan18.

6.5 Future directions

Having identified a novel tetraspanin-partner protein interaction, the most immediate investigation following this thesis should focus on elucidating the mechanism of regulation of Orai1 by Tspan18. As discussed in section 6.3, the potential role of Tspan18 in regulation of Orai1 expression is already being investigated through immunoprecipitation and western blotting methods using the Tspan18 deficient platelets. There are also experiments using fluorescence microscopy which could be used to investigate other potential mechanisms of action such as cellular localisation and clustering. Future experiments to further investigate the complex interplay of Tspan18 in Ca^{2+} signalling are also required, to elucidate whether this tetraspanin has roles in both release of Ca^{2+} from intracellular stores and SOCE, or whether it's function is limited to just one area of this signalling pathway. The additional experiments outlined in section 3.4, such as completion of platelet function testing in the presence of extracellular Ca^{2+} would help to clarify these questions.

Having described a comprehensive characterisation of the role of Tspan18 in platelet function in this thesis, it would also be interesting to investigate the roles of Tspan18 in other cell types. Perhaps the most obvious direction to move the project next would be to complete a full characterisation of the role of Tspan18 in endothelial cells. Previous studies have demonstrated Tspan18 expression in endothelial cells, and as shown by the preliminary work at the end of chapter 5, Tspan18 may have a role in normal endothelial cell function. It would be interesting to further investigate the potential role of endothelial Tspan18 in the bleeding phenotype observed in the Tspan18

knockout mouse, but would also be useful to analyse other aspects of endothelial cell function. For example, the role of Tspan18 in vascular development, vascular integrity and angiogenesis could be investigated. Interestingly, Tspan18 has been implicated in migration of chick neural crest cells due to regulation of cadherin 6B expression (Fairchild & Gammill, 2013). The potential role for Tspan18 in regulation of endothelial cell migration and thus angiogenesis should therefore be investigated. Interestingly, cadherin 6 is expressed on platelets, and has a potential role in platelet activation as a possible ligand for the integrin αIIbβ3 (Dunne et al., 2012). Preliminary investigation into cadherin 6 expression on Tspan18 deficient platelets using a commercially available antibody to measure surface expression by flow cytometry was unsuccessful (data not shown). It would be interesting to follow this up with an antibody that works to investigate the potential role for Tspan18 in regulation of cadherin 6 expression in platelets.

It is possible that Tspan18 has a wider expression profile and that it also plays roles in other cell types. In order to better investigate the expression profile of Tspan18 and to elucidate in which cell types it might be important, the expression profile of Tspan18 must be better characterised. In order to achieve this, ideally generation of a Tspan18 antibody is required. This would allow assessment of endogenous protein expression levels. Additionally, the Tspan18 knockout mouse is a useful tool in further characterising the expression profile of Tspan18. Due to the lactose operon (Lacz) which is included in the target vector used to generate the knockout mouse, 5-bromo-4-chloro-3-indolyl-β-D-galactopyranoside (Xgal) staining could be employed to measure in which tissues Tspan18 would have been expressed. Lacz

encodes for the β-galactosidase enzyme, therefore wherever Tspan18 would have been expressed in the mouse tissues, β-galactosidase will be expressed instead. This enzyme hydrolyses X-gal to form a blue compound; therefore X-gal staining produces blue staining in tissues which would have expressed Tspan18.

As outlined in section 1.3.5, Tspan18 has already been studied in the development of the nervous system and has also been identified as a susceptibility locus for schizophrenia (J. Yuan et al., 2013; Yue et al., 2011). It could be interesting to further investigate the role of Tspan18 in the developing brain and to elucidate whether Tspan18 mutations which lead to schizophrenia lead to defective Orai1 and reduced Ca^{2+} signalling.

In order to complete the Tspan18 story, the mechanism of Tspan18 action must be elucidated and the extent that it regulates other cell types must also be investigated. At first hand, it appears that Tspan18 may not provide a potential new drug target for thrombosis for treatment of heart attack and stroke, due to the haemostatic defects observed. However, not all of the Tspan18 deficient mice bled which, as discussed in chapter 5, may be due to a potential genetic modifier effect. If this can be better understood, then perhaps Tspan18 would offer an attractive target, to be able to specifically target Orai1 and Ca^{2+} signalling downstream of GPVI during platelet activation, without disruption to multiple other cell types.

APPENDICES

APPENDIX 1

Tspan18 knockout mice have normal body weight and normal heart weight.

As a basic assessment of overall health and development of the Tspan18 deficient mice, litter matched pairs at 8-9 weeks old were weighed. There was no difference in the bodyweight of Tspan18 deficient mice and wildtype mice (appendix figure 1a). Additionally, as a basic assessment of cardiac health, the hearts of litter matched pairs at 10-12 weeks old were weighed. There was no difference in the weight of hearts of Tspan18 deficient mice and wildtype mice (appendix figure 1b).

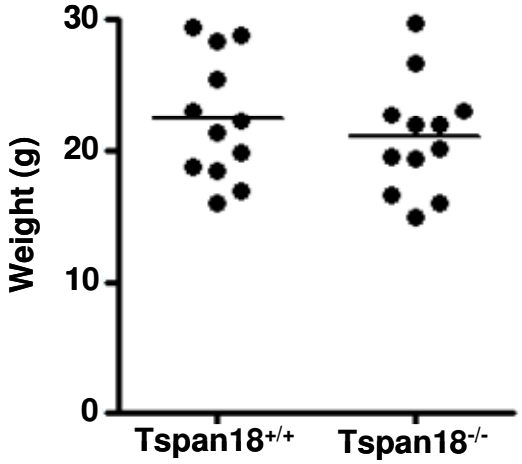

Appendix figure 1a – Bodyweight of the Tspan18 deficient mice is normal. Litter matched pairs of wildtype and Tspan18 deficient mice were weighed at 8-9 weeks old. Data were analysed by T-test. Each symbol represents an individual.

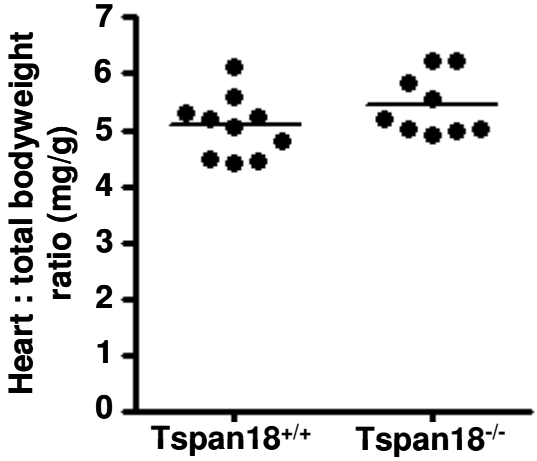

Appendix figure 1b –Tspan18 deficient mice have normal heart weight. Hearts were harvested from litter matched pairs of wildtype and Tspan18 deficient mice at 10-12 weeks old. Tissue was blotted to remove excess blood and hearts weighed. Data were normalised to total bodyweight for each individual, and analysed by T-test. Each symbol represents an individual.

APPENDIX 2

Optimisation of siRNA knockdown of Tspan18 in HUVEC

As a preliminary investigation into the potential role of Tspan18 on endothelial cells, *in vitro* assays using HUVEC were employed. Expression of Tspan18 was disrupted using two different siRNA duplexes in comparison to a control siRNA duplex.

To optimise knockdown of Tspan18, HUVEC were harvested either 48, 72, or 96 hours post-transfection, Tspan18 mRNA was assessed via real time quantitative PCR. Both duplexes induced the highest level of knockdown 48 hours post transfection, and no difference was observed in Tspan18 expression between non-transfected cells and a control siRNA duplex (appendix figure 2).

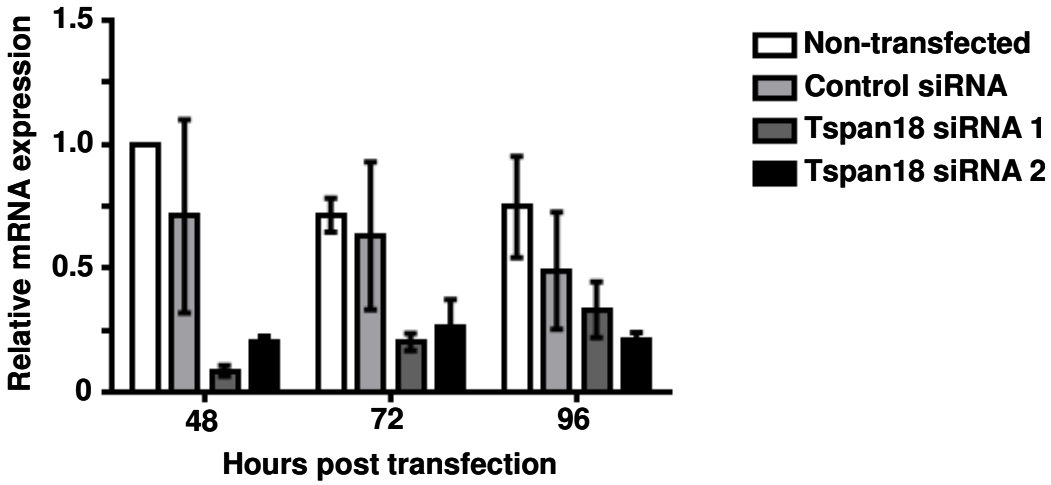

Appendix figure 2 – Optimisation of Tspan18 knockdown in HUVEC using siRNA. Expression of Tspan18 was disrupted using two different siRNA duplexes, compared with non-transfected cells and a control siRNA duplex. HUVEC were transfected with siRNA duplexes using RNAiMAX and were harvested 48, 72, or 96 hours post-transfection. Tspan18 expression was assessed via real time PCR. Relative mRNA levels of Tspan18 in each sample are shown. Error bars represent the standard error of the mean from 3 separate experiments.

APPENDIX 3

Characterising Orai1 antibodies

To better investigate the impact of Tspan18 on Orai1 and to be able to monitor endogenous levels of Orai1, rather than rely on over-expression systems, a suitable Orai1 antibody was required.

To characterise Orai1 antibodies for use in western blotting, HEK293T cells were transfected with two different Myc-tagged human Orai1 constructs. Cells were then lysed, samples separated by SDS-PAGE electrophoresis and protein expressed assessed by western blotting. Two different Orai1 antibodies were tested; ProSci 4281 (Orai1-CT), raised against a 16 amino acid region at the carboxyl terminus of Orai1, and ProSci 4041 (Orai1-NT), raised against an 18 amino acid region at the amino terminus of Orai1. Expression of Orai1 in the HEK293T cells was confirmed by blotting with an anti-Myc antibody. Blotting with either of the Orai1 antibodies detected bands corresponding to the correct molecular weight for Orai1 when HEK293T cells were transfected with either Orai1 construct, whereas no corresponding bands were observed in the non-transfected control sample (appendix figure 3a). To assess whether endogenous levels of Orai1 could be detected by western blotting, washed mouse platelets were prepared, lysed, separated by SDS-PAGE electrophoresis and blotted with the Orai1-CT antibody. Several non-specific bands were observed and no clear band corresponding to the molecular weight of Orai1 could be distinguished (appendix figure 3a, B). The

inability to distinguish the endogenous levels of Orai1 was probably due to the low levels of endogenous Orai1 present in mouse platelets.

To attempt to detect endogenous levels of Orai1, an immunoprecipitation approach was used. To characterise the Orai1 antibodies for immunoprecipitation, human platelets were used rather than mouse platelets, as they are abundant and readily available.

Human platelets were isolated from the blood and washed into modified Tyrode's buffer. The platelets were lysed, immunoprecipitated, and samples were separated by SDS-PAGE and western blotted. Immunoprecipitation for CD9 was completed alongside those for Orai1, as a positive control, and both MOPC and Rab IgG were used as negative controls. A band of approximately the correct molecular weight for Orai1 was observed after blotting with the Orai1-CT antibody following immunoprecipitation with either Orai1 antibody, and was also observed when blotting the platelet whole cell lysate (appendix figure 3b). Immunoprecipitation for CD9 resulted in enrichment of this tetraspanin.

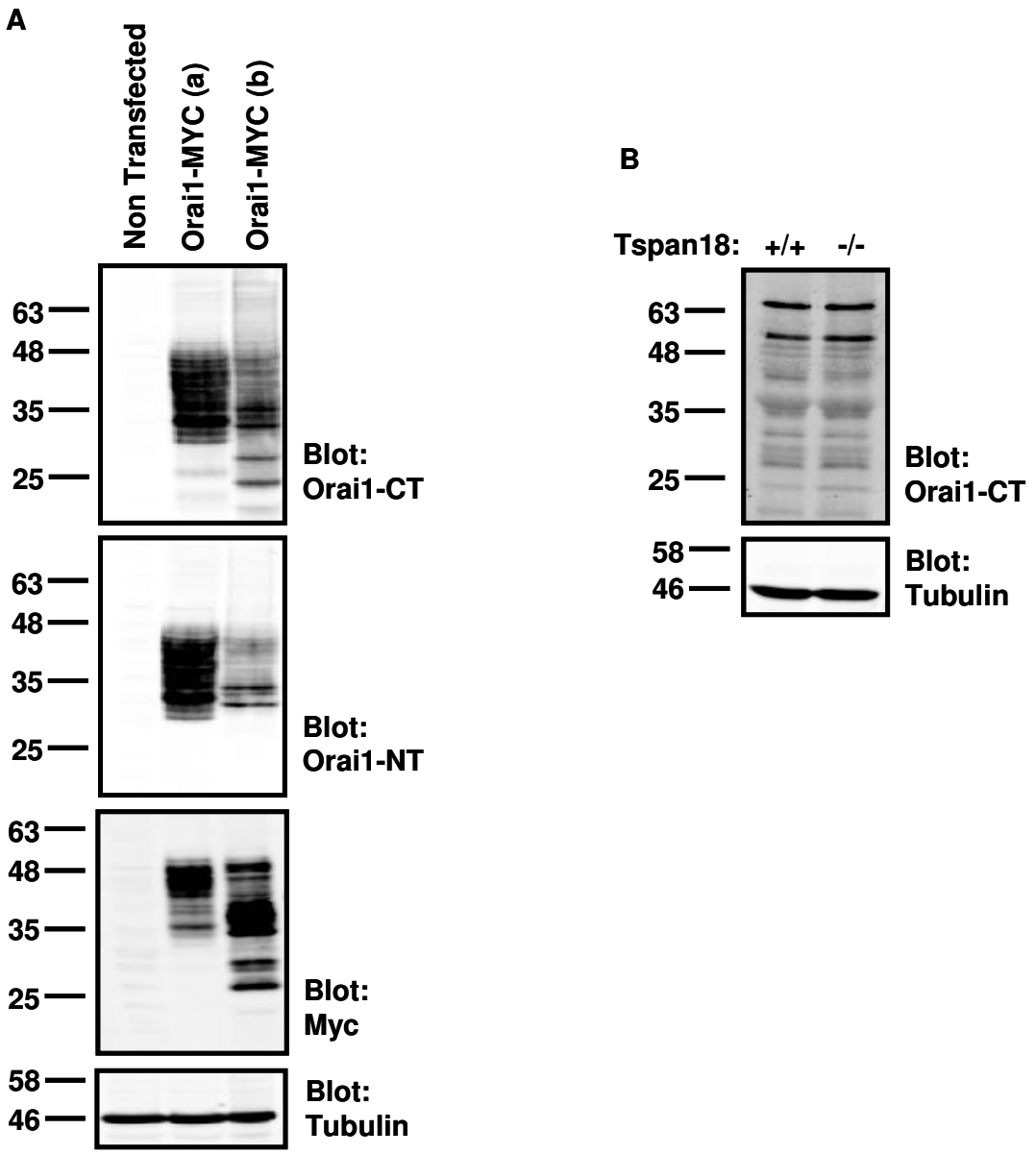

Appendix figure 3a - Characterising Orai1 antibodies for use in western blotting. HEK293T cells were transfected using PEI with Myc-tagged Orai1. Whole cell lysate samples were separated by SDS-PAGE and western blotted with either an Orai1 antibody, an anti-Myc antibody to check expression, or a tubulin antibody to control for loading (A). Mouse platelets were isolated from the whole blood and lysed in sample buffer. Samples were separated by SDS-PAGE and western blotted with an Orai1 antibody (B). Representative blots are shown from 3 separate experiments.

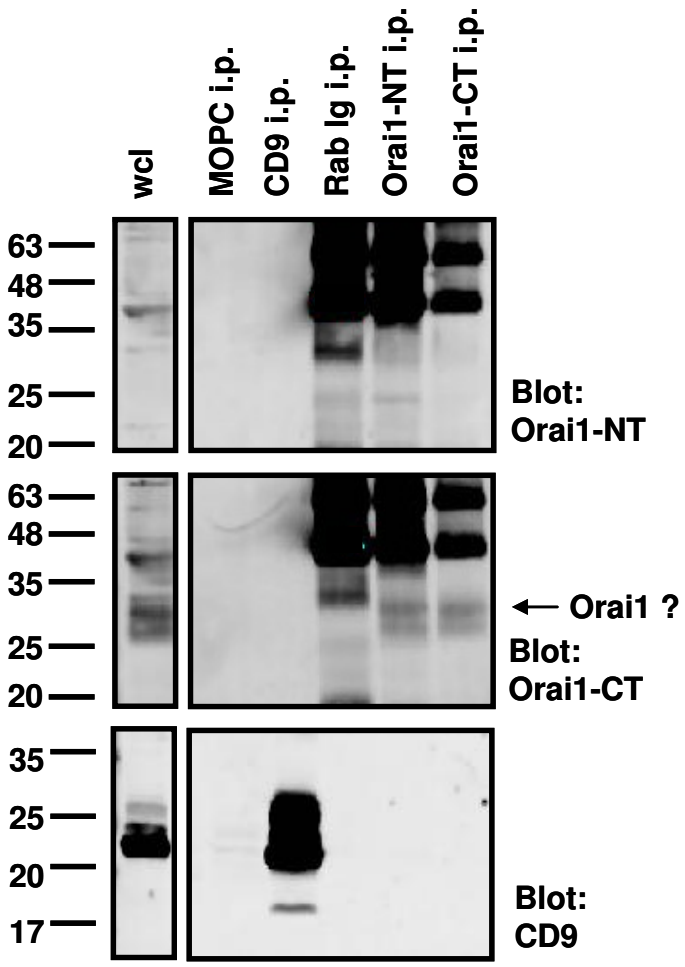

Appendix figure 3b – Characterising Orai1 antibodies for immunoprecipitation. Human platelets were isolated from the blood and lysed in Brij97 lysis buffer. Samples were immunoprecipitated as labelled above, separated by SDS-PAGE and western blotted as labelled above. A representative blot from 2 separate experiments is shown.

APPENIX 4

Published papers

Bailey R.L., Herbert J.M., Khan K., Heath V.L., Bicknell R. and Tomlinson M.G., 2011. The emerging role of tetraspanin microdomains on endothelial cells. *Biochemical Society Transactions*, 39(6), pp.1667–1673

Haining E.J., Yang J., **Bailey R.L.,** Khan K., Collier R., Tsai S., Watson S.P., Frampton J., Garcia P. and Tomlinson M.G., 2012. The TspanC8 subgroup of tetraspanins interacts with A disintegrin and metalloprotease 10 (ADAM10) and regulates its maturation and cell surface expression. *The Journal of biological chemistry*, 287(47), pp.39753–65

REFERENCES

Baba, Y., Matsumoto, M., & Kurosaki, T. (2014). Calcium signaling in B cells: Regulation of cytosolic Ca(2+) increase and its sensor molecules, STIM1 and STIM2. *Molecular Immunology*, *62*(2), 339–343. doi:10.1016/j.molimm.2013.10.006

Bailey, R. L., Herbert, J. M., Khan, K., Heath, V. L., Bicknell, R., & Tomlinson, M. G. (2011). The emerging role of tetraspanin microdomains on endothelial cells. *Biochemical Society Transactions*. doi:10.1042/BST20110745

Barreiro, O., Ovalle, S., Higginbottom, A., & Monk, P. N. (2005). Endothelial tetraspanin microdomains regulate leukocyte firm adhesion during extravasation. *Immunobiology*, *105*(7), 2852–2861. doi:10.1182/blood-2004-09-3606.

Barreiro, O., Zamai, M., Yáñez-Mó, M., Tejera, E., López-Romero, P., Monk, P. N., … Sánchez-Madrid, F. (2008). Endothelial adhesion receptors are recruited to adherent leukocytes by inclusion in preformed tetraspanin nanoplatforms. *The Journal of Cell Biology*, *183*(3), 527–42. doi:10.1083/jcb.200805076

Becker, B. F., Heindl, B., Kupatt, C., & Zahler, S. (2000). Endothelial function and hemostasis. *Zeitschrift Für Kardiologie*, *89*(3), 160–7.

Bénézech, C., & Nayar, S. (2014). CLEC-2 is required for development and maintenance of lymph nodes. *Blood*, *123*(20), 3200–3207. doi:10.1182/blood-2013-03-489286.

Bergmeier, W., Oh-hora, M., Mccarl, C., Roden, R. C., Bray, P. F., & Feske, S. (2009). Brief report R93W mutation in Orai1 causes impaired calcium influx in platelets. *Blood*, *113*(3), 675–678. doi:10.1182/blood-2008-08-174516.The

Berndt, M. C., & Andrews, R. K. (2011). Bernard-Soulier syndrome. *Haematologica*, *96*(3), 355–9. doi:10.3324/haematol.2010.039883

Berridge, M. J., & Irvine, R. F. (1984). Inositol trisphosphate, a novel second messenger in cellular signal transduction. *Nature*, *312*(22), 315 – 321.

Bertozzi, C. C., Schmaier, A. A., Mericko, P., Hess, P. R., Zou, Z., Chen, M., … Kahn, M. L. (2010). Platelets regulate lymphatic vascular development through CLEC-2 – SLP-76 signaling. *Blood*, *116*(4), 661–670. doi:10.1182/blood-2010-02-270876.

Best, L., Martin, T., Russel, R., & Preston, F. (1977). Prostacyclin increases cyclic AMP levels and adenylate cyclase activity in platelets. *Nature*, *267*, 850–852.

Blann, A. D. (2006). Plasma von Willebrand factor , thrombosis , and the endothelium: The first 30 years. *Thrombosis and Haemostasis*, *95*, 49–55. doi:10.1160/TH05

Boilard, E., Nigrovic, P. a, Larabee, K., Watts, G. F. M., Coblyn, J. S., Weinblatt, M. E., … Lee, D. M. (2010). Platelets amplify inflammation in arthritis via collagen-

dependent microparticle production. *Science (New York, N.Y.)*, *327*(5965), 580–3. doi:10.1126/science.1181928

Born, G. V. R. (1962). Aggregation of blood platelets by adenosine diphosphate and its reversal. *Nature*, *194*, 927–9.

Boulaftali, Y., Hess, P. R., Getz, T. M., Cholka, A., Stolla, M., Mackman, N., … Bergmeier, W. (2013). Platelet ITAM signaling is critical for vascular integrity in inflammation. *The Journal of Clinical Investigation*, *123*(2). doi:10.1172/JCI65154.908

Brass, L. F. (2003). Thrombin and platelet activation. *Chest*, *124*, 18S–25S. doi:10.1378/chest.124.3_suppl.18S

Braun, A., Varga-Szabo, D., Kleinschnitz, C., Pleines, I., Bender, M., Austinat, M., … Nieswandt, B. (2009). Orai1 (CRACM1) is the platelet SOC channel and essential for pathological thrombus formation. *Blood*, *113*(9), 2056–63. doi:10.1182/blood-2008-07-171611

Broos, K., Feys, H. B., De Meyer, S. F., Vanhoorelbeke, K., & Deckmyn, H. (2011). Platelets at work in primary hemostasis. *Blood Reviews*, *25*(4), 155–67. doi:10.1016/j.blre.2011.03.002

Bustin, S. a, Benes, V., Garson, J. a, Hellemans, J., Huggett, J., Kubista, M., … Wittwer, C. T. (2009). The MIQE guidelines: minimum information for publication of quantitative real-time PCR experiments. *Clinical Chemistry*, *55*(4), 611–22. doi:10.1373/clinchem.2008.112797

Charrin, S., Jouannet, S., Boucheix, C., & Rubinstein, E. (2014). Tetraspanins at a glance. *Journal of Cell Science*, *127*, 3641–3648. doi:10.1242/jcs.154906

Charrin, S., Le Naour, F., Oualid, M., Billard, M., Faure, G., Hanash, S. M., … Rubinstein, E. (2001). The major CD9 and CD81 molecular partner. Identification and characterization of the complexes. *The Journal of Biological Chemistry*, *276*(17), 14329–37. doi:10.1074/jbc.M011297200

Charrin, S., le Naour, F., Silvie, O., Milhiet, P.-E., Boucheix, C., & Rubinstein, E. (2009). Lateral organization of membrane proteins: tetraspanins spin their web. *The Biochemical Journal*, *420*(2), 133–54. doi:10.1042/BJ20082422

Charrin, S., Manié, S., Billard, M., Ashman, L., Gerlier, D., Boucheix, C., & Rubinstein, E. (2003). Multiple levels of interactions within the tetraspanin web. *Biochemical and Biophysical Research Communications*, *304*(1), 107–112. doi:10.1016/S0006-291X(03)00545-X

Charrin, S., Manié, S., Oualid, M., Billard, M., Boucheix, C., & Rubinstein, E. (2002). Differential stability of tetraspanin/tetraspanin interactions: role of palmitoylation. *FEBS Letters*, *516*(1-3), 139–44.

Charrin, S., Manié, S., Thiele, C., Billard, M., Gerlier, D., Boucheix, C., & Rubinstein, E. (2003). A physical and functional link between cholesterol and tetraspanins. *European Journal of Immunology*, *33*(9), 2479–89. doi:10.1002/eji.200323884

Cheli, Y., Jensen, D., Marchese, P., Habart, D., Wiltshire, T., Cooke, M., … Kunicki, T. J. (2008). The Modifier of hemostasis (Mh) locus on chromosome 4 controls in vivo hemostasis of Gp6 -/- mice. *Hemostasis, Thrombosis and Vascular Biology*, *111*(3), 1266–1273. doi:10.1182/blood-2007-09-111369.The

Chou, J., Mackman, N., Merrill-skoloff, G., Pedersen, B., Furie, B. C., & Furie, B. (2004). Hematopoietic cell-derived microparticle tissue factor contributes to fibrin formation during thrombus propagation. *Blood*, *104*(10), 3190–3197. doi:10.1182/blood-2004-03-0935.Supported

Colombo, D. (2010). CHARACTERIZATION OF THE TETRASPANIN PROTEIN TSPAN18. *PhD Thesis*, (September).

Crabtree, G. R., & Olson, E. N. (2002). NFAT signaling: choreographing the social lives of cells. *Cell*, *109 Suppl*, S67–79.

De Candia, E. (2012). Mechanisms of platelet activation by thrombin: a short history. *Thrombosis Research*, *129*(3), 250–6. doi:10.1016/j.thromres.2011.11.001

Dornier, E., Coumailleau, F., Ottavi, J.-F., Moretti, J., Boucheix, C., Mauduit, P., … Rubinstein, E. (2012). TspanC8 tetraspanins regulate ADAM10/Kuzbanian trafficking and promote Notch activation in flies and mammals. *The Journal of Cell Biology*, *199*(3), 481–96. doi:10.1083/jcb.201201133

Doyle, E. L., Ridger, V., Ferraro, F., Turmaine, M., Saftig, P., & Cutler, D. F. (2011). CD63 is an essential cofactor to leukocyte recruitment by endothelial P-selectin. *Blood*, *118*(15), 1–3. doi:10.1182/blood-2010-11-321489.

Drummer, H. E., Wilson, K. A., & Poumbourios, P. (2002). Identification of the Hepatitis C Virus E2 Glycoprotein Binding Site on the Large Extracellular Loop of CD81. *Journal of Virology*, *76*(21), 11143–11147. doi:10.1128/JVI.76.21.11143

Dütting, S., Bender, M., & Nieswandt, B. (2012). Platelet GPVI: a target for antithrombotic therapy?! *Trends in Pharmacological Sciences*, *33*(11), 583–90. doi:10.1016/j.tips.2012.07.004

Dunne, E., Spring, C. M., Reheman, A., Jin, W., Berndt, M. C., Newman, D. K., … Kenny, D. (2012). Cadherin 6 has a functional role in platelet aggregation and thrombus formation. *Arteriosclerosis, Thrombosis, and Vascular Biology*, *32*(7), 1724–31. doi:10.1161/ATVBAHA.112.250464

Eble, J. A., Po, S., Inoue, O., Gartner, T. K., Hughan, S. C., Pearce, A. C., … Watson, S. P. (2006). A novel Syk-dependent mechanism of platelet activation by the C-

type lectin receptor CLEC-2. *Blood*, *107*(16790533), 542–549. doi:10.1182/blood-2005-05-1994.

Echtler, K., Stark, K., Lorenz, M., Kerstan, S., Walch, A., Jennen, L., … Massberg, S. (2010). Platelets contribute to postnatal occlusion of the ductus arteriosus. *Nature Medicine*, *16*(1), 75–82. doi:10.1038/nm.2060

Ehrhardt, C., Schmolke, M., Matzke, A., Knoblauch, A., Will, C., Wixler, V., & Ludwig, S. (2006). Polyethylenimine, a cost-effective transfection reagent. *Signal Transduction*, *6*, 179–184. doi:10.1002/sita.200500073

Ema, H., & Nakauchi, H. (2015). Expansion of hematopoietic stem cells in the developing liver of a mouse embryo. *Blood*, *95*(7), 2284–2289.

Espenel, C., Margeat, E., Dosset, P., Arduise, C., Le Grimellec, C., Royer, C. a, … Milhiet, P.-E. (2008). Single-molecule analysis of CD9 dynamics and partitioning reveals multiple modes of interaction in the tetraspanin web. *The Journal of Cell Biology*, *182*(4), 765–76. doi:10.1083/jcb.200803010

Everett, L. a, Cleuren, A. C. a, Khoriaty, R. N., & Ginsburg, D. (2014). Murine coagulation factor VIII is synthesized in endothelial cells. *Blood*, *123*(24), 3697–705. doi:10.1182/blood-2014-02-554501

Fairchild, C. L., & Gammill, L. S. (2013). Tetraspanin18 is a FoxD3-responsive antagonist of cranial neural crest epithelial-to-mesenchymal transition that maintains cadherin-6B protein. *Journal of Cell Science*, *126*(Pt 6), 1464–76. doi:10.1242/jcs.120915

Farndale, R. W. (2006). Collagen-induced platelet activation. *Blood Cells, Molecules & Diseases*, *36*(2), 162–5. doi:10.1016/j.bcmd.2005.12.016

Feng, M., Grice, D. M., Faddy, H. M., Nguyen, N., Leitch, S., Wang, Y., … Rao, R. (2010). Store-independent activation of Orai1 by SPCA2 in mammary tumors. *Cell*, *143*(1), 84–98. doi:10.1016/j.cell.2010.08.040

Feske, S., Gwack, Y., Prakriya, M., Srikanth, S., Puppel, S.-H., Tanasa, B., … Rao, A. (2006). A mutation in Orai1 causes immune deficiency by abrogating CRAC channel function. *Nature*, *441*(7090), 179–85. doi:10.1038/nature04702

Finney, B. A., Schweighoffer, E., Navarro-nu, L., Hughes, C. E., Langan, S. A., Lowe, K. L., … Watson, S. P. (2012). CLEC-2 and Syk in the megakaryocytic / platelet lineage are essential for development. *Blood*, *119*(7), 1747–1756. doi:10.1182/blood-2011-09-380709.

Forrester, L. M., Bernstein, A., Rossant, J., & Nagy, A. (1991). Long-term reconstitution of the mouse hematopoietic system by embryonic stem cell-derived fetal liver. *Proceedings of the National Academy of Sciences of the United States of America*, *88*(September), 7514–7517.

Gilio, K., van Kruchten, R., Braun, A., Berna-Erro, A., Feijge, M. a H., Stegner, D., … Nieswandt, B. (2010). Roles of platelet STIM1 and Orai1 in glycoprotein VI- and thrombin-dependent procoagulant activity and thrombus formation. *The Journal of Biological Chemistry*, *285*(31), 23629–38. doi:10.1074/jbc.M110.108696

Giurisato, E., Gamberucci, a, Ulivieri, C., Marruganti, S., Rossi, E., Giacomello, E., … Sorrentino, V. (2014). The KSR2-calcineurin complex regulates STIM1-ORAI1 dynamics and store-operated calcium entry (SOCE). *Molecular Biology of the Cell*, *25*(11), 1769–81. doi:10.1091/mbc.E13-05-0292

Giustarini, D., Rossi, R., Milzani, A., & Dalle-Donne, I. (2008). Nitrite and Nitrate Measurement by Griess Reagent in Human Plasma: Evaluation of Interferences and Standardization. *Methods in Enzymology*. doi:10.1016/S0076-6879(07)00823-3

Goschnick, M. W., Lau, L. M., Wee, J. L., Liu, Y. S., Hogarth, P. M., Robb, L. M., … Jackson, D. E. (2006). Impaired "outside-in" integrin alphaIIbbeta3 signaling and thrombus stability in TSSC6-deficient mice. *Blood*, *108*(6), 1911–8. doi:10.1182/blood-2006-02-004267

Grosse, J., Braun, A., Varga-szabo, D., Beyersdorf, N., Schneider, B., Zeitlmann, L., … Nieswandt, B. (2007). An EF hand mutation in Stim1 causes premature platelet activation and bleeding in mice. *The Journal of Clinical Investigation*, *117*(11). doi:10.1172/JCI32312.3540

Grüner, S., Prostredna, M., Koch, M., Miura, Y., Schulte, V., Jung, S. M., … Nieswandt, B. (2005). Relative antithrombotic effect of soluble GPVI dimer compared with anti-GPVI antibodies in mice. *Blood*, *105*(4), 1492–9. doi:10.1182/blood-2004-06-2391

Grynkiewicz, G., Poenie, M., & Tsienb, R. Y. (1985). A New Generation of Ca2 + Indicators with Greatly Improved Fluorescence Properties *. *The Journal of Biological Chemistry*, *260*(6), 3440–3450.

Gwack, Y., Srikanth, S., Feske, S., Cruz-Guilloty, F., Oh-hora, M., Neems, D. S., … Rao, A. (2007). Biochemical and functional characterization of Orai proteins. *The Journal of Biological Chemistry*, *282*(22), 16232–43. doi:10.1074/jbc.M609630200

Haining, E. J., Yang, J., Bailey, R. L., Khan, K., Collier, R., Tsai, S., … Tomlinson, M. G. (2012). The TspanC8 subgroup of tetraspanins interacts with A disintegrin and metalloprotease 10 (ADAM10) and regulates its maturation and cell surface expression. *The Journal of Biological Chemistry*, *287*(47), 39753–65. doi:10.1074/jbc.M112.416503

Haining, E. J., Yang, J., & Tomlinson, M. G. (2011). Tetraspanin microdomains: fine-tuning platelet function. *Biochemical Society Transactions*, *39*(2), 518–23. doi:10.1042/BST0390518

Handschumacher, R. E., Harding, M. W., Rice, J., Drugge, R. J., & Speicher, D. W. (1984). Cyclophilin: a specific cytosolic binding protein for cyclosporin A. *Science (New York, N.Y.)*, *226*, 544–547. doi:10.1126/science.6238408

Heemskerk, J. W. M., Mattheij, N. J. a, & Cosemans, J. M. E. M. (2013). Platelet-based coagulation: different populations, different functions. *Journal of Thrombosis and Haemostasis : JTH*, *11*(1), 2–16. doi:10.1111/jth.12045

Hemler, M. E. (2003). Tetraspanin proteins mediate cellular penetration, invasion, and fusion events and define a novel type of membrane microdomain. *Annual Review of Cell and Developmental Biology*, *19*, 397–422. doi:10.1146/annurev.cellbio.19.111301.153609

Hemler, M. E. (2005). Tetraspanin functions and associated microdomains. *Nature Reviews. Molecular Cell Biology*, *6*(10), 801–11. doi:10.1038/nrm1736

Hemler, M. E. (2014). Tetraspanin proteins promote multiple cancer stages. *Nature Reviews Cancer*, *14*(1), 49–60. doi:10.1038/nrc3640

Herzog, B. H., Fu, J., Wilson, S. J., Hess, P. R., Sen, A., McDaniel, J. M., … Xia, L. (2013). Podoplanin maintains high endothelial venule integrity by interacting with platelet CLEC-2. *Nature*, *502*(7469), 105–9. doi:10.1038/nature12501

Hess, P. R., Rawnsley, D. R., Jakus, Z., Yang, Y., Sweet, D. T., Fu, J., … Kahn, M. L. (2014). Platelets mediate lymphovenous hemostasis to maintain blood-lymphatic separation throughout life. *The Journal of Clinical Investigation*, *124*(1), 273–284. doi:10.1172/JCI70422.Syk

Higginbottom, A., Quinn, E. R., Kuo, C. C., Flint, M., Wilson, L. H., Bianchi, E., … Levy, S. (2000). Identification of amino acid residues in CD81 critical for interaction with hepatitis C virus envelope glycoprotein E2. *Journal of Virology*, *74*, 3642–3649. doi:10.1128/JVI.74.8.3642-3649.2000

Hodivala-dilke, K. M., Mchugh, K. P., Tsakiris, D. A., Rayburn, H., Crowley, D., Ullman-culleré, M., … Hynes, R. O. (1999). β3 -integrin – deficient mice are a model for Glanzmann thrombasthenia showing placental defects and reduced survival. *The Journal of Clinical Investigation*, *103*(2), 229–238. doi:10.1172/JCI5487.

Horii, K., Kahn, M. L., & Herr, A. B. (2006). Structural basis for platelet collagen responses by the immune-type receptor glycoprotein VI. *Blood*, *108*(3), 936–942. doi:10.1182/blood-2006-01-010215.Supported

Hoth, M., & Niemeyer, B. A. (2013). The Neglected CRAC Proteins: Orai2, Orai3, and STIM2. *Current Topics in Membranes*, *71*, 237–271. doi:10.1016/B978-0-12-407870-3.00010-X

Hou, X., Pedi, L., Diver, M. M., & Long, S. B. (2012). Crystal structure of the calcium release-activated calcium channel Orai. *Science (New York, N.Y.)*, *338*(6112), 1308–13. doi:10.1126/science.1228757

Hughes, C. E., Auger, J. M., McGlade, J., Eble, J. a, Pearce, a C., & Watson, S. P. (2008). Differential roles for the adapters Gads and LAT in platelet activation by GPVI and CLEC-2. *Journal of Thrombosis and Haemostasis : JTH*, *6*(12), 2152–9. doi:10.1111/j.1538-7836.2008.03166.x

Hughes, C. E., Navarro-Núñez, L., Finney, B. A., Mourão-Sá, D., Pollitt, A. Y., & Watson, S. P. (2010). CLEC-2 is not required for platelet aggregation at arteriolar shear. *Journal of Thrombosis and Haemostasis : JTH*, *8*(10), 2328–32. doi:10.1111/j.1538-7836.2010.04006.x

Inoue, O., Suzuki-Inoue, K., Dean, W. L., Frampton, J., & Watson, S. P. (2003). Integrin alpha2beta1 mediates outside-in regulation of platelet spreading on collagen through activation of Src kinases and PLCgamma2. *The Journal of Cell Biology*, *160*(5), 769–80. doi:10.1083/jcb.200208043

Italiano, J. E. (2013). Unraveling mechanisms that control platelet production. *Seminars in Thrombosis and Hemostasis*, *39*(1), 15–24. doi:10.1055/s-0032-1331157

Italiano, J. E. I., Richardson, J. L., Patel-hett, S., Battinelli, E., Zaslavsky, A., Short, S., … Klement, G. L. (2008). Angiogenesis is regulated by a novel mechanism : pro- and antiangiogenic proteins are organized into separate platelet granules and differentially released. *Blood*, *111*(3), 1227–1233. doi:10.1182/blood-2007-09-113837.An

Ivanciu, L., Krishnaswamy, S., & Camire, R. M. (2014). New insights into the spatiotemporal localization of prothrombinase in vivo. *Blood*, *124*(11), 1705–1714. doi:10.1182/blood-2014-03-565010.The

Jardin, I., Gómez, L. J., Salido, G. M., & Rosado, J. a. (2009). Dynamic interaction of hTRPC6 with the Orai1-STIM1 complex or hTRPC3 mediates its role in capacitative or non-capacitative Ca(2+) entry pathways. *The Biochemical Journal*, *420*(2), 267–76. doi:10.1042/BJ20082179

Jardin, I., Lopez, J. J., Salido, G. M., & Rosado, J. a. (2008). Orai1 mediates the interaction between STIM1 and hTRPC1 and regulates the mode of activation of hTRPC1-forming Ca2+ channels. *The Journal of Biological Chemistry*, *283*(37), 25296–304. doi:10.1074/jbc.M802904200

Ji, W., Xu, P., Li, Z., Lu, J., Liu, L., Zhan, Y., … Chen, L. (2008). Functional stoichiometry of the unitary calcium-release-activated calcium channel. *Proceedings of the National Academy of Sciences of the United States of America*, *105*(36), 13668–73. doi:10.1073/pnas.0806499105

Jin, J., Daniel, J. L., & Kunapuli, S. P. (1998). Molecular basis for ADP-induced platelet activation. II. The P2Y1 receptor mediates ADP-induced intracellular calcium mobilization and shape change in platelets. *The Journal of Biological Chemistry*, *273*, 2030–2034. doi:10.1074/jbc.273.4.2030

Junge, H. J., Yang, S., Burton, J. B., Paes, K., Shu, X., French, D. M., … Ye, W. (2009). TSPAN12 regulates retinal vascular development by promoting Norrin- but not Wnt-induced FZD4/beta-catenin signaling. *Cell*, *139*(2), 299–311. doi:10.1016/j.cell.2009.07.048

Kaji, K., Oda, S., Shikano, T., Ohnuki, T., Uematsu, Y., Sakagami, J., … Kudo, a. (2000). The gamete fusion process is defective in eggs of Cd9-deficient mice. *Nature Genetics*, *24*(3), 279–82. doi:10.1038/73502

Kanaji, S., Fahs, S. a, Shi, Q., Haberichter, S. L., & Montgomery, R. R. (2012). Contribution of platelet vs. endothelial VWF to platelet adhesion and hemostasis. *Journal of Thrombosis and Haemostasis : JTH*, *10*(8), 1646–52. doi:10.1111/j.1538-7836.2012.04797.x

Karin, M. (1995). The regulation of AP-1 activity by mitogen-activated protein kinases. *The Journal of Biological Chemistry*, *270*(28), 16483 – 16486.

Kaur, S., Leszczynska, K., Abraham, S., Scarcia, M., Hiltbrunner, S., Marshall, C. J., … Heath, V. L. (2011). RhoJ/TCL regulates endothelial motility and tube formation and modulates actomyosin contractility and focal adhesion numbers. *Arteriosclerosis, Thrombosis, and Vascular Biology*, *31*(3), 657–64. doi:10.1161/ATVBAHA.110.216341

Kazarov, A. R., Yang, X., Stipp, C. S., Sehgal, B., & Hemler, M. E. (2002). An extracellular site on tetraspanin CD151 determines alpha 3 and alpha 6 integrin-dependent cellular morphology. *The Journal of Cell Biology*, *158*, 1299–1309. doi:10.1083/jcb.200204056

Kitadokoro, K., Bordo, D., Galli, G., Petracca, R., Falugi, F., Abrignani, S., … Bolognesi, M. (2001). CD81 extracellular domain 3D structure: insight into the tetraspanin superfamily structural motifs. *The EMBO Journal*, *20*(1-2), 12–8. doi:10.1093/emboj/20.1.12

Kleinschnitz, C., Pozgajova, M., Pham, M., Bendszus, M., Nieswandt, B., & Stoll, G. (2007). Targeting platelets in acute experimental stroke: impact of glycoprotein Ib, VI, and IIb/IIIa blockade on infarct size, functional outcome, and intracranial bleeding. *Circulation*, *115*(17), 2323–30. doi:10.1161/CIRCULATIONAHA.107.691279

Konopatskaya, O., Gilio, K., Harper, M. T., Zhao, Y., Cosemans, J. M. E. M., Karim, Z. A., … Poole, A. W. (2009). PKCalpha regulates platelet granule secretion and thrombus formation in mice. *The Journal of Clinical Investigation*, *119*, 399–407. doi:10.1172/JCI34665

Konopatskaya, O., Matthews, S. A., Harper, M. T., Gilio, K., Cosemans, J. M. E. M., Williams, C. M., … Poole, A. W. (2011). Protein kinase C mediates platelet secretion and thrombus formation through protein kinase D2. *Blood*, *118*(2), 416–424. doi:10.1182/blood-2010-10-312199.An

Kuijpers, M. J. E., van der Meijden, P. E. J., Feijge, M. a H., Mattheij, N. J. a, May, F., Govers-Riemslag, J., … Cosemans, J. M. E. M. (2014). Factor XII Regulates the Pathological Process of Thrombus Formation on Ruptured Plaques. *Arteriosclerosis, Thrombosis, and Vascular Biology*, *34*(8), 1674–80. doi:10.1161/ATVBAHA.114.303315

Landau, L. (1982). Direct activation of calcium-activated, phospholipid-dependent protein kinase by tumor-promoting phorbol esters. *The Journal of Biological Chemistry*, *257*, 7847–7851.

Lang, F., Münzer, P., Gawaz, M., & Borst, O. (2013). Regulation of STIM1/Orai1-dependent Ca2+ signalling in platelets. *Thrombosis and Haemostasis*, *110*(5), 925–30. doi:10.1160/TH13-02-0176

Lau, L. M., Wee, J. L., Wright, M. D., Moseley, G. W., Hogarth, P. M., Ashman, L. K., & Jackson, D. E. (2004). The tetraspanin superfamily member CD151 regulates outside-in integrin alphaIIbbeta3 signaling and platelet function. *Blood*, *104*(8), 2368–75. doi:10.1182/blood-2003-12-4430

Le Naour, F., Rubinstein, E., Jasmin, C., Prenant, M., & Boucheix, C. (2000). Severely reduced female fertility in CD9-deficient mice. *Science (New York, N.Y.)*, *287*(5451), 319–21.

Lewandrowski, U., Wortelkamp, S., Lohrig, K., Zahedi, R. P., Wolters, D. a, Walter, U., & Sickmann, A. (2009). Platelet membrane proteomics: a novel repository for functional research. *Blood*, *114*(1), 10–9. doi:10.1182/blood-2009-02-203828

Lewis, R. S. (2007). The molecular choreography of a store-operated calcium channel. *Nature*, *446*(7133), 284–7. doi:10.1038/nature05637

Liou, J., Fivaz, M., Inoue, T., & Meyer, T. (2007). Live-cell imaging reveals sequential oligomerization and local plasma membrane targeting of stromal interaction molecule 1 after Ca2+ store depletion. *Proceedings of the National Academy of Sciences of the United States of America*, *104*, 9301–9306. doi:10.1073/pnas.0702866104

Liu, C., & Hermann TE. (1978). Characterization of ionomycin as a calcium ionophore. *The Journal of Biological Chemistry*, *253*, 5892–5894.

Lowe, K. L., Navarro-Nunez, L., & Watson, S. P. (2012). Platelet CLEC-2 and podoplanin in cancer metastasis. *Thrombosis Research*, *129 Suppl* , S30–7. doi:10.1016/S0049-3848(12)70013-0

Lytton, J., Westlin, M., & Hanley, M. R. (1991). Thapsigargin inhibits the sarcoplasmic or endoplasmic reticulum Ca-ATPase family of calcium pumps. *The Journal of Biological Chemistry*, *266*(26), 17067–71.

Macaulay, I. C., Tijssen, M. R., Thijssen-Timmer, D. C., Gusnanto, A., Steward, M., Burns, P., … Ouwehand, W. H. (2007). Comparative gene expression profiling of in vitro differentiated megakaryocytes and erythroblasts identifies novel

activatory and inhibitory platelet membrane proteins. *Blood*, *109*(8), 3260–9. doi:10.1182/blood-2006-07-036269

Maciag, T., Cerundolo, J., Ilsley, S., Kelley, P. R., & Forand, R. (1979). An endothelial cell growth factor from bovine hypothalamus: Identification and partial characterization. *Proceedings of the National Academy of Sciences of the United States of America*, *76*(11), 5674–5678.

Madl, J., Weghuber, J., Fritsch, R., Derler, I., Fahrner, M., Frischauf, I., … Schütz, G. J. (2010). Resting state Orai1 diffuses as homotetramer in the plasma membrane of live mammalian cells. *The Journal of Biological Chemistry*, *285*(52), 41135–42. doi:10.1074/jbc.M110.177881

Mahaut-Smith, M. P., Jones, S., & Evans, R. J. (2011). The P2X1 receptor and platelet function. *Purinergic Signalling*, *7*(3), 341–56. doi:10.1007/s11302-011-9224-0

Maley, F., Trimble, R., Tarentino, A., & Plummer, T. (1989). Characterization of glycoproteins and their associated oligosaccharides through the use of endoglycosidases. *Analytical Biochemistry*, *180*(2), 195–204.

Mangin, P. H., Kleitz, L., Boucheix, C., Gachet, C., & Lanza, F. (2009). CD9 negatively regulates integrin alphaIIbbeta3 activation and could thus prevent excessive platelet recruitment at sites of vascular injury. *Journal of Thrombosis and Haemostasis : JTH*, *7*(5), 900–2. doi:10.1111/j.1538-7836.2009.03322.x

Marcus, a J., Broekman, M. J., Drosopoulos, J. H., Islam, N., Alyonycheva, T. N., Safier, L. B., … Maliszewski, C. R. (1997). The endothelial cell ecto-ADPase responsible for inhibition of platelet function is CD39. *The Journal of Clinical Investigation*, *99*(6), 1351–60. doi:10.1172/JCI119294

Maruyama, Y., Ogura, T., Mio, K., Kato, K., Kaneko, T., Kiyonaka, S., … Sato, C. (2009). Tetrameric Orai1 is a teardrop-shaped molecule with a long, tapered cytoplasmic domain. *The Journal of Biological Chemistry*, *284*(20), 13676–85. doi:10.1074/jbc.M900812200

Massberg, S., Gru, S., Konrad, I., Arguinzonis, M. I. G., Eigenthaler, M., Hemler, K., … Gawaz, M. (2004). Enhanced in vivo platelet adhesion in vasodilator-stimulated phosphoprotein (VASP)– deficient mice. *Blood*, *103*(1), 136–143. doi:10.1182/blood-2002-11-3417.

Massberg, S., Sausbier, M., Klatt, P., Bauer, M., Pfeifer, A., Siess, W., … Hofmann, F. (1999). Increased Adhesion and Aggregation of Platelets Lacking Cyclic Guanosine 3',5'-Monophosphate Kinase I. *J Exp Med*, *189*(8).

Mattila, P. S., Ullman, K. S., Fiering, S., Emmel, E. a, McCutcheon, M., Crabtree, G. R., & Herzenberg, L. a. (1990). The actions of cyclosporin A and FK506 suggest a novel step in the activation of T lymphocytes. *The EMBO Journal*, *9*(13), 4425–33.

May, F., Hagedorn, I., Pleines, I., Bender, M., Vögtle, T., Eble, J., … Nieswandt, B. (2009). CLEC-2 is an essential platelet-activating receptor in hemostasis and thrombosis. *Blood*, *114*(16), 3464–72. doi:10.1182/blood-2009-05-222273

Mendis, S., Puska, P., & Norrving, B. (2011). Global atlas on cardiovascular disease prevention and control. *World Health Organization*, 2–14.

Mercer, J. C., Dehaven, W. I., Smyth, J. T., Wedel, B., Boyles, R. R., Bird, G. S., & Putney, J. W. (2006). Large store-operated calcium selective currents due to co-expression of Orai1 or Orai2 with the intracellular calcium sensor, Stim1. *The Journal of Biological Chemistry*, *281*, 24979–24990. doi:10.1074/jbc.M604589200

Mignen, O., Thompson, J. L., & Shuttleworth, T. J. (2008). Orai1 subunit stoichiometry of the mammalian CRAC channel pore. *The Journal of Physiology*, *586*(2), 419–25. doi:10.1113/jphysiol.2007.147249

Min, G., Wang, H., Sun, T. T., & Kong, X. P. (2006). Structural basis for tetraspanin functions as revealed by the cryo-EM structure of uroplakin complexes at 6-A resolution. *The Journal of Cell Biology*, *173*(6), 975–83. doi:10.1083/jcb.200602086

Mishima, K., Kato, Y., Kaneko, M. K., Nishikawa, R., Hirose, T., & Matsutani, M. (2006). Increased expression of podoplanin in malignant astrocytic tumors as a novel molecular marker of malignant progression. *Acta Neuropathologica*, *111*(5), 483–8. doi:10.1007/s00401-006-0063-y

Mitchell, J. a, Ali, F., Bailey, L., Moreno, L., & Harrington, L. S. (2008). Role of nitric oxide and prostacyclin as vasoactive hormones released by the endothelium. *Experimental Physiology*, *93*(1), 141–7. doi:10.1113/expphysiol.2007.038588

Miyado, K., Yamada, G., Yamada, S., Hasuwa, H., Nakamura, Y., Ryu, F., … Okabe, M. (2014). Requirement of CD9 on the Egg Plasma Membrane for Fertilization. *Science*, *287*(5451), 321–324.

Miyata, K., Takagi, S., Sato, S., Morioka, H., Shiba, K., Minamisawa, T., … Fujita, N. (2014). Suppression of Aggrus/podoplanin-induced platelet aggregation and pulmonary metastasis by a single-chain antibody variable region fragment. *Cancer Medicine*, 1–10. doi:10.1002/cam4.320

Moncada, S. (1982). Biological Importance of prostacyclin. *Br. J. Pharmacol.*, *76*(December 1980), 3–31.

Moncada, S., & Higgs, E. a. (2006). The discovery of nitric oxide and its role in vascular biology. *British Journal of Pharmacology*, *147 Suppl* , S193–201. doi:10.1038/sj.bjp.0706458

Montpellier, C., Tews, B. A., Poitrimole, J., Rocha-Perugini, V., D'Arienzo, V., Potel, J., … Cocquerel, L. (2011). Interacting regions of CD81 and two of its partners,

EWI-2 and EWI-2wint, and their effect on hepatitis C virus infection. *The Journal of Biological Chemistry*, *286*(16), 13954–65. doi:10.1074/jbc.M111.220103

Moroi, M., & Jung, S. M. (2004). Platelet glycoprotein VI: its structure and function. *Thrombosis Research*, *114*(4), 221–33. doi:10.1016/j.thromres.2004.06.046

Moroi, M., Jung, S. M., Nomura, S., Sekiguchi, S., Ordinas, a, & Diaz-Ricart, M. (1997). Analysis of the involvement of the von Willebrand factor-glycoprotein Ib interaction in platelet adhesion to a collagen-coated surface under flow conditions. *Blood*, *90*(11), 4413–24.

Nieswandt, B., Aktas, B., Moers, a, & Sachs, U. J. H. (2005). Platelets in atherothrombosis: lessons from mouse models. *Journal of Thrombosis and Haemostasis : JTH*, *3*(8), 1725–36. doi:10.1111/j.1538-7836.2005.01488.x

Nieswandt, B., Brakebusch, C., Bergmeier, W., Schulte, V., Bouvard, D., Mokhtari-Nejad, R., … Fässler, R. (2001). Glycoprotein VI but not alpha2beta1 integrin is essential for platelet interaction with collagen. *The EMBO Journal*, *20*(9), 2120–30. doi:10.1093/emboj/20.9.2120

Nieswandt, B., Pleines, I., & Bender, M. (2011). Platelet adhesion and activation mechanisms in arterial thrombosis and ischaemic stroke. *Journal of Thrombosis and Haemostasis : JTH*, *9 Suppl 1*, 92–104. doi:10.1111/j.1538-7836.2011.04361.x

Nieswandt, B., Schulte, V., Bergmeier, W., Mokhtari-Nejad, R., Rackebrandt, K., Cazenave, J. P., … Zirngibl, H. (2001). Long-term antithrombotic protection by in vivo depletion of platelet glycoprotein VI in mice. *The Journal of Experimental Medicine*, *193*(4), 459–69.

Nieswandt, B., & Watson, S. P. (2003). Review article Platelet-collagen interaction : is GPVI the central receptor ? *Blood*, *102*(2), 449–461. doi:10.1182/blood-2002-12-3882.B.N.

Nikopoulos, K., Gilissen, C., Hoischen, A., van Nouhuys, C. E., Boonstra, F. N., Blokland, E. a W., … Collin, R. W. J. (2010). Next-generation sequencing of a 40 Mb linkage interval reveals TSPAN12 mutations in patients with familial exudative vitreoretinopathy. *American Journal of Human Genetics*, *86*(2), 240–7. doi:10.1016/j.ajhg.2009.12.016

Nourshargh, S., Hordijk, P. L., & Sixt, M. (2010). Breaching multiple barriers: leukocyte motility through venular walls and the interstitium. *Nature Reviews. Molecular Cell Biology*, *11*(5), 366–78. doi:10.1038/nrm2889

Orlowski, E., Chand, R., Yip, J., Wong, C., Goschnick, M. W., Wright, M. D., … Jackson, D. E. (2009). A platelet tetraspanin superfamily member, CD151, is required for regulation of thrombus growth and stability in vivo. *Journal of Thrombosis and Haemostasis : JTH*, *7*(12), 2074–84. doi:10.1111/j.1538-7836.2009.03612.x

Palomo, I., Toro, C., & Alarcón, M. (2008). The role of platelets in the pathophysiology of atherosclerosis (Review). *Molecular Medicine Reports*, *1*(2), 179–84.

Park, C. Y., Hoover, P. J., Mullins, F. M., Bachhawat, P., Covington, E. D., Raunser, S., … Lewis, R. S. (2009). STIM1 clusters and activates CRAC channels via direct binding of a cytosolic domain to Orai1. *Cell*, *136*(5), 876–90. doi:10.1016/j.cell.2009.02.014

Pearce, A. C., Senis, Y. A., Billadeau, D. D., Turner, M., Watson, S. P., & Vigorito, E. (2004). Vav1 and vav3 have critical but redundant roles in mediating platelet activation by collagen. *The Journal of Biological Chemistry*, *279*(52), 53955–62. doi:10.1074/jbc.M410355200

Penna, A., Demuro, A., Yeromin, A. V, Zhang, S. L., Safrina, O., Parker, I., & Cahalan, M. D. (2008). The CRAC channel consists of a tetramer formed by Stim-induced dimerization of Orai dimers. *Nature*, *456*(7218), 116–20. doi:10.1038/nature07338

Perron, J. C., & Bixby, J. L. (1999). Tetraspanins expressed in the embryonic chick nervous system. *FEBS Letters*, *461*(1-2), 86–90.

Pfaffl, M. W. (2001). A new mathematical model for relative quantification in real-time RT-PCR. *Nucleic Acids Research*, *29*(9), e45.

Poulter, J. a, Davidson, A. E., Ali, M., Gilmour, D. F., Parry, D. a, Mintz-Hittner, H. a, … Toomes, C. (2012). Recessive mutations in TSPAN12 cause retinal dysplasia and severe familial exudative vitreoretinopathy (FEVR). *Investigative Ophthalmology & Visual Science*, *53*(6), 2873–9. doi:10.1167/iovs.11-8629

Prakriya, M., Feske, S., Gwack, Y., Srikanth, S., Rao, A., & Hogan, P. G. (2006). Orai1 is an essential pore subunit of the CRAC channel. *Nature*, *443*(7108), 230–3. doi:10.1038/nature05122

Protty, M. B., Watkins, N. A., Colombo, D., Thomas, S. G., Heath, V. L., Herbert, J. M. J., … Tomlinson, M. G. (2009). Identification of Tspan9 as a novel platelet tetraspanin and the collagen receptor GPVI as a component of tetraspanin microdomains. *The Biochemical Journal*, *417*(1), 391–400. doi:10.1042/BJ20081126

Prox, J., Willenbrock, M., Weber, S., Lehmann, T., Schmidt-Arras, D., Schwanbeck, R., … Schwake, M. (2012). Tetraspanin15 regulates cellular trafficking and activity of the ectodomain sheddase ADAM10. *Cellular and Molecular Life Sciences : CMLS*, *69*(17), 2919–32. doi:10.1007/s00018-012-0960-2

Rajesh, S., Sridhar, P., Tews, B. A., Fénéant, L., Cocquerel, L., Ward, D. G., … Overduin, M. (2012). Structural basis of ligand interactions of the large extracellular domain of tetraspanin CD81. *Journal of Virology*, *86*(18), 9606–16. doi:10.1128/JVI.00559-12

Ramanathan, G., Gupta, S., Thielmann, I., Pleines, I., Varga-Szabo, D., May, F., … Braun, a. (2012). Defective diacylglycerol-induced Ca2+ entry but normal agonist-induced activation responses in TRPC6-deficient mouse platelets. *Journal of Thrombosis and Haemostasis : JTH*, *10*(3), 419–29. doi:10.1111/j.1538-7836.2011.04596.x

Renné, T., Pozgajová, M., Grüner, S., Schuh, K., Pauer, H.-U., Burfeind, P., … Nieswandt, B. (2005). Defective thrombus formation in mice lacking coagulation factor XII. *The Journal of Experimental Medicine*, *202*(2), 271–81. doi:10.1084/jem.20050664

Rink, T. J., & Sage, S. O. (1990). Calcium signalling in human platelets. *Annual Review of Physiology*, *52*(81), 431 – 49.

Rondaij, M. G., Bierings, R., Kragt, A., van Mourik, J. a, & Voorberg, J. (2006). Dynamics and plasticity of Weibel-Palade bodies in endothelial cells. *Arteriosclerosis, Thrombosis, and Vascular Biology*, *26*(5), 1002–7. doi:10.1161/01.ATV.0000209501.56852.6c

Rondina, M. T., Weyrich, A. S., & Zimmerman, G. a. (2013). Platelets as cellular effectors of inflammation in vascular diseases. *Circulation Research*, *112*(11), 1506–19. doi:10.1161/CIRCRESAHA.113.300512

Rowley, J. W., Oler, A. J., Tolley, N. D., Hunter, B. N., Low, E. N., Nix, D. a, … Weyrich, A. S. (2011). Genome-wide RNA-seq analysis of human and mouse platelet transcriptomes. *Blood*, *118*(14), e101–11. doi:10.1182/blood-2011-03-339705

Rubinstein, E. (2011). The complexity of tetraspanins. *Biochemical Society Transactions*, *39*(2), 501–5. doi:10.1042/BST0390501

Ruggeri, Z. M., Dent, J. A., & Saldívar, E. (1999). Contribution of distinct adhesive interactions to platelet aggregation in flowing blood. *Blood*, *94*, 172–178.

Sakakura, K., Nakano, M., Otsuka, F., Ladich, E., Kolodgie, F. D., & Virmani, R. (2013). Pathophysiology of atherosclerosis plaque progression. *Heart, Lung & Circulation*, *22*(6), 399–411. doi:10.1016/j.hlc.2013.03.001

Sako, Y., Minoghchi, S., & Yanagida, T. (2000). Single-molecule imaging of EGFR signalling on the surface of living cells. *Nature Cell Biology*, *2*(3), 168–72. doi:10.1038/35004044

Schröder, J., Lüllmann-Rauch, R., Himmerkus, N., Pleines, I., Nieswandt, B., Orinska, Z., … Saftig, P. (2009). Deficiency of the tetraspanin CD63 associated with kidney pathology but normal lysosomal function. *Molecular and Cellular Biology*, *29*(4), 1083–94. doi:10.1128/MCB.01163-08

Schütz, G. J., Kada, G., Pastushenko, V. P., & Schindler, H. (2000). Properties of lipid microdomains in a muscle cell membrane visualized by single molecule microscopy. *The EMBO Journal*, *19*(5), 892–901. doi:10.1093/emboj/19.5.892

Schwarz, U. R., Walter, U., & Eigenthaler, M. (2001). Taming platelets with cyclic nucleotides. *Biochemical Pharmacology*, *62*(9), 1153–61.

Sebastiano, C., Bromberg, M., Breen, K., & Hurford, M. T. (2010). Case Report Glanzmann ' s thrombasthenia : report of a case and review of the literature. *International Journal of Experimental Pathology*, *3*(4), 443–447.

Seigneuret, M. (2006). Complete predicted three-dimensional structure of the facilitator transmembrane protein and hepatitis C virus receptor CD81: conserved and variable structural domains in the tetraspanin superfamily. *Biophysical Journal*, *90*, 212–227. doi:10.1529/biophysj.105.069666

Seigneuret, M., Delaguillaumie, a, Lagaudrière-Gesbert, C., & Conjeaud, H. (2001). Structure of the tetraspanin main extracellular domain. A partially conserved fold with a structurally variable domain insertion. *The Journal of Biological Chemistry*, *276*(43), 40055–64. doi:10.1074/jbc.M105557200

Senis, Y. a, Mazharian, A., & Mori, J. (2014). *Src family kinases: at the forefront of platelet activation. Blood* (Vol. 44). doi:10.1182/blood-2014-01-453134

Senis, Y. A., Tomlinson, M. G., Ellison, S., Mazharian, A., Lim, J., Zhao, Y., … Watson, S. P. (2009). The tyrosine phosphatase CD148 is an essential positive regulator of platelet activation and thrombosis. *Blood*, *113*(20), 4942–54. doi:10.1182/blood-2008-08-174318

Serru, V., Le Naour, F., Billard, M., Azorsa, D. O., Lanza, F., Boucheix, C., & Rubinstein, E. (1999). Selective tetraspan-integrin complexes (CD81/alpha4beta1, CD151/alpha3beta1, CD151/alpha6beta1) under conditions disrupting tetraspan interactions. *The Biochemical Journal*, *340 (Pt 1*, 103–111. doi:10.1042/0264-6021:3400103

Shapiro, V. S., Mollenauer, M. N., Greene, W. C., & Weiss, A. (1996). c-rel regulation of IL-2 gene expression may be mediated through activation of AP-1. *The Journal of Experimental Medicine*, *184*(5), 1663–9.

Shoham, T., Rajapaksa, R., Boucheix, C., Rubinstein, E., Poe, J. C., Tedder, T. F., & Levy, S. (2003). The Tetraspanin CD81 Regulates the Expression of CD19 During B Cell Development in a Postendoplasmic Reticulum Compartment. *The Journal of Immunology*, *171*(8), 4062–4072. doi:10.4049/jimmunol.171.8.4062

Shuttleworth, T. J. (2012). Orai3--the "exceptional" Orai? *The Journal of Physiology*, *590*(Pt 2), 241–57. doi:10.1113/jphysiol.2011.220574

Smolenski, a. (2012). Novel roles of cAMP/cGMP-dependent signaling in platelets. *Journal of Thrombosis and Haemostasis : JTH*, *10*(2), 167–76. doi:10.1111/j.1538-7836.2011.04576.x

Smyth, J. T., Hwang, S.-Y., Tomita, T., DeHaven, W. I., Mercer, J. C., & Putney, J. W. (2010). Activation and regulation of store-operated calcium entry. *Journal of*

Cellular and Molecular Medicine, *14*(10), 2337–49. doi:10.1111/j.1582-4934.2010.01168.x

Soboloff, J., Rothberg, B. S., Madesh, M., & Gill, D. L. (2012). STIM proteins: dynamic calcium signal transducers. *Nature Reviews. Molecular Cell Biology*, *13*(9), 549–65. doi:10.1038/nrm3414

Soboloff, J., Spassova, M. a, Tang, X. D., Hewavitharana, T., Xu, W., & Gill, D. L. (2006). Orai1 and STIM reconstitute store-operated calcium channel function. *The Journal of Biological Chemistry*, *281*(30), 20661–5. doi:10.1074/jbc.C600126200

Srikanth, S., & Gwack, Y. (2012). Orai1, STIM1, and their associating partners. *The Journal of Physiology*, *590*(Pt 17), 4169–77. doi:10.1113/jphysiol.2012.231522

Stathopulos, P. B., Zheng, L., & Ikura, M. (2009). Stromal interaction molecule (STIM) 1 and STIM2 calcium sensing regions exhibit distinct unfolding and oligomerization kinetics. *The Journal of Biological Chemistry*, *284*(2), 728–32. doi:10.1074/jbc.C800178200

Stathopulos, P. B., Zheng, L., Li, G.-Y., Plevin, M. J., & Ikura, M. (2008). Structural and mechanistic insights into STIM1-mediated initiation of store-operated calcium entry. *Cell*, *135*(1), 110–22. doi:10.1016/j.cell.2008.08.006

Stegner, D., Haining, E. J., & Nieswandt, B. (2014). Targeting glycoprotein VI and the immunoreceptor tyrosine-based activation motif signaling pathway. *Arteriosclerosis, Thrombosis, and Vascular Biology*, *34*(8), 1615–20. doi:10.1161/ATVBAHA.114.303408

Stegner, D., & Nieswandt, B. (2011). Platelet receptor signaling in thrombus formation. *Journal of Molecular Medicine (Berlin, Germany)*, *89*(2), 109–21. doi:10.1007/s00109-010-0691-5

Sterk, L., & Geuijen, C. (2002). Association of the tetraspanin CD151 with the laminin-binding integrinsα 3β1, α6β1, α6β4 and α7β1 in cells in culture and in vivo. *Journal of Cell Science*, *115*, 1161 – 1173.

Stipp, C. S., Kolesnikova, T. V, & Hemler, M. E. (2003). Functional domains in tetraspanin proteins. *Trends in Biochemical Sciences*, *28*(2), 106–12. doi:10.1016/S0968-0004(02)00014-2

Suzuki-Inoue, K., Inoue, O., Ding, G., Nishimura, S., Hokamura, K., Eto, K., … Ozaki, Y. (2010). Essential in vivo roles of the C-type lectin receptor CLEC-2: embryonic/neonatal lethality of CLEC-2-deficient mice by blood/lymphatic misconnections and impaired thrombus formation of CLEC-2-deficient platelets. *The Journal of Biological Chemistry*, *285*(32), 24494–507. doi:10.1074/jbc.M110.130575

Suzuki-Inoue, K., Kato, Y., Inoue, O., Kaneko, M. K., Mishima, K., Yatomi, Y., … Ozaki, Y. (2007). Involvement of the snake toxin receptor CLEC-2, in

podoplanin-mediated platelet activation, by cancer cells. *The Journal of Biological Chemistry*, *282*(36), 25993–6001. doi:10.1074/jbc.M702327200

Tang, T., Li, L., Tang, J., Li, Y., Lin, W. Y., Martin, F., … de Sauvage, F. J. (2010). A mouse knockout library for secreted and transmembrane proteins. *Nature Biotechnology*, *28*(7), 749–55. doi:10.1038/nbt.1644

Taylor, K. a, Wright, J. R., Vial, C., Evans, R. J., & Mahaut-Smith, M. P. (2014). Amplification of human platelet activation by surface pannexin-1 channels. *Journal of Thrombosis and Haemostasis : JTH*, *12*(6), 987–98. doi:10.1111/jth.12566

Thiel, M., Lis, A., & Penner, R. (2013). STIM2 drives Ca2+ oscillations through store-operated Ca2+ entry caused by mild store depletion. *The Journal of Physiology*, *591*(Pt 6), 1433–45. doi:10.1113/jphysiol.2012.245399

Thomas, G. D. (2011). Neural control of the circulation. *Advances in Physiology Education*, *35*(1), 28–32. doi:10.1152/advan.00114.2010

Thompson, J. L., & Shuttleworth, T. J. (2013). How many Orai's does it take to make a CRAC channel? *Scientific Reports*, *3*, 1961. doi:10.1038/srep01961

Tognon, C. E., Kirk, H. E., Passmore, L. A., Whitehead, P., Der, C. J., Kay, R. J., & Whitehead, I. A. N. P. (1998). Regulation of RasGRP via a Phorbol Ester-Responsive C1 Domain Regulation of RasGRP via a Phorbol Ester-Responsive C1 Domain. *Molecular and Cellular Biology*, *18*(12).

Tomlinson, M. G., Calaminus, S. D., Berlanga, O., Auger, J. M., Bori-Sanz, T., Meyaard, L., & Watson, S. P. (2007). Collagen promotes sustained glycoprotein VI signaling in platelets and cell lines. *Journal of Thrombosis and Haemostasis : JTH*, *5*(11), 2274–83. doi:10.1111/j.1538-7836.2007.02746.x

Tomlinson, M. G., Kane, L. P., Su, J., Kadlecek, T. A., Mollenauer, M. N., & Weiss, A. (2004). Expression and Function of Tec , Itk , and Btk in Lymphocytes : Evidence for a Unique Role for Tec. *Molecular and Cellular Biology*, *24*(6), 2455–2466. doi:10.1128/MCB.24.6.2455

Tronik-Le Roux, D., Roullot, V., Poujol, C., Kortulewski, T., Nurden, P., & Marguerie, G. (2000). Thrombasthenic mice generated by replacement of the integrin alpha(IIb) gene: demonstration that transcriptional activation of this megakaryocytic locus precedes lineage commitment. *Blood*, *96*(4), 1399–408.

Uhrin, P., Zaujec, J., Breuss, J. M., Olcaydu, D., Chrenek, P., Stockinger, H., … Kerjaschki, D. (2010). Novel function for blood platelets and podoplanin in developmental separation of blood and lymphatic circulation. *Blood*, *115*(19), 3997–4005. doi:10.1182/blood-2009-04-216069.

Van Hinsbergh, V. W. M. (2012). Endothelium--role in regulation of coagulation and inflammation. *Seminars in Immunopathology*, *34*(1), 93–106. doi:10.1007/s00281-011-0285-5

Van Montfoort, M. L., Kuijpers, M. J. E., Knaup, V. L., Bhanot, S., Monia, B. P., Roelofs, J. J. T. H., … Meijers, J. C. M. (2014). Factor XI Regulates Pathological Thrombus Formation on Acutely Ruptured Atherosclerotic Plaques. *Arteriosclerosis, Thrombosis, and Vascular Biology*, *34*, 1668–73. doi:10.1161/ATVBAHA.114.303209

Varga-Szabo, D., Authi, K. S., Braun, A., Bender, M., Ambily, A., Hassock, S. R., … Nieswandt, B. (2008). Store-operated Ca2+ entry in platelets occurs independently of transient receptor potential (TRP) C1. *Pflugers Archiv European Journal of Physiology*, *457*, 377–387. doi:10.1007/s00424-008-0531-4

Varga-Szabo, D., Braun, a, & Nieswandt, B. (2009). Calcium signaling in platelets. *Journal of Thrombosis and Haemostasis : JTH*, *7*(7), 1057–66. doi:10.1111/j.1538-7836.2009.03455.x

Varga-Szabo, D., Braun, A., Kleinschnitz, C., Bender, M., Pleines, I., Pham, M., … Nieswandt, B. (2008). The calcium sensor STIM1 is an essential mediator of arterial thrombosis and ischemic brain infarction. *The Journal of Experimental Medicine*, *205*(7), 1583–91. doi:10.1084/jem.20080302

Vig, M., Beck, A., Billingsley, J. M., Lis, A., Parvez, S., Peinelt, C., … Penner, R. (2006). CRACM1 multimers form the ion-selective pore of the CRAC channel. *Current Biology : CB*, *16*(20), 2073–9. doi:10.1016/j.cub.2006.08.085

Wang, H.-X., Li, Q., Sharma, C., Knoblich, K., & Hemler, M. E. (2011). Tetraspanin protein contributions to cancer. *Biochemical Society Transactions*, *39*(2), 547–52. doi:10.1042/BST0390547

Wang, X., Wang, Y., Zhou, Y., Hendron, E., Mancarella, S., Andrake, M. D., … Gill, D. L. (2014). Distinct Orai-coupling domains in STIM1 and STIM2 define the Orai-activating site. *Nature Communications*, *5*, 3183. doi:10.1038/ncomms4183

Watson, S. P., Auger, J. M., McCarty, O. J. T., & Pearce, a C. (2005). GPVI and integrin alphaIIb beta3 signaling in platelets. *Journal of Thrombosis and Haemostasis : JTH*, *3*(8), 1752–62. doi:10.1111/j.1538-7836.2005.01429.x

Wilson, D. P., Susnjar, M., Kiss, E., Sutherland, C., & Walsh, M. P. (2005). Thromboxane A2-induced contraction of rat caudal arterial smooth muscle involves activation of Ca2+ entry and Ca2+ sensitization: Rho-associated kinase-mediated phosphorylation of MYPT1 at Thr-855, but not Thr-697. *The Biochemical Journal*, *389*(Pt 3), 763–74. doi:10.1042/BJ20050237

Winterwood, N. E., Varzavand, A., Meland, M. N., Ashman, L. K., & Stipp, C. S. (2006). A Critical Role for Tetraspanin CD151 in alpha3beta1 and alpha6beta4 Integrin – dependent Tumor Cell Functions on Laminin-5. *Molecular Biology of the Cell*, *17*(June), 2707–2721. doi:10.1091/mbc.E05

Wright, M. D., Geary, S. M., Fitter, S., Gregory, W., Lau, L., Sheng, K., … Apostolopoulos, V. (2004). Characterization of Mice Lacking the Tetraspanin Superfamily Member CD151 Characterization of Mice Lacking the Tetraspanin

Superfamily Member CD151. *Molecular and Cellular Biology*, *24*(13), 5978 – 5988. doi:10.1128/MCB.24.13.5978

Yáñez-Mó, M., Alfranca, a, Cabañas, C., Marazuela, M., Tejedor, R., Ursa, M. a, … Sánchez-Madrid, F. (1998). Regulation of endothelial cell motility by complexes of tetraspan molecules CD81/TAPA-1 and CD151/PETA-3 with alpha3 beta1 integrin localized at endothelial lateral junctions. *The Journal of Cell Biology*, *141*(3), 791–804.

Yáñez-Mó, M., Barreiro, O., Gordon-Alonso, M., Sala-Valdés, M., & Sánchez-Madrid, F. (2009). Tetraspanin-enriched microdomains: a functional unit in cell plasma membranes. *Trends in Cell Biology*, *19*(9), 434–46. doi:10.1016/j.tcb.2009.06.004

Yang, X. H., Mirchev, R., Deng, X., Yacono, P., Yang, H. L., Golan, D. E., & Hemler, M. E. (2012). CD151 restricts the α6 integrin diffusion mode. *Journal of Cell Science*, *125*(Pt 6), 1478–87. doi:10.1242/jcs.093963

Yang, X. H., Richardson, A. L., Torres-Arzayus, M. I., Zhou, P., Sharma, C., Kazarov, A. R., … Hemler, M. E. (2008). CD151 accelerates breast cancer by regulating alpha 6 integrin function, signaling, and molecular organization. *Cancer Research*, *68*(9), 3204–13. doi:10.1158/0008-5472.CAN-07-2949

Yang, X., Jin, H., Cai, X., Li, S., & Shen, Y. (2012). Structural and mechanistic insights into the activation of Stromal interaction molecule 1 (STIM1). *Proceedings of the National Academy of Sciences of the United States of America*, *109*(15), 5657–62. doi:10.1073/pnas.1118947109

Yauch, R. L., Berditchevski, F., Harler, M. B., Reichner, J., & Hemler, M. E. (1998). Highly stoichiometric, stable, and specific association of integrin alpha3beta1 with CD151 provides a major link to phosphatidylinositol 4-kinase, and may regulate cell migration. *Molecular Biology of the Cell*, *9*(10), 2751–65.

Ye, X., Wang, Y., & Nathans, J. (2010). The Norrin/Frizzled4 signaling pathway in retinal vascular development and disease. *Trends in Molecular Medicine*, *16*(9), 417–25. doi:10.1016/j.molmed.2010.07.003

Yuan, J., Jin, C., Qin, H. De, Wang, J., Sha, W., Wang, M., … Shugart, Y. Y. (2013). Replication study confirms link between TSPAN18 mutation and schizophrenia in Han Chinese. *PloS One*, *8*(3), e58785. doi:10.1371/journal.pone.0058785

Yuan, P., Temam, S., El-Naggar, A., Zhou, X., Liu, D. D., Lee, J. J., & Mao, L. (2006). Overexpression of podoplanin in oral cancer and its association with poor clinical outcome. *Cancer*, *107*(3), 563–9. doi:10.1002/cncr.22061

Yue, W. H., Wang, H. F., Sun, L. D., Tang, F. L., Liu, Z. H., Zhang, H. X., … Zhang, D. (2011). Genome-wide association study identifies a susceptibility locus for schizophrenia in Han Chinese at 11p11.2. *Nature Genetics*, *43*(12), 1228–31. doi:10.1038/ng.979

Zahid, M., Mangin, P., Loyau, S., Hechler, B., Billiald, P., Gachet, C., & Jandrot-Perrus, M. (2012). The future of glycoprotein VI as an antithrombotic target. *Journal of Thrombosis and Haemostasis : JTH*, *10*(12), 2418–27. doi:10.1111/jth.12009

Zbidi, H., Jardin, I., Woodard, G. E., Lopez, J. J., Berna-Erro, A., Salido, G. M., & Rosado, J. a. (2011). STIM1 and STIM2 are located in the acidic Ca2+ stores and associates with Orai1 upon depletion of the acidic stores in human platelets. *The Journal of Biological Chemistry*, *286*(14), 12257–70. doi:10.1074/jbc.M110.190694

Zelm, M. C. Van, Smet, J., Adams, B., Mascart, F., Schandené, L., Janssen, F., … Burg, M. Van Der. (2010). CD81 gene defect in humans disrupts CD19 complex formation and leads to antibody deficiency. *The Journal of Clinical investigationJournal of Cli*, *120*(4). doi:10.1172/JCI39748.eases

Zhang, F. L., Luo, L., Gustafson, E., Lachowicz, J., Smith, M., Qiao, X., … Monsma, F. J. (2001). ADP is the cognate ligand for the orphan G protein-coupled receptor SP1999. *The Journal of Biological Chemistry*, *276*, 8608–8615. doi:10.1074/jbc.M009718200

Zhou, Y., Srinivasan, P., Razavi, S., Seymour, S., Meraner, P., Gudlur, A., … Hogan, P. G. (2013). Initial activation of STIM1, the regulator of store-operated calcium entry. *Nature Structural & Molecular Biology*, *20*(8), 973–81. doi:10.1038/nsmb.2625